Changes in vascular elasticity due to the consumption of high salt: Sex differences

by

©Eric Abonah Mensah

A thesis submitted to the School of Graduate Studies in partial fulfilment of the requirements for the degree of

Doctor of Philosophy in Medicine

Division of Biomedical Sciences (Cardiovascular and Renal Sciences)

Faculty of Medicine

Memorial University of Newfoundland

October 2024

St. John's, Newfoundland

Abstract

Arterial stiffness and alteration in vascular biomechanics play pivotal roles in circulatory dysfunction. Furthermore, the pharmacological responses of vasoactive agents on biomechanics are less defined in salt-induced hypertension in males versus females. Therefore, the studies undertaken for this thesis investigated the changes in the structure and biomechanics of small resistance arteries from salt-sensitive male and female Dahl rats fed regular and high salt diets for 6-7 weeks (n=6-8/group). Third-order mesenteric arteries were used, and the effects of pharmacological agents on biomechanics were assessed using pressure myography. Rats on a high salt diet (H) developed hypertension with elevated pulse wave velocity compared to rats on a regular diet (R). Morphometric assessment of the vessel wall indicated the possible development of hypertrophy with a significant increase in collagen and smooth muscle cell areas in males (H) compared (R) and the corresponding females. While no significant differences in composite Young's modulus (CYM) were found between groups, vasoconstriction (phenylephrine, 0.3 μM) resulted in significantly higher CYM in males (H) than (R) and the corresponding females on a high salt diet or regular diet. In contrast, vasodilation (sodium nitroprusside, 0.3 μM) significantly reduced CYM in the male groups (H) compared to the corresponding values in females (H). Inhibition of endothelial cell function using (L-NAME 0.3 μM, Ouabain 100 μM, and $BaCl_2$ 100 μM) or by denudation significantly increased CYM in male (R), female (R) and female (H) but not in male (H). Immunohistochemical assessment of biomechanical markers of arterial stiffness revealed significant sex differences, which may contribute to differential mechanisms of arterial stiffness in males versus females. Assessment of sex-specific contributions of Piezo 1 channels in vascular biomechanics indicated a differential expression of Piezo 1 mechanosensitive ion channels. In intact tissue, Piezo 1 antagonist,

GsMTx-4 (2 μM), led to significant increases in CYM in male (R), female (R) and female (H) but not male (H). In contrast, in endothelial denuded vessels, GsMTx-4 produced a significant increase in CYM but only in females (R). These findings point to sex-specific changes in the ultrastructure and function of these arteries, which seem to alter the biomechanics and, thus, ultimately, the integrated function of macro- and micro-circulations.

General Lay Summary

The impact of high salt consumption on health has spurred intensive scientific investigation. Eating too much salt has been linked to serious health problems, especially elevated blood pressure, heightened cardiovascular morbidity and mortality. Annually, approximately 1.65 million cardiovascular-related deaths worldwide are attributed to high salt intake, with a majority occurring in males compared to females, representing a significant portion of cardiovascular-related deaths. Reducing dietary salt intake is suggested to have a beneficial effect on the cardiovascular system. This is particularly true for older adults, where a high salt intake is strongly associated with high blood pressure. Excessive salt intake can impact cardiovascular health by influencing vascular biology and hormonal changes, potentially leading to altered vascular elasticity.

Arterial stiffness indicates how elastic or stiff the arteries are and is an important marker for cardiovascular health, closely linked to various vascular disorders like stroke and heart failure. Sex differences in arterial stiffness are suggested to be due to biological differences. Studies done prior to this research suggested that the markers of arterial stiffness differ between men and women and between people with and without high cardiovascular risk factors. Understanding these differences and the mechanisms by which a high salt diet influences arterial stiffness is key to reducing cardiovascular risk. This study focuses on how high salt intake affects blood vessel elasticity, particularly in males and females.

We used a type of rat sensitive to salt and fed them both normal and high salt diets for 6-7 weeks. Both male and female rats developed high blood pressure on the high salt diet, which affected the structure and function of their blood vessels. Although overall arterial stiffness (measured by the Composite Young modulus) did not differ much between groups, the responses

to substances(drugs) that cause a change in blood vessel diameter did vary. Male rats on a high salt diet had stiffer blood vessels when constricted, but their blood vessels became significantly more elastic when dilated than females on the same diet. We also found sex-specific differences in biochemical markers of arterial stiffness and specific ion channels that respond to mechanical changes in blood vessels. These findings suggest that while males and females experienced increased arterial blood pressure due to high salt intake, different changes occur in their blood vessel structure and function.

Acknowledgement

I want to take this opportunity to express my heartfelt gratitude to the many individuals who have played a significant role in my journey as a doctoral candidate. Their unwavering support, guidance, and encouragement have been instrumental in shaping my research and personal growth.

First and foremost, I am deeply indebted to my PhD supervisors, Dr. Reza Tabrizchi and Dr. Noriko Daneshtalab. Their expertise, wisdom, and dedication to research have been invaluable. They have provided me with valuable guidance throughout this process and served as mentors and role models. I am truly fortunate to have had the privilege of working under their supervision.

I would also like to sincerely thank the members of my PhD committee, Dr. Bruce Van Vliet and Dr. Graham Fraser, for their insightful feedback and constructive criticism. Their expertise and commitment to academic excellence have contributed significantly to the refinement and depth of my research.

I am grateful to all the professors and faculty members who have shared their knowledge and expertise with me throughout my academic journey. Their lectures, seminars, and discussions have broadened my understanding of my field and enriched my research.

I would also like to acknowledge the invaluable support of the faculty support staff, including administrative assistants, librarians, and technicians. Their efficiency and willingness to assist have facilitated my research endeavors, making the process smoother and more manageable.

In addition, I am thankful to my fellow research students and colleagues, who have been a source of inspiration, intellectual stimulation, and camaraderie. Their insights and discussions have shaped my thinking and provided a supportive community throughout my doctoral studies.

Finally, I would like to express my deepest gratitude to my family and friends for their unwavering love, encouragement, and understanding. Their belief in me has been a constant source of motivation, and their support has sustained me during challenging times.

To all those who have directly and indirectly contributed to my research, your involvement and support have been immeasurable. I am truly grateful for your contributions and acknowledge your impact on my academic and personal growth.

Thank you all for being a part of this incredible journey.

Table of Contents

List of Tables

List of Figures

List of Abbreviations

Adenosine triphosphate (ATP)
Angiotensin II (AII)
Antidiuretic hormone (ADH)
ATP-sensitive potassium channels (KATP)
Basement membrane (BM)
Calcium ion (Ca^{2+})
Calcium-activated chloride channels (CaCCs)
Calcium-activated potassium (KCa)
Calcium channel blockers (CCBs)
Cardiac output (CO)
Chloride ion (Cl^-)
Composite Young modulus (CYM)
Cyclooxygenase (COX)
Cyclic adenosine monophosphate (cAMP)
Cyclic guanosine monophosphate (cGMP)
4' 6-Diamindino-2-Phenylindole (DPI)
Diacylglycerol (DAG)
Extracellular matrix (ECM)
Endothelial cells (ECs)
Endothelin (ET-1)
Endothelin-converting enzyme (ECE)
Endothelium-derived hyperpolarizing factor (EDHF)
Endothelium-derived relaxing factor (EDRF)
Female high salt diet (FHS)
Female regular diet (FRD)
Grammostola mechanotoxin #4 (GsMTx-4, GsMTx4, GsMTx-IV)
G protein-coupled receptors (GPCRs)
Guanosine-5'-diphosphate (GDP)
Guanosine-5'-triphosphate (GTP)
Immunohistochemistry (IHC)
Inositol 1,4,5 trisphosphate (IP3)
Inward rectifier potassium channels (Kir)
L-NG-nitro arginine methyl ester (L-NAME)
Male high salt diet (MHS)
Male regular diet (MRD)
Matrix metalloprotease (MMP)
Matrix metallopeptidase 9 (MMP-9)
Mean arterial pressure (MAP)
Mean gray value (MGV)
Myosin light chain (MLC)
Myosin light chain kinase (MLCK)
Myosin light chain phosphatase (MLCP)
Nicotinamide adenine dinucleotide phosphate (NADPH)
Nitric oxide synthase (NOS)
Normal goat serum (NGS)
Non-steroidal anti-inflammatory drugs (NSAIDs)
Phosphate-buffered saline (PBS)
Potassium ions (K+)
Pulse pressure (PP)
Pulse wave velocity (PWV)
Reactive oxygen species (ROS)
Sodium ions (Na+)
Sodium-potassium pump (Na+–K+-ATPase)
Sympathetic nervous system (SNS)
Tandem two-pore k channels (K2P)
Tetraethylammonium (TEA)
Tissue inhibitors of metalloproteinases (TIMPs)
Total peripheral resistance (TPR)
Vascular smooth muscle cell (VSMC)
Voltage-gated potassium channels (VGKC)
Volume-regulated chloride channels (CLVR)

List of Publications

Chapter 2 was published in *Journal of Hypertension* in March 2022 as **"Differential biomechanics in resistance arteries of male compared with female Dahl hypertensive rats"** (DOI: 10.1097/HJH.0000000000003053).

Chapter 3 was published in *Journal of Pharmacology Research Perspective* in February 2024 as **"Effects of vasoactive substances on biomechanics of small resistance arteries of male and female Dahl salt-sensitive rats"** (DOI: 10.1002/prp2.1180).

Chapter 4 was published in *Journal of Pharmacology Research Perspective* in June 2024 as **"Involvement of Piezo 1 mechanoceptors in vascular stiffness in isolated small resistance arteries of male and female Dahl salt-sensitive hypertensive rats"** (DOI: 10.1002/prp2.1227).

Authors' Contributions

The candidate confirms that all authors (Dr. Reza Tabrizchi and Dr. Noriko Daneshtalab) mentioned in the publications (Chapters 2, 3 and 4) contributed to the conception of the studies, analysis of the data and writing, editing, and revising of the manuscripts.

Chapter 1 INTRODUCTION

1.1 Overview of the cardiovascular system

An essential feature as organisms transitioned from unicellular to more complex multicellular organisms is the development of an extensive network of blood vessels and a pump referred to as the cardiovascular system (Stefanovska & Bracic, 1999). This system facilitates the distribution of blood to the various tissues in the body. The cardiovascular network circulates oxygen and provides nutrients, removes carbon dioxide (CO_2) and waste products of metabolism to the appropriate excretory organs for disposal, and carries antibodies that protects the body against infections and diseases (Senior, 2010). In mammals, the cardiovascular system consists of a muscular pump (heart) and a closed system of blood vessels that perform specific functions. The heart is one of the crucial organs responsible for sustaining life. The heart's primary function is maintaining constant blood flow throughout the body. The heart also works with other body systems to maintain adequate blood pressure and heart rate (Hall & Hall, 2020; Senior, 2010).

Two circulatory loops are found in the human cardiovascular system. The systemic circulatory loop is the primary circulatory system that transports oxygenated blood to the body's organs, tissues and cells and removes CO_2 and waste. In contrast, the pulmonary circulatory loop transports deoxygenated blood from the right side of the heart to the lungs, where the blood is reoxygenated and returned to the left side of the heart (Hall & Hall, 2020).

The blood vessels that form part of the cardiovascular system perform specific functions based on their location in the circulatory system (Tucker et al., 2017). They consist of arteries, capillaries and veins. In general, arteries carry oxygenated blood from the heart to other body tissues except in the pulmonary trunks of the pulmonary circulatory loop, where arteries carry

deoxygenated blood from the heart to the lungs to be oxygenated. Capillaries enable the exchange of gases, nutrients and excretory waste products between the circulatory system and body cells, while veins return deoxygenated blood to the heart. The venous system serves as the body's blood reservoir and contains up to 75 percent of the total blood volume at a given time (Peters et al., 2001; Tucker et al., 2017). The intrinsic ability of veins to hold this high blood volume is due to their ability to distend and store large volumes of blood at low pressures (high capacitance) (Caro et al., 2012; Hall & Hall, 2020; Senior, 2010).

1.2 Components of the blood vessel wall

Variations in the functional and mechanical properties of the segments of the arterial tree result from the contributions of the different vessel wall components (Shadwick, 1999). The arterial wall consists primarily of cellular and extracellular matrix (ECM) components (Figure 1.1). The cellular components consist mainly of the vascular smooth muscle cells (VSMCs), the primary stromal cells of the vascular wall and the endothelial cells (ECs) (Shadwick, 1999). The ECM component of the vascular wall consists primarily of the connective tissues, collagen and elastin deposited by VSMCs that account for most of the mechanical properties of the arterial wall (Wagenseil & Mecham, 2009). Together, connective tissues, matrix fibers and cells of the arterial wall are organized into three tunics: intima, media, and adventitia (Figure 1.1) (Hassanisaber et al., 2019; Wagenseil & Mecham, 2007; Wagenseil & Mecham, 2009).

The intima is the innermost luminal layer of the arterial wall, extending from the lumen to the internal elastic lamina (a layer of elastic tissue that forms a boundary between the intimal and medial layers). It consists of a monolayer of ECs that lines the intimal luminal surface and rests on a thin subendothelial extracellular matrix and a basal layer of internal elastic lamina that separates the intima from the media (Halper, 2018; Wagenseil & Mecham, 2009).

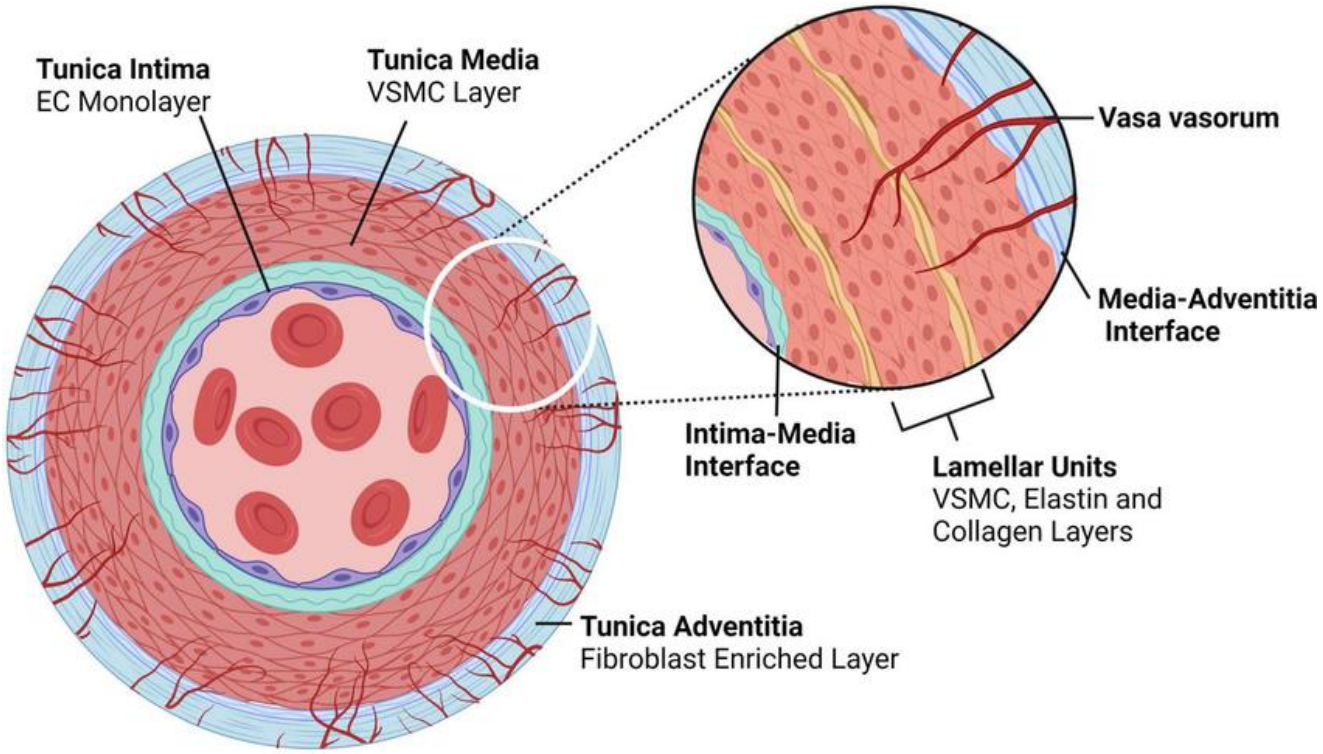

Figure 1.1 Schematic representation of the constituent component of the arterial wall. The arterial wall is composed of three main layers: the intima (internal), the media (middle), and the adventitia (external). Figure adapted from (Bax et al., 2022)

The tunica media consists of VSMCs embedded in highly organized elastin, collagen fibers and proteoglycans (Halper, 2018). The media is continuous from the internal to the external elastic lamina (a layer of elastic tissue that forms a boundary between the medial and adventitia layers).

The media is the chief determinant of arterial wall mechanical properties at physiological pressures (Halper, 2018). The adventitia extends from the external elastic lamina and forms the outermost layer of the vessel, usually contiguous with the perivascular connective tissue (Halper, 2018). Generally, adventitial cells are sparse and consist mainly of fibroblasts. The adventitia contains vasa vasorum (a network of microvessels that perfuses the vessel wall itself) providing nutrition to the adventitia and media, and nerves that contribute to regulating the medial smooth muscle function (Halper, 2018; Heistad & Marcus, 1979).

1.3 Structural and mechanical properties of the arterial wall

The transition from an open to a closed circulatory system in multicellular organisms required the development of mechanically efficient blood vessels that support blood flow. The walls of arteries are thicker, very elastic and muscular compared to the other vessels in the circulatory system (Tucker et al., 2017). This structural adaptation defines the mechanical properties of the arterial wall.

1.3.1 Arterial wall elasticity

The mechanical properties of the arterial wall serve as an essential determinant of hemodynamic functions (Humphrey, 1995). According to Hooke's law, elastic materials exhibit a linear relation between the applied force (stress) and the deformation (strain) due to the applied force (Mooney, 1940; Ugural & Fenster, 2011). The ratio of the stress/strain relationship, referred to as the modulus of elasticity, defines the elastic properties of the material (Mooney,

1940; Ugural & Fenster, 2011). However, arteries can be described as anisotropic tissues exhibiting viscous (or fluid-like) and elastic (or ideal solid-like) properties in a time-dependent manner (viscoelasticity) (Humphrey, 1995; Mooney, 1940). As a result, when arteries are subjected to deformation, there's a delay in the return to its original form once the applied stress is removed within its viscoelastic limit. Beyond the viscoelastic limit, arteries may deform and never return to their original form (plastic deformation). The viscoelastic property allows the arterial wall to store and dissipate mechanical energy (Bergel, 1960; Humphrey, 1995).

Compared with other blood vessels, the large arteries close to the heart have a high percentage of elastic tissues that allow them to stretch and accommodate the pulsatile pressure generated from the heart. As such, these arteries act as elastic reservoirs that enable them to undergo significant changes in volume with little changes in pressure, a phenomenon referred to as the Windkessel effect (Figure 1.2) (Silva et al., 2019; Westerhof et al., 2009). The Windkessel property allows arteries to store some portion of the stroke volume during each systole and release this volume during diastole, ensuring a more continuous flow of blood throughout circulation rather than the would-be pulsatile flow by the conversion of the stored elastic potential energy during systole into kinetic energy during diastole (Caro et al., 2012; Silva et al., 2019; Westerhof et al., 2009). The Windkessel effect also helps minimize the workload on the heart by reducing cardiac afterload (the pressure that the heart must work against to expel blood during systole) (Figure 1.2) (Kolh et al., 2000; Silva et al., 2019).

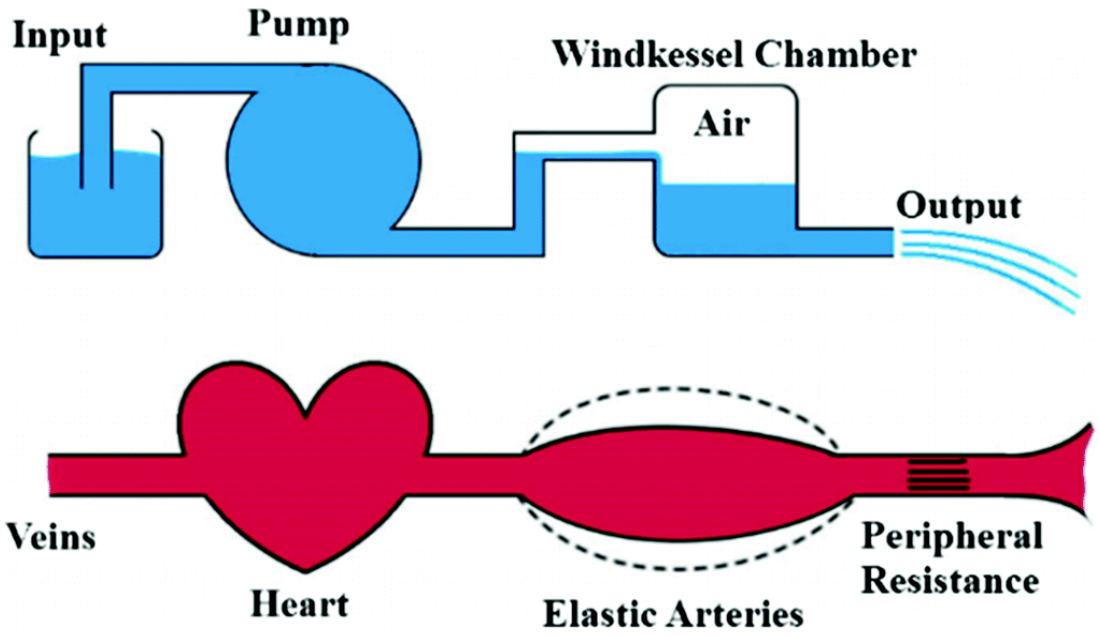

Figure 1.2 Schematic illustration of the elastic buffering property of the large elastic arteries compared to that of the Windkessel chamber. The Windkessel effect of large elastic artery compliance enables energy conversion between blood flow and the elastic vessel wall, while resistance arteries contribute to peripheral vascular resistance. Figure adapted with permission from (Silva et al., 2019)

1.3.2 Hemodynamic forces acting on the arterial wall.

Hemodynamic forces resulting from blood flow affect the structure and function of the arterial wall. The most relevant hemodynamic forces experienced by blood vessels are circumferential stress, axial stress and wall shear stress (Patel et al., 1974; Secomb, 2016). These forces are essential for the homeostasis of the arterial wall; changes in these forces can result in changes in vessel wall structure and function (remodeling) to normalize these forces (Patel et al., 1974; Secomb, 2016). Wall shear stress is defined as the tangential force exerted on the luminal surface of the blood vessel wall (Patel et al., 1974; Secomb, 2016), while axial stress refers to the force acting parallel to the vessel wall that governs length adaptations (Patel et al., 1974; Secomb, 2016). Circumferential stress on the other hand, is the force acting perpendicularly to the vessel wall (Patel et al., 1974; Secomb, 2016). The magnitude of circumferential stress acting on the arterial wall is determined by the diameter, blood pressure, and thickness of the vessel wall (Secomb, 2016).

For a given arterial segment, the circumferential wall stress can be related to the tension, blood pressure exerted on the vessel wall and the geometric properties (wall thickness, lumen diameter) of the vessel wall using Laplace's law. Laplace's law states that the tension (T) in a blood vessel wall is directly proportional to the radius (r) of the vessel lumen and the blood pressure (P) exerted by blood on the vessel wall; ($T = P * r$) (Humphrey, 1995; Secomb, 2016).

This implies that, for a given blood pressure, an increase in the radius of a blood vessel results in a linear rise in wall tension. Therefore, the large arteries close to the heart must have thicker walls to withstand the wall tension generated during systole compared to the smaller arteries in the periphery. Furthermore, the circumferential wall stress (σ) experienced in a particular segment of the arterial tree is proportional to the wall tension (T) but inversely

proportional to two times the wall thickness (h); ($\sigma = T/h = P*r/h$) (Humphrey, 1995; Secomb, 2016). As a result, a distension of the artery (increase in diameter) due to elevated blood pressure would subsequently result in vessel wall remodeling (increase in vessel wall thickness) in order to withstand the generated wall tension and keep the circumferential stress constant.

As blood is transported away from the heart to the various tissues, the large elastic arteries differentiate into more muscular arteries, which serve primarily as conduits for the transport of blood, having the ability to contract or relax to regulate the flow of blood to the various part of the body (Caro et al., 2012; Christensen & Mulvany, 2001; Senior, 2010). As the lumen diameter of the blood vessels decreases towards a particular organ in systemic circulation, the blood flow velocity also declines (Owen & Roberts, 2007).

The flow of blood throughout the arterial tree from the heart to the various tissues can be conceptualized as an electrical circuit based on Ohm's Law, where the voltage difference in the circuit (ΔV) is equal to the product of the current (I) and the resistance provided by the conductor to the flow of current (R); ($\Delta V = I * R$) (Owen & Roberts, 2007). Based on this analogy, the resistance to the flow of blood in systemic circulation can be defined as the ratio of the pressure difference between any two points along the length of the vessel (ΔP) to the flow rate of blood (Q) (Owen & Roberts, 2007).

More importantly, the resistance to blood flow in the arterial tree depends on the geometrical properties of the vessel wall (vessel length and diameter, which is influenced by the contractile state of the VSMCs) and the viscosity of blood (Owen & Roberts, 2007; Robertson & Watton, 2013). According to Poiseuille's law, the resistance (R) is directly proportional to the length (l) of the vessel and the viscosity (η) of the blood and inversely proportional to the radius of the fourth power (r^4); ($R = \frac{8\eta l}{\pi r^4}$), thus, slight alterations in arterial lumen diameter, either functional or

structural, result in significant changes in arterial resistance (Robertson & Watton, 2013; Schiffrin, 1992; Secomb, 2016).

1.3.3 Resistance arteries

Resistance arteries are segments of the arterial tree that regulate vascular resistance (Christensen & Mulvany, 2001). Resistance arteries provide blood to the microcirculation and are defined by the lumen diameter and the number of VSMC layers in the vessel wall (Intengan & Schiffrin, 2000; Segal, 2000). Resistance arteries consist of small arteries with two or more layers of VSMC and an internal diameter measuring between 100 μm to ≈500 μm in a relaxed state (values differ among authors) and arterioles with a single layer of VSMC with an internal diameter measuring < 100 μm that serves as a primary site for the generation of peripheral vascular resistance (Fronek & Zweifach, 1975; Intengan & Schiffrin, 2000; Segal, 2000; Segal & Duling, 1986)

1.3.4 Macro- and Microcirculation

Arteries can be further organized into macrocirculation and microcirculation based on their structure and function. Macrocirculation refers to the part of the arterial tree involved in pulsatile pressure and flow (Nichols et al., 2015; Safar & Struijker-Boudier, 2010). Macrocirculation consists of the proximal large elastic arteries (aorta) that function as a temporal buffer for blood during the ejection phase of the heart (Windkessel function), effectively reducing the load and ensuring a continuous blood flow during diastole (Christensen & Mulvany, 2001; Safar & Struijker-Boudier, 2010). In contrast, microcirculation refers to the part of the arterial tree involved with steady pressure and flow. The microcirculation is a segment of the vascular tree in which pulsations have almost completely dampened (Safar & Struijker-Boudier, 2010). Microcirculation contributes to total peripheral resistance (TPR) and plays a crucial role

in regulating blood pressure and the perfusion of the various tissues in the body. (Christensen & Mulvany, 2001; Safar & Struijker-Boudier, 2010). The relationship between TPR, mean arterial pressure (MAP), and cardiac output (CO) can be expressed mathematically as TPR = CO / MAP. As such, pathological conditions such as hypertension and subsequent vascular remodeling that leads to an increase in TPR would result in an elevation in mean arterial pressure.

1.3.5 Crosstalk between Macro- and Microcirculation

The different hemodynamic aspects of the arterial tree can be attributed to the considerable heterogeneity in the structure and function of the different segments of the arterial wall. A crosstalk is suggested to exist between the macrocirculation and the microcirculation, where changes in large artery structure and elasticity influences the structure and function of the smaller arteries and arterioles while modifications in the small arteries and arterioles affect the structure and function of the large arteries. (Nichols et al., 2015; Safar & Struijker-Boudier, 2010).

The structure and function of the small arteries are a significant determinant of TPR. In pathological conditions, alterations in the structure and function of the small arteries result in an increased MAP and structural remodeling of the large elastic arteries (Nichols et al., 2015; Safar & Struijker-Boudier, 2010). Insidiously, the elevated MAP results in large artery stiffening and subsequent remodeling of the small resistance arteries, further increasing TPR and MAP (Nichols et al., 2015; Safar & Struijker-Boudier, 2010).

The crosstalk between macro- and microcirculation results from the relationship between the pulsatile pressure and flow experienced in the large elastic arteries and the impedance to blood flow characteristic of the resistance arteries. During systole, ventricular ejection of blood into the aorta and large arteries generates a pressure waveform that propagates along the entire

length of the arterial tree. The pressure waveform consists of a forward-travelling component resulting from ventricular ejection and a backward wave reflected off peripheral arteries at the branching origins of arterioles. The velocity at which the pressure waveform propagates through the arterial tree is referred to as pulse wave velocity (PWV). The Windkessel property characteristic of the large elastic arteries of macrocirculation serves to effectively buffer the pulsatile flow of blood and regulate the transmission and timing of both the forward and reflected pressure wave (Safar & Struijker-Boudier, 2010). Furthermore, the resistance arteries of microcirculation serve as an important site for the reflection of the forward wave (Safar & Struijker-Boudier, 2010). Hence, a combination of large artery stiffness and changes in the geometry, structure and function of resistance arteries results in an elevated PWV and a return of the reflected wave during mid-to-late systole (Laurent et al., 2019; Nichols et al., 2015). The effect of this interaction is an augmentation of systolic pressure and an increase in pulse pressure due to a decrease in diastolic pressure (Nichols et al., 2015; Safar et al., 2009).

1.4 Structural component of the arterial wall

The structural components of the arterial wall, primarily collagen and elastin deposited in the medial layer by VSMCs, account for the passive mechanical properties of the arterial wall (Wagenseil & Mecham, 2009). Along with VSMCs, the structural component of the arterial wall determines the blood vessel's viscoelastic properties (ability to exhibit both elastic and viscous behavior when deformed) (Bergel, 1960).

The distensibility of the arterial wall is mainly determined by its elastin component (Baltgaile, 2012; Wagenseil & Mecham, 2009). Woven into a three-dimensional interconnected lamellar network, elastin behaves mechanically as though it were composed of long, extensive, independent chains that allow it to transfer stress throughout the vessel wall (Gundiah et al.,

2009). Elastogenesis, the production of elastin, occurs within a narrow timeframe (from fetal life to the end of adolescence), while elastin lasts for the entire lifespan (Cocciolone et al., 2018). In the arterial wall, elastin is produced by VSMCs; however, under pathological conditions, ECs and fibroblasts make elastin in response to increased stress on the vessel wall (Xu & Shi, 2014). Elastin is produced from the precursor-soluble tropoelastin (Eoh et al., 2017). The final product is a complex elastic fiber that consists of elastin and microfibrils (Eoh et al., 2017). The expression of the tropoelastin gene is regulated in response to different growth factors, cytokines and bioactive molecules (Eoh et al., 2017; Yue, 2014).

In addition to its structural and mechanical role, elastin also regulates the proliferation and migration of VSMCs (Brooke et al., 2003). Its mechanical properties and ability to regulate the proliferation of VSMCs make elastin an integral component of the arterial wall. However, despite the longevity of elastin in the vascular wall, repair or replacement of elastin during injury, stress or age-related calcification is incomplete because elastin expression is switched off in adults. Instead, the arterial wall shifts to producing stiff collagen fibers to maintain the integrity of the vessel wall (Wagenseil & Mecham, 2012; Xu & Shi, 2014).

Collagen is a fibrous protein that contributes to vessel mechanics primarily at larger distension (higher pressures) (Shadwick, 1999). Collagen fibers are suggested to be only minimally engaged at low pressures, while more collagen fibers are recruited to maintain the wall tension as the vessel becomes more distensible at higher pressures (Shadwick, 1999; Sokolis et al., 2006). The collagen family consists of different subtypes, and at least 13 different subtypes are present in the vascular wall (Malfait, 2018). The expression of collagen depends on the region of the vascular tree being investigated (Malfait, 2018; Myllyharju & Kivirikko, 2001; Wagenseil & Mecham, 2009). Collagen biosynthesis by VSMCs, fibroblasts and ECs is a

complex process involving intracellular collagen synthesis and an extracellular maturation of collagen into collagen fibers, with the different collagen molecules having the ability to form other classes of collagen based on their macromolecular properties (Malfait, 2018; Plant et al., 2009). Like elastin, collagen interacts with the various vascular cells, providing cues for maintaining the vessel wall function.

1.5 The vascular endothelium

The vascular endothelium consists of a single layer of ECs that lines the inner walls of the vasculature (Figure 1.1) (Krüger-Genge et al., 2019). The ECs form the inner lining of the arteries, veins and capillaries and are in direct contact with the components and cells of the blood (Sumpio et al., 2002). The endothelium is not just a barrier but also serves as an endocrine and paracrine organ modulating the function of the underlying blood vessel components and regulating blood circulation (Krüger-Genge et al., 2019; Sumpio et al., 2002). The vascular endothelium is separated from the underlying cell components by a basal lamina (a thin layer of ECM proteins), and together, both the ECs and basal lamina constitute the intima of the vessel wall anchored to a basement membrane (Krüger-Genge et al., 2019; Sumpio et al., 2002).

The subendothelial basement membrane (BM) not only serves as the foundation to which ECs attach but is also the tissue compartment boundary between the endothelium and vascular connective tissue (Eble & Niland, 2009). The ECs are, therefore, luminal cells with a luminal membrane exposed to the circulating blood while their basolateral surface is anchored to the basal lamina (Eble & Niland, 2009; Krüger-Genge et al., 2019). The ECs are oriented along the axis of the vessel wall in order to minimize the forces exerted by circulating blood (Campinho et al., 2020). ECs have many functions specific to their location and show considerable phenotypic heterogeneity across the vascular bed (Aird, 2007). The endothelium actively controls the degree

of vascular relaxation and constriction and the extravasation of solutes, fluids, hormones and macromolecules from platelets and blood cells (Krüger-Genge et al., 2019). In addition, ECs actively repress the intermediate VSMCs in the underlying tunica media to prevent outgrowth into the tunica-intima layer and interfere with normal vascular function (Adams & Alitalo, 2007; Krüger-Genge et al., 2019).

1.6 Vascular smooth muscle cells

The VSMCs are an essential component of the blood vessel wall. They are located in the tunica media of blood vessels (Figure 1.1) (Bacakova et al., 2018) and chiefly regulate the diameter of the vessel wall lumen through contraction and relaxation (Bacakova et al., 2018; Brozovich et al., 2016). The contractile and relaxation mechanism of the VSMCs are regulated by neural innervation from the autonomic nervous system in addition to various hormones, autocrine and paracrine agents from the vascular endothelium and other local chemical and physical stimuli (Brozovich et al., 2016; Busse et al., 1985; Walsh et al., 1995). VSMCs predominantly display a contractile phenotype in the vessel wall, allowing them to maintain vascular tone and contribute to viscoelastic properties (Matsumoto et al., 2016; Williams, 1998). However, VSMCs can also undergo phenotypic switching a phenomenon that enables VSMCs to differentiate into a synthetic phenotype (exhibiting high proliferative and migratory traits) characteristic of arterial remodeling in pathological states (Lacolley et al., 2012; Sorokin et al., 2020).

The contraction of VSMC can be initiated by a mechanical, electrical, or chemical stimulus (Belik & Stephens, 1993; Brozovich et al., 2016; Busse et al., 1985; Yang et al., 2003). Furthermore, passive stretching in response to changes in load or length results in contractions originating from the VSMC itself, which is referred to as a myogenic response (Davis & Hill,

1999; Yang et al., 2003). Myogenic response is a distinctive feature of resistance arteries in regulating blood flow (Jackson, 2021). Regardless of the stimulus, VSMCs use cross-bridge coupling between actin and myosin filaments to develop the force for contracting, while intracellular Ca^{2+} initiates the contraction (Webb, 2003). The mechanism of contraction and relaxation of VSMCs involves different signal transduction pathways specific to the stimulus applied (Althoff & Offermanns, 2015; Webb, 2003). Contraction results from an increase in intracellular Ca^{2+} due to either the influx of Ca^{2+} into the cell via calcium channels, or the release of Ca^{2+} into the cytosol from the internal Ca^{2+} stores. The free Ca^{2+} binds to calmodulin (a unique calcium-binding protein) (Rembold, 1992; Webb, 2003). The calcium-calmodulin complex then activates the myosin light chain kinase, an enzyme that phosphorylates the myosin light chains in the presence of adenosine triphosphate (ATP). In contrast, myosin light chain (MLC) can be activated independently of calcium through the RhoA-Rho kinase (ROCK) signaling pathway (Puetz et al., 2009). The phosphorylation of the myosin light chain leads to cross-bridge formation between the myosin heads and actin filaments, causing smooth muscle contraction (Webb, 2003). VSMC relaxation occurs by a reduction in MLC phosphorylation by halting the release of Ca^{2+} by the SR or reduced Ca^{2+} entry into the cytosol, inhibition of myosin light chain kinase (MLCK) action and the activation of myosin light chain phosphatase (MLCP), which dephosphorylates MLC (Rembold, 1992; Webb, 2003).

1.7 Control of Vascular Tone

Vascular tone is an essential factor that contributes to the vessel wall's mechanics. It refers to the degree of constriction or relaxation experienced by the vessel wall related to its maximally dilated state (Bevan & Laher, 1991; Davis et al., 2023; Johansson, 1989). Vascular tone is primarily determined by the balance of competing vasoconstrictor and vasodilator

influences on the underlying VSMCs (Davis & Hill, 1999). In resistance arteries and arterioles, the arterial tone contributes to total peripheral resistance, a major determinant of blood pressure that regulates tissue blood flow (Jackson, 2017; Magder, 2018; Schiffrin, 2020).

The vasoactive factors influencing vascular tone can be grouped into extrinsic and intrinsic factors. The extrinsic vasoactive factors originate from outside the blood vessel or surrounding tissues and modulate blood pressure by altering the total peripheral resistance (Edis & Shepherd, 1970). Intrinsic vasoactive factors arise from the vessel wall and are involved in local blood flow regulation (Hill & Davis, 2012; Sandoo et al., 2010).

Extrinsic or neurohumoral factors include neurotransmitters and peptides (Ball, 1989). Intrinsic factors include endothelial factors (originating from the endothelium), myogenic responses from VSMC stretch, metabolic factors and local hormones or chemicals (Hansen et al., 1998). The mechanisms by which extrinsic and intrinsic factors influence vascular tone involve diverse signal transduction mechanisms that ultimately affect the interaction between actin and myosin in the VSMC contraction or relaxation (Edwards, 2013; Orshal & Khalil, 2004). This mechanism primarily consists of a signal transduction triad (receptor-transducer-effector) and the various second messengers involving calcium, adenylate and guanylate cyclases (cAMP and cGMP), inositol 1,4,5 trisphosphate (IP3), diacylglycerol (DAG) and phospholipases (Althoff & Offermanns, 2015; Lincoln et al., 2001; Touyz & Schiffrin, 2000). The primary signal transduction pathway in regulating vascular tone is through G protein-coupled receptors (GPCRs), an integral membrane proteins used by cells to convert extracellular signals into intracellular responses (Chachisvilis et al., 2006; Nobles et al., 2005; Vögler et al., 2008).

In the vascular system, GPCRs are associated with heteromeric G proteins with alpha (Gα), beta (Gβ) and Gamma (G γ) subunits (Kaur et al., 2023; Penela et al., 2006; Vögler et al.,

2008). The activity of GPCR is regulated by an active (GTP) or inactive (GDP) state (Vögler et al., 2008). Activation of the GPCR interacts with various downstream enzymes and channels that regulate intracellular second messengers catalyzed by their α subunits: $G\alpha_s$, $G\alpha_i$ and $G\alpha_q$ or $G\alpha_o$ (Kaur et al., 2023; Martins et al.; Nobles et al., 2005; Penela et al., 2006).

1.7.1 Sympathetic regulation of vascular tone

Neurogenic control of vascular tone and blood pressure plays a role in maintaining vascular homeostasis. In particular, the sympathetic nervous system (SNS) modulates vascular tone primarily by inducing vasoconstriction (Bruno et al., 2012; Sheng & Zhu, 2018). In pathophysiological conditions, sympathetic nerve overactivity results in elevated vasoconstriction and increased vascular tone, which affects blood pressure and vessel wall mechanics, promoting arterial remodeling (Byrne et al., 2018; Masi et al., 2019; Sauzeau et al., 2006). Neurogenic control of vascular tone involves neurotransmitters that act on membrane-bound receptors expressed by VSMCs and endothelial cells to evoke changes in cellular function (Sheng & Zhu, 2018). Vascular sympathetic neurotransmitter activation of the Gq protein subunit of the GPCR signal transduction pathway stimulates the release of Ca^{2+} from intracellular Ca^{2+} stores mediated by IP3 and Ca^{2+} efflux into the cell via calcium channels (Cooper & Dimri, 2021; Masi et al., 2019). Increasing Ca^{2+} activates Rhokinase, an enzyme that inhibits myosin light chain phosphatase, resulting in smooth muscle contraction (Cooper & Dimri, 2021; Masi et al., 2019; Perez-Zoghbi et al., 2009; Taylor & Cassagnol, 2022).

Furthermore, activation of the Gi protein subunit by sympathetic neurotransmitters such as norepinephrine or the synthetic catecholamines, including phenylephrine, inhibits adenyl cyclase activity, causing a decrease in cAMP (which inhibits MLCK), increasing MLC phosphorylation and constricting the VSMCs (Cooper & Dimri, 2021; Gao, 2022; Masi et al.,

2019; Nausch et al., 2012). On the other hand, activation of the Gs protein subunit by neurotransmitters stimulates adenyl cyclase activity, leading to increased levels of cAMP, which inhibits MLCK activity, reducing MLC phosphorylation and relaxing VSMCs (Cooper & Dimri, 2021; Masi et al., 2019).

1.7.2 Endothelial regulation of vascular tone

The vascular endothelium plays a vital role in the local regulation of vascular homeostasis. The endothelium contributes to the control of vascular tone and blood pressure via the release of paracrine signaling molecules to the underlying VSMC that generally act to attenuate vascular contraction and promote vasorelaxation (Cooke, 2000; Krüger-Genge et al., 2019). A healthy endothelium maintains a balance between vasodilation and vasoconstriction by the production of several vasoactive factors including vasorelaxing factors such as nitric oxide (NO), prostacyclin (PGI2), endothelium-derived hyperpolarizing factor (EDHF) as well as vasoconstrictors including endothelin (ET-1) (Cooke, 2000; Krüger-Genge et al., 2019). However, there is a switch in pathophysiological conditions, from a decreased vasoconstrictor response to an increased vasoconstrictor response and a reduced vasodilator production with endothelial dysfunction (Böhm & Pernow, 2007; Daiber et al., 2017; Münzel et al., 1997; Yannoutsos et al., 2014). As such, the endothelium can elicit vasoconstrictor and vasodilator effects that regulate the vascular tone (Rubanyi, 1991). The primary mechanisms in which the endothelium relaxes the blood vessels involve endothelium-derived relaxing factor (EDRF) nitric oxide activation of guanyl cyclase and EDHF (Bauer & Sotníková, 2010; Cohen & Vanhoutte, 1995; Stankevičius et al., 2003). These endothelial-derived vasoactive factors are produced in response to physical stimuli such as shear stress, neurotransmitters, hormones, and products from metabolism (Inagami et al., 1995; Noori et al., 2007).

1.7.2.1 *Endothelium-Derived Relaxation Factor*

The EDRF is an endogenous vasodilator produced by vascular ECs in response to a number of vessel wall stresses and chemical stimuli (Inagami et al., 1995; Noori et al., 2007). Structurally, EDRF is in the form of NO or a compound containing nitric oxide (Myers et al., 1990). NO is produced from the amino acid arginine by the enzymatic action of nitric oxide synthase (NOS), which is dependent on calcium, calmodulin and nicotinamide adenine dinucleotide phosphate (NADPH) (Gough, 2008; Myers et al., 1990; Pirahanchi et al., 2019; Snyder & Bredt, 1992). Exogenous NO can also be obtained from the organic sodium salt, (e.g., sodium nitroprusside), which reacts with sulfhydryl-containing molecules to produce NO (Holme & Sharman, 2020). There are two endothelial isoforms of NOS, the constitutive NOS (cNOS) and the inducible NOS (iNOS), both of which can be inhibited by arginine analogues, such as L-NAME (used in this thesis) (Griffith & Stuehr, 1995; Pirahanchi et al., 2019). The NO produced diffuses into the underlying VSMC, exerting paracrine effects by activating guanyl cyclase, which catalyzes GTP's dephosphorylation to cGMP. Intracellular cGMP induces smooth muscle relaxation by decreasing intracellular Ca2+ concentration, activating potassium channel hyperpolarization of VSMC and stimulating cGMP-dependent protein kinase that activates myosin light chain phosphatase (Griffith & Stuehr, 1995; Noori et al., 2007; Pirahanchi et al., 2019).

1.7.2.2 *Endothelial-derived hyperpolarisation Factor*

The EDHF is another endothelium relaxation factor. EDHF is suggested to cause vasorelaxation via VSMC hyperpolarization by activating the ATP-sensitive potassium channels and sodium-potassium ATPase in VSMC (Busse et al., 2002; Garland et al., 2011).

EDHF is not affected by inhibitors of NO synthase. However, its effects can be blocked by agents that target K channels (Doughty et al., 1999; Lacy et al., 2000; Ozkor & Quyyumi, 2011). The generally adopted pathway for EDHF to act on VSMC includes: (1) an endothelial-derived diffusible substance that crosses the internal elastic lamina into the underlying VSMC and activates various ion channels to cause vasorelaxation, and (2) an electrical event that involves contact-mediated mechanisms that primarily spreads endothelial hyperpolarization to VSMC through inter-cellular coupling (Busse et al., 2002; Félétou & Vanhoutte, 2004; Garland et al., 2011). A combination of ouabain and $BaCl_2$ used in this thesis is known to block EDHF effects in the vascular system (Van de Voorde & Vanheel, 2000).

Several phenomena have been suggested to trigger EDHF, including:

I. Synthesis of cytochrome P450 (CYP450) metabolites,
II. Transmission of endothelial cell hyperpolarization factors to VSMC via gap junctions
III. K^+ derived from endothelial calcium-activated potassium channels that activate electrogenic Na^+–K^+-ATPase followed by hyperpolarization and smooth muscle cell relaxation.

1.7.2.3 *The Endothelial Cyclooxygenase Pathway*

The endothelial cyclooxygenase pathway involves cyclooxygenase enzymes that form part of the metabolic cascade that converts arachidonic acid into a range of prostanoid lipid mediators that cause either vasorelaxation or vasoconstriction of the underlying VSMCs (Cipollone et al., 2008; Luo et al., 2016). Prostanoids are fatty acid compounds derived from membrane phospholipids primarily in homeostasis and during inflammation but are also involved in modulating vascular tone (Luo et al., 2016; Stables & Gilroy, 2011). Endogenous arachidonic acid-derived phospholipase A2 breakdown of phospholipids results in three

important metabolic pathways; the cyclooxygenase (COX) pathway, where arachidonic acid is metabolized by (COX) 1 and 2 into prostaglandins (PGs) and thromboxane (TX), (inhibited by nonsteroidal anti-inflammatory drugs (NSAIDs) (Mitchell et al., 2021; Sanchez et al., 2010; Zewde & Mattson, 2004), the lipooxygenase pathway where arachidonic acid is metabolized by lipooxygenase to leukotrienes (which can be blocked by inhibitors of lipoxygenase) (Pfister, 2011; Sasaki et al., 1997) and, by multiple cytochrome P450 enzymes to produce epoxides and hydroxyeicosatetraenoic acids (which can be blocked by inhibitors of cytochrome P450) (Chen & Cheung, 1996; Ozkor & Quyyumi, 2011; Zygmunt et al., 1996).

In the vascular endothelium, prostacyclin is the primary by-product of arachidonic acid metabolism (Stables & Gilroy, 2011). Prostacyclin increases cAMP in VSMC via the Gs-protein pathway, causing vasorelaxation (Orie & Clapp, 2011; Tanaka et al., 2004; Yang et al., 2010). In platelets, VSMCs and leukocytes, the production of thromboxane, prostaglandin, and leukotrienes such as LTC4, respectively, acts as potent vasoconstrictors acting through the Gq - protein pathway of the GPCR signal transduction (Malmsten, 1986; Yamaguchi et al., 2022). The cyclooxygenase pathway is also a source of superoxide anions, which modulate endothelium-dependent increase in vascular tone by the breakdown of nitric oxide or by the direct effects on VSMC constriction (Katusic, 1996; Lüscher & Tanner, 1993; Versari et al., 2009b).

1.7.2.4 *Endothelin*

Endothelin (ET-1) is a 21-amino acid peptide produced by the vascular endothelium from an amino acid precursor through the actions of an endothelin-converting enzyme (ECE) located on the EC membrane (Davenport et al., 2016). The formation and release of ET-1 is triggered by angiotensin II, antidiuretic hormone, thrombin, cytokines, reactive oxygen species, and shear

forces acting on the vascular endothelium (Davenport et al., 2016; Marasciulo et al., 2006). In contrast, the release of ET-1 is inhibited by prostacyclin, atrial natriuretic peptide, and NO (Kuchan & Frangos, 1993; Marasciulo et al., 2006). Once ET-1 is produced, it binds to receptors on the target tissues (Marasciulo et al., 2006). There are two basic types of ET-1 receptors: ETA and ETB. Both receptors are coupled to a Gq protein and the formation of IP3, which causes Ca^{2+} release from the sarcoplasmic reticulum and subsequent VSMC contraction (Gomez Sandoval et al., 2014; Marasciulo et al., 2006). In addition to ETA and ETB receptors found on VSMCs, there are also ETB receptors on the endothelium (Gomez Sandoval et al., 2014). Under normal conditions, the ETA receptor is the dominant receptor in eliciting ET-1 VSMC contraction in blood vessels (Gomez Sandoval et al., 2014; Pollock et al., 1995). However, binding of ET-1 to endothelial ETB receptors stimulates NO formation, which causes vasodilation in the absence of VSMC ETA and ETB activation (Eguchi et al., 1993; Luscher & Barton, 2000).

1.7.3 Ion Channels

Ion channels in the plasma membrane of vascular cells, primarily VSMC, play an important role in regulating vascular tone and the resistance to blood flow. The various vasoconstrictor and vasodilator stimuli that modulate the contractile responses of VSMC elicit their effects on ion channels; hence, ion channels are involved in all aspects of generating and regulating vascular tone (Figure 1.3). The cell membrane is permeable to several ions, the most important of which are involved in regulating vascular tone are Na^+, K^+, Ca^{2+} and Cl^- (Jackson, 2000; Morgado et al., 2012; Nilius & Droogmans, 2001; Tykocki et al., 2017). The movement of ions across the cell membrane is facilitated by specific gated ion channels, which open when

activated and are closed in an inactive state (Alberts et al., 2002; Unwin, 1989). These channels open and close in response to various stimuli, including membrane voltage changes (voltage-gated channels), ligand activation of receptors (receptor-gated channels), specific ions, chemical ligands and physical stress (Adams et al., 1989; Jackson, 2000; Nilius & Droogmans, 2001; Unwin, 1989). In endothelial cells, the activation of ion channels by agonists and mechanical forces are responsible for the mechanosensing and vasoregulatory properties of the vascular wall (Cheng et al., 2019; Nilius & Droogmans, 2001). Movement of ions across these gated channels results in changes to the electrical conductance and intracellular signaling mechanisms that regulate the contractile state of VSMCs, which is dependent on the complex interplay of vasodilator and vasoconstrictor stimuli (Adams et al., 1989; Alberts et al., 2002; Jackson, 2000; Unwin, 1989). The stimuli input modulates the activity of the ion channels that control membrane potential and the magnitude of intracellular ion concentration. Among the many ion channels, calcium channels, potassium channels, and chloride channels are selective ion channels expressed by VSMC and ECs, along with the recently discovered nonselective cation channel, Piezo 1, fundamental to transducing mechanical force, establishing membrane potential, and regulating vascular tone.

1.7.3.1 *Calcium channels*

Calcium ions play an essential role in the contraction of VSMC. Elevated intracellular Ca^{2+} due to the influx of Ca^{2+} through the cell membrane and its release from intracellular stores determines the degree of vasoconstriction (Figure 1.3) (Jackson, 2000; Ottolini et al., 2019). In endothelial cells, the influx of Ca^{2+} through calcium channels is crucial for the synthesis and release of various vasoactive substances that modulate vascular tone (Cheng et al., 2019; Nilius & Droogmans, 2001).VSMC expresses different types of calcium channels (Ghosh et al., 2017;

Hughes, 1995). Primarily, voltage-gated calcium channels of the plasma membrane serve as the primary source of extracellular Ca^{2+} in response to changes in cell membrane potential. Calcium channels are comprised of a family of structurally related proteins (Cribbs, 2001; Hughes, 1995). They are classified as either high voltage-activated (HVA) or low voltage-activated (LVA) and can be further subdivided based on their pharmacological properties (Cribbs, 2001; Hughes, 1995). HVA channels include L, N, P/Q, and R types, and LVA channels are referred to as T type (Cribbs, 2001; Ghosh et al., 2017; Hughes, 1995). The L-type calcium channels are a family of structurally related proteins that exhibit tissue-specific expression and are the primary calcium channels that serve as classic targets of calcium channel blockers (CCBs) (Eid et al., 2018; Ghosh et al., 2017). CCBs including verapamil (used as pharmacological agent that blocks the L-type calcium channels in this thesis), diltiazem and nifedipine exhibit vasodiloatory properties by the inhibition of Ca^{2+} influx through calcium channels (Achike & Dai, 1990; Ashida et al., 1991; Katz et al., 1985). The T type, along with other calcium channels including store and stretch-operated calcium channels further contribute to the intracellular Ca^{2+} concentration in vascular injury and pathological conditions (Ghosh et al., 2017; Hughes, 1995; Iftinca, 2011; Laher & Van Breemen, 2012; Morgado et al., 2012; Touyz et al., 2018; Wynne et al., 2009; Zamponi et al., 2015).

1.7.3.2 *Potassium Channels*

Potassium channels are the dominant ion conductive pathway in VSMC (Beech, 2007). Potassium channels serve as a critical regulator of vascular tone by regulating the membrane potential (Figure 1.3) (Beech, 2007; Dogan et al., 2019). As a result of the electrochemical gradient of potassium ions, the opening of potassium channels results in the efflux of potassium ions out of the cell (Dogan et al., 2019; Jackson, 2017). As such, the activation of potassium

channels leads to membrane hyperpolarization and subsequent vasodilation, while inhibiting the channel with potassium channel blockers such as Tetraethylammonium chloride (TEA) results in membrane depolarization and subsequent vasoconstriction (Dogan et al., 2019; O'Rourke, 1996). Different types of potassium channels are expressed in the VSMC, i.e. calcium-activated potassium (KCa), voltage-gated potassium channels (VGKC), ATP-sensitive potassium channels (KATP), inward rectifier potassium channels (Kir) and tandem two-pore k channels (K2P) (Dogan et al., 2019; Jackson, 2017; Kshatri et al., 2018; López-López et al., 2018). The activity and expression of potassium channels are altered in severe vascular diseases such as hypertension (Mandegar et al., 2002; Sobey, 2001). Increased potassium channel function and expression are suggested to help avert increased abnormal vascular tone (Jackson, 2017; López-López et al., 2018). A malfunction of potassium channels is often associated with impaired vascular responses, likely resulting in potassium ion dysregulation in vascular diseases (Dogan et al., 2019; López-López et al., 2018).

1.7.3.3 *Chloride Channels*

Chloride ions and transporters have been proposed to regulate vascular tone by modulating the membrane potential of vascular cells (Hübner et al., 2015; Li et al., 2009). In the VSMC, the electrochemical gradient for chloride is such that opening chloride channels results in the efflux of chloride from the cell, thereby triggering vasoconstriction (Goto & Kitazono, 2022; Hübner et al., 2015). In contrast, inhibition of chloride channels by chloride channel blockers such as indanyloxyacetic acid (IAA-94) and 4,4'-diisothiocyanatostilbene-2,2'-disulphonic acid (DIDS) leads to hyperpolarization and VSMC relaxation (Goto & Kitazono, 2022; Hübner et al., 2015; Li et al., 2009; Nelson et al., 1997). VSMC expresses two types of chloride channels, i.e. calcium-activated chloride channels (CaCCs) and volume-regulated chloride channels (CLVR)

(Almohanna, 2019; Goto & Kitazono, 2022). CaCCs are activated by an elevation in intracellular Ca^{2+} due to the actions of various vasoconstrictors and are involved in the depolarization associated with vasoconstrictor-induced vascular tone (Goto & Kitazono, 2022; Hübner et al., 2015). An upregulation of CaCC channels contributes to increased vascular contractility and elevated blood pressure associated with hypertension (Hübner et al., 2015; Li et al., 2009).

1.7.3.4 *Piezo 1 ion channel*

Piezo 1 ion channels are nonselective mechanosensitive ion channels required for early vascular development, and their expression persists in both VSMC and ECs of resistance arteries (Davies & Tripathi, 1993; Kefauver et al., 2020; Volkers et al., 2015). They are a class of mechanosensory membrane proteins that act as molecular transducers of mechanical stimuli on a microsecond time scale (earliest cellular events of vascular mechanotransduction) and convert them into intracellular biochemical signals, allowing the movement of ions and solutes across the cell membrane when they are open (Davies & Tripathi, 1993; Kefauver et al., 2020). The Piezo family of mechanosensitive ion channels consists of two members, Piezo1 and Piezo 2 (Beech & Kalli, 2019; Douguet et al., 2019). Piezo 1 is primarily expressed in peripheral tissues, including endothelial cells and VSMCs and plays a crucial role in vascular development and homeostasis (Beech & Kalli, 2019; Douguet et al., 2019). Piezo 2 is suggested to be predominantly expressed in mechanosensory neurons involved in the senses of touch, hearing, and proprioception (Beech & Kalli, 2019; Douguet et al., 2019).

Piezo 1 activation is thought to be involved in the modulation of the myogenic and trophic effects of the vessel wall (Endesh, 2018; Garcia Robledo MD, 2019; Robledo, 2019). The activation of Piezo 1 channels by stretch or shear stress is suggested to cause the movement of ions, primarily Ca^{2+}, across the cell membrane. Furthermore, Piezo 1 can be activated by

pharmacological modulators such as Yoda 1 (used in this thesis), Jedi 1 and Jedi 2, as well as inhibited by antagonists such as Dooku 1 and the peptide toxin Grammostola mechanotoxin #4 (GsMTx-4) from Grammostola spatulata spider venom (used in this thesis) (Douguet et al., 2019). The result is the induction of cell depolarization, hyperpolarization or contraction due to the elevation of intracellular Ca^{2+} depending on the particular vascular cells involved (Davies & Tripathi, 1993; Kefauver et al., 2020; Nourse & Pathak, 2017; Volkers et al., 2015). The vasoactive effects of Piezo 1 channels depend on its location within the vascular wall. In ECs, Piezo 1 channels play an important role in sensing and responding to shear stress by triggering the increase in intracellular Ca^{2+} concentration, leading to activating the calmodulin-binding domain of eNOS and the production of endothelial-derived relaxation factors (EDRF) that relaxes the underlying VSMCs (Garcia Robledo MD, 2019; Volkers et al., 2015; Wang et al., 2021). However, the increase in intracellular Ca^{2+} in VSMC stimulates VSMC contraction as the calcium-calmodulin complex activates myosin light chains kinase that increases the tone of the vessel wall in response to the stretch (Wang et al., 2021). Furthermore, a likely efflux of K^+ from VSMC due to the activation of VSMC-Piezo 1 channels would result in hyperpolarization and relaxation of the VSMCs (Touyz, 2005; Touyz et al., 2018).

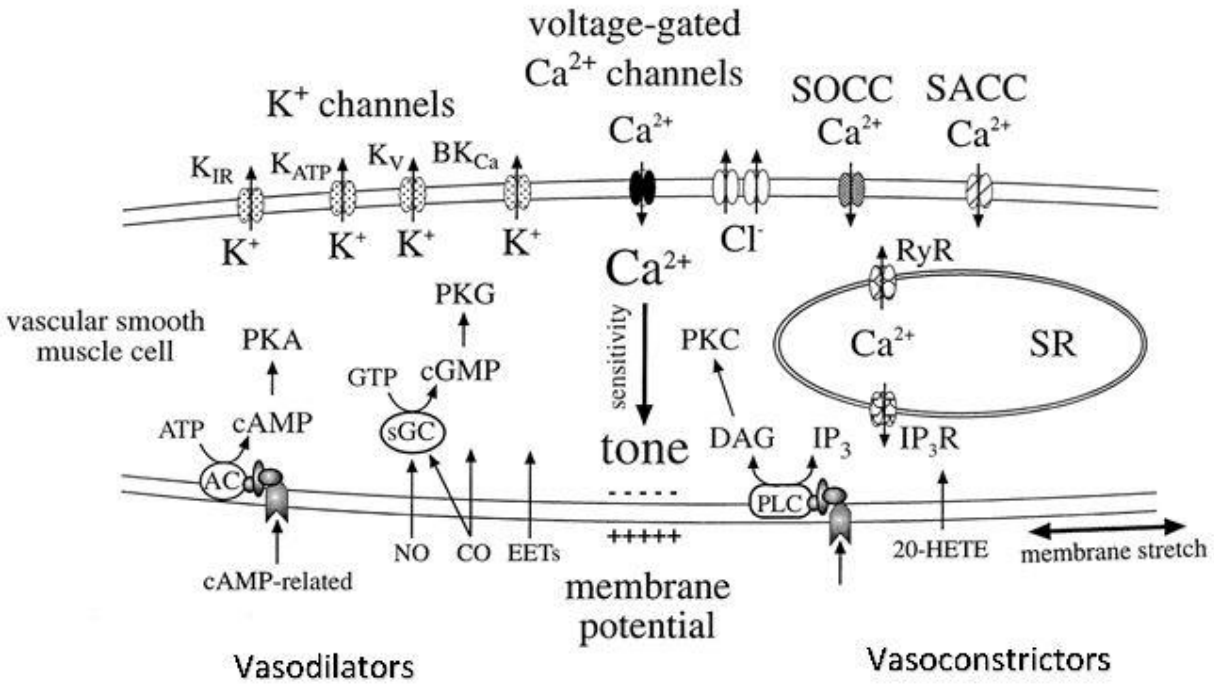

Figure 1.3 Contributions of the various ion channels to the regulation of vascular tone. Schematic of a cross-section through part of a vascular muscle cell. KIR, KATP, KV, and BKCa channels are shown along the top membrane. Also shown are voltage-gated Ca^{2+} channels, 2 types of Cl^{-} channels, SOC channels (SOCC), and SAC channels (SACC). Shown in the membranes of the sarcoplasmic reticulum (SR) are ryanodine receptors (RyR) and inositol 1,4,5-trisphosphate receptors (IP3R). AC indicates adenylate cyclase; PKA, cAMP-dependent protein kinase; sGC, soluble guanylate cyclase; PKG, cGMP-dependent protein kinase; EETs, epoxyeicostetraenoic acid (epoxides of arachidonic acid); PLC,phospholipase C; DAG,diacylglycerol; PKC=protein kinase C; and 20-HETE, 20-OH-arachidonic acid. Figure adapted with permission from (Jackson, 2000).

1.8 Arterial stiffness and remodeling

A critical factor in the evolutionary transition from an open to a closed circulatory system was the change in the vessel wall's structure and composition, which enabled the large elastic arteries to store and release energy during the cardiac cycle (Camasão & Mantovani, 2021; Levick, 2013). The Windkessel effect of the large elastic arteries reduces the pressure load on the heart during systole. It also ensures a continuous, steady flow of blood in the periphery to the various organs rather than the characteristic pulsatile flow of blood in the absence of this property (Camasão & Mantovani, 2021; Laurent & Boutouyrie, 2015; Levick, 2013).

Resistance arteries, on the other hand, play an essential role in controlling blood flow to the various organs in the periphery. While resistance arteries are smaller in size and lumen diameter compared to large elastic arteries, changes in the lumen diameter of the resistance arteries can significantly result in changes in TPR, an essential determinant of blood pressure (Camasão & Mantovani, 2021; Laurent & Boutouyrie, 2015). The differences in the mechanism, structure and function of these different components of the vascular bed result from the considerable heterogeneity in the vessel wall components (Levick, 2013; Xu & Shi, 2014).

The Windkessel property of the large elastic arteries results from the predominant elastic component of the arterial wall, enabling it to distend with changing pressure (Bank & Kaiser, 2002; Shadwick, 1999). On the other hand, the dominant VSMC component in resistance arteries enables it to regulate the lumen diameter and blood flow to various tissues by means of contracting or relaxing based on the tissue's needs (Conger, 1994; Lüscher & Tanner, 1993). A vital coupling between the ECM and cellular components of the vessel wall maintains proper vessel wall function in physiological conditions (Bank & Kaiser, 2002; Shadwick, 1999). Arterial stiffness is a pathophysiological condition that occurs when changes in the vessel wall

mechanics result in stiffer and less distensible arteries (Shadwick, 1999; Zieman et al., 2005). The myriad of structural and functional changes in the arterial wall in response to the chronic changes in vessel wall mechanics is referred to as arterial remodeling (Shadwick, 1999; Shirwany & Zou, 2010; Zieman et al., 2005). The pathological conditions can ultimately end in target organ damage, morbidity, and mortality (Glasser et al., 1997; Shirwany & Zou, 2010). Arterial remodeling is facilitated by intrinsic factors such as genetics, changes in the structural, cellular and hemodynamic functions of the vessel wall with ageing, as well as by external factors, including salt, glucose regulation (diabetes), chronic renal disease, dyslipidemia, changes in neurohumoral regulation (Glasser et al., 1997; Zieman et al., 2005).

Arterial stiffness, an initial adaptive response of the vessel wall to the changes in mechanical and hemodynamic stress in order to accommodate higher loading pressures without any structural changes, eventually becomes maladaptive, resulting in arterial remodeling characterized by alterations in the structure and function of the arterial wall (Shirwany & Zou, 2010; Zieman et al., 2005). Based on the type and location of the vessel in the vasculature, arterial remodeling can be either hypertrophic (thickening of the vessel wall), eutrophic (constant wall thickness) or hypotrophic (thinning of the vessel wall) (Feihl et al., 2008; Man & Wang, 2017; Shirwany & Zou, 2010). Furthermore, the remodeling can be inward or outward (Figure 1.4). (Feihl et al., 2009; Man & Wang, 2017; Shirwany & Zou, 2010).

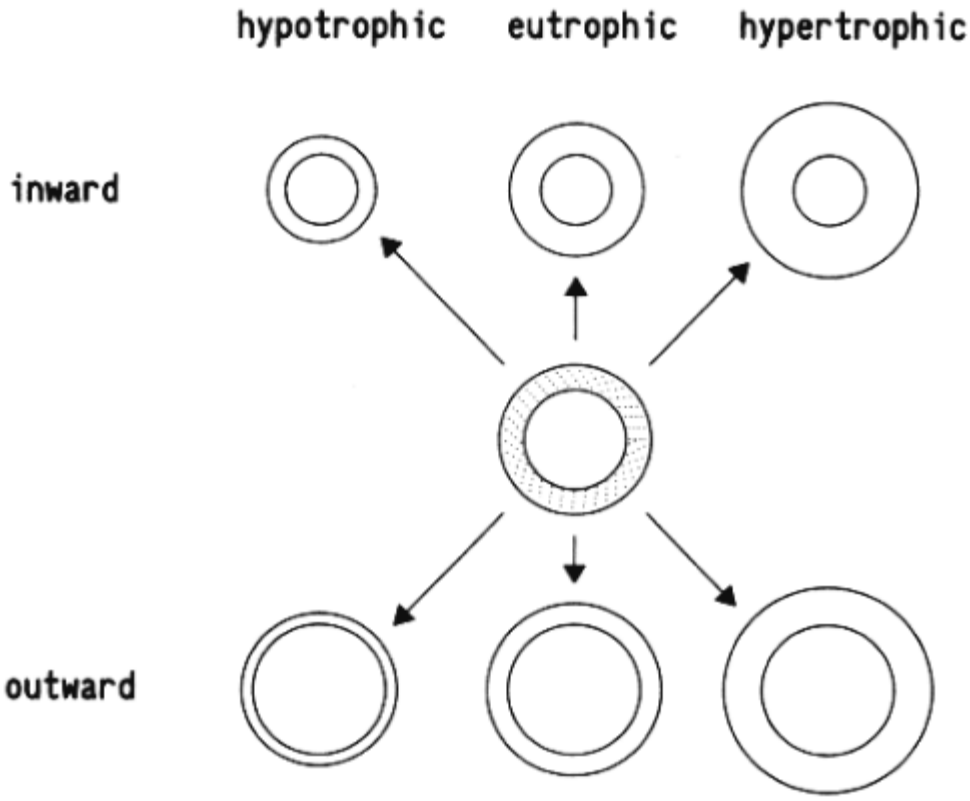

Figure 1.4 Classification of the different types of arterial remodeling according to the structural changes in the arteries. Starting from the vessel at the center (shaded), arterial wall remodeling can be hypertrophic (doubling of cross-sectional area, vessels in right column), eutrophic (no change in cross-sectional area, vessels in center column, or hypotrophic (halving of cross-sectional area, vessels in left column). These forms of remodeling can be inward (e.g., 30% reduction in lumen diameter, vessels in top row), or outward (e.g., 30% increase in lumen diameter, vessels in bottom row). Figure adapted with permission from (Mulvany et al., 1996)

In large elastic arteries, arterial remodeling is characterized by an outward hypertrophic remodeling (increased vessel diameter and thickened internal and medial layers of the vessel wall), which reduces the wall stress on the vessel wall that accompanies increases in blood pressure in accordance with LaPlace's law of wall tension (Laurent, 1995). In peripheral arteries, remodeling is characterized by inward eutrophic and hypertrophic remodeling, which results in increased peripheral vascular resistance to blood flow depending on the pathological condition (Feihl et al., 2008; Méndez-Barbero et al., 2021; Renna et al., 2013). The pathophysiological changes that result in arterial stiffness can also be separated into structural and cellular remodeling (Feihl et al., 2008; Renna et al., 2013).

Arterial stiffness is a complex interplay of changes in the arterial wall's structural and cellular components involving a highly regulated and interrelated process in response to vessel wall stress. The structural changes in arterial stiffness encompass the changes in the composition of the ECM components, primarily collagen and elastin (Méndez-Barbero et al., 2021; Renna et al., 2013). The elastic lamellae of a typical arterial wall are composed of elastic fibers arranged in parallel concentric fenestrated layers, alternating with layers of VSMCs anchored by elastic structural fibers of glycoproteins and integrins. (Eble & Niland, 2009; Robertson & Watton, 2013; van Varik et al., 2012). During arterial remodeling, the normal composition and layer of the elastic lamella are lost as they become increasingly fragmented and fibrotic (Cai et al., 2021; Robertson & Watton, 2013). Furthermore, the increased pressure on the vessel wall due to elastin breakdown stimulates excess collagen production to withstand the increased stress on the vessel wall (Cai et al., 2021; Robertson & Watton, 2013). A slow but dynamic process of production and degradation normally maintains the relative proportions of these ECM components of the vessel wall. However, a combination of decreased elastin content and increased collagen

deposition in the vessel wall in response to stress contributes to the stiffening and remodeling of the vascular wall (Cai et al., 2021; Robertson & Watton, 2013). A balance of elastin and collagen ratio in the vascular wall is regulated primarily by the elastolytic and collagenolytic actions of matrix metalloprotease (MMP), which is influenced by the various factors that trigger arterial remodeling (Díez, 2007; Jacob, 2003; P. Lacolley et al., 2017). The activity of MMP is modulated by various factors that cause arterial remodeling (Chen et al., 2013; Cui et al., 2017). MMP activity is upregulated by increased gene expression, post-translational activation by changes of the pro-MMP protein, MMP-MMP-interaction, plasmin, thrombin and reactive oxygen species (ROS) (Cui et al., 2017; Díez, 2007). The tissue inhibitor of MMP (TIMPs) counteracts the activity of MMP (Cabral-Pacheco et al., 2020; Díez, 2007). A balance between the MMP and TIMPs is crucial in arterial remodeling (Busti et al., 2010; Cabral et al., 2008; Díez, 2007).

In addition to the changes in the structural components of the arterial wall during remodeling, the endothelial layer and the VSMC also contribute to arterial stiffness and remodeling (Lemarié et al., 2010; Méndez-Barbero et al., 2021). The VSMC contributes to the maintenance of a physiological vessel wall tone in response to various mechanical, physical and neurohumoral stimuli as well as local endothelial-derived vasoactive substances (Méndez-Barbero et al., 2021; Touyz et al., 2013). On the other hand, the endothelium produces a balance of both vasoconstrictor and vasodilator substances that maintain homeostasis of the vessel wall (Félétou, 2011; Méndez-Barbero et al., 2021). However, a dysfunction of the endothelium in pathological conditions results in increased vasoconstrictor substances that increase vascular tone and vessel wall stiffness (Félétou, 2011; Vanhoutte et al., 2017; Yannoutsos et al., 2014). The endothelial layer also produces various factors that stimulate VSMCs to switch from contractile

to synthetic phenotypes and promote the deposition of ECM material (primarily collagen) to reinforce the vessel wall in response to stress (Ahmed & Warren, 2018; Frismantiene et al., 2018; Stegemann et al., 2005).

1.8.1 Assessment of arterial stiffness

Arterial stiffness is a complex property of the vessel wall that changes not only with acute changes in the vascular tone due to physical, chemical, and neurohumoral stimuli but also due to a long-term remodeling of the vessel wall in response to stress (Boyle, 2001; Folkow, 1987; Tesauro et al., 2017). Characterizing the mechanical properties of the vascular wall and the specific factors that cause changes in vessel wall function in physiological and pathophysiological states involves both invasive and non-invasive techniques (Chirinos, 2012; Palombo & Kozakova, 2016; Quinn et al., 2012). Animal models of arterial stiffness are primarily carried out using invasive techniques that allow the estimation of specific or global measurements of the arterial tree (Davis et al., 2023). Clinically, arterial stiffness plays a role in the pathogenesis of cardiovascular disease, and its assessment involves non-invasive techniques (Quinn et al., 2012; Tomiyama & Yamashina, 2010). The conventional clinical method for assessing arterial stiffness involves the analysis of the pulse pressure (PP) waveform generated by ventricular ejection (Augmentation index and PWV (Chirinos, 2012; Quinn et al., 2012).

The augmentation index estimates the increase in systolic blood pressure caused by the early return of reflected waves to the heart and is quantified by the difference between the second and first peak systolic values expressed as a percentage of abnormal PP (Gkaliagkousi & Douma, 2009; Quinn et al., 2012; Sharman et al., 2009). Although pulse wave analysis is a widely used measure of arterial stiffness, it may be confounded by factors related to cardiac function, such as

heart rate, stroke volume and ventricular ejection pattern (Gkaliagkousi & Douma, 2009; Mitchell, 2009).

PWV is the most widely used measurement of arterial stiffness clinically and experimentally. It is considered the gold standard measure of arterial stiffness because it is a non-invasive and relatively easy method for estimating arterial stiffness (Covic & Siriopol, 2015; Lim & Lip, 2008). PWV is the velocity at which the pressure waves generated by the systolic contraction of the heart propagate along the arterial tree. PWV is measured from two pressure waveforms, and assessment is usually done in two different arteries (for example, the carotid and the femoral arteries) (Covic & Siriopol, 2015; Lim & Lip, 2008; Vermeersch et al., 2009). PWV estimates represent the pulse wave's average velocity between the two remote measurement locations. The evaluation of the PWV provides additional information about the elastic properties (stiffness) of the arterial system. The higher PWV corresponds to a lower distensibility of the vessels and, therefore, a higher arterial stiffness (Covic & Siriopol, 2015; Lim & Lip, 2008; Vermeersch et al., 2009). The velocity at which the pressure waves propagate through the arterial tree depends on the mechanical properties of the vessel. Although PWV measurements represent the overall properties of the arterial wall, they fail to account for the structural and functional changes occurring in a particular segment of the arterial tree (Chirinos, 2012; Ma et al., 2018; Townsend et al., 2015)

Another important measure of arterial wall stiffness is the ability of the vessel wall to distend and increase in volume with increasing transmural pressure. The slope of the volume-pressure relationship of the vessel wall is quantified as arterial compliance, which represents the change in volume with pressure (Chirinos, 2012; Shirwany & Zou, 2010). Due to the heterogeneity of the vessel wall, different vessel wall components are recruited at different

strains with predominantly elastic elastin at lower pressure. In comparison, the less distensible collagen is recruited to support wall tension at higher pressure (Patrick Lacolley et al., 2017). As such, the compliance of vessels tends to be reduced at higher pressures and volumes (Patrick Lacolley et al., 2017; Mayet & Hughes, 2003; Shadwick, 1999).

The contractile state (tone) of the VSMC also contributes to the compliance of the vessel wall. Contraction of VSMC regulates the size of the blood vessel lumen, thereby decreasing blood volume and increasing blood pressure in the arterial system (Jaminon et al., 2019). The compliance of the vessel wall tends to reduce with increasing wall stiffness (Mayet & Hughes, 2003; Shadwick, 1999). A shortcoming in using compliance as a measure of arterial stiffness is that the compliance of the vessel wall depends on the changes in volume with distending pressure, which is influenced by the size of the lumen and the vessel wall (London & Pannier, 2010).

In comparison to compliance, which provides information about the stiffness of the artery as a hollow material which is dependent on size and geometry, the composite Young's modulus describes the stiffness of a segment of the arterial wall based on the changes in wall stress for a given change in strain (Intengan & Schiffrin, 1998; Park & Schiffrin, 2001). Different vessel wall components contribute differently to the vessel wall mechanics at various distending pressures (Intengan et al., 1999; Park & Schiffrin, 2001). Therefore, the composite Young's modulus is a quantitative measure of the sum contributions of the vessel wall components to the arterial stiffness independent of vessel size (Chirinos, 2012; Intengan et al., 1999; Park & Schiffrin, 2001; Safar, 2007; Saphirstein & Morgan, 2014). However, since the relationship between stress and strain in blood vessels is nonlinear due to the composite material and

viscoelastic properties of the arterial wall, the stiffness of the arterial wall segment cannot be accurately quantified using a single value of composite Young's modulus.

1.9 Changes in vascular elasticity due to the consumption of high salt

The consumption of high salt as part of a diet has been the subject of intense scientific research due to its association with elevated systemic blood pressure, increased cardiovascular morbidity and mortality, and, recently, activation of the inflammation by the immune system (Aguiar et al., 2017; Rodríguez-Iturbe et al., 2012; Uetake et al., 2015). Globally, an estimated 1.65 million cardiovascular-related deaths have been attributed to high sodium intake annually; 61.9% of deaths occurred in males and 38.1% in females (Mozaffarian et al., 2014). These deaths account for 1 of every 10 deaths from cardiovascular-related causes (9.5%).

In 2010, the estimated mean level of global salt consumption by individuals was 3.95 g per day, which is nearly double the WHO's recommended limit of 2.0g per day with men consuming approximately 10% more sodium than women (Powles et al., 2013). The average daily salt intake in the population is currently estimated at 2.76 g per day, which is higher than the estimated goal of 2.3 g per day. High salt intake has been established to result in elevated blood pressure. In a community interest study, it was reported that the threshold intake levels of 60-70 mmol of sodium daily are a prerequisite for the development of high blood pressure (Safar et al., 2009).

Reducing in dietary salt intake is suggested to benefit the cardiovascular system (Bibbins-Domingo et al., 2010; Cook et al., 2007; Ha, 2014; He & MacGregor, 2007). Dietary salt reduction is suggested to lower intravascular pressure, especially in older populations with isolated systolic hypertension, but only modestly affects diastolic blood pressure (Chobanian et al., 2003). A consistent correlation between sodium intake and blood pressure has been observed,

particularly in the older population (i.e., greater than 65 years of age) (Bibbins-Domingo et al., 2010; Cook et al., 2007; Ha, 2014; He & MacGregor, 2007; Safar et al., 2009) but little is known about the underlying vascular mechanisms responsible for the long term effect of salt.

Excess sodium intake may influence cardiovascular morbidity and mortality, mainly through its contributions to alteration in vascular biology and hormonal changes that could ultimately lead to altered vascular elasticity (Benetos et al., 2002; Safar et al., 2009). Elevated arterial stiffness is recognized as a surrogate endpoint for cardiovascular diseases due to its association with a number of vascular disorders (e.g., stroke and heart failure). Several investigations have also established a blood pressure-independent correlation between dietary sodium intake and arterial stiffness (Appel et al., 2011; P. Boutouyrie et al., 2011; Safar et al., 2009).

Chronic intake of high sodium is suggested to be associated with alteration in vascular biology, i.e., hypertrophy of the arterial wall and ECM remodelling independent of elevated intravascular pressure (Safar & O'Rourke, 2006). Thus, salt consumption could directly increase vascular stiffness. This effect can be moderately reversed by reducing sodium consumption or using diuretics to lower body salt content independent of blood pressure (He & MacGregor, 2007; Safar & O'Rourke, 2006; Safar et al., 2000).

Arterial stiffness is suggested to result from multiple mechanisms involving reduced elastin/collagen ratio, reactive oxygen species–induced inflammation, calcification, VSMC stiffness, and endothelial dysfunction. As observed with ageing, arterial stiffness is more pronounced in males than females, with estrogen suggested to provide a cardioprotective layer in females. However, this cardioprotective effect is lost during menopause as arterial stiffness becomes more prominent in females compared to males (Ahimastos et al., 2003; Benetos et al.,

2002; Kingwell et al., 2001; Lee & Oh, 2010). The sex differences in arterial stiffness are suggested to be both intrinsic and influenced by sex steroids (Ahimastos et al., 2003). Markers of arterial stiffness, including PWV, PP and central aortic pressure, have been suggested to differ between males and females as well as between groups with high cardiovascular risk factors and those in normal states (Ahimastos et al., 2003; Benetos et al., 2002; Kim et al., 2014; Kingwell et al., 2001; Lee & Oh, 2010). In the Dahl salt-sensitive hypertensive rat model, sex-specific quantitative trait loci associated with arterial stiffness have been identified, suggesting a potential sex-specific genetic determinant for arterial stiffness (Decano et al., 2016).

Despite the substantial progress that has been made in narrowing the gaps in our knowledge of the detrimental effects of salt on the cardiovascular system, our understanding of the mechanistic differences, manifestations and progression of arterial stiffness remains incomplete. More importantly, few studies directly compared males and females regarding salt-induced arterial stiffness. In addition, little is known about the underlying sex-specific factors that drive these sex-related differences. Understanding the underlying fundamental mechanisms leading to sex-specific differences in arterial stiffness offers the possibility of identifying novel selective treatments and therapies to reduce the risk of cardiovascular disease.

In the current thesis, Dahl salt-sensitive male and female rats fed on a 4% NaCl diet were used to investigate sex differences in arterial stiffness due to high salt consumption. This study used the Dahl salt-sensitive rat model because of its predisposition to hypertension caused by an interaction of genetic and environmental factors (sensitivity to dietary salt) (Abais-Battad et al., 2019; Rapp, 1982). More importantly, Van Vliet et al. (2006) reported two distinct and separable stages of salt-induced hypertension in Dahl salt-sensitive rats fed 4% NaCl. This makes the Dahl salt-sensitive rat model relevant for understanding the long-term effects of salt intake on the

vascular system. The changes in the structure and function of the arterial wall due to dietary salt were compared between Dahl salt-sensitive male and female rats on a high salt diet and regular diet. In addition, using a segment of the arterial wall (third-order mesenteric arteries), some mechanisms and sex-related factors contributing to sex differences in arterial stiffness were investigated using various vasoactive drugs and antibodies listed in appendix B.

1.10 Objectives

The current research aims to establish how high salt consumption alters blood vessel wall stiffness in males and females. The present study will:

I. Investigate sex-specific effects of high salt consumption and elevation in arterial pressure on vascular biomechanics and function in small resistant arteries of Dahl salt-sensitive male and female rats.

II. Examine sex-specific structural changes of the vessel wall and responses to some pharmacological agents on the biomechanics of small resistant arteries of Dahl salt-sensitive male and female rats.

III. Determine the sex-specific contributions of the mechanosensitive Piezo 1 ion channels in regulating blood vessel wall stiffness.

1.11 Hypothesis

There are limited reports on the changes in vascular elasticity due to high salt intake in both male and female rats. An attempt was made to address three hypotheses in this thesis. First, there would be sex-specific differences in biomechanics and function of small resistant arteries of Dahl salt-sensitive male and female rats. Secondly, the behavior of isolated small resistance arteries to pharmacological agents will differ in the context of vascular stiffness in normotensive versus salt-induced hypertensive state, with associated sex-specific structural and functional differences. Finally, I hypothesize that there will be sex-specific differences in the contributions of Piezo 1 channels to biomechanics in the resistance arteries of hypertensive males versus females.

Chapter 2 Differential biomechanics in the resistance arteries of male and female Dahl hypertensive rats

2.1 Abstract

An increase in vascular stiffness is associated with a higher risk of cardiovascular morbidity and mortality and is likely sex-specific. Our objectives were to compare structural and functional alterations in small resistance arteries (3rd order mesenteric) related to vascular stiffness from Dahl salt-sensitive male and female rats (n=8, mean ± s.e.m.). Arterial blood pressure and pulse wave velocity assessed in vitro were significantly ($p < 0.05$) elevated in males (161 ± 3 mmHg; 6.4 ± 0.2 m s−1) and females (147 ± 2 mmHg; 5.5 ± 0.1 m s−1) on a high (H) salt compared to regular (R) diets but were significantly higher in males (H) compared to females. Significant increases in collagen and smooth muscle cell areas were evident in the ultrastructure of mesenteric arteries of hypertensive males compared to normotensive or corresponding females. There were no significant differences in composite Young's modulus (CYM) between groups. Vasoconstriction (phenylephrine, 0.3 μM) resulted in significantly higher CYM in males (H: 8.6 ± 1 KPa) than R (4.5 ± 0.8 KPa), and the corresponding females (H: 5.6 ± 0.6 KPa and R: 5 ± 0.9 KPa). In contrast, vasodilation (sodium nitroprusside, 0.3 μM) significantly reduced CYM in the male groups (H: 2.5 ± 0.4 KPa and R: 2.7 ± 0.5 KPa) compared to the corresponding values in females (H: 4.2 ± 0.6 KPa and R: 5 ± 0.5 KPa). Moreover, the slope of the pressure-volume curves revealed significantly greater distended vascular compliance in male H than in R and the corresponding females. Our findings are supportive of a link between high salt intake and elevated blood pressure as being sex-specific, likely involving sex-dependent changes in the

ultrastructure of the vessels, which ultimately can alter the biomechanics and thus, the hemodynamic functions of both macro- and micro-circulations.

2.2 Introduction

Arterial stiffness is defined primarily in terms of the changes to the mechanical properties (i.e., stress/strain relationships) of the arteries and associated fundamental morphological changes to the wall (Bevan & Bevan, 1984; Khamdaeng et al., 2012). In addition to the substantial changes in elastin and collagen that forms the main load-bearing component of the arterial wall, there is also a significant adaptation of both the passive and active components of the vessel to accommodate the stresses (Cox, 1975, 1983; Holzapfel et al., 2000; Nagasawa et al., 1982). Arterial stiffness of the large central arteries is the primary determinant of vascular impedance influencing the systemic pressure-flow relationship (Adamson, 1999; Cecelja et al., 2009). The result of arterial wall stiffness is changes in hemodynamic function such as pulse wave velocity (PWV) and arterial pulse pressure. This is due to the underlying structural changes and modifications in large conduit arteries, which can significantly increase cardiovascular risk factors and mortality (Cosson et al., 2007; Fitch et al., 2001; Marque et al., 2001). Remodeling of the arteries is an initially adaptive response to the stress posed on the blood vessel. Causally, it involves shear stress from the flow of blood across the vessel lumen, longitudinal stress from the surrounding tissues, and circumferential stress from the blood pressure in response to physiological and pathophysiological changes in the body (Chatzizisis et al., 2007; Gibbons & Dzau, 1994; Intengan & Schiffrin, 2001). The change eventually becomes maladaptive as it compromises vessel wall function, contributing to cardiovascular complications.

Arterial stiffness can be considered to have two distinct but interconnected components, which are structural and dynamic (Janić et al., 2014). The structural component consists of collagen, elastin fibers, and other associated molecular components of the extracellular matrix,

while the dynamic component consists of the smooth muscle tone. The dynamic component of arterial stiffness is tone-dependent and is influenced mainly by the vasoactive substances released by the endothelium as well as the nerves innervating the blood vessels (Anderson, 2006; Janić et al., 2014).

Elevated arterial stiffness in large arteries is recognized as a surrogate endpoint for cardiovascular diseases due to its association with subclinical atherosclerosis and cardiovascular diseases, including angina, myocardial infarction, stroke, and heart failure (Laurent & Boutouyrie, 2013). Chronic high sodium intake is also suggested to be linked to hypertrophy of the aorta and extracellular matrix (ECM) development independent of blood pressure (Safar & O'Rourke, 2006). This results in a subsequent increase in vascular stiffness and modified secretory populations of vascular smooth muscle cells (VSMCs) (He & MacGregor, 2007; Safar & O'Rourke, 2006; Safar et al., 2000).

There Dahl salt-sensitive rats have been used as a model for hypertension over decades, while both abnormal vasoconstriction and vasodilation have been described in blood vessels of this strain (McLoone et al., 2009). Distinct rapid (days) and slow phases (5 weeks) for elevation in blood pressure in Dahl salt-sensitive rats have been described for this model of hypertension (Van Vliet et al., 2006; Zicha et al., 2012). In addition, differential functional responses to sympathetic nerve stimulation were found to exist in vasculature such as the mesenteric bed in Dahl salt-sensitives rats (Gamoh et al., 2019). Further, morphological and structural changes have been also described in blood vessels from this strain (Parai & Tabrizchi, 2005; Sandow et al., 2009).

In general, the evidence in the literature seems to mainly be concerned with stiffness of the larger conduit arteries and there is less emphasis on regional and local changes in smaller arteries

in hypertension. Nonetheless, there is evidence in the current literature that suggests increased stiffness and augmented pressure wave (e.g. abnormal wave reflection) could additively contribute to the onset of hypertension (Tomiyama et al., 2018; Tomiyama et al., 2020). It is possible that the crosstalk between micro-circulation and macro-circulation and the inter-connection between them leads to additive detrimental effects on the circulation due to increased global vascular stiffness (Pan et al., 2018; Takahashi et al., 2021). There are limited reports on the direct relationship between the changes in vascular elasticity due to high sodium intake in both males and females. Thus, the primary objectives of this study were to compare the effects of high salt consumption and elevation in systemic arterial pressure on vascular biomechanics and function in small resistant arteries in males and females, which has not been previously studied. Accordingly, in the current study, we made comparisons on the biomechanical and pharmacomechanical functions (i.e. composite modules and compliance) and ultrastructure in small resistance arteries (150–200 μm) using pressure myography.

2.3 Materials and Methods

2.3.1 Animals:

All procedures on animals were carried out in accordance with the guidelines of the Canadian Council on Animal Care, with the approval of the Institutional Animal Care Committee of Memorial University of Newfoundland and the Canadian Council of Animal Care (Guide to Care and Use of Experimental Animals, Vol 1, 2nd Edition). Male and female Dahl salt-sensitive rats (age 5–6 weeks) were purchased from Charles River Laboratories. (Saint Constant, Quebec, Canada), housed two per cage and were kept in a temperature-controlled environment (22 ± 2° C) on a 12 h-12 h light-dark cycle. They were given access to normal tap water and standard

chow (regular) or Japanese style stroke-prone high salt diet containing 4% NaCl (Zeigler Bros., Inc. Gardners, Pennsylvania, USA) *ad libitum* for 6–7 weeks.

2.3.2 Experimental Design:

At 6–7 weeks, each animal was anesthetized (induction 5% isoflurane in 100% O_2, maintenance 1.5–1.25% isoflurane in 100% O_2), and were injected with the analgesic, buprenorphine (0.01 mg/kg, subcutaneously). The core body temperature was maintained at 37 ± 1° C using a heating lamp and monitored with a rectal thermometer. The external iliac and carotid arteries were isolated and catheterized using polyethylene tubing [I.D. 0.58 mm, O.D. 0.965 mm (9 cm) connected to I.D. 0.28 mm, O.D. 0.61 mm (7 cm)]. The catheters were advanced forward (approximately 2 cm) such that the catheter in the femoral artery was just at the distal end of the abdominal aorta, while the catheter in the carotid artery was just beyond the aortic arch and in the proximal end of the thoracic aorta (Leblanc & Tabrizchi, 2018). All catheters were filled with heparinized physiological (0.9% NaCl) saline (25 iu/ml). Central (aortic) and peripheral (femoral artery) blood pressure, as well as heart rate were continuously recorded by AcqKnowledge (3.9.1.6) software (Biopac Systems Inc., Goleta, California, USA) with a pressure transducer (P23XL; Spectramed Statham; Viggo-Spectramed, Oxnard, California, USA) for 20–25 min. The signals were amplified (DA 100A; Biopac Systems Inc.), wherein the amplifier was connected to a universal interface module (UIM 100; Biopac Systems Inc.), and to an acquisition unit (MP100; Biopac Systems Inc.). The analogue output signal was then converted to a digital signal (USB1W; Biopac Systems Inc.), and displayed in AcqKnowledge (3.9.1.6). Animals were euthanized by anaesthetic overdose and thoracotomy. The mesenteric arteries were removed and prepared for functional and histological studies. As well, the heart of each animal was excised,

and the right ventricle and left ventricle as well as septum were separated and weighed. In addition, the length between the carotid artery catheter and the femoral artery catheter was measured at postmortem, and PWV was then calculated with the following formula PWV = $d/\Delta t$ (Leblanc & Tabrizchi, 2018).

2.3.3 Pressure Myograph Experiments:

All chemicals used in the pressure myograph experiments were purchase from Sigma Aldrich (Montreal, Canada) unless otherwise stated. The mesenteric bed was placed in a dissecting dish containing modified Krebs buffer with the following composition (mmol/l): 120 NaCl, 4 KCl, 1.2 $MgCl_2.6H_2O$, 1.5 $CaCl_2H_2O$, 25 $NaHCO_3$, 1.2 KH_2PO_4 and 0.1 EDTA in an oxygenated (95% O_2 and 5% CO_2) environment. The third-order branch of the mesenteric artery was determined to be the third branch off the superior mesenteric artery of the gut. A length of approximately 5 mm was isolated and carefully cleaned of surrounding tissues under a dissecting microscope as described by (Jadeja et al., 2015). The mechanical properties of isolated third-order mesenteric arteries were studied with a pressure myograph. Isolated vessels were mounted onto the Single Vessel Chamber component of the Pressure Servo System (Living System Instrumentations, Model CH-1-SH/CH-1-QT P100; St. Albans City, Vermont, USA) for the pressure myograph studies. In detail, the mesenteric arteries were mounted on two glass micropipettes, secured with 0.2 metric (10–0) surgical nylon suture obtained from Covidien (Monosof, Covidien LLC, Mansfield, Massachusettss, USA). The vessel length was adjusted so that the vessel walls were parallel without stretch. Intraluminal pressure was then set to a baseline pressure of 3.9996 KPa (1.0 mmHg = 0.1333 KPa), and allowed to equilibrate for 20 min at 37 ± 1°C in a modified Krebs buffer gassed with a mixture of 95% O_2 and 5% CO_2. Vascular response was imaged using an inverted microscope and measured using a Video

Dimension Analyzer (Living Systems Instrumentation) and the iWORX Data Recording Software (Dover, New Hampshire, USA). Three different groups of experiments were undertaken in assessment of the mechanical function of the blood vessel using two vasoactive agents phenylephrine (0.3 μmol/l), sodium nitroprusside (0.3 μmol/l) or equivalent volume (24 μl) of vehicle (distilled water). Five minutes after the additions of the vasoactive agents or vehicle, intraluminal pressure was raised stepwise at an increasing transmural pressure of 5.3329, 7.9993, 10.6658 and 13.3322 KPa to obtain a pressure-diameter (D) curves. For each vessel, the left wall and right wall thickness was also measured. In another group of experiments without the presence of any vasoactive agents, isolated third-order mesenteric arteries were pressure-fixed (13.3322 KPa) with Karnovsky fixative at 37 ± 1°C for 30 min for ultrastructure assessment using electron microscopy.

2.3.4 Calculation of mechanical parameters

The luminal diameter at baseline D_0, LW and RW were measured at various intraluminal pressures, (5.3, 7.9, 10.6, and 13.3 KPa) using a video frame capture and real-time edge-detection system available with the Video Dimension Analyzer. The wall thickness (WT) was calculated using the following formula: WT = (LW+RW)/2.

Vascular compliance (C), which is the ability of a vessel to distend and increase volume with an increasing transmural pressure is equal to changes in vessel volume ($\Delta V = \pi r2\ h$), divided by changes in transmural pressure (ΔP) (i.e., $C = \Delta V/\Delta P$).

The following mechanical parameters were calculated according to the methods by Intengan and Schiffrin (Intengan & Schiffrin, 1998). Circumferential wall strain (ε) = $(D - D_0)/ D_0$, where D_0 is the diameter at baseline transmural pressure and D is the observed luminal diameter for a

given transmural pressure. Circumferential wall stress (σ) = (PD)/(2WT), where P is the intramural pressure, D and WT are the luminal diameter and wall thickness respectively.

To estimate the arterial stiffness independent of vessel geometry, the composite Young's modulus of the vessel was determined where Ec = stress/strain. The non-linear nature of the stress/strain relationship was compensated for by fitting the stress/strain data from each vessel to an exponential curve $y = ae^{bx}$ where $\sigma = \sigma_0 e^{x\beta}$ (plots of ln y vs. x), σ_0 is the stress at baseline transmural pressure and β is a constant directly proportional to Ec, related to the rate of increase of the stress/strain curve. An increase in β implies an increase in Ec (increase in stiffness).

2.3.5 Preparation of tissues for morphometry ultrastructure:

For transmission electron microscopy (TEM), blood vessels were fixed in Karnovsky fixative at 4^o C overnight (Karnovsky, 1964). Tissues were then washed in 0.1 M sodium cacodylate buffer (pH 7.4), post-fixed in 1% Osmium tetroxide, dehydrated in increasing concentrations of ethanol and acetone, followed by infiltration with EPON resin using a modified protocol by Hyam (1981). Resin blocks were polymerized in BEEM capsules (Electron Microscopy Sciences, EMS) overnight at 70^o C and cut to 100 nm with a diamond knife (Diatome), mounted on 300 mesh copper grids, stained with uranyl acetate and lead citrate (EMS), and examined using a Tecnai Spirit transmission electron microscope (FEI) with an accelerating voltage of 80 kV.

For light microscopy, the same processing protocol was used, but the sections were 1 µm and placed on a glass slide and stained with toluidine blue in 1% sodium borate solution. Each section was examined on an Olympus FV300 microscope with a SC50 5 MP digital color camera (Olympus Canada, Richmond Hill, Ontario, Canada).

2.3.6 Morphometry

The morphometric parameters were calculated using a test system (grid) consisting of a coherent square lattice of points generated by a JAVA-written stereological tool (STEPanizer) (Tschanz et al., 2011). The cross-sectional area of the various vessel wall components was then estimated as the area of the component per unit containing area according to the method described by Lee et al. (Lee et al., 1983), cross-sectional area $(A_A) = \left(\frac{\Sigma a}{\Sigma A}\right) t$, where: t = thickness of serial sections, a = area of the profiles for a, and A= area of the section. In order to compensate for eccentricity due to sectioning, the correction factor (d1/d2) was used to estimate the true (corrected) cross-sectional area AC = AA (d1/d2), where d1 = short axial diameter and d2 = long axial diameter.

2.3.7 Statistical analysis

All the data (haemodynamics, morphometric, ultrastructure, composite elastic modulus and compliance values) were analysed using two-way analysis of variance (ANOVA) followed by Bonferroni test and/or one-way ANOVA followed by Bonferroni test. The statistical analysis was carried out with the SigmaPlot statistical package (Systat Software, San Jose, California, USA). The data are presented as means ± s.e.m., and the sample size is the number of animals used in each experiment (n = 5–8). A value of P less than 0.05 was considered significant.

2.4 Results

The bodyweight of Dahl salt-sensitive female rats was generally lower than that of the Dahl-salt-sensitive male rats in both groups (high salt & regular diets), and within both groups (male and female), there was no significant difference between the body weights; male regular diet (MRD): 363.3 ± 7.7 g, male high salt diet (MHS): 373.9 ± 8.6 g, female regular diet (FRD): 241.3± 8.1 g, and female high salt diet (FHS): 251.0± 4.7 g.

There were significant differences between heart rate of males and females either within or between groups on regular compared to high salt diets. Consumption of high salt diet caused significant increases in heart rate in both male and females (Table 2.1). Moreover, consumption of high salt elevated central and peripheral, systolic and diastolic, blood pressures independent of sex. Central and peripheral, systolic, and diastolic, blood pressures of males on high salt diet were significantly higher than the corresponding values in females. However, there were no differences in the central and peripheral, systolic, and diastolic, blood pressures of male and female on regular diet (Table 2.1). Central pulse pressure was elevated following high salt consumption in male but not female animals. However, PWV (an index of central vascular stiffness) became significantly elevated in both male and female animals on high salt compared to those regular diet. PWV was also found to be significantly higher in males compared to corresponding females on high salt diet (Table 2.1).

Table 2.1: Hemodynamic measurements in Dahl salt-sensitive male and female rats on regular or high salt (HS; 4% NaCl) diets for 6-7 weeks.

Hemodynamic	SSM (R diet)	SSM (HS diet)	SSF (R diet)	SSF (HS diet)
HR (beats/min)	373 ± 2[b]	386 ± 3[ac]	356 ± 5	367 ± 4[b]
cSBP (mmHg)	131 ± 2	161 ± 3[ac]	132 ± 2	147 ± 2[b]
cDBP (mmHg)	96 ± 1	117 ± 3[ac]	99 ± 2	108 ± 2[b]
cPP (mmHg)	37 ± 1[b]	44 ± 1[ac]	40 ± 1	39 ± 1
pSBP (mmHg)	130 ± 2	158 ± 3[ac]	130 ± 2	144 ± 2[b]
pDBP (mmHg)	92 ± 1	118 ± 3[ac]	91 ± 1	104 ± 2[b]
pPP (mmHg)	38 ± 1	40 ± 1	39 ± 1	42 ± 1[b]
PWV (m/sec)	4.9 ± 06	6.4 ± 0.8[ac]	4.5 ± 0.1	5.5 ± 0.1[b]

Each value is expressed as a mean ± s.e.m. (n = 8). cDBP, central DBP; cPP, central pulse pressure; cSBP, central SBP; FHS, female high salt diet FRD, female regular diet; HR, heart rate; MHS, male high salt diet; MRD, male regular diet; pDBP, peripheral DBP; pPP, peripheral pulse pressure; pSBP, peripheral SBP; PWV, pulse wave velocity.

[a] Significantly different from SSM R diet; $p < 0.05$

[b] Significantly different from SSF R diet; $p < 0.05$

[c] Significantly different from SSF HS diet; $p < 0.05$

The ratio of the left ventricle and septum to right ventricle of MHS (5.8 ± 0.2) was significantly greater than that of the MRD (4.5 ± 0.3), and female groups FRD (4.7 ± 0.1) and FHS (4.7 ± 0.2). It is apparent that the significant left ventricular hypertrophy found in MHS group is likely due to greater increase in systemic arterial pressure as well as vascular stiffness.

2.4.2 Morphometric analysis

There was a significant increase in the area of media in the 3rd order mesenteric blood vessels of males on high salt compared to those on regular diet or the corresponding females. There were no other significant changes in areas of adventitia, intima, internal elastic lamina, or external elastic lamina associated with either sex or diet (Table 2.2).

Table 2.2: Morphometric analysis from electron microscopy images of third-order mesenteric blood vessels fixed at 13.33 KPa (1 mmHg = 0.1333 KPa) obtained from Dahl salt-sensitive male and female rats on regular or high salt (4% NaCl) diets for 6–7 weeks

	SSM (R diet)	SSM (HS diet)	SSF (R diet)	SSF (HS diet)
Adventitia (μm^2)	39 ± 5	34 ± 4	41 ± 9	41 ± 8
Media (μm^2)	89 ± 18	158 ± 15[ab]	80 ± 18	86 ± 14
Intima (μm^2)	18 ± 5	21 ± 3	21 ± 6	35 ± 10
IEL (μm^2)	2.4 ± 0.7	4.0 ± 0.7	3.6 ± 1	4.0 ± 0.4
EEL (μm^2)	0.2 ± 0.05	0.3 ± 0.09	0.27 ± 0.1	0.23 ± 0.05

Each value is expressed as a mean ± s.e.m. (n = 5). EEL, external elastic lamina; FHS, female high salt diet; FRD, female regular diet; IEL, internal elastic lamina; MHS, male high salt diet; MRD, male regular diet.

[a]Significantly different from SSM R diet; $p < 0.05$

[b]Significantly different from SSF HS diet; $p < 0.05$

The internal and external elastic laminae demarcating the medial layer of the 3rd order of the mesenteric blood vessel were prominent in both male and female groups (Figure 2.1). However, the external elastic lamina was poorly developed in both sexes compared to the well-developed internal lamina regardless of diet. Ultrastructural assessment indicated a distorted, fragmented, and discontinuous endothelia cell layer in the arteries of males on a high salt diet. The medial layer of the vessel wall appeared to be thicker in the males on high salt diet with increased layers of smooth muscle cells compared to the other groups. The medial layer consist of mostly smooth muscle cell with discontinuous layers of elastic lamina and collagen sparsely distributed in the media layer (Figure 2.1).

MRD

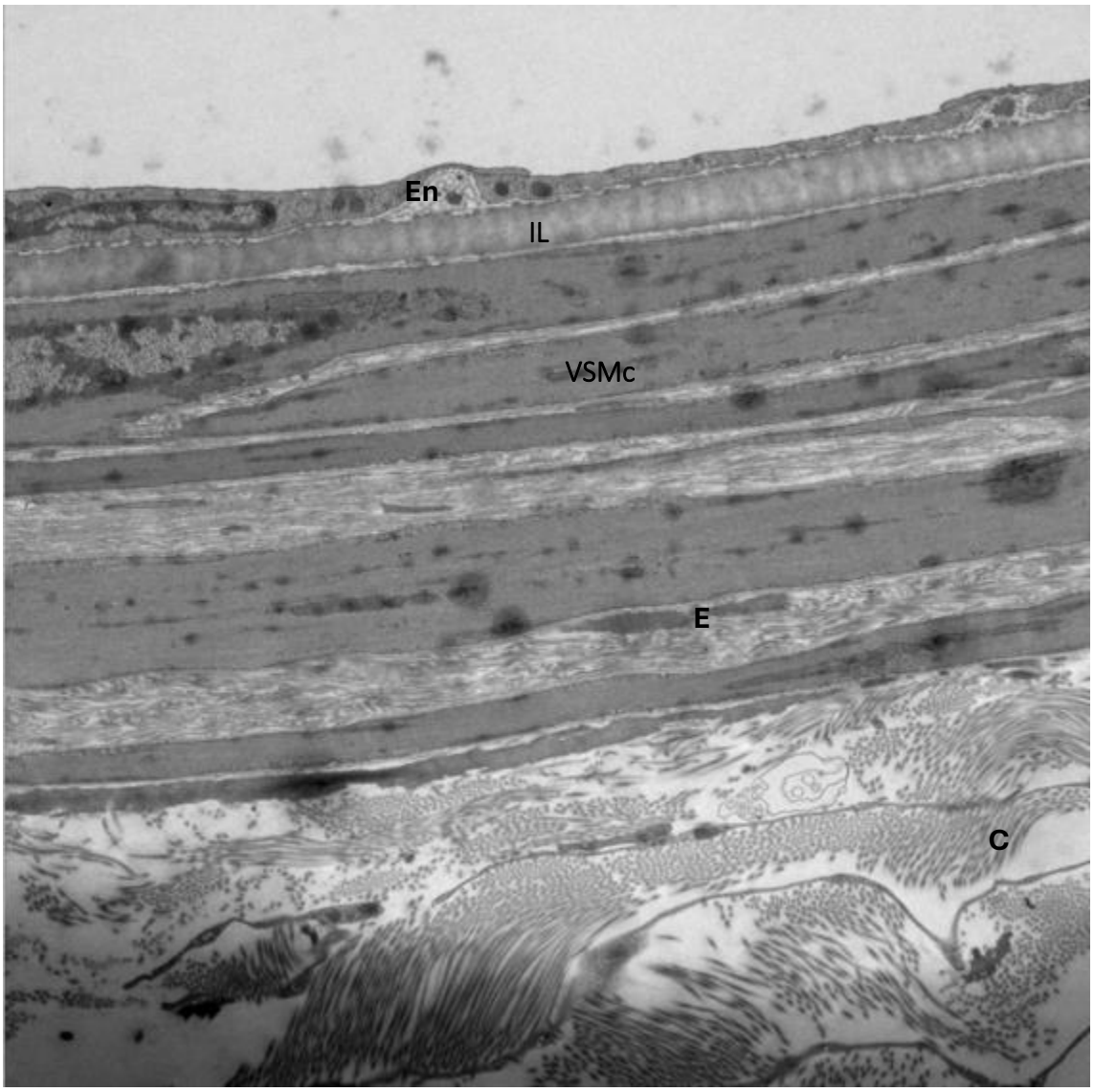

2.0 µm

MHSD

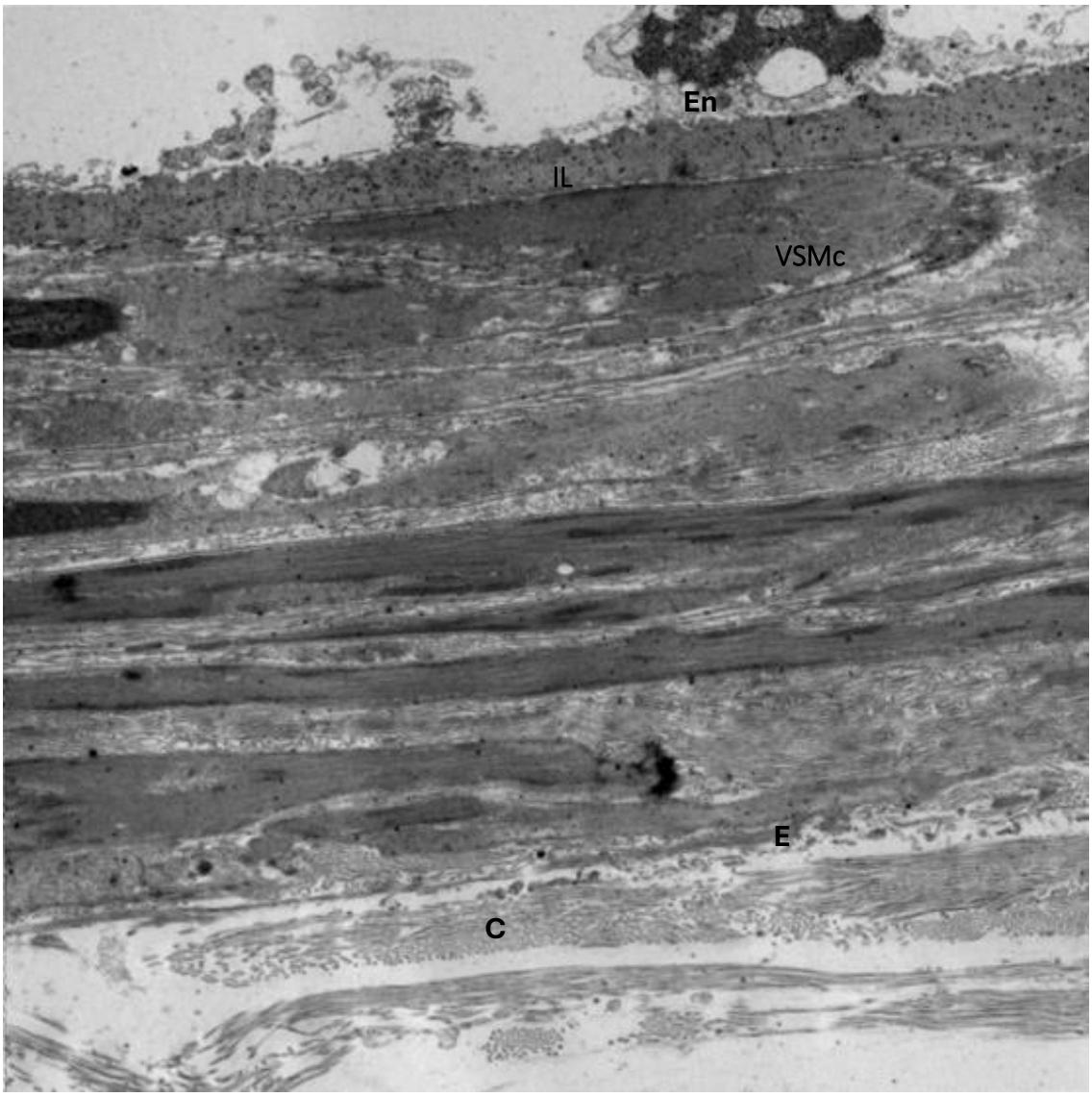

2.0 µm

FRD

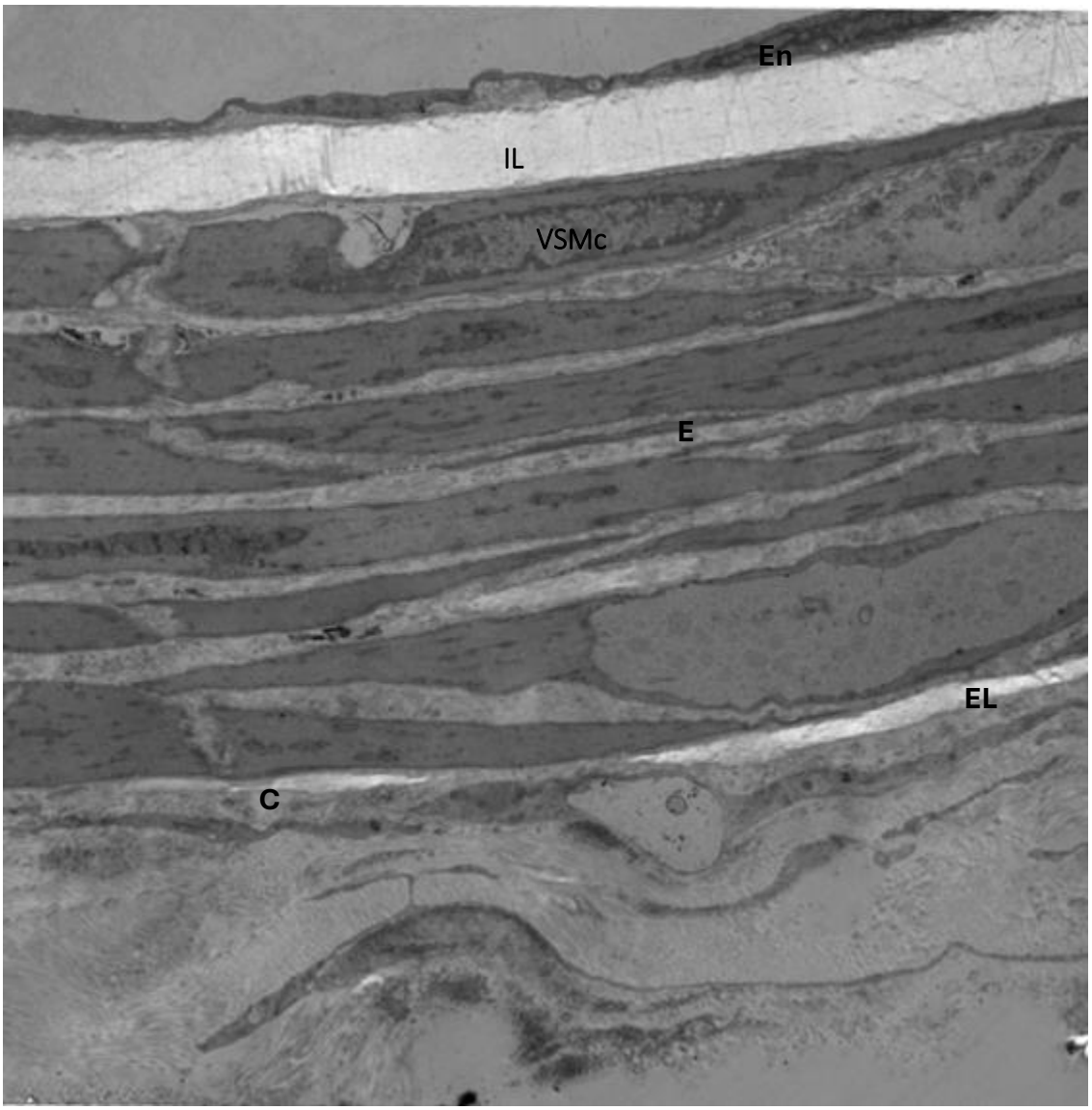

2.0 μm

FHSD

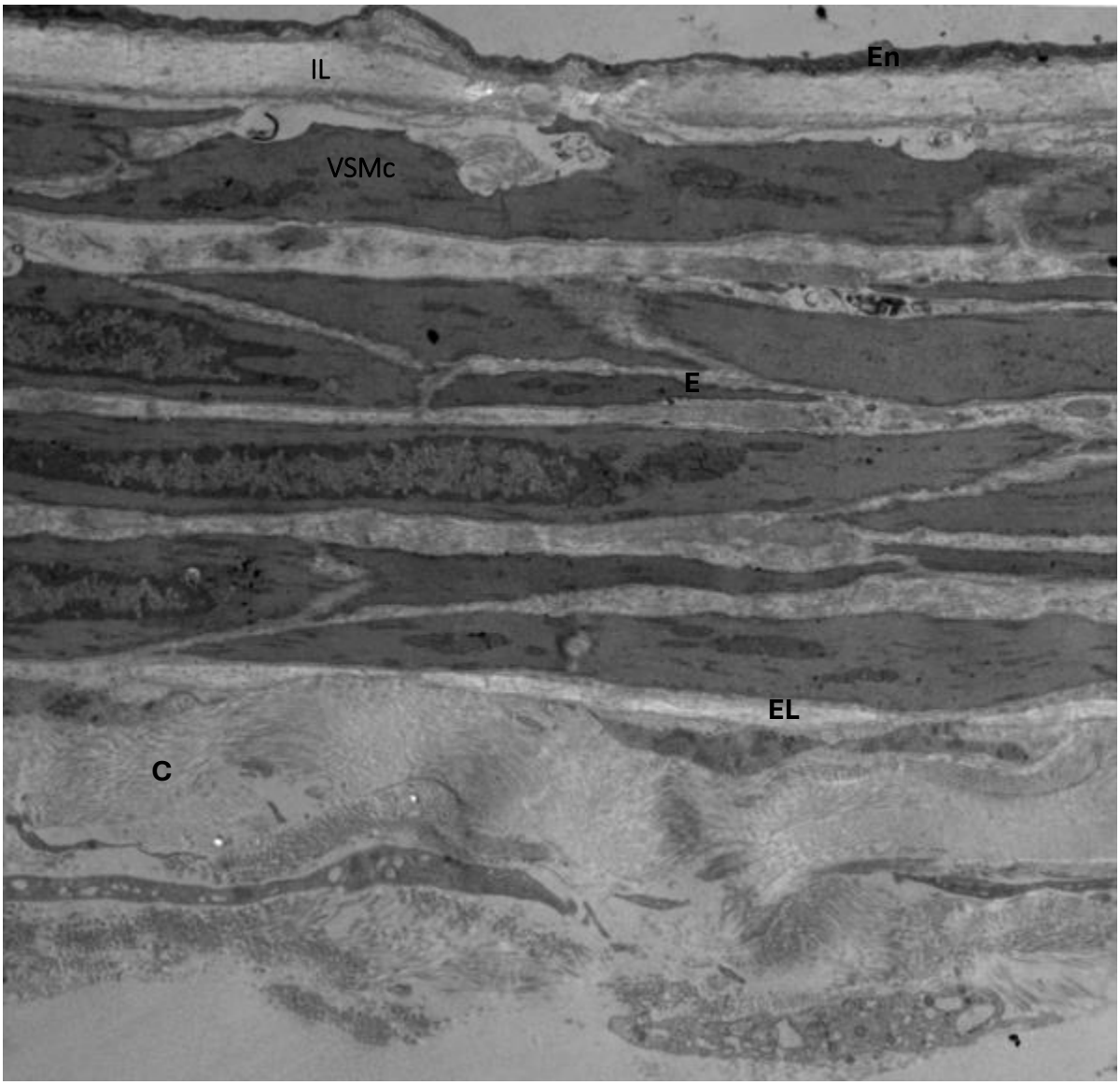

2.0 µm

Figure 2.1 Electron micrograph cross-sectional areas (direct mag: x1100) of the third-order mesenteric arteries from Dahl salt-sensitive male and female rats on regular or high salt (4% NaCl) diets for 6–7 weeks. C, collagen; E, elastin; EL, external elastic lamina; En, Endothelium; FHS, female high salt diet; FRD, female regular diet; IL, internal elastic lamina; MHS, male high salt diet; MRD, male regular diet.

There were significant increases in collagen and smooth muscle cell areas in the 3rd order mesenteric blood arteries of males on high salt compared to either males on regular diet or corresponding females. There were no significant changes noted in elastin area for these blood vessels within or between any of the experimental groups (Figure 2.2). Furthermore, no significant differences were observed in the ratio of the areas of collagen/elastin, vascular smooth muscle/collagen, or vascular smooth muscle/elastin within and between the various groups (Table 2.3).

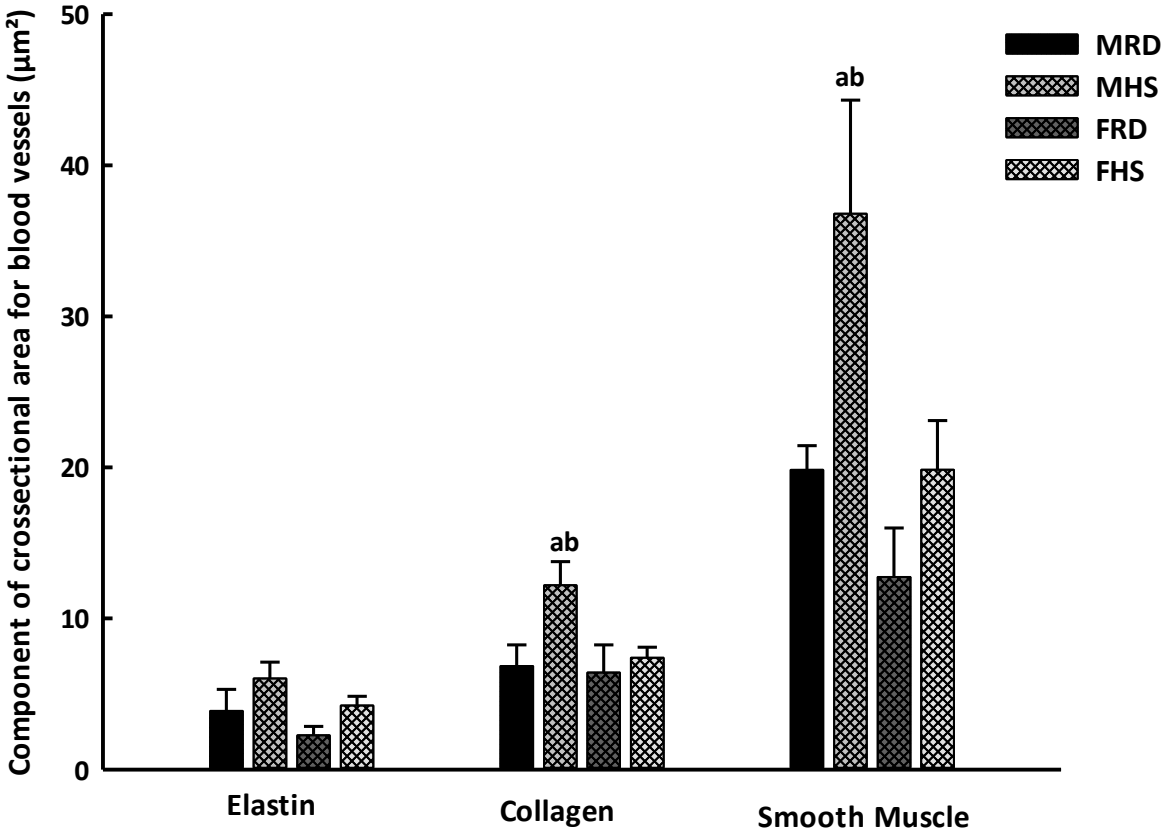
Component of crossectional area for blood vessels (µm²)
50
40
30
20
10
0
MRD
MHS
FRD
FHS
ab
ab
Elastin
Collagen
Smooth Muscle

Figure 2.2: Morphometric determination from electron microscopy images of content for elastin, collagen, vascular smooth muscle cell from third-order mesenteric blood vessels fixed at 13.33 KPa [1 mmHg = 0.1333 KPa) obtained from Dahl salt-sensitive] male and female rats on regular or high salt (4% NaCl) diets for 6–7 weeks. Each value is expressed as a mean ± s.e.m. (n = 5). FHS, female high salt diet; FRD, female regular diet; MHS, male high salt diet; MRD, male regular diet. [a]Significantly different from MRD diet; $P < 0.05$; [b]Significantly different from FRD; $P < 0.05$; [c]Significantly different from FHS; $P < 0.05$.

Table 2.3: Morphometric determination from electron microscopy images of content for ratios for elastin, collagen and vascular smooth muscle cell (VSMC) from third-order mesenteric blood vessels fixed at 13.33 KPa (1 mmHg = 0.1333 KPa) obtained from Dahl salt-sensitive male and female rats on regular or high salt (4% NaCl) diets for 6–7 weeks.

	SSM (R diet)	SSM (HS diet)	SSF (R diet)	SSF (HS diet)
Collagen/Elastin	2.68 ± 1.0	2.42 ± 0.6	3.14 ± 0.7	1.86 ± 0.2
VSMC/Collagen	3.23 ± 0.7	2.75 ± 0.3	2.27 ± 0.5	2.75 ± 0.3
VSMC/Elastin	6.96 ± 1.7	5.99 ± 0.9	6.18 ± 1.0	5.05 ± 0.8

Each value is expressed as a mean ± s.e.m. (n = 5).FHS, female high salt diet; FRD, female regular diet; MHS, male high salt diet; MRD, male regular diet.

2.4.3 Vascular Mechanics

The composite Young's modulus, a measure of vascular stiffness independent of geometry, was found not to be significantly altered in the 3rd order mesenteric blood vessels among the experimental groups (Figure 2.3A). However, in the presence of a vasoconstrictor, phenylephrine (0.3 μM), the composite Young's modulus was significantly higher in blood vessels from males on high salt compared to males on regular diets and the corresponding females (Figure 2.3B). The presence of the vasodilator and NO donor, sodium nitroprusside (0.3 μM), resulted in a significant reduction in the composite Young's modulus in blood vessels of males on regular and high salt diets compared to the corresponding values in females (Figure 2.3C).

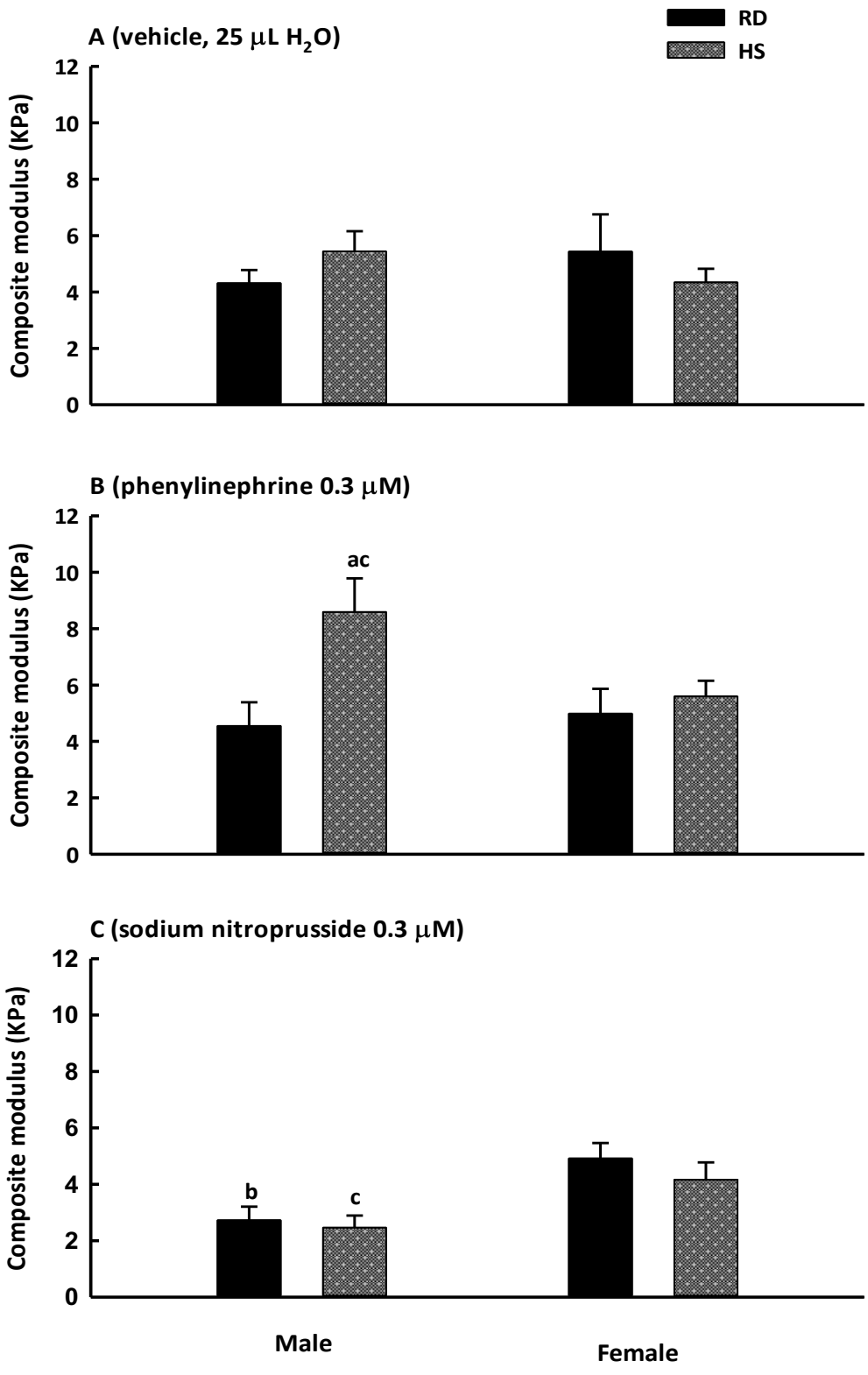
RD
HS
A (vehicle, 25 μL H2O)
B (phenylinephrine 0.3 μM)
C (sodium nitroprusside 0.3 μM)
Composite modulus (KPa)
0
2
4
6
8
10
12
ac
b
c
Male
Female

Figure 2.3: Calculated values of composite Young's modulus (Kpa) using stress-strain plots in isolated third-order mesenteric arteries at various intravascular pressures from Dahl salt-sensitive male and female rats on regular or high salt (4% NaCl) diets for 6–7 weeks. Each value is expressed as a mean ± s.e.m. (n = 8). FHS, female high salt diet; FRD, female regular diet; MHS, male high salt diet; MRD, male regular diet. [a]Significantly different from MRD; $P < 0.05$; [b]Significantly different from FRD; $P < 0.05$; [c]Significantly different from FHS; $P < 0.05$.

The evidence from pressure-volume curves in the 3rd order mesenteric arteries revealed significant elevation in the volume at the two highest pressures in males on high salt compared to males on regular diets and the corresponding values in females (Figure 2.4A). There were no significant differences between pressure-volume curves for females due to diet. In the presence of the vasoconstrictor, phenylephrine (0.3 μM), a significantly higher volume was observed with females on high salt diet compared to those on regular diets, at the two higher pressures (Figure 2.4B). Also, a significantly higher volume was observed at the highest pressure in males on HSD with PE treatment compared to the corresponding females on regular diet and females on HSD (Figure 2.4B). The presence of vasodilator, sodium nitroprusside (0.3 μM), caused significant increases of volume in response to the two highest pressures in males on regular diet compared to corresponding females on regular diet (Figure 2.4C). It was evident that at the two highest pressures, significant increases in volume were observed in blood vessels from male compared to the corresponding females on high salt diet (Figure 2.4C).

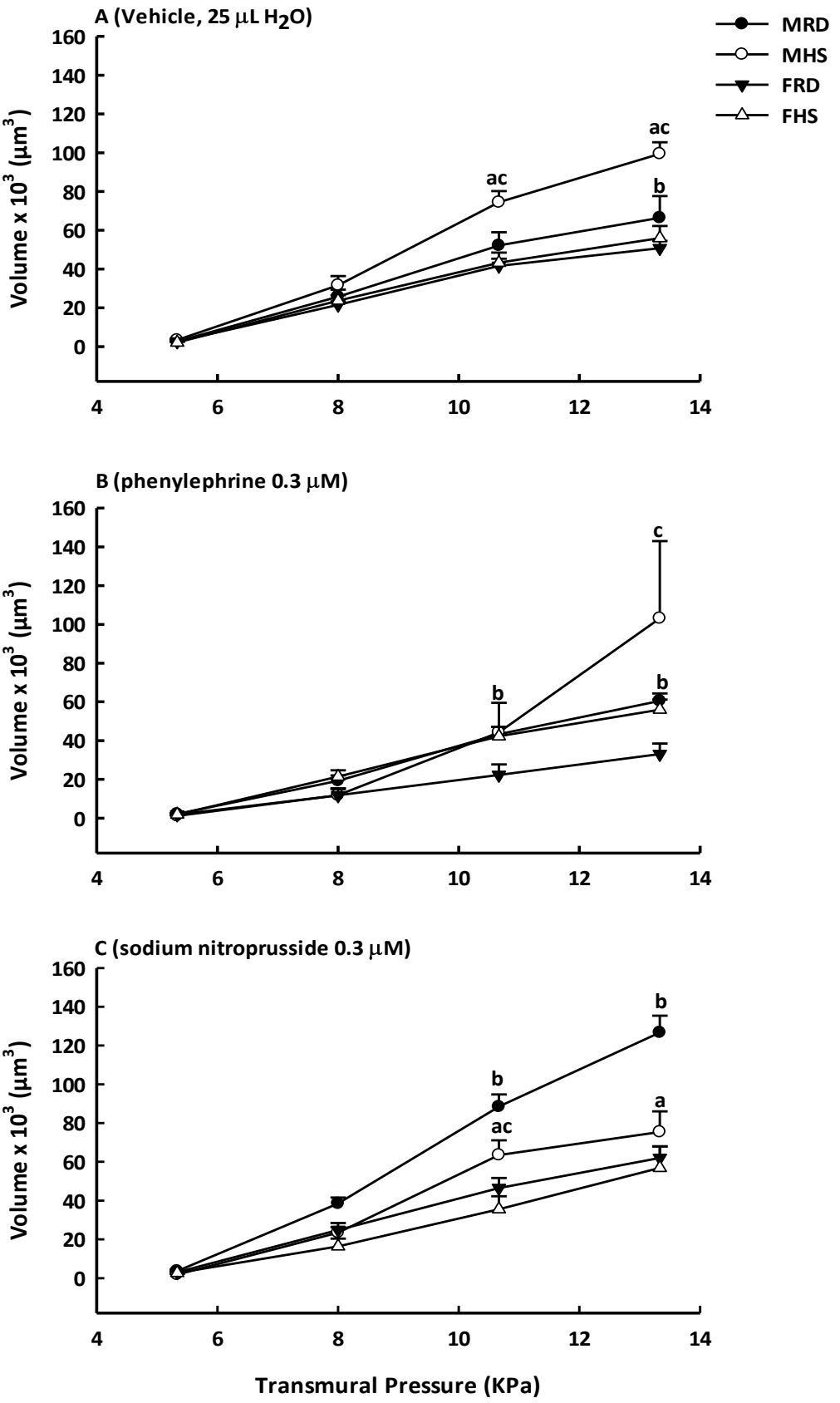
A (Vehicle, 25 μL H2O)
MRD
MHS
FRD
FHS
Volume x 10^3 (μm^3)
ac
ac
b
B (phenylephrine 0.3 μM)
c
b
b
C (sodium nitroprusside 0.3 μM)
b
b
a
ac
Transmural Pressure (KPa)

Figure 2.4: Pressure-volume plots in isolated pressurised third-order mesenteric arteries from Dahl salt-sensitive male and female rats on regular or high salt (4% NaCl) diets for 6–7 weeks. Each value is expressed as a mean ± s.e.m. (n = 8). FHS, female high salt diet; FRD, female regular diet; MHS, male high salt diet; MRD, male regular diet. [a]Significantly different from MRD; $P < 0.05$; [b]Significantly different from FRD; $P < 0.05$; [c]Significantly different from FHS; $P < 0.05$.

The calculated slope from the pressure-volume curves revealed significantly greater distended vascular compliance in males on high salt compared to males on regular diets, and the corresponding females on high salt diet (Figure 2.5A). The presence of phenylephrine (0.3 μM) did not significantly affect vascular compliance in males on regular compared to high salt diets (Figure 2.5B). In contrast, phenylephrine significantly increased compliance in blood vessels of females on high salt compared to regular diets (Figure 2.5B). The presence of sodium nitroprusside (0.3 μM) significantly reduced vascular compliance in males on high salt compared to regular diets (Figure 2.5C). The latter vasodilator also significantly increased vascular compliance in males on regular diet compared to the corresponding values in females also supporting the differential nature of the pressure-volume relationships in different sexes (Figure 2.5C).

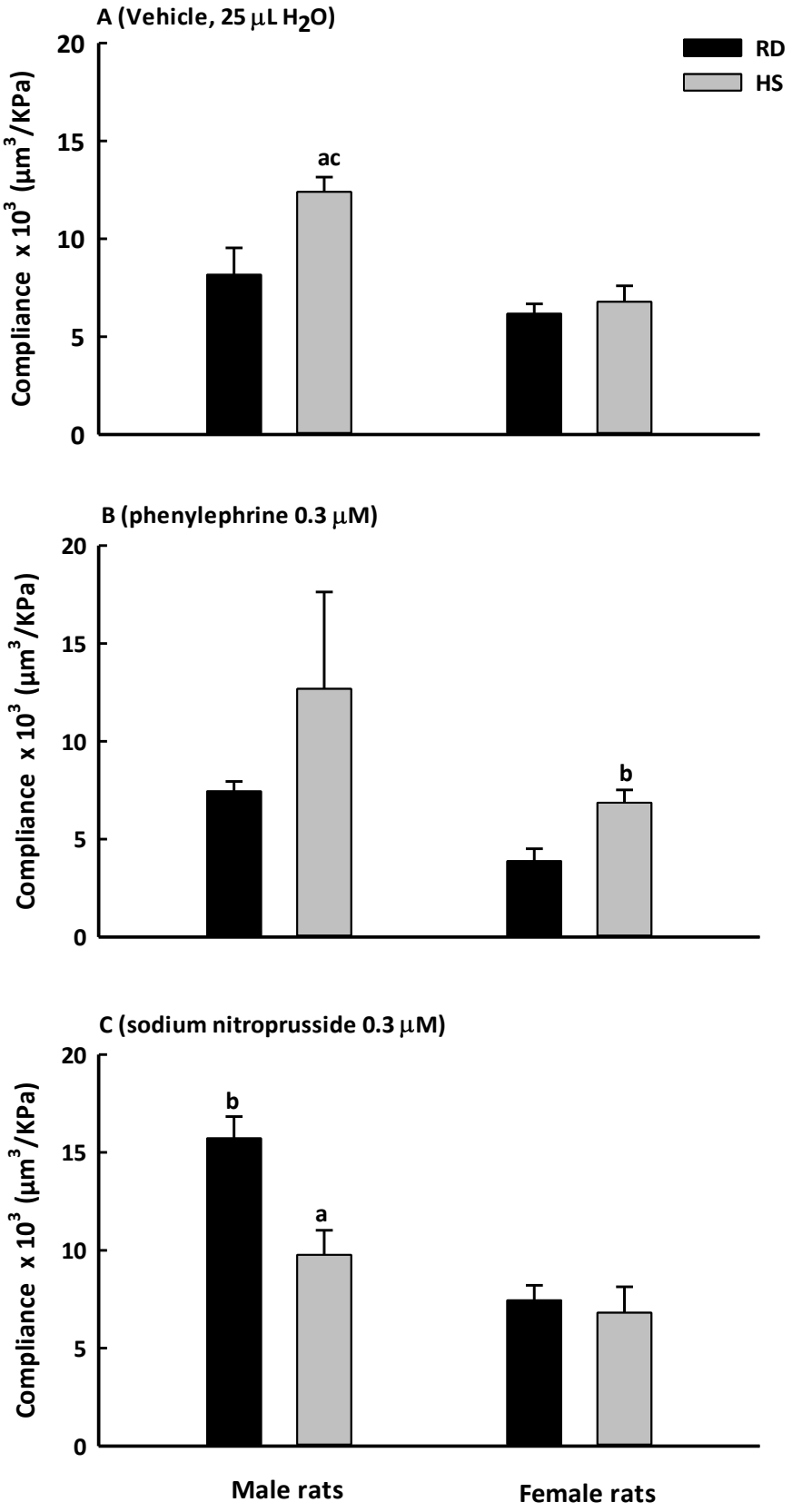
A (Vehicle, 25 μL H2O)
RD
HS
Compliance x 10³ (μm³/KPa)
20
15
10
5
0
ac
B (phenylephrine 0.3 μM)
b
C (sodium nitroprusside 0.3 μM)
b
a
Male rats
Female rats

Figure 2.5: Calculated values of compliance from pressure-volume plots in isolated third-order mesenteric arteries from Dahl salt-sensitive male and female rats on regular or high salt (4% NaCl) diets for 6–7 weeks. Each value is expressed as a mean ± s.e.m. (n = 8). FHS, female high salt diet; FRD, female regular diet; MHS, male high salt diet; MRD, male regular diet. [a]Significantly different from MRD; $P < 0.05$; [b]Significantly different from FRD; $P < 0.05$; [c]Significantly different from FHS; $P < 0.05$.

2.5 Discussion

Arterial wall stiffness results from complex interactions that involve structural and cellular elements, and whose changes are responsible for maintaining the mechanical properties of the arterial wall. The consequence of the alteration in the properties of load-bearing components of the arterial wall is the modifications of its mechanical characteristics which are influenced by both intrinsic and extrinsic factors, such as sex differences and nutritional content (Díez, 2007; Grillo et al., 2019; Manrique et al., 2016; Nichols et al., 2007; Zieman et al., 2005). Arterial stiffness and the resultant hemodynamic changes are now considered to be predictors of increase in morbidity and mortality; arterial stiffness is positively associated with increased risk of cardiovascular disease, including hypertension, myocardial infarction, heart failure, stroke (Kim et al., 2019; Mitchell et al., 2010; Said et al., 2018; Vasan et al., 2019; Zoungas & Asmar, 2007). Moreover, differential characteristics of the development of arterial stiffness between men and women appear to involve sex-specific mechanisms (Collier et al., 2011; Coutinho et al., 2013; DuPont et al., 2019; Guajardo et al., 2018; Nishiwaki et al., 2014).

Our investigation in Dahl salt-sensitive rats suggests that increased high salt consumption in the diet induced a significant increase in both central and peripheral (systolic and diastolic) blood pressures, and heart rate of both males and females. However, the central and peripheral SBP and DBPs of the males were significantly higher than the corresponding female groups on high salt diet. This difference was absent in the male and female rats on a regular diet. Furthermore, the central pulse pressure, a surrogate of arterial stiffness, was elevated with increased salt consumption in males but not female animals. Sex-specific patterns have been reported in the association between high salt intake and arterial stiffness measured by PWV (Baldo et al., 2019; Coutinho et al., 2013; Wu et al., 2021). We found the PWV was significantly elevated in both

male and females on high salt compared to regular diet. However, PWV was also significantly greater in males than the corresponding females on high salt diet. Surprisingly, based on significant increase in the ratio of left ventricle plus septum to right ventricle in male on high-salt compared to all other groups, ventricular hypertrophy seems to only present in hypertensive males (Arnal et al., 1993; Kihara et al., 1985; Yuan & Leenen, 1991). The results suggest the significant increase in systemic arterial blood pressure and PWV but not pulse pressure may lead to the existence of accommodating circumstance in the circulatory system of females on high salt diet that circumvents ventricular hypertrophy.

Evidence from several studies indicate a direct relationship between sodium intake and systemic arterial blood pressure (Grillo et al., 2019; Louis et al., 1971; Vollmer et al., 2001). Accordingly, chronic consumption of high salt has been found to result in a significant increase in systemic arterial blood pressure linked to the onset of hypertension and increase morbidity and mortality (Meneely et al., 1961; Moreira et al., 2014; Sanders et al., 2005). In contrast, a decrease in salt consumption has been shown to decrease blood pressure, lower incidence of cardiovascular complications, and better health outcomes (Kawasaki et al., 1978; Vollmer et al., 2001; Ylitalo et al., 1976). Further, blood pressure responses to salt intake have also been reported to vary with sex and age (He et al., 2009; Myers & Morgan, 1983; Weinberger & Fineberg, 1991).

Vascular changes from the large elastic arteries to microcirculation are known to occur as a result of elevated blood pressure (Feihl et al., 2009; Grey et al., 2003; Struijker-Boudier, 2014). Several studies have reported thickening of the walls of elastic and muscular arteries, remodeling of small muscular resistance arteries causing in an increased wall to lumen ratio, as well as a reduction in the number of vessels in the microcirculation associated with elevated systemic arterial blood pressure (Lee & Smeda, 1985; Prewitt et al., 2002; Yannoutsos et al., 2014). Our

current findings show that there is structural remodeling in the third-order mesenteric vascular bed of the male group i.e., an increase in collagen and smooth muscle component of the vascular wall. An effect that was absent in the parallel female group. Under normal physiological conditions, VSMCs are embedded in an elastin-rich extracellular matrix localized primarily in the media of the vascular wall. In hypertension, there is an increase in collagen synthesis and subsequent VSMC proliferation and migration that has been reported in the mesenteric and other vascular beds of several rat strains in response to increased stress on the vessel wall (Briones et al., 2006; Nissen et al., 1978; Robert et al., 1994).

In contrast to the increased deposition of collagen due to the elevation of arterial blood pressure, collagen fibers are engaged over time at higher intravascular pressures to support passive tension resulting in increased vessel wall stiffening. Evidence in the literature also suggest that during elevated blood pressure, VSMCs undergo hyperplasia and hypertrophy, which is crucial for vascular remodeling and subsequent increase in the total peripheral resistance in response to stress from higher blood pressure (Brown et al., 2018). In our present investigation, the increase in vessel wall media thickness, cross-sectional area, and increased media/lumen ratios suggest the possible development of hypertrophy and eutrophic remodeling associated with elevated blood pressure due to the consumption of high salt diet. The consequence of such modifications is an alteration of the stress/strain characteristics of the vessel wall, compliance, and composite Young's modulus, which may predispose the circulatory tree to abnormal behavior and hence, risks related to cardiovascular morbidity and mortality.

Morphological and physiological (functional) changes in the vasculature have been reported to occur during hypertension (Barbaro et al., 2015; Linde et al., 2012). Salt-induced changes in vascular function is a consequential and/or contributing factor to the remodeling of the arterial

wall that underlies elevated blood pressure. Our results from the pressure-volume curves reveal significantly greater distended vascular compliance in hypertensive (high salt diet) than normotensive (regular diet) males and the corresponding females on high salt diet. Our finding in these small resistance arteries is in contrast to other studies in large conduit vessels that suggest a decrease in compliance with hypertension due to the intake of high salt diet (Engberink et al., 2015; Intengan & Schiffrin, 1998; Kanbay et al., 2011; Kusche-Vihrog et al., 2015). Sympathetic neural control is involved in the modulation of large artery function and vasomotor control of small resistance arteries. The influence of sympathetic nervous system as well as those of the local vasoactive mediators on vascular function are crucial elements in the development hypertension and related cardiovascular events.

In our current investigation, vasoconstriction due to the action of phenylephrine did not significantly affect vascular compliance in males on a regular compared to high salt diets. In contrast, phenylephrine significantly increased compliance in vessels of females on high salt compared to regular diets, likely due to the initial smaller lumen size diameter in males. Vasodilation using a NO donor, sodium nitroprusside, significantly reduced vascular compliance in males on high salt compared to regular diets. Furthermore, vasodilation significantly increased vascular compliance in males compared to females on regular diet. However, there was a significant decrease in vascular compliance in male compared with female on salt diet in the presence vasodilator, sodium nitroprusside, supporting the view that initial lumen diameter is likely responsible for the observed differences in vascular compliance over the pressure range in our investigation. The observed results may be due to differences in salt sensitivity and NO regulation between sexes as a result of the impact of hormonal regulation of endothelial function (Eisenach et al., 2012).

The composite elastic Young's modulus, a measure of vascular stiffness independent of geometry, was not significantly altered in the 3rd order mesenteric blood vessels among the experimental groups under baseline conditions. This is perhaps not surprising as we noted that the ratios of the various components (i.e., collagen/elastin, VSM/collagen, VSMC/elastin) of vascular wall were significantly different in animals fed regular versus high salt diets. However, in the presence of a vasoconstrictor (phenylephrine), the composite Young's modulus was significantly higher in blood vessels from males on high salt than males on regular diets and the corresponding females. This can likely be attributed to the combination of functional (i.e., pharmacomechanical coupling) and morphological changes (VSMC proliferation) in blood vessels of male animals on high salt diet (Anderson et al., 1989; Carlson et al., 2000; Velez-Roa et al., 2004).

In our studies, the presence of the exogenous nitric oxide donor, sodium nitroprusside, resulted in a significant reduction in the composite Young's modulus in blood vessels of males on regular and high salt diets compared with the corresponding values in females. Accordingly, such a response would be expected to mask the role of the active component of the vascular wall in modulating vascular function. The outcome may support the view that vascular tone is elevated *in vivo* due to reduction in endothelial cell function with increased salt consumption. The latter alteration in function may accentuate vascular stiffness due to the presence of vasoconstrictors even though under baseline condition composite Young's modulus was noted to be unchanged in animals fed a high salt diet. Moreover, this is an effect that seems to be suppressed in females perhaps due to the presence of other vasculoprotective factors such as sex steroid hormones.

In summary, our findings suggest the link that exits between high salt diet and elevated blood pressure is sex specific. It likely involves sex-dependent changes in the ultrastructure of the blood vessel which ultimately could alter the biomechanics. Moreover, it is likely that both high salt intake and pressure play a role in the vascular remodelling, and the combination seem to produce a greater effect in male compared with female animals in our study. It is also possible that the haemodynamic functions of both micro-circulation and macro-circulation may lead to additive detrimental outcomes, and this is a novel concept that requires systematic clinical investigation.

2.6 Perspective

The Windkessel property of the large arteries is a fundamental determinant of the relationship between the pulsatile pressure and flow, enabling a steady flow in the microcirculation for efficient perfusion of organs and tissues. It is recognized that the resistance vessels serve not only as the site for vascular resistance, but also as an origin of wave reflections generating increased central systolic pressure. Accordingly, increase in vascular stiffness is an adaptive response to an increase in hemodynamic stress, and the comparative study of the structural and mechanical alterations of resistance vessels in males and females are essential for a better understanding and insight of sex differences in the circulatory system. The increase in arterial stiffness of large arteries results in a combination of reduced storage capacity of the arteries during systole and wave propagation along the arterial tree. The consequence is an increase in ventricular load and hypertrophy and elevated blood pressure, pulse pressure and PWV. The downstream effect is a reduction in tissue perfusion by the resistance arteries, which are predictors of cardiovascular morbidity and mortality. Crosstalk between the micro- and macro-circulation plays a vital role in regulating vascular hemodynamics. A disruption in function of the microvascular circulation can trigger a change in structural and mechanical alterations of the microcirculation, which can be corrected with certain pharmacological agents that produce vasodilation to reduce workload and dampen wave reflection, but such an approach may need to be different based on sex.

Chapter 3 Effects of vasoactive substances on the biomechanics of small resistance arteries of male and female Dahl salt-sensitive rats

3.1 Abstract

Changes in vascular biomechanics leading to increase in arterial stiffness play a pivotal role in circulatory dysfunction. Our objectives were to examine sex-specific pharmacological changes related to the biomechanics and any structural modifications in small resistance arteries of Dahl salt-sensitive male and female rats. The composite Young modulus (CYM) was determined using pressure myograph recordings, and immunohistochemistry was used for the evaluation of any structural changes in the third-order mesenteric arteries ($n = 6$). Animals on high-salt diet developed hypertension with significant elevation in central and peripheral blood pressures and pulse wave velocity compared to those on regular diet. There were no significant differences observed in the CYM between any of the groups (i.e., males and females) in vehicle-treated time-control studies. The presence of verapamil (0.3 μM) significantly reduced CYM in hypertensive males without changes within females compared to vehicle. This effect was abolished by phenylephrine (0.3 μM). $BaCl_2$ (100 μM), ouabain (100 μM), and L-NAME (0.3 μM) combined significantly increased CYM in vessels from in normotensive males and females but not in hypertensive males compared to vehicle. The increase in CYM was abolished in the presence of phenylephrine. Sodium nitroprusside (0.3 μM), in the presence of phenylephrine, significantly reduced CYM in male normotensive versus hypertensive, with no differences within females. Significant differences were observed in immunohistochemical assessment of biomechanical markers of arterial stiffness between males and females. Our

findings suggest sex possibly due to pressure differences to be responsible for adaptive changes in biomechanics, and varied pharmacological responses in hypertensive state.

3.2 Introduction

Alterations in the mechanical characteristics of the arterial wall occur when an initial adaptive mechanism becomes maladaptive with resulting vascular complications (Cecelja & Chowienczyk, 2012; Mozos et al., 2017; Veerasamy et al., 2014). The interactions between structural and dynamic components of the vessel wall are vital in providing the structural and mechanical properties required for proper vascular function (Intengan & Schiffrin, 2000; Ribeiro-Silva et al., 2021), with the dysregulation of each component being crucial to the vessel wall remodeling process. Hence, alterations in the biomechanics and the ensuing malfunction of the arterial wall have emerged as an important risk factor for future cardiovascular events in males and females (Cecelja & Chowienczyk, 2012; Mozos et al., 2017; Veerasamy et al., 2014). There are, however, sex-specific differences in arterial stiffness, which are suggested to be intrinsic and influenced by many factors, including sex hormones (Colafella & Denton, 2018; DuPont et al., 2019; Rossi et al., 2011). Although several mechanisms have been suggested to be involved in the development of arterial stiffness, there remains many gaps in our knowledge of the mechanistic differences and factors involved in arterial remodeling in males versus females. We recently reported structural alterations to the vessel wall with increased collagen and vascular smooth muscle cell (VSMC) in the small mesenteric arteries of hypertensive male rats compared to normotensive or their corresponding female rats (Mensah et al., 2022). Our findings from assessing the vessel wall mechanics using phenylephrine (vasoconstrictor) and sodium nitroprusside (vasodilator) suggest sex-specific mechanisms is likely involved in changes in the ultrastructure of the vessels. These sex-specific structural alterations alter biomechanics and hemodynamics (Mensah et al., 2022).

Resistance arteries serve as a crucial site for blood pressure regulation, and this effect depends on the contractile state of the arterial VSMCs (W. F. Jackson, 2021; Jiang et al., 2016). Moreover, L-type voltage-operated Ca channels play an important role in the development of blood vessel tone, making them an important target in regulating vasoconstriction and peripheral resistance (Thompson & Khalil, 2003; Tykocki et al., 2017). Accordingly, sex-differences may exist in vascular biomechanics due to functional alterations in voltage-operated calcium channels that have yet to be investigated. Furthermore, arterial remodeling seems to be initiated by myriad of complex mechanisms that affect the structural, as well as the dynamic components of the arterial wall (e.g., endothelial cells), where sex-differences may exist (Cecelja & Chowienczyk, 2012; Mozos et al., 2017). Several marker proteins, including matrix metallopeptidase 9 (MMP-9), nicotinamide adenine dinucleotide phosphate (NADPH) oxidase and β1 integrin, have been reported to modulate the mechanisms involved in the development and progression of arterial stiffness through alterations in extracellular matrix (ECM), oxidative stress, endothelial permeability and adherence and VSMC stiffening (Hays et al., 2018; Sanchez et al., 2006; Yasmin et al., 2005; Yun et al., 2016). The possibility that changes in vascular biomechanics due to sex differences are associated with alterations in MMP-9, NADPH and/or β1 integrin levels in small resistance arteries is yet to be determined.

Thus, our working hypothesis was that differential changes of biomechanics in small mesenteric resistance arteries (~220 μm) of male compared to female salt-hypertensive animals will be of both structural and functional nature. Therefore, the primary aim of our investigation was to examine whether males and females differ in response to salt-induced hypertension in terms of the degree of hypertension produced and whether this is reflected in pharmacological

responses in isolated blood vessels. The secondary goal was to determine any underlying structural alterations using immunohistochemistry.

3.3 Materials and Methods

3.3.1 Animals:

All procedures on animals were carried out in accordance with the guidelines of the Canadian Council on Animal Care, with the approval of the Institutional Animal Care Committee of Memorial University of Newfoundland and the Canadian Council of Animal Care (Guide to care and Use of Experimental Animals, Vol 1, 2nd Edition). Male and female Dahl salt-sensitive rats (age 5–6 weeks) were purchased from Charles River Laboratories (Saint Constant, QC, Canada), housed two per cage, and were kept in a temperature-controlled environment (22 ± 2°C) on a 12 h–12 h light–dark cycle. They were given access to normal tap water and standard chow (regular) or high-salt diet containing 4% NaCl (Zeigler Bros., Inc. Gardners, PA, USA) ad libitum for 6–7 weeks (approximately 84–91 days of life).

3.3.2 Experimental Design:

Each animal (age 12–14 weeks) was anesthetized (induction 5% isoflurane in 100% O_2, maintenance 1.25%–1.5% isoflurane in 100% O_2), and was injected with the analgesic, buprenorphine (0.01 mg/kg, s.c.). The core body temperature was maintained at 37 ± 1°C using a heating lamp and monitored with a rectal thermometer. The external iliac and carotid arteries were isolated and catheterized using polyethylene tubing (I.D. 0.58 mm, O.D. 0.965 mm [9 cm] connected to I.D. 0.28 mm, O.D. 0.61 mm [7 cm]). The catheters were advanced forward (approximately 2 cm) such that the catheter in the femoral artery was just at the distal end of the abdominal aorta while the catheter in the carotid artery was just beyond the aortic arch and in the

proximal end of the thoracic aorta (Leblanc & Tabrizchi, 2018). All catheters were filled with heparinized normal saline (25 iu/mL). Central (aortic) and peripheral (femoral artery) blood pressure, as well as heart rate, were continuously recorded by AcqKnowledge (3.9.1.6) software (Biopac Systems Inc., Goleta, CA, USA) with a pressure transducer (P23XL; Spectramed Statham; Viggo-Spectramed, Oxnard, CA, USA) for 20–25 min. The signals were amplified (DA 100A; Biopac Systems Inc., Goleta, CA, USA), where the amplifier was connected to a universal interface module (UIM 100; Biopac Systems Inc., Goleta, CA, USA), and to an acquisition unit (MP100; Biopac Systems Inc., Goleta, CA, USA). The analog output signal was then converted to a digital signal (USB1W; Biopac Systems Inc., Goleta, CA, USA), and displayed in AcqKnowledge (3.9.1.6). Animals were euthanized by anesthetic overdose and thoracotomy. The mesenteric arteries were removed and prepared for functional and histological studies. The heart of each animal was excised, and the right ventricle and left ventricle plus septum were separated and weighed. In addition, the length between the carotid artery catheter and the femoral artery catheter was measured at post-mortem, and pulse wave velocity (PWV) was then calculated with the following formula $PWV = d/\Delta t$ (Leblanc & Tabrizchi, 2018).

3.3.3 Pressure Myograph Experiments:

All chemicals used in the pressure myograph experiments were purchase from Sigma Aldrich (Montreal, Canada) unless otherwise stated. The mesenteric bed was placed in a dissecting dish containing modified Krebs buffer with the following composition (mM): 120 NaCl, 4 KCl, 1.2 $MgCl_2.6H_2O$, 1.5 $CaCl_2H_2O$, 25 $NaHCO_3$, 1.2 KH_2PO_4, and 0.1 EDTA in an oxygenated (95% O_2 and 5% CO_2) environment. The third-order branch of the mesenteric artery was determined to be the third branch off the superior mesenteric artery of the gut. A length of approximately 5

mm was isolated and carefully cleaned of surrounding tissues under a dissecting microscope as described by Jadeja et al (Jadeja et al., 2015).

The mechanical properties of isolated third-order mesenteric arteries were studied with a pressure myograph. Isolated vessels were mounted onto the Single Vessel Chamber component of the Pressure Servo System (Living system instrumentations, Model CH-1-SH/CH-1-QT P100, St. Albans City, VT, USA) for the pressure myograph studies. In detail, the isolated third -order mesenteric artery were mounted on two glass micropipettes, secured with 0.2 metric (10-0) surgical nylon suture obtained from CovidienTM . The vessel length was adjusted so that the vessel walls were parallel and without stretch. Intraluminal pressure was then set to a baseline pressure of 3.9 KPa (30 mmHg) and allowed to equilibrate for 20 min at 37 ± 1°C in a modified Krebs buffer gassed with a mixture of 95% O_2 and 5% CO_2.

Vascular response was imaged using an inverted microscope Accu-Scope 3032 (Accu-Scope INC, NY, USA) and measured using a Video Dimension Analyzer (Living Systems Instrumentation, VT, USA) and the iWORX Data Recording Software (Dover, NH, USA). Six different groups of experiments were undertaken in assessment of the mechanical function of the blood vessel with different interventions: (i) equivalent volume (24 µL) of vehicle (distilled water) time-control, (ii) verapamil (0.3 µM), (iii) phenylephrine (0.3 µM) plus verapamil (0.3 µM), (iv) $BaCl_2$, (100 µM), ouabain (100 µM) and L-N^{ω}-Nitro arginine methyl ester (0.3 µM) combined, (v) phenylephrine (0.3 µM) plus $BaCl_2$, (100 µM), ouabain (100 µM) plus L-N^{ω}-Nitro arginine methyl ester (0.3 µM) combined, and (vi) phenylephrine (0.3 µM) plus sodium nitroprusside (0.3 µM). Five minutes after the additions of the vasoactive agents or vehicle, intraluminal pressure was raised stepwise at an increasing transmural pressure of 5.3, 7.9, 10.6, and 13.3 Kpa to obtain a pressure-diameter (D) curve. For each vessel, the thickness of the left

wall (LW) and right wall (RW) were also measured. In another group of experiments isolated third order mesenteric arteries were pressure-fixed (7.9 KPa), without the presence of any vasoactive agents, with Karnovsky fixative at 37 ± 1°C for 30 min for immunohistochemistry studies.

3.3.4 Tissue immunofluorescence

Isolated third-order mesenteric vessels were pressure-fixed in formalin and embedded in the paraffin wax. The paraffin-embedded vessels were sliced into 6 μm sections using a cryotome (Fisher Scientific, Pittsburgh, PA, USA), placed on charged slides (4–6 slices/slide), and stored at −20°C until processed for immunofluorescence (IF) studies. The expression of the following proteins was tested: MMP9 (Anti-MMP9 antibody [EP1254] ab76003 (1:200); Abcam, MA, USA), NADPH (Anti-NADPH oxidase 4 antibody [UOTR1B493] ab133303 (1:100); Abcam, MA, USA), and integrin beta 1 (Anti-Integrin beta 1 antibody [EPR16895] ab179471 (1:250); Abcam, MA, USA). For day 1 of testing, the slides were thawed, deparaffinized using, two washes of xylene (10 min each), 1:1 Xylene:100% Ethanol, 100% ethanol, 95% ethanol, 70% ethanol, 50% ethanol, and washed in 1 × PBS (5 min each). All antibody staining required heat-mediated antigen retrieval with citrate buffer pH 6.0 at 100°C for 30 min (for anti-MMP9 and -NADPH oxidase 4 antibodies) and Tris/EDTA buffer pH 9.0 at 100°C for 30 min (for Anti-Integrin beta 1 antibody) and allowed to cool down at room temperature for 20 min and washed in 1 × PBS (5 min each at room temperature) before tissue permeabilization and blocking. The blocking solutions consisted of 10% normal goat serum (NGS) with 0.1% Triton-X in 1 × PBS, incubated for 1 h at room temperature. Following the wash step (2 × PBS for 10 min at room temperature), the samples were incubated with the primary antibodies for the proteins of interest at the concentrations indicated above.

For day 2 of testing, after five washes (2 × PBS for 10 min at room temperature), sections were incubated with secondary antibody [Cy5-Goat Anti-Rabbit (1:200) for Anti-MMP9; Cy5-Goat Anti-Rabbit (1:250) for NADPH oxidase 4 and Cy5-Goat Anti-Rabbit (1:200) for Anti-Integrin beta 1; all Cy5 conjugated antibodies were from Jackson Immunoresearch, PA, USA]. 4′,6-diamindino-2-phenylindole [DAPI (1:1000); ThermoFisher Scientific, ON, CAN] was used as a nuclear counterstain.

For all the immunofluorescence staining, stacks of images at 1 μm increments (a total of 10 slices) were collected for a Z-stack using Zeiss LSM900 with airyscan 2 with Zen Blue software. Semi-quantitative analysis of the images was done using ImageJ software (US National Institutes of Health), and a step-by-step protocol outlined by (Crowe & Yue, 2019) was used to determine the mean gray value (MGV) of the vessel for the various antibodies used as the average pixel intensity of the IHC threshold image (Mean).

3.3.5 Calculation of mechanical parameters

The luminal diameter at baseline D_0, left LW and RW were measured at various intraluminal pressures, (5.3329, 7.9993, 10.6658, and 13.3322 KPa) using a video frame capture and real-time edge-detection system available with the Video Dimension Analyzer. The wall thickness (WT) was calculated using the following formula: WT = (LW+RW)/2.

Vascular compliance (C), which is the ability of a vessel to distend and increase volume with an increasing transmural pressure is equal to changes in vessel volume ($\Delta V = \pi r2\ h$), divided by changes in transmural pressure (ΔP) (i.e., $C = \Delta V/\Delta P$).

The following mechanical parameters were calculated according to the methods by Intengan and Schiffrin (Intengan & Schiffrin, 1998). Circumferential wall strain (ε) = $(D - D_0)/ D_0$, where D_0

is the diameter at baseline transmural pressure and D is the observed luminal diameter for a given transmural pressure. Circumferential wall stress (σ) = (PD)/(2WT), where P is the intramural pressure, D and WT are the luminal diameter and wall thickness respectively.

To estimate the arterial stiffness independent of vessel geometry, the composite Young's modulus of the vessel was determined where Ec = stress/strain. The non-linear nature of the stress/strain relationship was compensated for by fitting the stress/strain data from each vessel to an exponential curve $y = ae^{bx}$ where $\sigma = \sigma_0 e^{x\beta}$ (plots of ln y vs. x), σ_0 is the stress at baseline transmural pressure and β is a constant directly proportional to Ec, related to the rate of increase of the stress/strain curve. An increase in β implies an increase in Ec (increase in stiffness).

3.3.6 Statistical analysis

The hemodynamics, composite Young's modulus, and compliance values, immunohistochemistry was analyzed using two-way analysis of variance (ANOVA) followed by Bonferroni test and/or one-way analysis of variance followed by Bonferroni test. The statistical analysis was carried out with the SigmaPlot statistical package (Systat Software, San Jose, CA, USA). The data are presented as means ± s.e.m., and the sample size is the number of animals used in each experiment (n = 6). A value of $P < 0.05$ was considered significant.

3.4 Results

The body weight of Dahl salt-sensitive female rats was significantly lower than that of the Dahl-salt-sensitive male rats in both groups (high salt & regular diets). There were no significant differences between the body weights within the groups (i.e., males and females); male regular diet: 318.3 ± 17.4 g, male high salt diet: 357.7 ± 26.7 g, female regular diet: 233.3 ± 6.1 g, and female high salt diet: 242.3 ± 4.8 g.

Hemodynamic values for the groups are presented in Table 3.1. Animals that consumed a high salt diet had a significantly elevated central, peripheral, systolic, and diastolic, blood pressures, independent of sex. There were no differences in the central and peripheral, systolic, and diastolic, blood pressures of male versus female on regular diet. The central and peripheral pulse pressures were significantly elevated following high salt consumption in males but not. PWV (an index of the large central arteries stiffness) became significantly elevated in both male and female animals on high salt compared to those on regular diet. However, we did find that PWV was significantly greater in males compared to corresponding females on high salt diet (Table 3.1).

Table 3.1: Hemodynamic measurements in Dahl salt-sensitive male and female rats on regular (R) or high salt (HS; 4% NaCl) diets for 6-7 weeks. Each value is expressed as a mean ± s.e.m. (n = 6)

Hemodynamic	Male (R diet)	Male (HS diet)	Female (R diet)	Female (HS diet)
HR (beats/min)	361 ± 14	387 ± 6	351 ± 14	362 ± 7
cSBP (mmHg)	131 ± 0.6	164 ± 2.4[ac]	134 ± 2.7	145 ± 1.0[b]
cDBP (mmHg)	95 ± 0.6	118 ± 3.1[ac]	96 ± 2.2	105 ± 0.7[b]
cPP (mmHg)	36 ± 0.3	46 ± 2.6[ac]	36 ± 0.9	40 ± 0.6
pSBP (mmHg)	128 ± 1.3	158 ± 2.5[ac]	131 ± 2.9	143 ± 0.8[b]
pDBP (mmHg)	92 ± 0.5	115 ± 2.2[ac]	93 ± 2.7	102 ± 0.7[b]
pPP (mmHg)	36 ± 1.2	43 ± 1.8[a]	37 ± 1.4	41 ± 1.3
PWV (m/sec)	4.8 ± 0.2	6.7 ± 0.4[ac]	4.4 ± 0.4	5.5 ± 0.3[b]

Abbreviations: cDBP, central diastolic blood pressure; cPP, central pulse pressure; cSBP, central systolic blood pressure; HR, heart rate; pDBP, peripheral diastolic blood pressure; pPP, peripheral pulse pressure; pSBP, peripheral systolic blood pressure; PWV, pulse wave velocity.

[a] Significantly different from Male R diet; $p < 0.05$

[b] Significantly different from Female R diet; $p < 0.05$

[c] Significantly different from Female HS diet; $p < 0.05$

The ratio of the left ventricle plus septum to right ventricle of males on high salt diet (6.0 ± 0.3), was significantly greater than that of the males on regular diet (4.8 ± 0.3), or female groups either on regular (4.6 ± 0.3) or high salt diets (4.5 ± 0.2). It is likely that the significant left ventricular hypertrophy found in males on high salt diet is due to greater increase in systemic arterial pressure as well as vascular stiffness (Table 3.1).

3.4.2 Vascular mechanics

There were no significant differences observed in the CYM between any of the groups (i.e., males and females) in vehicle-treated time-control studies (Figure 3.1A). The presence of verapamil (0.3 μM) significantly reduced the CYM in vessels from male animals on high salt compared to regular diets while no changes were noted in the corresponding female groups (Figure 3.1B). In addition, verapamil also significantly changed the CYM of blood vessels in male compared to the corresponding female animals on regular diet (Figure 3.1B). The presence of the vasoconstrictor, phenylephrine (0.3 μM), completely reversed the effects of verapamil in vessels from male animals leading to no significant differences among the groups (Figure 3.1C). A comparison of the percent changes of CYM in the presence of vasoactive agents to vehicle-treated tissues revealed that verapamil significantly decreased blood vessel stiffness in vessels from male on high salt compared to males or regular diet and females on high salt diet (Table 3.2).

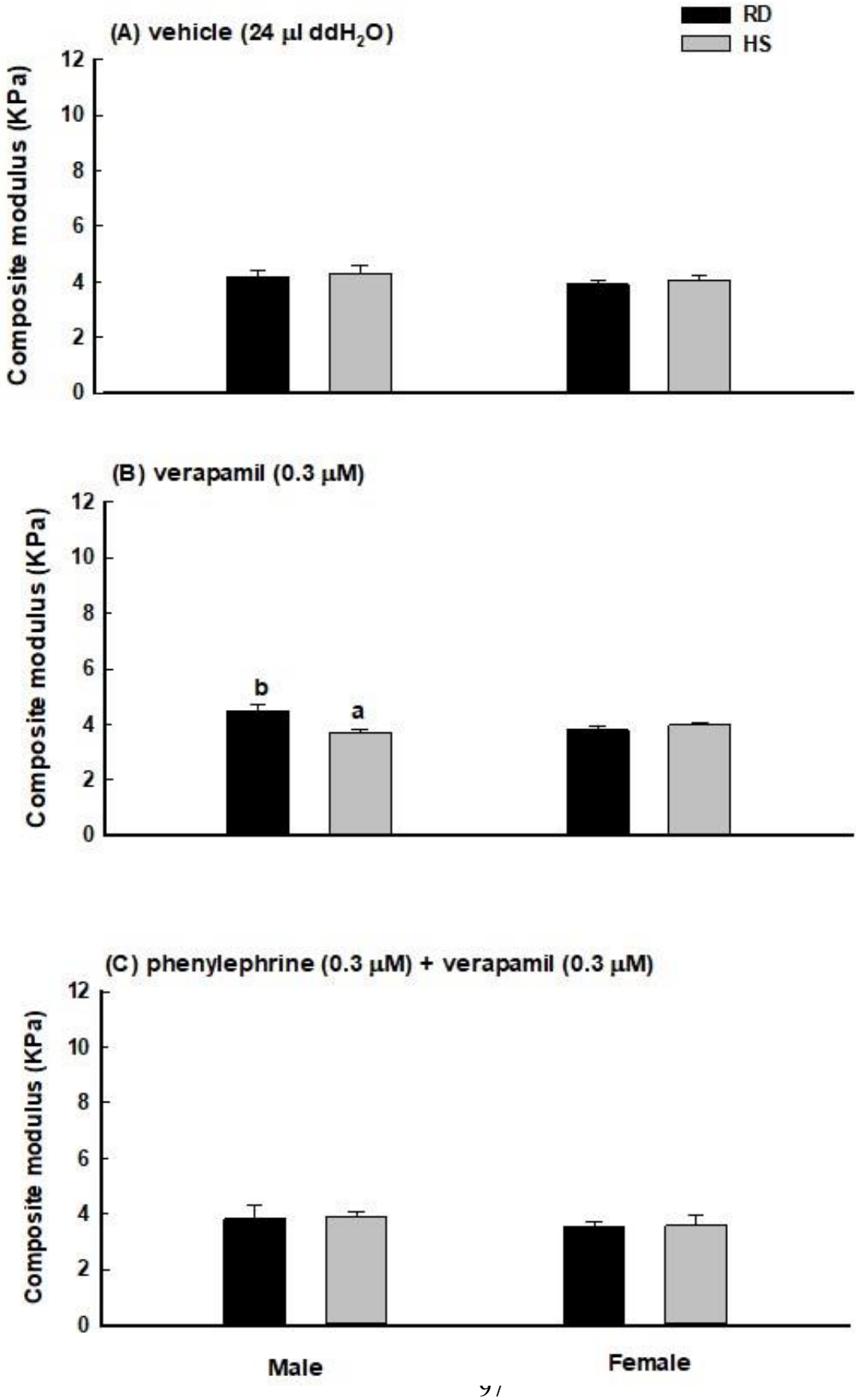
(A) vehicle (24 μl ddH2O)
RD
HS
Composite modulus (KPa)
12
10
8
6
4
2
0
(B) verapamil (0.3 μM)
b
a
(C) phenylephrine (0.3 μM) + verapamil (0.3 μM)
Male
Female

Figure 3.1: Calculated values of composite Young's modulus using stress–strain plots in isolated third-order mesenteric arteries at various intravascular pressures from Dahl salt-sensitive male and female rats on regular or high-salt (4% NaCl) diets for 6–7 weeks; time-control (A) presence of vehicle (B) verapamil (0.3 μM) and (C) phenylephrine (0.3 μM) plus verapamil (0.3 μM). Each value is expressed as a mean ± s.e.m. ($n = 6$). [a]Significantly different from Male RD; $p < .05$; [b]Significantly different from Female RD; $p < .05$. HS, high-salt diet; RD, regular diet.

Table 3.2: Percent changes in composite Young's modulus (CYM) from vehicle-treated mesenteric arteries from Dahl salt-sensitive male and female rats on regular (R) or high-salt (HS; 4% NaCl) diets for 6–7 weeks.

Treatment	SSM (R diet)	SSM (HS diet)	SSF (R diet)	SSF (HS diet)
Verapamil	-7.3 ± 6%	14.0 ± 2.5%[a]	2.8 ± 2.8%	2.5 ± 2.4%
PE+Verapamil	8.3 ± 12%	9.9 ± 4.7%	10.2 ± 4.9%	11.9 ± 8.6%
BOL	77.2 ± 16%	9.4 ± 2%[ab]	120 ± 33%	73 ± 8.5%
PE+BOL	-15.5 ± 3.7%	-53.5 ± 6.8%[ab]	-24.2 ± 6%	-22.9 ± 2.5%
PE+SNP	23.5 ± 2.8	-7.4 ± 8.9%[a]	23.2 ± 6.6%	8.6 ± 3%

The percent values were calculated from the respective mean average of vehicle-treated time-control group. Each value is expressed as a mean ± s.e.m. ($n = 6$). Verapamil (0.3 μM); Phenylephrine (PE) (0.3 μM); $BaCl_2$ (B) (100 μM) + Ouabain (100 μM) (O) + L-N^{ω}-nitro arginine methyl ester (L) (0.3 μM) (BOL); Sodium Nitroprusside (SNP) (0.3 μM).

[a] Significantly different from SSM R diet; $P < 0.05$

[b] Significantly different from SSF HS diet; $P < 0.05$

The presence of $BaCl_2$ (100 μM), ouabain (100 μM) and L-Nω-nitro arginine methyl ester (0.3 μM) combined, (i.e., attenuation of endothelia cell basal relaxing function), resulted in an increase in CYM in blood vessels from males on regular and females on regular and high salt diets but not males on high salt diet (Figure 3.2A). The presence of the vasoconstrictor, phenylephrine (0.3 μM), completely reversed the effects of $BaCl_2$, ouabain and L-Nω-nitro arginine methyl ester, resulting in no significant differences in the CYM in blood vessels of any of the groups, males or females (Figure 3.2B). In comparison, the addition of NO donor/vasodilator, sodium nitroprusside (0.3 μM), in the presence of the vasoconstrictor, phenylephrine (0.3 μM), caused significant reductions in the CYM in blood vessels within males on regular compared to high salt diets while no differences were found within females on regular and high salt diets (Figure 3.2C). Further, the CYM was significantly larger in males on high salt compared to females on high salt diet while no differences were noted between males versus females on regular diet, in the presence of phenylephrine and sodium nitroprusside combined (Figure 3.2C). In addition, inhibition of basal endothelial cell function by the presence of $BaCl_2$, ouabain and L-Nω-nitro arginine methyl ester resulted in significant increase in the stiffness of vasculature in males on regular diet and females on regular and high diets but not males on high salt diet (Table 3.2).

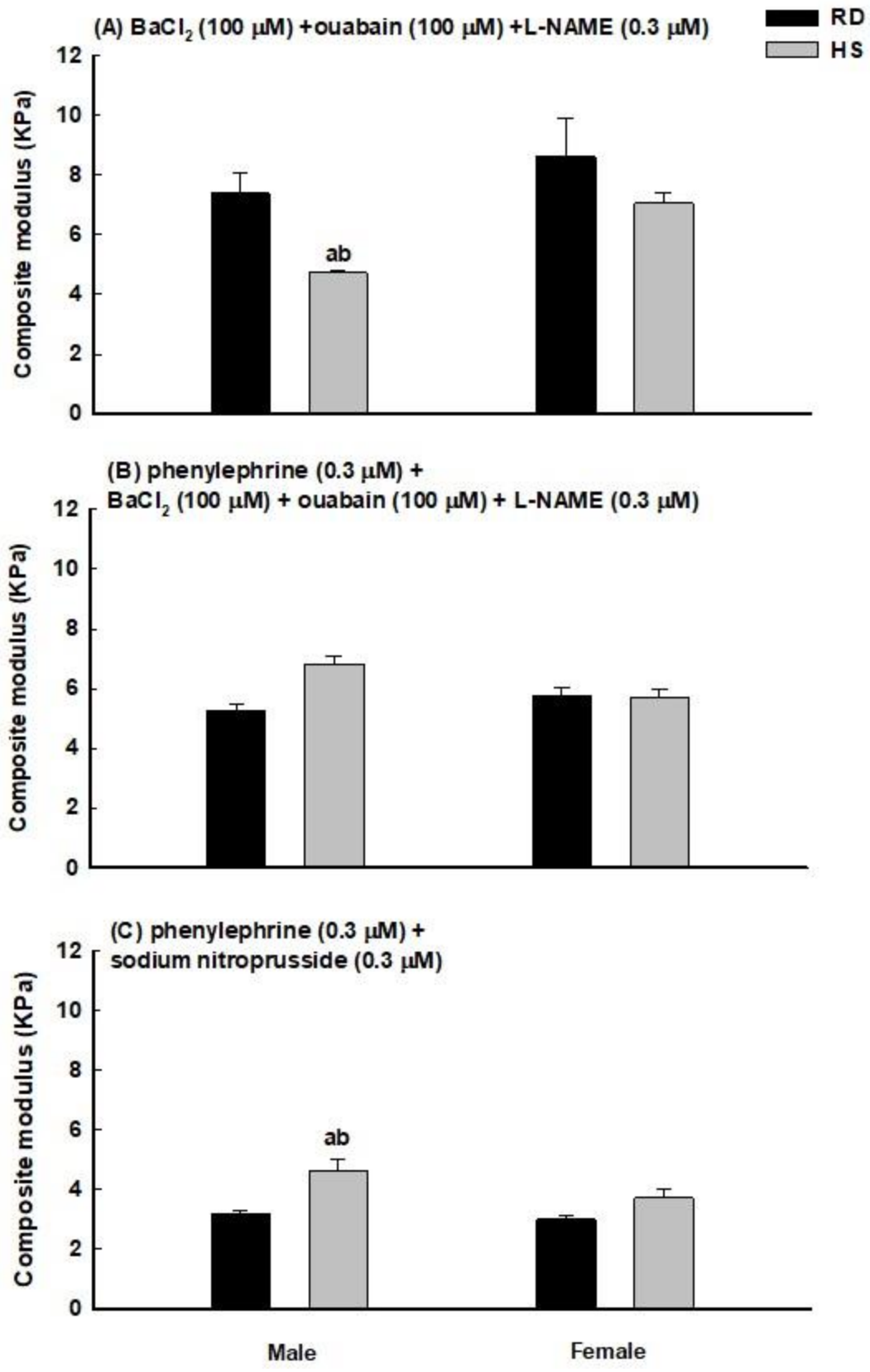
(A) BaCl2 (100 μM) +ouabain (100 μM) +L-NAME (0.3 μM)
RD
HS
Composite modulus (KPa)
12
10
8
6
4
2
0
ab
(B) phenylephrine (0.3 μM) +
BaCl2 (100 μM) + ouabain (100 μM) + L-NAME (0.3 μM)
Composite modulus (KPa)
(C) phenylephrine (0.3 μM) +
sodium nitroprusside (0.3 μM)
Composite modulus (KPa)
ab
Male
Female

Figure 3.2: Calculated values of composite Young's modulus using stress–strain plots in isolated third-order mesenteric arteries at various intravascular pressures from Dahl salt-sensitive male and female rats on regular or high-salt (4% NaCl) diets for 6–7 weeks in the presence of (A) $BaCl_2$ (100 μM) + ouabain (100 μM) + L-N^{ω}-nitro arginine methyl ester (L) (0.3 μM), (B) phenylephrine (0.3 μM) plus $BaCl_2$ (100 μM) + ouabain (100 μM) + L-N^{ω}-nitro arginine methyl ester (0.3 μM) and (C) phenylephrine (0.3 μM) plus sodium nitroprusside (0.3 μM). Each value is expressed as a mean ± s.e.m. ($n = 6$). [a]Significantly different from Male RD; $p < .05$; [b]Significantly different from Female HS; $p < .05$. HS, high-salt diet; RD, regular diet.

Calculation of compliance values in these vessels from pressure-volume curves indicates a significantly higher compliance of vessels in males on high salt diet compared to males on regular and the corresponding females on high salt diets (Figure 3.3A). Moreover, the presence of verapamil negated the greater level of compliance noted in males on high salt diet, while the presence of vasoconstrictor, phenylephrine, was able to reverse the effects of verapamil in vessels from males on high salt diet (Figure 3.3C).

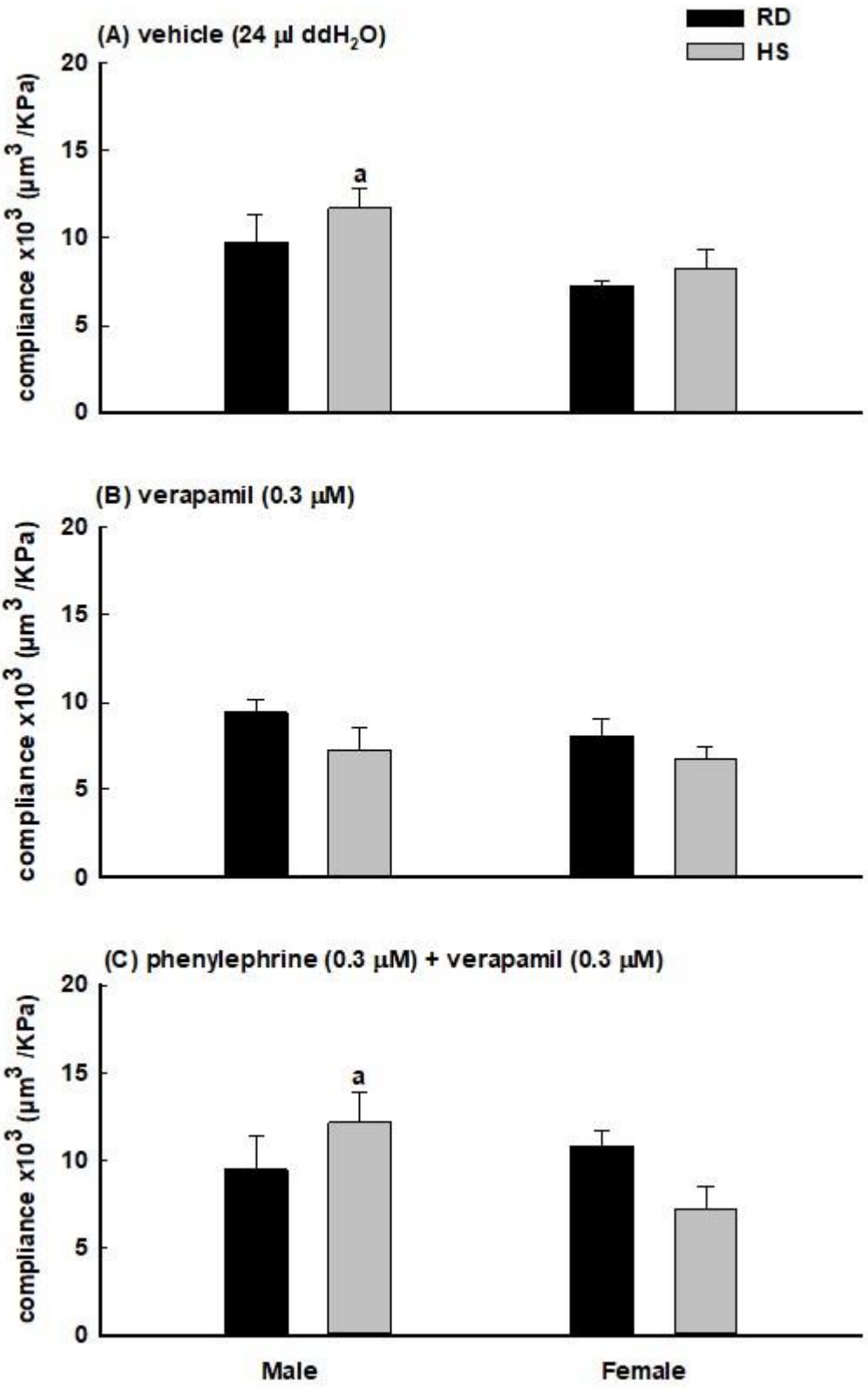
RD
HS
(A) vehicle (24 μl ddH2O)
compliance x10^3 (μm^3 /KPa)
20
15
10
5
0
a
(B) verapamil (0.3 μM)
compliance x10^3 (μm^3 /KPa)
20
15
10
5
0
(C) phenylephrine (0.3 μM) + verapamil (0.3 μM)
compliance x10^3 (μm^3 /KPa)
20
15
10
5
0
a
Male
Female

Figure 3.3: Calculated values of compliance from pressure–volume plots in isolated third-order mesenteric arteries from Dahl salt-sensitive male and female rats on regular or high-salt (4% NaCl) diets for 6–7 weeks; time-control (A) presence of vehicle (B) verapamil (0.3 μM) and (C) phenylephrine (0.3 μM) plus verapamil (0.3 μM). Each value is expressed as a mean ± s.e.m. ($n = 6$). [a]Significantly different from Female HS; $p < .05$. HS, high-salt diet; RD, regular diet.

The presence of $BaCl_2$, ouabain and L-Nω-nitro arginine methyl ester reduced vascular compliance. A significant reduction was found between blood vessels of male on regular compared to males on high salt diets (Figure 3.4A). However, there were no difference between females on regular versus high salt diets (Figure 3.4A). The concomitant presence of vasoconstrictor, phenylephrine, and $BaCl_2$, ouabain and L-Nω-nitro arginine methyl ester resulted in significant reductions of vascular compliance in males on high salt compared to males on regular diet. In contrast, an increase in vascular compliance was found in blood vessels of females on high salt compared to females on regular diet (Figure 3.4B). The addition of sodium nitroprusside in the presence the vasoconstrictor, phenylephrine, resulted in an increase in the vascular compliance in males on regular and high salt diets that were comparable, as well as in females on high salt diet but not females on regular diet (Figure 3.4C).

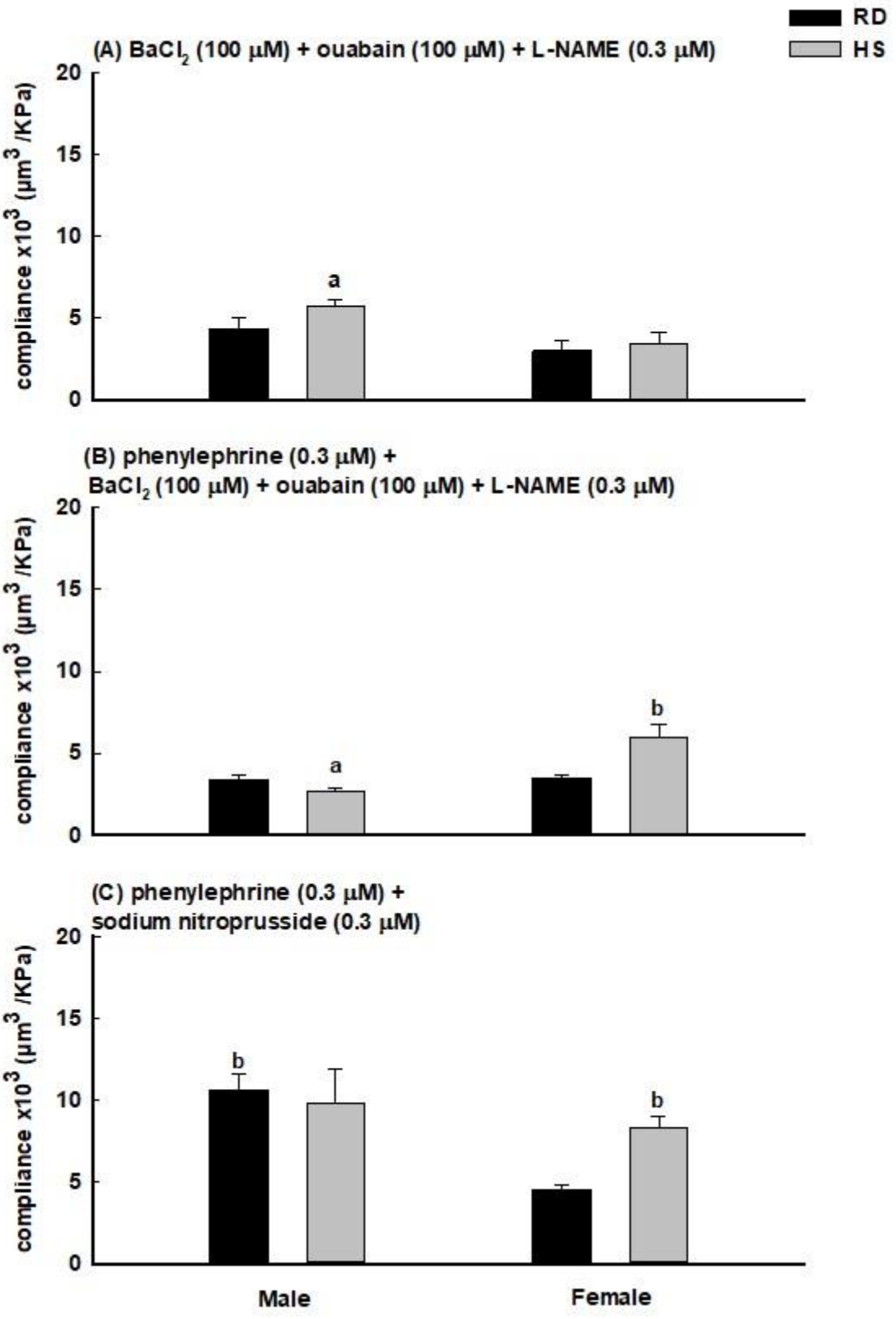
RD
HS
(A) BaCl2 (100 μM) + ouabain (100 μM) + L-NAME (0.3 μM)
compliance x10^3 (μm^3 /KPa)
20
15
10
5
0
a
(B) phenylephrine (0.3 μM) +
BaCl2 (100 μM) + ouabain (100 μM) + L-NAME (0.3 μM)
compliance x10^3 (μm^3 /KPa)
20
15
10
5
0
a
b
(C) phenylephrine (0.3 μM) +
sodium nitroprusside (0.3 μM)
compliance x10^3 (μm^3 /KPa)
20
15
10
5
0
b
b
Male
Female

Figure 3.4: Calculated values of compliance from pressure–volume plots in isolated third-order mesenteric arteries from Dahl salt-sensitive male and female rats on regular or high-salt (4% NaCl) diets for 6–7 weeks; (A) $BaCl_2$ (100 μM) + ouabain (100 μM) + L-N^{ω}-nitro arginine methyl ester (L) (0.3 μM), (B) phenylephrine (0.3 μM) plus $BaCl_2$ (100 μM) + ouabain (100 μM) + L-N^{ω}-nitro arginine methyl ester (0.3 μM) (C) phenylephrine (0.3 μM) plus sodium nitroprusside (0.3 μM). Each value is expressed as a mean ± s.e.m. ($n = 6$). [a]Significantly different from Female HS; $p < .05$; [b]Significantly different from Female RD; $p < .05$. HS, high-salt diet; RD, regular diet.

3.4.3 Immunohistochemistry

MMP-9 is expressed in both VSMCs and endothelial cells. In the third-order mesenteric arteries fixed at 7.9 KPa pressure, there was an elevated expression of MMP-9 in the intima, media and adventitia in males on high salt compared to the other groups. A semi-quantitative analysis of the changes in MMP-9 indicated a significant increase in its levels of expression in males on high salt compared to males on a regular diet, without any changes in the corresponding female groups (Figure 3.5).

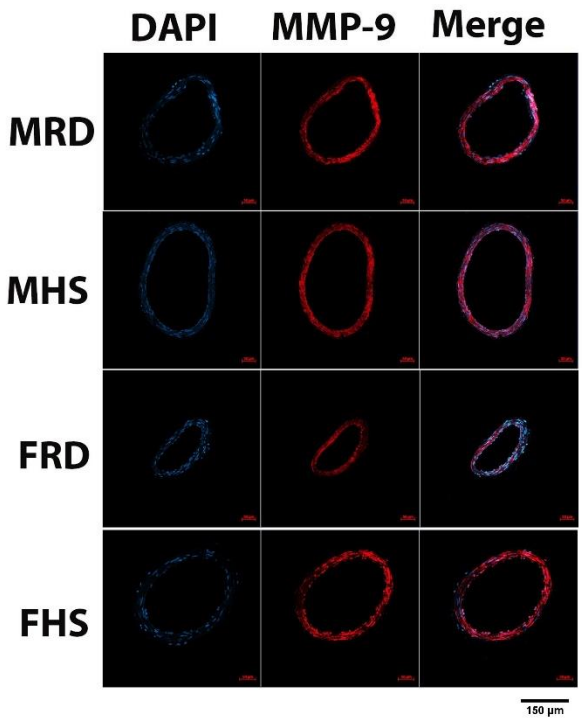
DAPI
MMP-9
Merge
MRD
MHS
FRD
FHS
150 µm

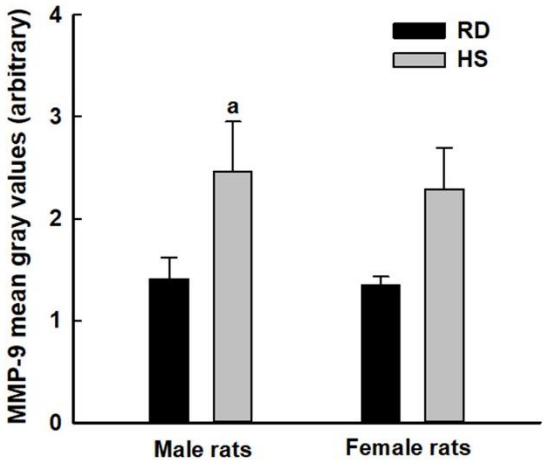
MMP-9 mean gray values (arbitrary)
4
3
2
1
0
a
RD
HS
Male rats
Female rats

Figure 3.5: Representative photographs of immunohistochemical staining of MMP-9 in the third-order mesenteric arteries from Dahl salt-sensitive male and female rats on regular or high-salt (4% NaCl) diets for 6–7 weeks, fixed under 7.9993 kPa pressure. Inset plot of semi-quantitative assessment of the gray area for MMP-9. Each value is expressed as a mean ± s.e.m. ($n = 6$). [a]Significantly different from Male RD; $p < .05$. HS, high-salt diet; RD, regular diet.

NADPH was expressed in the intima and predominantly in the media of the vessel wall towards the adventitia. Comparison of NADPH in blood vessels revealed a significant increase of expression in males on high salt compared to males on a regular diet, but no significant changes in the corresponding female groups (Figure 3.6).

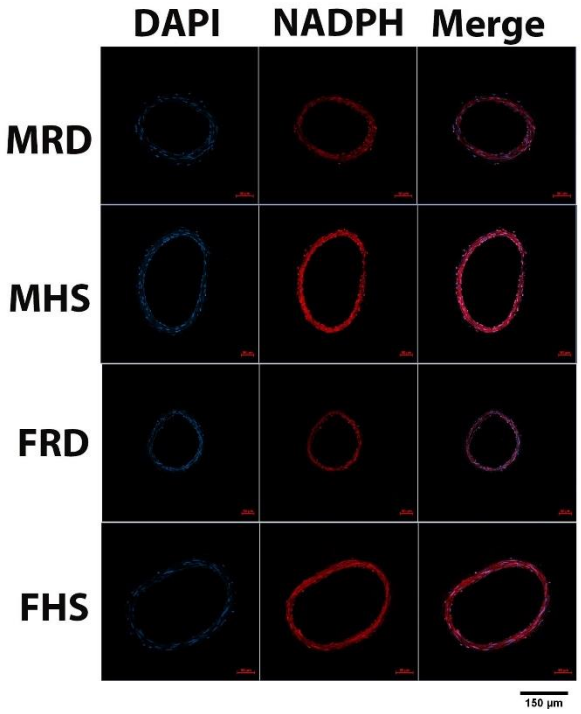
DAPI
NADPH
Merge
MRD
MHS
FRD
FHS
150 μm

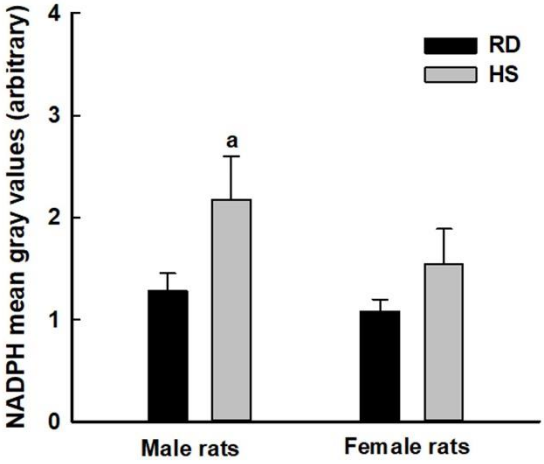
NADPH mean gray values (arbitrary)
4
3
2
1
0
a
RD
HS
Male rats
Female rats

Figure 3.6: Representative photographs of immunohistochemical staining of NADPH in the third-order mesenteric arteries from Dahl salt-sensitive male and female rats on regular or high-salt (4% NaCl) diets for 6–7 weeks, fixed under 7.9993 kPa pressure. Inset plot of semi-quantitative assessment of the gray area for NADPH. Each value is expressed as a mean ± s.e.m. ($n = 6$). [a]Significantly different from Male RD; $p < .05$. HS, high-salt diet; RD, regular diet.

β1-Integrin was found to be expressed in the intima and adventitia of all the groups and predominantly expressed in the media of the high salt diet groups (Figure 3.7). A semi-quantitative analysis revealed significant increases in the levels of β1-integrin in blood vessels of male and female animals on high salt diet when compared to their corresponding group on regular diets (Figure 3.7).

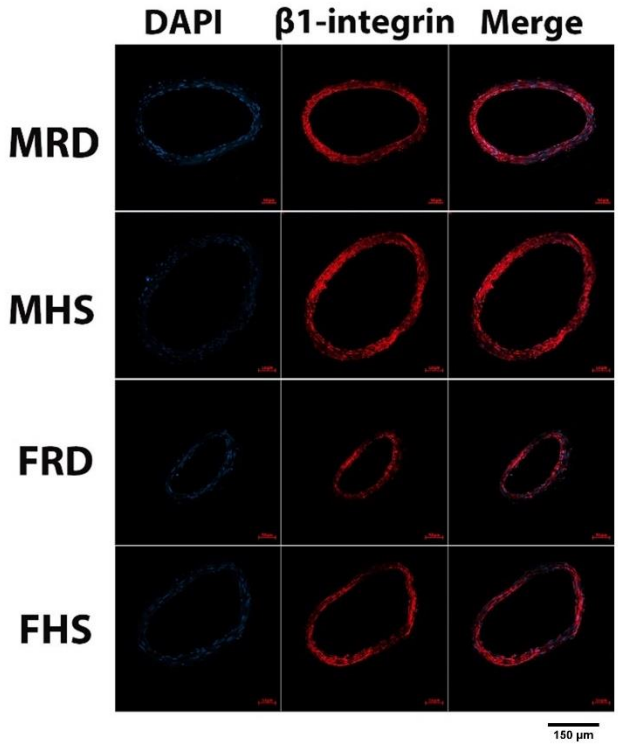
DAPI
β1-integrin
Merge
MRD
MHS
FRD
FHS
150 μm

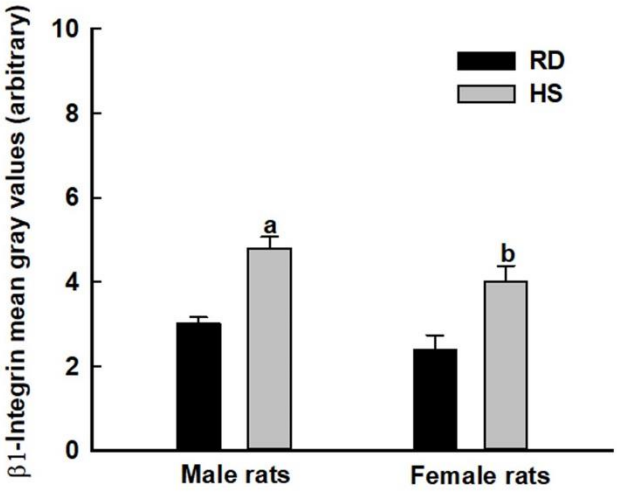
β1-Integrin mean gray values (arbitrary)
10
8
6
4
2
0
RD
HS
a
b
Male rats
Female rats

Figure 3.7: Representative photographs of immunohistochemical staining of β1-integrin in the third-order mesenteric arteries from Dahl salt-sensitive male and female rats on regular or high-salt (4% NaCl) diets for 6–7 weeks, fixed under 7.9993 kPa pressure. Inset plot of semi-quantitative assessment of the gray area for β1-integrin. Each value is expressed as a mean ± s.e.m. ($n = 6$). [a]Significantly different from Male RD; $p < .05$; [b]Significantly different from Female RD; $p < .05$. HS, high-salt diet; RD, regular diet.

3.5 Discussion

In our current investigation, using small resistance arteries, the presence of L-type Ca channel antagonist, verapamil, resulted in reductions in CYM in the male hypertensive animals with no changes in female groups. In addition, inhibition of endothelial cell function by treatment with $BaCl_2$, ouabain and L-Nω-nitro arginine methyl ester, led to significant increases in blood vessel stiffness (i.e., increase in CYM) in the male normotensive and both female groups but not in the male hypertensive group. Immunohistochemical assessments of the biochemical properties of the arterial wall showed significant differential expressions of MMP-9, NADPH, and β1-integrin between sexes.

Alterations in wall structure of blood vessels leading to the elevation in arterial stiffness are accompanied by an increase in CYM (Bank et al., 1996; Lee & Oh, 2010; Messas et al., 2013; Wagenseil & Mecham, 2009). We have previously reported sex-specific changes in CYM in small resistance arteries between male and female hypertensive rats due to high salt consumption following exposure to phenylephrine (vasoconstrictor) and sodium nitroprusside (vasodilator) (Mensah et al., 2022). At baseline, we found no differences in CYM among the experimental groups in our current study, and as we had previously reported (Mensah et al., 2022). However, when treated with verapamil, there were significant changes in CYM within the males but not the female groups. Moreover, pre-constriction with phenylephrine completely abolished the vascular actions of verapamil on CYM in males without affecting females. These findings indicate a sex-specific sensitivity in the L-type calcium channels to verapamil that can significantly influence arterial biomechanics in males but not females.

Inhibition of endothelial cell function revealed significant increases in CYM from baseline in all groups except the male hypertensive group, unmasking endothelial dysfunction in

the male hypertensive rats that could contribute to increased arterial stiffness in the latter group but not in any other group (Gallo et al., 2021; Guo et al., 2014). Furthermore, the increase in CYM in females on high salt supports the functionality of the endothelial cell layer despite significant elevation in blood pressure, heart rate and PWV. Here, we have demonstrated the potential for a sex-specific vasculoprotective phenomenon that may oppose, and possibly delay or prevent, the progression of arterial remodelling and function in females. Our current findings are consistent with our previous publication, where the electron micrograph images of the third order mesenteric arteries in the male hypertensive group had revealed damaged, discontinuous and fragmented endothelial cell layer, a feature which was absent in the male and female normotensives, and female hypertensive rats (Mensah et al., 2022). Pre-constriction of these arteries with phenylephrine before treatment with sodium nitroprusside (NO donor) increased CYM in the male hypertensive group compared to the normotensive and female hypertensive groups. This would suggest that this increase in CYM results from a possible reduction in NO bioavailability, an increase in sensitivity to the effects of phenylephrine vasoconstriction and possibly the structural alterations in the male hypertensive group due to high salt intake and elevation in blood pressure.

Several mechanisms have been suggested to account for the development and progression of arterial stiffness (Avolio, 2013; DuPont et al., 2019; Luft, 2012; Palombo & Kozakova, 2016; Zieman et al., 2005). However, the sex-specific mechanisms contributing to arterial stiffness that we have described in our current studies were unknown, and not studied. Arterial remodeling is a complex pathophysiological adaptation involving the structural and dynamic components of the arterial wall (Lemarié et al., 2010; van Varik et al., 2012). Structural alterations involve the enhanced deposition of collagen and increased elastin turnover/breakdown

of the ECM. Matrix metalloproteinases (MMP) are zinc-dependent endopeptidases that degrade various ECM proteins, including collagen and elastin, and influence endothelial cell and VSMC function. MMP is regulated by endogenous tissue inhibitors of metalloproteinases (TIMPs). A balance between MMP and TIMP is crucial in pathophysiological conditions serving as a biomarker in arterial remodeling (Díez, 2007; Lemarié et al., 2010).

The current study in male and female rats demonstrated sex-specific change in the expression of MMP-9 in the vascular wall, with males being more susceptible after the consumptions of a high salt diet. Elevated MMP-9 expression in the hypertensive males suggests there is more remodeling of the resistance artery wall in response to increased hemodynamic stress (Kalani et al., 2016; Yasmin et al., 2005). The molecular mechanisms underlying ECM remodeling in mesenteric resistance arteries have not been studied extensively. The increase in the expression of MMP-9 is a clear indication of ECM turnover from increased salt consumption, which is consistent with our ultrastructure findings (Mensah et al., 2022). Furthermore, the subsequent increase in the expression of MMP-9 in the male hypertensive group compared to the female group suggests a different possible timeline in the initiation and progression of arterial remodeling between males and females. Moreover, the present studies on MMP-9 expression in the cardiovascular system report a significant increase of MMP-9 expression in males compared to females with an underlying cardiovascular diseases suggesting a sex disparity of MMP-9 expression, which could account for the sex-specific differences in functional response and arterial remodeling (Kobayashi et al., 2011; Sokolis & Iliopoulos, 2014; Sullivan et al., 2018).

Evidence from several studies suggests that VSMCs directly contribute to elevated arterial stiffness as a consequence of the alterations in the cytoskeleton and integrin complex

within the ECM (Gao et al., 2014; Hays et al., 2018; Kajuluri et al., 2021; Patrick Lacolley et al., 2017; Qiu et al., 2010). A direct interaction between the arterial wall (i.e., ECM) and VSMCs components involves the ECM integrin-cytoskeleton complex. The ECM integrin-cytoskeleton complex is a mechanosensing apparatus allowing VSMCs to detect and respond to intraluminal stress on the vessel wall (Hill et al., 2007; Lacolley et al., 2012). In our current study, the increased expression of β1-integrin in male and female hypertensive groups is consistent with increased VSMCs/wall ratio in our previous morphometric analysis of the vascular wall (Mensah et al., 2022). Thus, we suggest that β1-integrin is involved in cellular hypertrophy in response to high salt intake and/or elevated blood pressure. This is also aligned with a higher value of CYM in response to phenylephrine in the male hypertensive group due to the vessel wall/VSMC ratio (Mensah et al., 2022). Moreover, it is also possible that increase in β1-integrin occurs with inflammation, and it will affect cytoskeletal tension and alters cell-cell junctions (Pulous & Petrich, 2019).

However, these changes are not consistent with the change of CYM in female hypertensive rats in response to phenylephrine, suggesting a protective mechanism that regulates the vessel wall tone and VSMC proliferation in females despite the increased expression of β1-integrin (Turlo et al., 2013). Our results point to the concept that β1-integrin could be an early marker in the induction and progression of arterial remodeling and stiffness in small resistance arteries, an interesting finding that requires further investigation.

The increased expression of NADPH in the hypertensive group may suggest an increased endogenous superoxide anion production, and possibly reduced NO bioavailability. These results support the view of an intact endothelial cell layer as reported in our previous studies in male and female normotensive, and female hypertensive groups (Mensah et al., 2022). It also points to an

important functional role for intrinsic sex-specific mediators such as estrogen in the maintenance of a functional endothelium and bioavailability of endothelium-dependent relaxing/hyperpolarizing factors in small resistance arteries of females despite the elevated salt consumption and hypertension.

Treatment of blood vessels with verapamil did not affect compliance in either male or female groups. However, after pre-constricting the vessels with phenylephrine before verapamil, there was a significant increase in compliance in the male hypertensive compared to the normotensive group. In contrast, verapamil did not affect the compliance of the female groups. The observed result suggests a difference in sensitivity to verapamil in the males versus females, which is unmasked under elevated vessel tone. The changes in the compliance in the rat phenotypes when the endothelial function was inhibited also unmask the contributions of vascular endothelium to the vessel wall compliance and how a dysfunctional endothelium impacts compliance. Furthermore, the overall increase in compliance in the males compared to the females when vessels were treated with sodium nitroprusside after pre-constriction with phenylephrine reinforces the differences NO bioavailability and regulation of vascular tone between males and females (Huang et al., 1998; Sader & Celermajer, 2002; White et al., 2000).

Our findings suggest multiple differential mechanisms involved in altering wall biomechanics, which is sex-specific in salt-induced hypertension. Thus, understanding how sex-specific effects influence these mechanisms could present a gender-specific therapeutic approach to lessen cardiovascular risk.

Chapter 4 The role of Piezo 1 channels in vascular stiffness in isolated small resistance arteries of male and female Dahl salt-sensitive hypertensive rats

4.1 Abstract

Piezo are mechanosensitive non-selective cation channels that are suggested to be involved in vascular development and function. The aim of our study was to determine any sex-specific contributions of the mechanosensitive Piezo 1 channels on blood vessel wall stiffness. Composite Young modulus (CYM) was determined using pressure myograph experimental approach using third-order mesenteric arteries (intact and denuded) from Dahl salt-sensitive male and female normotensive and hypertensive rats (n = 6–8). The effects of Piezo 1 agonist (Yoda 1; 10 μM), and antagonist (GsMTx-4; 2 μM) were studied in intact and denuded vessels. The distribution of Piezo 1 was identified using immunohistochemistry. In intact blood vessels, there were no differences in CYM between the experimental groups, however, removal of the endothelium unmasked significant increases in CYM in normotensive males and female groups compared to hypertensive males. The presence of Yoda 1 did not affect CYM in any groups. In the intact tissues, GsMTx-4 led to significant increases in CYM in hypertensive females, and normotensive males and females, but not in hypertensive males. In the denuded vessels, GsMTx-4, produced a significant increase in CYM but only in the female normotensives. Differential expression of Piezo 1 were found in male versus female blood vessels. Our findings support a greater contribution of Piezo 1 mechanoceptors to vascular biomechanics of male hypertensive compared to male normotensive or female groups. The evidence also points to a possible

differential vasoregulatory role for Piezo 1 in endothelial versus vascular smooth cells, with a greater contribution in males than females.

4.2 Introduction

Piezo are mechanosensitive non-selective cation channels that are involved in vascular development and function (Kefauver et al., 2020; Volkers et al., 2015). These channels allow the passage of cations across the cell membrane and detect mechanical stress (Kefauver et al., 2020; Nourse & Pathak, 2017; Wang et al., 2021). Activation of Piezo 1 is suggested to influence myogenic activity of blood vessels as well have trophic effects (Robledo, 2019; Wang et al., 2021). Ion channels in the membrane of vascular endothelial and vascular smooth muscle cells (VSMCs) play a crucial role in maintaining and regulating vascular tone in resistance arteries, which are pivotal for generating vascular resistance (Jackson, 2000). This essential function ensures blood flow to vital organs while maintaining vascular reserve (Jacob et al., 2016).

Chronic elevation in blood pressure is characterized by the structural remodeling of the arterial wall (Humphrey & Schwartz, 2021; Touyz et al., 2018). Elevated intravascular pressure can lead to increased mechanical stress on the vessel wall components, which can significantly impact vascular development (Humphrey & Schwartz, 2021; Jacob et al., 2016). Hypertensive state can lead to endothelial dysfunction, possibly damage, and increased stress on the blood vessel wall (Humphrey & Schwartz, 2021; Martinez-Quinones et al., 2018). Endothelial cells and VSMCs have the ability to detect changes in pressure and its related stress on the vessel wall (i.e., mechanosensing) (Davis et al., 2023; Humphrey & Schwartz, 2021). This process requires unique proteins (mechanotransducers) that convert the mechanical forces generated by blood pressure and flow on the vessel walls into biochemical signals primarily via mechanically activated ion channels such as Piezo 1 (Davies & Tripathi, 1993; Davis et al., 2023; Humphrey

& Schwartz, 2021). As such, the presence of Piezo 1 channels have been reported in both VSMCs and endothelial cells (Beech, 2018; Fels & Kusche-Vihrog, 2020).

Piezo 1 has been suggested to be involved in arterial wall remodeling in different models of hypertension (i.e., angiotensin II infused, and deoxycorticosterone acetate salt-induced/uninephrectomized) (Retailleau et al., 2015). A decrease in blood vessel lumen diameter and an increase in wall thickness in the mentioned hypertensive states can be reversed in Piezo 1 knockout animals (Beech, 2018; Retailleau et al., 2015). However, there is very limited information describing the functional contributions of Piezo 1 in the mechanics of resistance arteries in a hypertensive state. In addition, no studies have examined sex differences for Piezo 1 in relation to vascular pharmacology. Moreover, in recent studies, we had suggested that sex differences could be responsible for adaptive changes in biomechanics, and varied pharmacological responses in Dahl hypertensive animals (e.g., the presence of verapamil reduced composite Young modulus (CYM) in the male hypertensive animals with no changes in females) (Mensah et al., 2022, 2024). Therefore, our working hypothesis is that there are differences in the contributions of Piezo 1 mechanoreceptors to biomechanics in the resistance arteries of hypertensive males versus females. Accordingly, the aim of our current study was to describe the sex-specific contributions of the mechanosensitive Piezo 1 channels in resistance artery biomechanics in normotensive and a hypertensive rat model and define the role of these channels in the pathophysiology of salt-induced hypertension as an emerging pharmacological target.

4.3 Materials and Methods

4.3.1 Animals:

All procedures on animals were carried out in accordance with the guidelines of the Canadian Council on Animal Care, with the approval of the Institutional Animal Care Committee of Memorial University of Newfoundland and the Canadian Council of Animal Care (Guide to care and Use of Experimental Animals, Vol 1, 2nd Edition). Male and female Dahl salt-sensitive rats (age 5-6 weeks) were purchased from Charles River Laboratories (Saint Constant, QC, Canada), housed two per cage, and were kept in a temperature-controlled environment (22 ± 2° C) on a 12h-12h light-dark cycle. They were given access to normal tap water and standard chow (0.65% NaCl) or a high salt diet containing 4% NaCl (Zeigler Bros., Inc. Gardners, PA, USA) ad libitum for 6-7 weeks.

4.3.2 Experimental Design:

Each animal (age 12–14 weeks) was anesthetized (induction 5% isoflurane in 100% O2, maintenance 1.5%–1.25% isoflurane in 100% O2) (Fresenius Kabi ON, Canada), and were injected with the analgesic, buprenorphine (0.01 mg/kg, s.c.). The core body temperature was maintained at 37 ± 1°C using a heating lamp and monitored with a rectal thermometer. The external iliac and carotid arteries were isolated and catheterized using polyethylene tubing (I.D. 0.58 mm, O.D. 0.965 mm [9 cm] connected to I.D. 0.28 mm, O.D. 0.61 mm [7 cm]). The catheters were advanced forward (approximately 2 cm) such that the catheter in the femoral artery was just at the distal end of the abdominal aorta while the catheter in the carotid artery was just beyond the aortic arch and in the proximal end of the thoracic aorta.19 All catheters were filled with heparinized normal saline (25 IU/mL). Central (aortic) and peripheral (femoral artery) blood pressure, as well as heart rate were continuously recorded by AcqKnowledge (3.9.1.6)

software (Biopac Systems Inc., Goleta, CA, USA) with a pressure transducer (P23XL; Spectramed Statham; Viggo-Spectramed, Oxnard, CA, USA) for 20–25 min. The signals were amplified (DA 100A; Biopac Systems Inc., Goleta, CA, USA), where the amplifier was connected to a universal interface module (UIM 100; Biopac Systems Inc., Goleta, CA, USA), and to an acquisition unit (MP100; Biopac Systems Inc., Goleta, CA, USA). The analog output signal was then converted to a digital signal (USB1W; Biopac Systems Inc., Goleta, CA, USA), and displayed in AcqKnowledge (3.9.1.6). Animals were euthanized by anesthetic overdose and thoracotomy. The mesenteric arteries were removed and prepared for functional and immunofluorescence studies. The heart of each animal was excised, and the right ventricle and left ventricle plus septum were separated and weighed. In addition, the length between the carotid artery catheter and the femoral artery catheter was measured at post-mortem, and pulse wave velocity (PWV) was then calculated with the following formula $PWV = d/\Delta t$ (Leblanc & Tabrizchi, 2018).

4.3.3 Pressure Myograph Experiments:

All chemicals used in the pressure myograph experiments were purchase from Sigma Aldrich (Montreal, Canada) unless otherwise stated. The mesenteric bed was placed in a dissecting dish containing modified Krebs buffer with the following composition (mM): 120 NaCl, 4 KCl, 1.2 $MgCl_2.6H_2O$, 1.5 $CaCl_2H_2O$, 25 $NaHCO_3$, 1.2 KH_2PO_4, 0.1 EDTA and 11 glucose in an oxygenated (95% O_2 and 5% CO_2) environment. The third-order branch of the mesenteric artery was determined to be the third branch off the superior mesenteric artery of the gut. A length of approximately 5 mm was isolated and carefully cleaned of surrounding tissues under a dissecting microscope as described by (Jadeja et al., 2015). The mechanical properties of isolated third-order mesenteric arteries were studied with a pressure myograph. Isolated vessels were mounted

onto the Single Vessel Chamber component of the Pressure Servo System (Living system instrumentations, Model CH-1-SH/CH-1-QT P100, St. Albans City, VT, USA) for the pressure myograph studies. In detail, the isolated third -order mesenteric artery were mounted on two glass micropipettes, secured with 0.2 metric (10-0) surgical nylon suture obtained from CovidienTM . The vessel length was adjusted so that the vessel walls were parallel and without stretch. Intraluminal pressure was then set to a baseline pressure of 3.9 KPa (30 mmHg) and allowed to equilibrate for 20 min at 37 ± 1°C in a modified Krebs buffer gassed with a mixture of 95% O_2 and 5% CO_2. Vascular response was imaged using an inverted microscope Accu-Scope 3032 (Accu-Scope INC, NY, USA) and measured using a Video Dimension Analyzer (Living Systems Instrumentation, VT, USA) and the iWORX Data Recording Software (Dover, NH, USA). The isolated blood vessels were either assigned as endothelial intact or denuded. The arteries were denuded by slowly passing of air bubbles through the lumen of the isolated vessels for 2 minutes. The absence of endothelium was confirmed after the completion of the protocols as each vessel was contracted with phenylephrine (0.3 μM), followed by the addition of methacholine (3 μM). An absence of relaxation in response to methacholine was taken as a measure of denudation of the blood vessels. Six different groups of experiments were undertaken in assessment of the mechanical function of the blood vessel with different interventions: (i) vehicle treatment (24 μL) of DMSO, (ii) Yoda (10 μM) (Bio-Techne Canada (Tocris Bioscience), ON, Canada), (iii) phenylephrine (0.3 μM) plus Yoda (10 μM) (iv) Grammostola Mechanotoxin 4 (GsMTx-4) (2 μM) (Alomone labs, JBP, Israel). Five minutes after the additions of the vasoactive agents or vehicle, intraluminal pressure was raised stepwise at an increasing transmural pressure of 2.6, 5.3, 7.9, 10.6, and 13.3 Kpa to obtain pressure-diameter (D) curves. For each vessel, the left wall (LW) and right wall (RW) thickness was also

measured. In another group of experiments isolated third order mesenteric arteries were pressure-fixed (7.9 KPa), without the presence of any vasoactive agents, with Karnovsky fixative at 37 ± 1°C for 30 minutes for immunohistochemistry (IHC) studies.

4.3.4 Immunofluorescence Studies

The isolated third-order mesenteric vessels were pressure-fixed in formalin and embedded in paraffin wax. The paraffin-embedded vessels were sliced into 6 µm sections using a cryotome (Fisher Scientific, Pittsburgh, PA, USA), placed on charged slides (4-6 slices/slide), and stored at -20° C until processed for immunofluorescence studies. The expression of the following Piezo 1 proteins was tested using Anti-Piezo1 Antibody (#APC-087) (1: 200); Alomone labs, JBP, Israel). For day 1 of testing, the slides were thawed, deparaffinized using; two washes of xylene (10 minutes each), 1:1 Xylene:100% Ethanol, 100% ethanol, 95% ethanol, 70% ethanol, 50% ethanol and washed in 1 x phosphate-buffered saline (PBS) (5 minutes each). Antibody staining required heat-mediated antigen retrieval with citrate buffer pH 6.0 at 100^{o} C for 30 minutes and allowed to cool down at room temperature for 20 mins and washed in 1 x PBS (5 minutes each at room temperature) before tissue permeabilization and blocking. The blocking solutions consisted of 10% normal goat serum (NGS) with 0.1% Triton-X in 1X PBS, incubated for 1 hr at room temperature. Following the wash step (2 x PBS for 10 minutes at room temperature), the samples were incubated with the primary antibodies for the proteins of interest at the concentrations indicated above.

For day 2 of testing, after five washes (2 x PBS for 10 minutes at room temperature), sections were incubated with secondary antibody [Cy5-Goat Anti-Rabbit (1:250); Cy5 conjugated antibodies were from Jackson Immunoresearch, PA, USA]. 4' 6-Diamindino-2-phenylindole

[DAPI (1:1,000); ThermoFisher Scientific, ON, CAN] was used as a nuclear counterstain. For all the immunofluorescence staining, stacks of images at 1µm increments (a total of ten slices) were collected for a Z-stack using Zeiss LSM900 with Airyscan 2 with Zen Blue software. Semi-quantitative analysis of the images was done using ImageJ software (U. S. National Institutes of Health), and a step-by-step protocol outlined by (Crowe & Yue, 2019) was used to determine the mean gray value (MGV) of the vessel for the various antibodies used as the average pixel intensity of the immunohistochemistry (IHC) threshold image (Mean).

4.3.5 Calculation of mechanical parameters

The luminal diameter at baseline D_0, LW and right wall RW were measured at various intraluminal pressures, (5.3329, 7.9993, 10.6658, and 13.3322 KPa) using a video frame capture and real-time edge-detection system available with the Video Dimension Analyzer. The wall thickness (WT) was calculated using the following formula: WT = (LW+RW)/2.

Vascular compliance (C), which is the ability of a vessel to distend and increase volume with an increasing transmural pressure is equal to changes in vessel volume ($\Delta V = \pi r2\ h$), divided by changes in transmural pressure (ΔP) (i.e., $C = \Delta V/\Delta P$).

The following mechanical parameters were calculated according to the methods by Intengan and Schiffrin (Intengan & Schiffrin, 1998). Circumferential wall strain (ε) = $(D - D_0)/ D_0$, where D_0 is the diameter at baseline transmural pressure and D is the observed luminal diameter for a given transmural pressure. Circumferential wall stress (σ) = (PD)/(2WT), where P is the intramural pressure, D and WT are the luminal diameter and wall thickness respectively.

To estimate the arterial stiffness independent of vessel geometry, the composite Young's modulus of the vessel was determined where Ec = stress/strain. The non-linear nature of the

stress/strain relationship was compensated for by fitting the stress/strain data from each vessel to an exponential curve $y = ae^{bx}$ where $\sigma = \sigma_0 e^{x\beta}$ (plots of ln y vs. x), σ_0 is the stress at baseline transmural pressure and β is a constant directly proportional to Ec, related to the rate of increase of the stress/strain curve. An increase in β implies an increase in Ec (increase in stiffness).

4.3.6 Statistical analysis

The data (hemodynamics, composite Young's modulus, and compliance values, immunohistochemistry) were analyzed using two-way analysis of variance (ANOVA) followed by Bonferroni test and/or one-way analysis of variance followed by Bonferroni test. The statistical analysis was carried out with the SigmaPlot statistical package (Systat Software, San Jose, CA, USA). The data are presented as means ± SEM, and the sample size is the number of animals used in each experiment (n =8). A value of $P < 0.05$ was considered significant.

4.4 Results

The body weight of Dahl salt-sensitive female rats were significantly lower than that of the males in both groups (regular and high salt diets). There were no significant differences between the body weights within the groups (i.e., males and females); male regular diet (MRD): 342.2 ± 20.1 g, male high salt diet (MHS): 374.0 ± 10.8 g, female regular diet (FRD): 232.3 ± 7.1 g, and female high salt diet (FHS): 242.7 ± 5.7 g.

The animals that consumed the high salt diet had a significantly higher heart rate, central, peripheral, systolic, and diastolic blood pressures, independent of sex (Table 4.1). There were also significant differences observed in the central and peripheral, systolic pressures of males versus females on a regular diet. The central and peripheral pulse pressures were also

significantly elevated following high salt diet consumption within groups, and between males versus females on a high salt diet. PWV (an index of systemic arterial stiffness) was significantly elevated in males and females on the high salt compared to those on a regular diet. However, we found that PWV was significantly greater in males compared to females on a high salt diet (Table 4.1).

Table 4.1: Hemodynamic measurements in Dahl salt-sensitive male (M) and female (F) rats on regular (R) or high salt (HS; 4% NaCl) diets for 6-7 weeks.

Hemodynamics	M (R diet)	M (HS diet)	F (R diet)	F (HS diet)
HR (beats/min)	369 ± 3**	391± 7* ***	337± 10	366± 11**
cSBP (mmHg)	133± 0.8**	161± 3.3* ***	124± 2.5	140± 2.6**
cDBP (mmHg)	94± 1.0**	113± 3.7* ***	88± 1.6	97± 1.6**
cPP (mmHg)	39± 1.6	47± 2.3* ***	35± 1.8	43± 2.6**
pSBP (mmHg)	129± 0.7**	150± 4* ***	119± 1.5	139± 2.6**
pDBP (mmHg)	89± 1.3	105± 4.1* ***	83± 2.2	96± 2.5**
pPP (mmHg)	39± 1.2	44± 6.1	35± 2.6	42± 1.8**
PWV (m/s)	4.6± 0.2	8.3± 1.0* ***	4.9± 0.2	5.6± 0.5**

Each value is expressed as a mean ± SEM. (n = 8)

Abbreviations: cDBP, central diastolic blood pressure; cPP, central pulse pressure; cSBP, central systolic blood pressure; HR, heart rate; pDBP, peripheral diastolic blood pressure; pPP, peripheral pulse pressure; pSBP, peripheral systolic blood pressure; PWV, pulse wave velocity.

* Significantly different from M (R diet); $P < 0.05$

** Significantly different from F (R diet); $P < 0.05$

*** Significantly different from F (HS diet); $P < 0.05$

The ratio of the left ventricle plus septum to the right ventricle, of males (5.8 ± 0.2) on a high salt diet was significantly greater than males (4.4 ± 0.3) on a regular diet and the females (4.4 ± 0.6) on a high salt diet. However, there were no significant changes within the female groups (female regular diet (4.3 ± 0.2)). It is likely that the larger left ventricular hypertrophy found in males on a high salt diet was due to a greater increase in systemic arterial pressure as well as vascular stiffness compared to the other groups (Table 4.1).

4.4.2 Vascular mechanics

In vehicle-treated time-control studies, there were no significant differences in the composite Young's modulus (CYM) value in any of the groups (i.e., both sexes) in arteries with the endothelium intact (Figure 4.1A). In contrast, in the denuded vessels, the CYM value was significantly lower in males on high salt compared to males on a regular diet, while no differences were found within the female groups (Figure 4.1B). In addition, CYM values were significantly higher in males compared to females on a regular diet (Figure 4.1B).

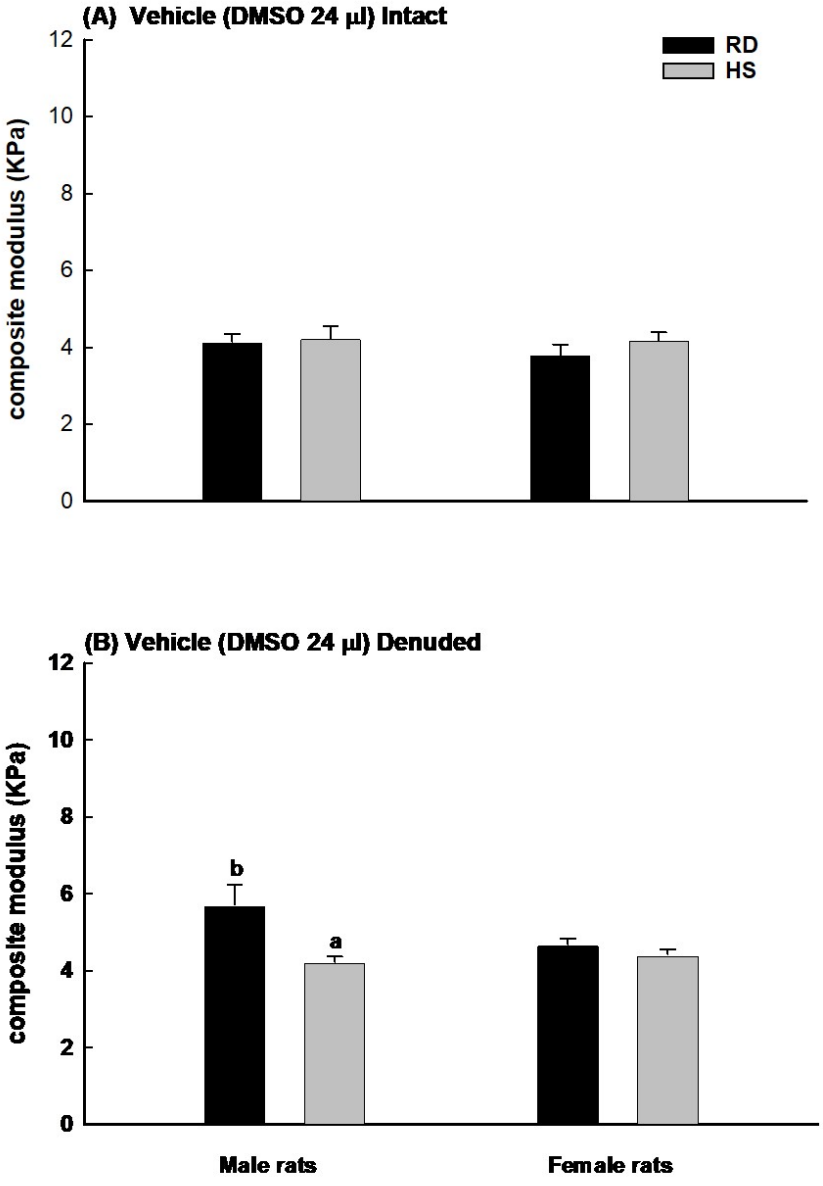
(A) Vehicle (DMSO 24 µl) Intact
RD
HS
composite modulus (KPa)
12
10
8
6
4
2
0
(B) Vehicle (DMSO 24 µl) Denuded
composite modulus (KPa)
12
10
8
6
4
2
0
b
a
Male rats
Female rats

Figure 4.1: Composite Young's modulus (KPa) values calculated using stress–strain plots in isolated third-order mesenteric arteries at various intravascular pressures from Dahl salt-sensitive male and female rats on regular or high salt (4% NaCl) diets for 6–7 weeks; time-control (A) intact endothelium and (B) denuded endothelium. Each value is expressed as a mean ± SEM ($n = 8$). [a]Significantly different from male regular diet; $p < .05$; [b]Significantly different from female regular diet; $p < .05$. Significance reported is within denuded groups. HS, high-salt diet; RD, regular diet.

4.4.3 Effect of Yoda and GSMTx-4 on CYM in third order mesenteric arteries

There were no significant differences in CYM values between any groups (i.e., males and females groups) in the intact or denuded vessels in the presence of the putative Piezo 1 agonist, Yoda 1 (10 μM)(Syeda et al., 2015) (Figure 4.2AB). The percent change in CYM from vehicle-treated time-controlled, to those treated with Yoda 1, revealed no significant differences in either the intact or the denuded tissues with the exception of a significant difference in denuded vessels of males (-3.2 ± 3.7%) versus females (-16.2 ± 3.7%) on the regular diet (Table 4.2).

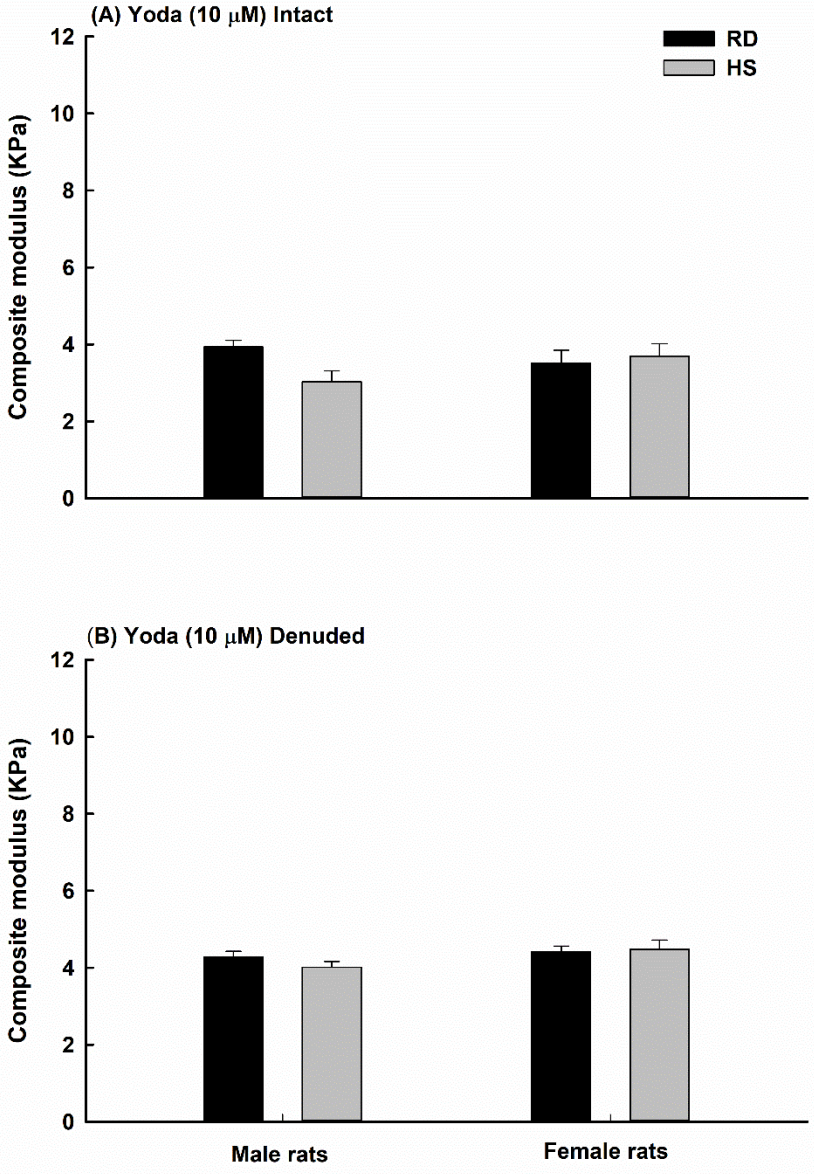
(A) Yoda (10 μM) Intact
RD
HS
Composite modulus (KPa)
12
10
8
6
4
2
0
(B) Yoda (10 μM) Denuded
Composite modulus (KPa)
12
10
8
6
4
2
0
Male rats
Female rats

Figure 4.2: Composite Young's modulus (KPa) values calculated using stress–strain plots in isolated third-order mesenteric arteries at various intravascular pressures from Dahl salt-sensitive male (M) and female (F) rats on regular or high salt (4% NaCl) diets for 6–7 weeks in presence of Yoda 1 (10 μM). (A) intact endothelium, (B) denuded endothelium. Each value is expressed as a mean ± SEM. (n = 8).

Table 4.2: Percent changes in composite Young's modulus (CYM) from vehicle-treated time-controlled experiments in mesenteric arteries from Dahl salt-sensitive male (M) and female (F) rats on regular (R) or high salt (HS; 4% NaCl) diets for 6–7 weeks.

Treatment	M (R diet)	M (HS diet)	F (R diet)	F (HS diet)
Yoda 1 (intact)	4.9 ± 4.0%	28.3 ± 6.7%	2.8 ± 2.8%	12.0 ± 7.7%
Yoda 1 (denuded)	-3.2 ± 3.7%	5.1 ± 3.6%	-16.2 ± 3.7%*	-6.6 ± 5.6%
GsMTx-4 (intact)	-19.0 ± 6.7%	-0.2 ± 3.3%* ***	-43.9 ± 7.9%*	-26.6 ± 4.1%**
GsMTx-4 (denuded)	-26.0 ± 7.6%	-33.2 ± 7.1%	-69.1 ± 9.0%*	-27.3 ± 9.7%**
PE+Yoda 1 (intact)	11.1 ± 7.9%	52.6 ± 4.6%* ***	6.6 ± 8.2%	17.2 ± 12.3%
PE+Yoda 1 (denuded)	-17.6 ± 9.3	13.3 ± 11.6%	-15.1 ± 8.8%	1.5 ± 12.5%

Note: The percent values were calculated from the respective mean average of vehicle treated time-control groups. Each value is expressed as a mean ± SEM. (n = 8). Yoda 1 (10 μM); GsMTx-4 (2.0 μM); Phenylephrine (PE) (0.3 μM).

* Significantly different from M (R diet); $p < .05$.

** Significantly different from F (R diet); $p < .05$.

*** Significantly different from F (HS diet); $p < .05$.

The presence of the Piezo 1 channel blocker, GsMTx-4 (2 μM), resulted in a significant reduction in the CYM value of intact vessels from male animals on high salt compared to regular diets (Figure 4.3A). In contrast, no changes were noted within the female groups. In addition, GsMTx-4 also significantly increased the CYM of intact blood vessels in females compared to the corresponding male animals on a high salt diet (Figure 4.3A). In the endothelium-denuded group, GsMTx-4, resulted in a significant increase in CYM value in females on a regular diet compared to a high salt diet, with no significant changes within the male group. Furthermore, GsMTx-4, caused a significant increase in CYM in denuded blood vessels of females compared to males on a regular diet (Figure 4.3B). The percent change in CYM in the presence of GsMTx-4 from vehicle-treated time-controlled, intact blood vessels, was found to be significantly different between males and females, within the groups and, the respective groups, on regular and high salt diets (Table 4.2). In denuded blood vessels, there were no significant differences in the per cent change in CYM within the males, while significant differences were found between, the respective, males versus females on regular compared to high salt diets (Table 4.2).

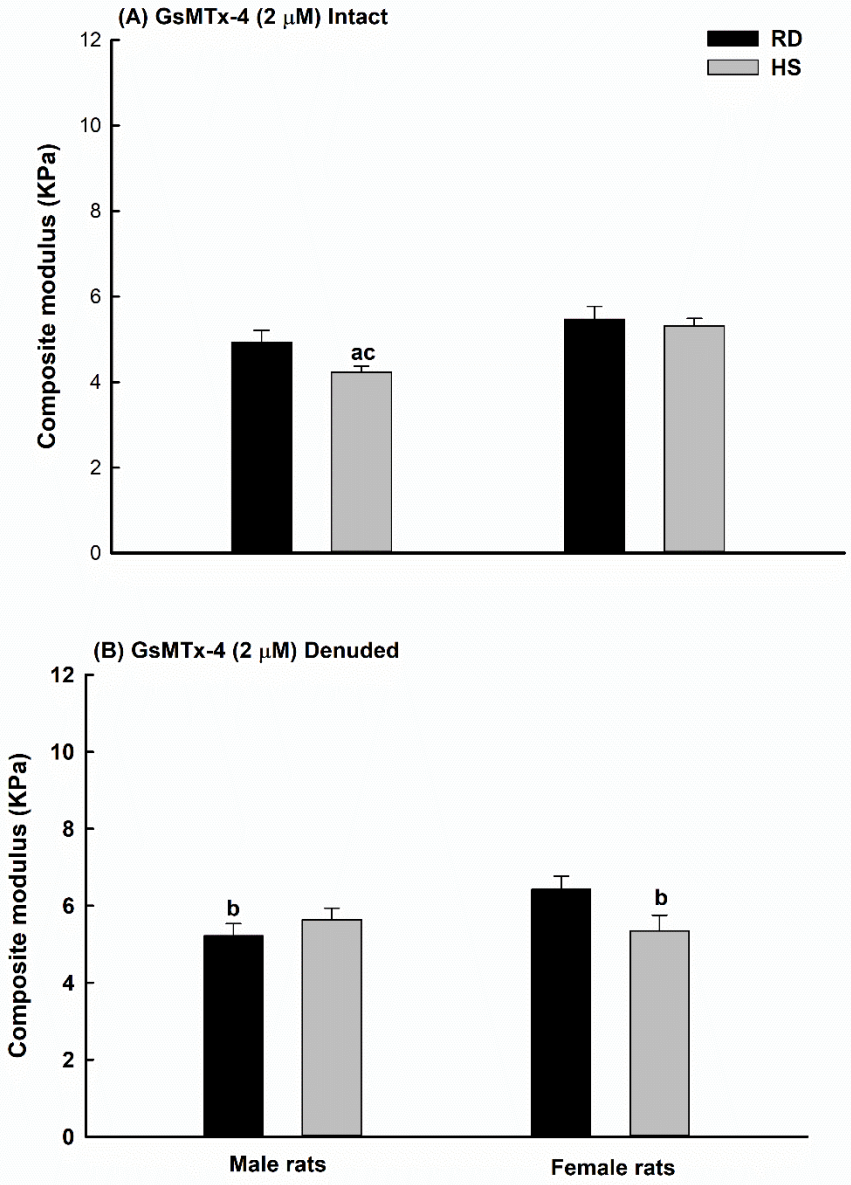
(A) GsMTx-4 (2 μM) Intact
RD
HS
Composite modulus (KPa)
12
10
8
6
4
2
0
ac
(B) GsMTx-4 (2 μM) Denuded
Composite modulus (KPa)
12
10
8
6
4
2
0
b
b
Male rats
Female rats

Figure 4.3: Composite Young's modulus (KPa) values calculated using stress–strain plots in isolated third-order mesenteric arteries at various intravascular pressures from Dahl salt-sensitive male and female rats on regular or high salt (4% NaCl) diets for 6–7 weeks in presence of GsMTx-4 (2 μM). (A) intact endothelium, (B) denuded endothelium. Each value is expressed as a mean ± SEM ($n = 8$). [a]Significantly different from male regular diet; $p < .05$; [b]Significantly different from female regular diet; $p < .05$; [c]Significantly different from female high-salt diet; $p < .05$. Significances reported are within intact and denuded groups. HS, high-salt die; RD, regular diet.

In the intact blood vessels pre-constricted with the α1-adrenoceptor agonist, phenylephrine (0.3 μM), the addition of Yoda (10 μM) caused significant reductions in the CYM within males on high salt compared to regular diets and the corresponding females on a high salt diet, while no differences were found within females (Figure 4.4A). The removal of the endothelium abolished any significant differences as was noted in the intact vessels (Figure 4.4B). In intact blood vessels pre-constricted with phenylephrine, and exposed to Yoda, the per cent change in CYM from vehicle-treated time-controlled indicated significant differences between males and females within the groups but no differences between, the respective, males versus females on regular compared to high salt diets (Table 4.2). In contrast, no significant differences were found in the parallel denuded blood vessels (Table 4.2).

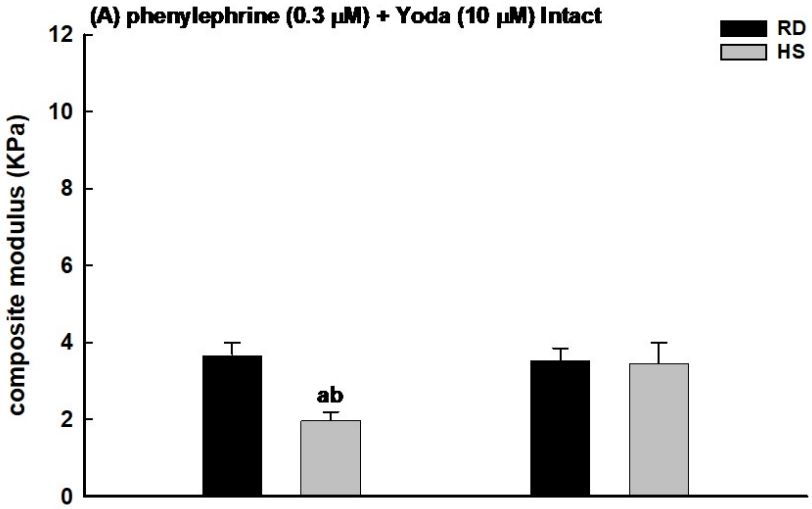
(A) phenylephrine (0.3 µM) + Yoda (10 µM) Intact
RD
HS
composite modulus (KPa)
12
10
8
6
4
2
0
ab

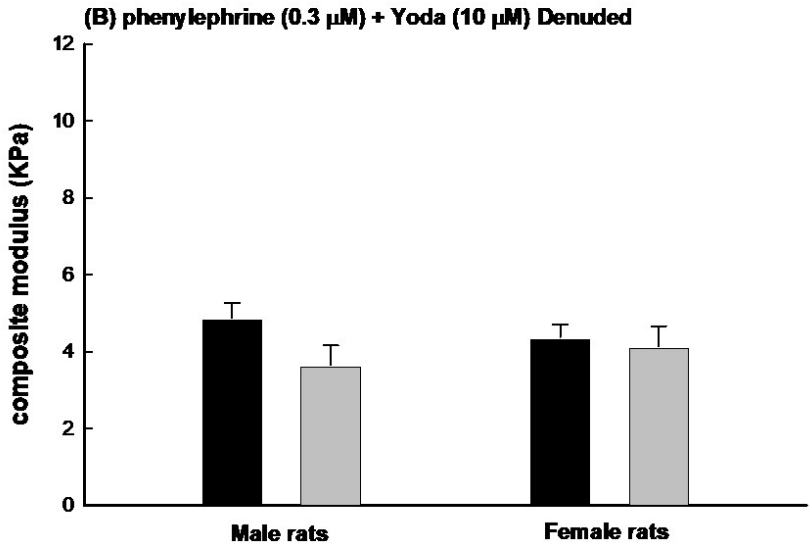
(B) phenylephrine (0.3 µM) + Yoda (10 µM) Denuded
composite modulus (KPa)
12
10
8
6
4
2
0
Male rats
Female rats

Figure 4.4: Composite Young's modulus (KPa) values calculated using stress–strain plots in isolated third-order mesenteric arteries at various intravascular pressures from Dahl salt-sensitive male and female rats on regular or high salt (4% NaCl) diets for 6–7 weeks in presence of phenylephrine (0.3 μM) plus Yoda 1 (10 μM). (A) intact endothelium, (B) denuded endothelium. Each value is expressed as a mean ± SEM ($n = 8$). [a]Significantly different from male regular diet; $p < .05$; [b]Significantly different from female high-salt diet; $p < .05$. Significances reported are within intact and denuded groups. HS, high-salt diet; RD, regular diet.

4.4.4 Vascular Compliance in third-order mesenteric arteries

Calculation of vascular compliance in these vessels were made using the pressure-volume curves. There were no significant differences in compliance between any groups (i.e., males and females) in vehicle-treated time-control, intact vessels (Figure 4.5A). However, in the denuded vessels, a significant increase in compliance was found within the male groups, but there were no differences within the females (Figure 4.5B).

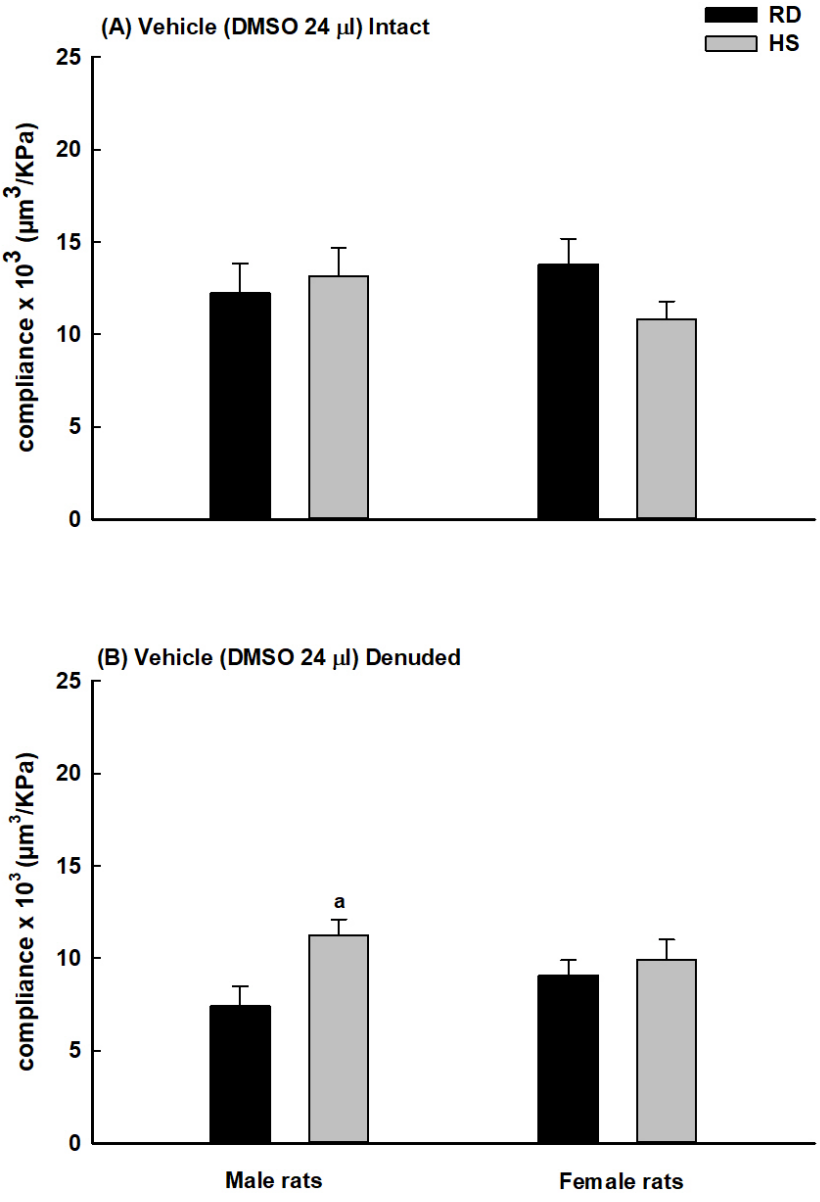
(A) Vehicle (DMSO 24 µl) Intact
RD
HS
compliance x 10^3 (µm^3/KPa)
25
20
15
10
5
0
(B) Vehicle (DMSO 24 µl) Denuded
compliance x 10^3 (µm^3/KPa)
a
Male rats
Female rats

Figure 4.5: Compliance (μm^3 KPa^{-1}) calculated from pressure–volume plots in isolated third-order mesenteric arteries from Dahl salt-sensitive male and female rats on regular or high salt (4% NaCl) diets for 6–7 weeks; time-control (A) intact endothelium, (B) denuded endothelium. Each value is expressed as a mean ± SEM.
($n = 8$). [a]Significantly different from male regular diet; $p < .05$. Significance reported is within denuded groups., HS, high-salt diet; RD, regular diet.

4.4.5 Effects of Yoda and GSMTx-4 on compliance in the third order mesenteric arteries

The presence of Yoda (10 μM) resulted in no significant changes in compliance among any on the groups (i.e., males and females) in the intact blood vessels (Figure 4.6A). In the denuded blood vessels, Yoda caused a significant increase in compliance within the male groups, without any changes in the female groups (Figure 4.6B). There was also a significant increase in compliance among the males in high salt compared to the corresponding females (Figure 4.6B).

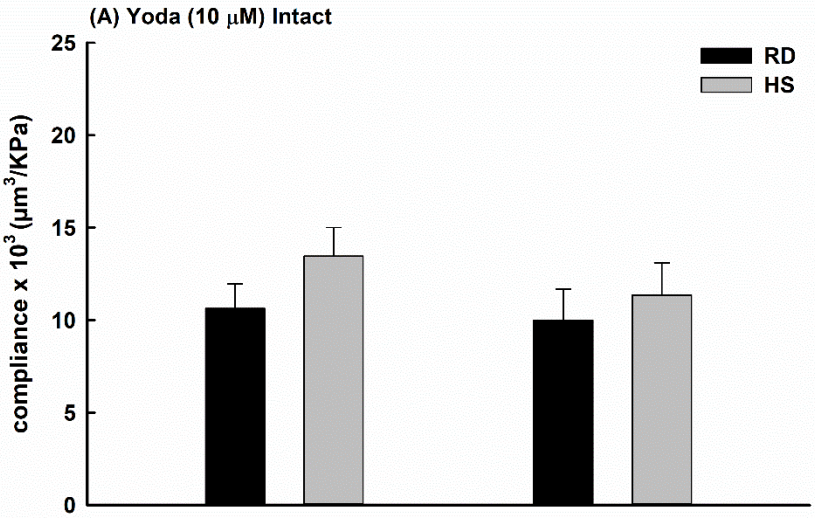
(A) Yoda (10 μM) Intact
RD
HS
compliance x 10³ (μm³/KPa)
25
20
15
10
5
0

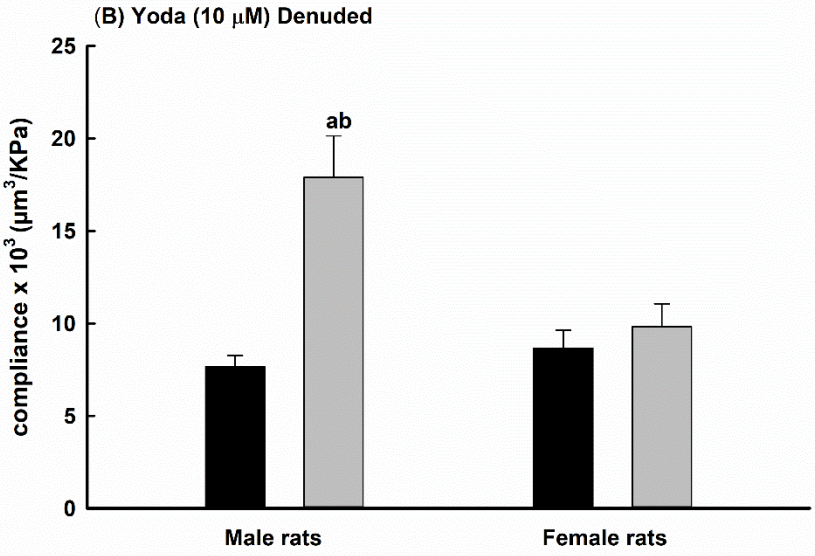
(B) Yoda (10 μM) Denuded
ab
compliance x 10³ (μm³/KPa)
25
20
15
10
5
0
Male rats
Female rats

Figure 4.6: Compliance (μm^3 KPa^{-1}) calculated from pressure–volume plots in isolated third-order mesenteric arteries from Dahl salt-sensitive male and female rats on regular or high salt (4% NaCl) diets for 6–7 weeks in presence of Yoda 1 (10 μM). (A) intact endothelium, (B) denuded endothelium. Each value is expressed as a mean ± SEM ($n = 8$). [a]Significantly different from male regular diet; $p < .05$; [b]Significantly different from female regular diet; $p < .05$. Significance reported is within denuded groups. RD = regular diet, HS = high-salt diet.

In the intact blood vessels, the presence of GsMTx-4 (2 μM) significantly reduced compliance of the vessels from the respective females compared to males on a high salt diet, while no changes were noted within either the male or female groups (Figure 4.7A). In the denuded vessels, the presence of GsMTx-4, resulted in a significant increase in compliance in the males on a high salt diet compared to males on a regular diet and females on a high salt diet. However, there was no significant difference in compliance noted within the female groups (Figure 4.7B).

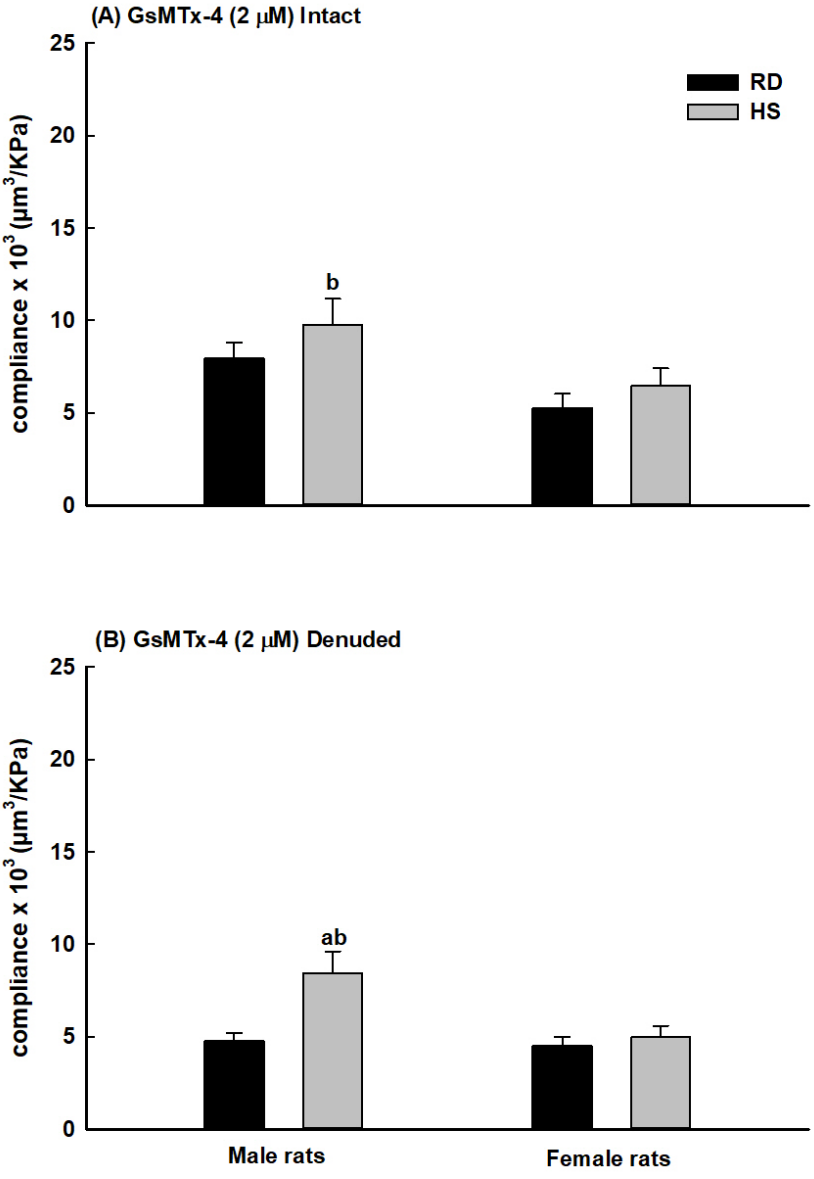
(A) GsMTx-4 (2 μM) Intact
compliance x 10³ (μm³/KPa)
25
20
15
10
5
0
RD
HS
b
(B) GsMTx-4 (2 μM) Denuded
compliance x 10³ (μm³/KPa)
25
20
15
10
5
0
ab
Male rats
Female rats

Figure 4.7: Compliance (μm^3 KPa^{-1}) calculated from pressure–volume plots in isolated third-order mesenteric arteries from Dahl salt-sensitive male and female rats on regular or high salt (4% NaCl) diets for 6–7 weeks in presence of GsMTx-4. (2 μM). (A) intact endothelium, (B) denuded endothelium. Each value is expressed as a mean ± SEM. ($n = 8$). [a]Significantly different from male regular diet; $p < .05$; [b]Significantly different from female high-salt diet; $p < .05$. Significances reported are within intact and denuded groups. HS, high-salt diet; RD, regular diet.

The addition of Yoda in blood vessels pre-constricted with, the α1-adrenoceptor agonist, phenylephrine, revealed no significant differences in compliance between any of the groups (i.e., males and females) in either intact or denuded tissues (Figure 4.8AB).

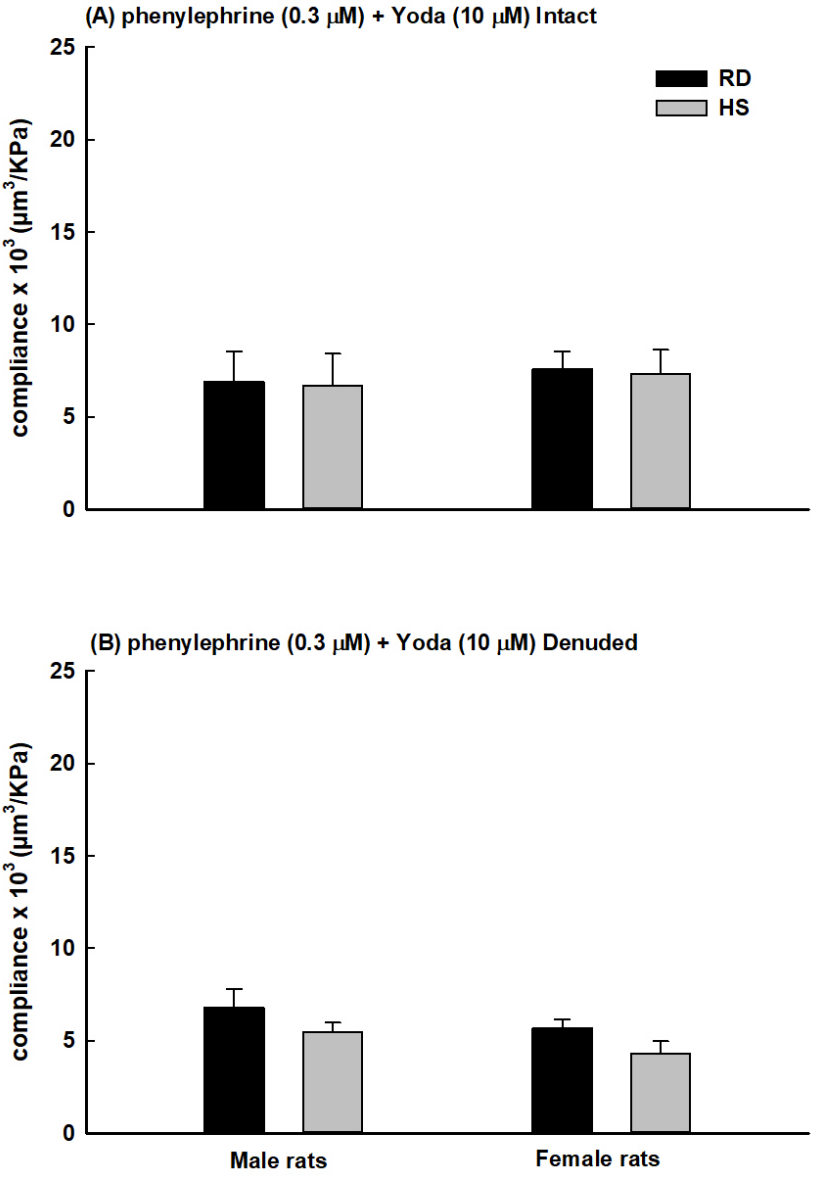
(A) phenylephrine (0.3 μM) + Yoda (10 μM) Intact
RD
HS
compliance x 10³ (μm³/KPa)
25
20
15
10
5
0
(B) phenylephrine (0.3 μM) + Yoda (10 μM) Denuded
compliance x 10³ (μm³/KPa)
25
20
15
10
5
0
Male rats
Female rats

Figure 4.8: Compliance (μm^3 KPa^{-1}) calculated from pressure–volume plots in isolated third-order mesenteric arteries from Dahl salt-sensitive male and female rats on regular or high salt (4% NaCl) diets for 6–7 weeks in presence of phenylephrine (0.3 μM) plus Yoda 1 (10 μM). (A) intact endothelium, (B) denuded endothelium. Each value is expressed as a mean ± SEM ($n = 8$). HS, high-salt diet; RD, regular diet.

4.4.6 Immunohistochemistry

In the third order mesenteric arteries fixed under a pressure of 7.9993 Kpa (60 mmHg), Piezo 1 was found to be expressed in both VSMCs, endothelial cells and adventitia (Figure 4.9). The expression of Piezo 1 was greater in the intima, media and adventitia in males on high salt compared to the other groups. A semi-quantitative analysis indicated a significant increase in the expression of Piezo 1 in males on high salt, predominantly in the media of the vessel wall towards the adventitia (VSMCs), compared to males on a regular diet, without any significant changes in the corresponding female groups (Figure 4.9).

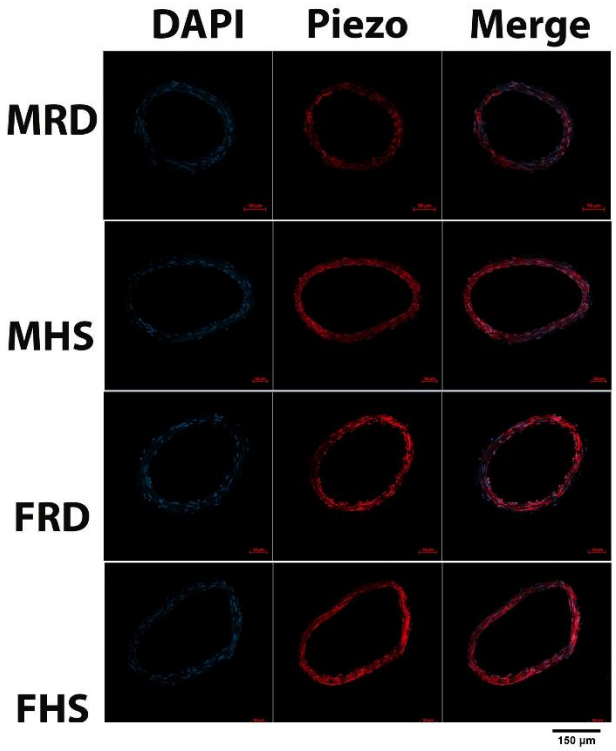
DAPI
Piezo
Merge
MRD
MHS
FRD
FHS
150 µm

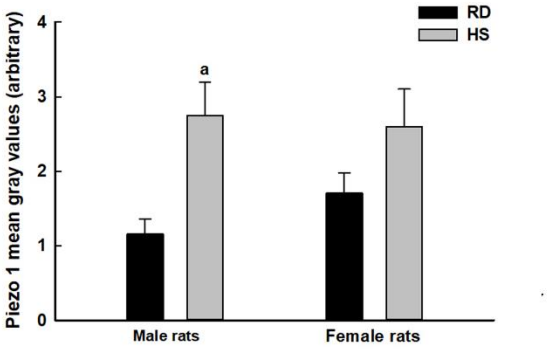
RD
HS
Piezo 1 mean gray values (arbitrary)
0
1
2
3
4
a
Male rats
Female rats

Figure 4.9: Representative photographs of immunohistochemical staining of Piezo 1 antibody in the third-order mesenteric arteries from Dahl salt-sensitive male and female rats on regular or high salt (4% NaCl) diets for 6–7 weeks, fixed under 7.9993 kPa pressure. Inset plot of semi-quantitative assessment of the gray area for Piezo 1 antibody. Each value is expressed as a mean ± SEM ($n = 6$). [a]Significantly different from male regular diet; $p < .05$. Male regular diet; male high-slat diet; female regular diet; female high-salt diet.

4.5 Discussion

The current investigation demonstrates, for the first time, the expression of Piezo 1 mechanosensitive ion channels in small mesenteric arteries. We have also found that antagonism and/or stimulation of Piezo 1 channels can unmask a functional role for the mechanoreceptors in controlling blood vessel wall stiffness. Moreover, the outcomes from our studies support a greater contribution of Piezo 1 to the biomechanics of male hypertensive compared to male normotensive and female hypertensive animals.

Vascular mechanotransduction is the conversion of mechanical forces into biochemical signals. Such mechanical forces play a pivotal role in vascular development and physiology (Volkers et al., 2015). In the vasculature, mechanical (hemodynamic) forces generated by blood flow and changes in transmural pressure can significantly influence vessel wall function and mechanics, especially in diseased states such as hypertension (Humphrey & Schwartz, 2021; Lemarié et al., 2010; Pries et al., 1996). The ensuing response to this mechanical stress involves the exchange of critical mechanical cues between the cellular and structural components of the vessel wall, facilitated by multiple ion channels (Humphrey & Schwartz, 2021; Lemarié et al., 2010). Hemodynamic forces are suggested to activate the vascular mechanosensitive channels that modulate blood vessel tone and remodeling (Humphrey & Schwartz, 2021; Pries et al., 1996).

Piezo 1 and 2 are nonselective mechanosensitive ion channels that are involved in early vascular development (Davies & Tripathi, 1993; Honoré et al., 2015; Volkers et al., 2015). Their expression are suggested to persist in both VSMCs and endothelial cells of the resistance arteries (Davies & Tripathi, 1993; Kefauver et al., 2020; Volkers et al., 2015). These ion channels are a class of mechanosensory membrane proteins that serve as molecular transducers of mechanical

stimuli on a microsecond time scale (earliest cellular events) and convert them into intracellular biochemical signals that allow the movement of ions and solutes across the cell membrane (Davies & Tripathi, 1993; Kefauver et al., 2020). Activation of the Piezo 1 channels by stretch or shear stress is suggested to cause the movement of Na^+, K^+ and Ca^{2+} across the cell membrane. The result could be the induction of either depolarization or hyperpolarization due to the elevation of intracellular of cations (e.g., Ca^{2+}) (Davies & Tripathi, 1993; Kefauver et al., 2020; Nourse & Pathak, 2017; Volkers et al., 2015). For example, in the endothelial cells, the increase in intracellular Ca^{2+} concentration can lead to the activation of the calmodulin-binding domain of eNOS and the production of endothelial-derived relaxation factors (Robledo, 2019; Volkers et al., 2015; Wang et al., 2021). In contrast, an increase in intracellular Ca^{2+} in the VSMC stimulates the Ca-calmodulin complex activation of the myosin light chains kinase leading to contractions that increases the tone of the vessel wall in response to the stretch (Robledo, 2019; Wang et al., 2021).

Consistent with our previous findings (Mensah et al., 2022), the arterial blood pressure and PWV, an index of arterial stiffness of the large central arteries, were significantly elevated in hypertensive compared to normotensive males and females. In the current investigation, while in intact blood vessels (i.e., vehicle treated time control), we found no differences in CYM between the experimental groups, while the removal of the endothelium unmasked significantly higher CYM in normotensive males and corresponding females compared to the hypertensive male in denuded vessels. The latter findings aligns with our previous histological evidence of endothelial cell damage in the third order mesenteric arteries of the Dahl male hypertensive but not male normotensive and female hypertensive or normotensive (Chapter 2). Thus, the observed increase in CYM in the denuded blood vessels reinforces the importance of a functional

endothelium in control of the blood vessel wall stiffness. Accordingly, this could perhaps suggest, (a) adaptive change in the vasculature of male hypertensive animals so as to curtail increases in the blood vessel wall stiffness in intact vessels, and/or (b) that endothelial cells play a greater functional role in the management of arterial stiffness in normotensive males, and females (i.e., normotensive and hypertensive).

While it is recognized that Piezo1 are nonselective cation channels in the endothelial cells and VSMCs (Robledo, 2019; Volkers et al., 2015), there is little known about the vascular cell-specific regulation of these channels and their vasoregulatory role in physiological and pathological conditions in blood vessels. Here in the intact tissues, we found that Yoda 1, a putative Piezo1 agonist, had no effect on the CYM. In contrast, GsMTx-4, an antagonist of Piezo 1 produced an increase in CYM in hypertensive females and normotensive males and females. This lack of effect due to actions of Yoda could be due to a possible constitutive activity of the Piezo 1 channels (Rode et al., 2017), and this view is supported in part by the effects of GsMTx-4. While the concertation of GsMTx-4 used in our current studies was well within the IC50 (23), this compound has been found to block other channels. Nonetheless, the calculated percent changes in CYM from vehicle treated time-controlled experiments also revealed sex-specific differences of functionally of Piezo 1 channels in the intact vessels within the normotensive groups and between hypertensive groups. Taken together, the outcome suggest a different vasoregulatory function for these channels in physiological versus pathological conditions.

The findings from intact tissues also suggest that GsMTx-4 exhibits a vascular-cell-specific effect on vascular tone by blocking the activation of endothelial Piezo 1 channels with minimal effect on VSMC-related Piezo 1 channel. This effect could account for the observed

reduction of CYM in the male hypertensive group compared to the normotensive males and hypertensive females in the intact vessels when treated with GsMTx-4. Therefore, the attenuated effect of GsMTx-4 on the CYM as observed in blood vessels of the hypertensive males could possibly be due to an impaired endothelial function. This is in accord with evidence from our laboratory where electron micrograph images of the third order mesenteric arteries indicated damaged, discontinuous and fragmented endothelial cell layer in male hypertensive but not in the male and female normotensives, or female hypertensive rats (Mensah et al., 2022).

More importantly, pre-constriction of the intact tissues with phenylephrine led to the unmasking of the vasodilatory effects of Yoda via the activation of Piezo 1 channels. The reduction in CYM in the male hypertensive group confirms the possible vasodilatory actions of VSMC Piezo 1 channels in pathological conditions. Furthermore, the significant reduction in CYM in the males compared to female hypertensive groups suggests sex-specific contributions of the Piezo 1 channels in the modulation of vascular tone in pathological conditions (Dogan et al., 2019). We have also demonstrated increased expression of Piezo 1 especially in the tunica media of the hypertensive groups compared to the normotensive groups from our IHC analysis. Furthermore, the activation of Piezo 1 channels by Yoda in our experimental setting requires an applied mechanical force or a change in vascular tone (i.e., vasoconstriction due the actions of phenylephrine).

In the denuded vessels Yoda 1 also produced no effects on CYM in any groups. However, in the denuded vessels, GsMTx-4, produced a significant increase in CYM but only in the female normotensive compared to female hypertensive. It is possible that combined actions of endothelial relaxing and hyperpolarizing, factors and Piezo 1 channel activity could account for the sex-specific cardiovascular protection noted in females. Taken together, these

observations support the view of a role for the Piezo-1 channels in VSMCs in the modulation of blood vessel stiffness. Collectively, our findings seem to indicate that Piezo 1 channel activity may well influence blood vessel wall stiffness in small resistance arteries in the presence and/or absence of functional endothelial cells.

The significant increase in vascular compliance observed in the male hypertensive groups compared to the other groups in the various treatments was consistent with our previous studies (Chapter 2). This is likely due to the initial baseline lumen size of the male hypertensive groups to other groups despite the effects of the various pharmacological interventions. The difference in the volume-pressure relationship of the vessel wall, quantified as compliance, suggests a structural and mechanical adaptive response in the hypertensive male group to maintain functional distensibility in response to increasing vessel wall stress in pathological conditions.

In summary, we have shown for the first time that there are sex-specific contributions of Piezo 1 mechanoreceptors to the biomechanics of resistance arteries. The results demonstrate an increase in Piezo-1 expression in pathological conditions in male hypertensive rats. Furthermore, our findings suggest a different vasoregulatory role of Piezo 1 mechanoreceptors that is either endothelium-specific or VSMC-specific, with a more significant impact in males than females. Taken together, this indicates that blocking Piezo 1 mechanoreceptors results in increased stiffness in resistance arteries, an effect that may in part be endothelium-dependent, and this could be a potential pharmacological target in the modulation and exploration of vascular stiffness.

Appendix B

There was no significant difference between the baseline lumen diameter (μm) of the third-order branch of the mesenteric artery within the male and female groups (Table 1.1 of appendix B). However, there were significant differences in lumen diameter (μm) between the male groups compared to corresponding female groups on either regular diet or high salt diet. Baseline lumen diameters (μm) of the third-order mesenteric arteries measured at the initial pressure of 3.9 KPa (30 mmHg) can be found in Table 1.1 of the appendix B.

In endothelium intact groups, there was no significant differences between baseline diameter (μm) within the male and female groups (Table 1.2 of appendix B). However, there were significant differences in lumen diameter (μm) between the male groups compared to corresponding female groups on either regular diet or high salt diet. Endothelial denudation resulted in a significant difference in lumen diameter (μm) between the male groups (Table 1.2 of appendix B). Furthermore, there were significant differences in lumen diameter (μm) between the male groups compared to corresponding female groups on either regular diet or high salt diet. Baseline lumen diameters (μm) of the third-order mesenteric arteries measured at the initial pressure of 1.99 KPa (15 mmHg) can be found in Table 1.2 of the appendix B.

Chapter 5 Final Summary

The studies in this thesis focused on investigating the sex differences in arterial wall elasticity caused by high salt consumption. The relationship between high salt consumption and cardiovascular adverse effects has been well established (Cappuccio, 2013; Chrysant, 2016; Susic & Frohlich, 2012). However, the mechanisms by which the high salt intake triggers elevated blood pressure and arterial stiffness have not been well defined. Furthermore, the nature, extent, or pattern of sex-related differences in arterial stiffness seem poorly understood, and the underlying mechanisms responsible for the sex-specific differences in arterial stiffness remain to be determined. Therefore, the studies undertaken for this thesis investigated the changes in the structure and biomechanics of mesenteric resistance arteries from salt-sensitive male and female Dahl rats fed with high salt diets. Specifically, third-order mesenteric arteries were used for the studies. The third-order mesenteric arteries are resistance arteries that contribute significantly to total peripheral resistance, acting as one of the regulatory sites for the distribution of cardiac output.

5.1 Effects of high salt consumption

High salt consumption is linked with elevated blood pressure (Liao et al., 1999; Safar & O'Rourke, 2006). Reduction in dietary salt intake is suggested not only to lower blood pressure and the incidence of hypertension but is also associated with reducing morbidity and mortality from cardiovascular diseases (Frisoli et al., 2012; Grillo et al., 2019; Ha, 2014; He et al., 2013; Pechère-Bertschi & Burnier, 2004). The available evidence from this work confirms the relationship between salt intake and elevated blood pressure. High salt intake increased systolic blood pressure and pulse pressure in salt-sensitive Dahl rat models in all three studies (Table 2.

1, 3.1 and 4.1). An important observation from our hemodynamic measurements was the significant increases in the systolic blood pressure, pulse pressure and PWV in the male group compared to the female group on a high salt diet, suggesting a possible protective factor in the females that delays the progress of hypertension in females. The observed hemodynamic differences could be attributed to sex-specific mechanisms that are responsible for the sex differences in the manifestation and progression of hypertension (Ahimastos et al., 2003; Gilbert & Nijland, 2008; Kim et al., 2015).

The mechanisms underlying arterial wall stiffness resulting from a high salt diet are somewhat unclear (Agbaje, 2022; Daemen, 2013; Shirwany & Zou, 2010). Furthermore, studies examining the factors involved in mechanistic sex differences have remained limited (DuPont et al., 2019; Ogola et al., 2018; Rossi et al., 2011). In general, a decline in arterial wall elasticity is suggested to develop from a complex interaction between the structural and cellular elements of the arterial wall (Arribas et al., 2006; Patrick Lacolley et al., 2017; Shirwany & Zou, 2010). The structural changes involve an increase in collagen (fibrosis) and the fragmentation and degradation of elastin that confers elasticity (Arribas et al., 2006; Díez, 2014; Shirwany & Zou, 2010). The cellular factors include changes in EC signaling and function and an increase in VSMC tone and proliferation (Patrick Lacolley et al., 2017; Shirwany & Zou, 2010; Zieman et al., 2005). Additionally, vascular stiffness is suggested not to be uniformly distributed and characteristically different within different sections of the arterial tree. In large elastic arteries, stiffness of the arterial wall is characterized by an outward hypertrophic remodeling while remodeling in resistance arteries, consistent with the observation in this study, is characterized by an inward eutrophic and hypertrophic remodeling (Patrick Lacolley et al., 2017; Savoia, 2019; Schiffrin & Hayoz, 1997).

5.2 Changes within the vascular wall

Ultrastructure and morphometric analysis of pressure-fixed third-order mesenteric arteries revealed an abnormal, damaged, fragmented, discontinuous and disarranged endothelial cell only in the male rats on a high salt diet (Figure 2.1), suggesting a potential diminishment or loss of function in the vascular endothelial layer. Furthermore, we reported increased collagen in the vessel wall of males on a high salt diet with no structural changes in the female counterparts (Figure 2.2). In contrast to the findings from other studies in the literature indicating a degradation of elastin component associated with arterial stiffness, the observation from our ultrastructural analysis in chapter 2 suggests a different pathophysiology of salt-induced-high blood pressure changes in arterial wall elasticity, which is as a result of increased collagen deposition and changes in the cellular components in the arterial wall with no significant changes in elastin composition.

An important factor in the development of hypertension and arterial wall stiffness is the cross-talk between macrocirculation and microcirculation and how the functional and structural abnormalities in one of these circulatory components induce functional and structural abnormalities in another, thus maintaining a vicious cycle (Laurent et al., 2022; Laurent & Boutouyrie, 2020; Safar & Struijker-Boudier, 2010). The increased collagen and smooth muscle cell areas evident in the ultrastructure of mesenteric arteries of hypertensive males compared to normotensive or corresponding females align with the observed difference in hemodynamic and PWV measurements, suggesting how changes in vessel wall components impact overall circulatory function. A remodelling of the arterial wall as a result of increased collagen and smooth muscle cells, an initial adaptive response to increased hemodynamic stress, eventually becomes maladaptive and plays a crucial role in increased vascular resistance. Furthermore, the

results from morphometric and ultrastructure analysis in Chapter 2 may reinforce the presence of a protective factor in the female group, resulting in sex-specific differences in the remodeling of the arterial wall due to salt-induced elevation of blood pressure.

5.3 Vascular stiffness and its indices

Arterial stiffness is an important prognostic biomarker for the prevention of cardiovascular disease. Therefore, effective assessment of arterial wall stiffness identifies cardiovascular risks and provides elastic indices for developing potential therapeutic interventions. Various methods have been used to assess arterial stiffness in both local and specific arterial beds (O'Rourke & Mancia, 1999; Rhee et al., 2008). While elastic indices derived from compliance and PWV provide insights into vascular stiffness and cardiovascular health, the composite elastic Young's used in this study defines the elastic properties of the artery wall and quantifies the intrinsic changes in wall stress for a given change in strain, taking into account all vessel wall components (i.e., structural and cellular components that contribute to the viscoelasticity of the artery wall) (Shadwick, 1999).

The suggested consequence of salt-induced structural and cellular modifications are changes in the functional and mechanical properties of the vessel wall. Overall, our results also showed an increase in vascular compliance in the male groups on a higher salt than the female group (Figure 2.5). The differences in vessel wall compliance were likely influenced by vascular-specific intrinsic factors such as smaller lumen size in the female blood vessels compared to the male counterpart.

The study in Chapter 2 emphasizes using the composite elastic Young's as a better index in the quantitative measurement of wall stiffness. This is particularly important because the composite Young's modulus encompasses changes in all the different components of the vessel wall as a

result of arterial remodeling. The CYM was not significantly altered among the experimental groups in the third-order mesenteric blood vessels at baseline conditions (Figure 2.3). The reason for this observation most probably relates to the vessel wall's structural and functional coupling, as discussed in Chapter 2.

5.4 Effect of high salt diet on vascular tone

High salt consumption is not only linked to an increase in blood pressure but is also suggested to contribute to an increase in systemic peripheral resistance, alterations in endothelial function and the elevation of sympathetic nerve activity (Simmonds et al., 2014; Simon et al., 2003; Sofola et al., 2002). Alterations in sympathetic nerve function is integral to the establishment and progression of many cardiovascular diseases, including hypertension. Females are suggested to be relatively more resistant to salt-induced hypertension than males (Belanger et al., 2020; Grillo et al., 2019; Nakano & Pollock, 2009). However, the mechanisms involved are not fully understood. Using the α1-adrenergic receptor agonist, phenylephrine, we observed a significantly higher CYM in the males on a high salt diet than their corresponding females. The greater value observed for CYM in the presence of the sympathomimetic agent in the blood vessels from male hypertensive animals could be attributed to a combination of functional (i.e., pharmacomechanical coupling) and morphological changes observed in the male animals on a high salt diet (Figure 2.3). This effect was absent in female hypertensive animals and may be an essential factor in the initiation and development of salt-induced hypertension and vascular remodeling. The absence of altered sympathetic nerve activity in the females could also be linked to the proposed protective factor(s) that inhibit or delay the occurrence of hypertension and vascular remodeling in females on a high salt diet. The study in Chapter 2 of this thesis provides insights into the sex-specific differences in resistance artery biomechanics, which could

contribute to identifying novel selective treatments and therapies to reduce the risk of cardiovascular disease.

5.5 Vascular endothelium

Endothelial dysfunction is an impairment in the ability of vascular endothelial cells to produce balanced vasodilator and vasoconstrictor factors that modulate vessel wall tone and vascular remodeling. The relationship between endothelial dysfunction and elevated blood pressure remains a chicken or egg dilemma, where endothelial dysfunction could be a product of elevated intravascular pressure. Accordingly, a dysfunction in the endothelial could lead to elevated blood pressure. The differences in mechanical responses to the various pharmacological inhibitors of nitric oxide synthase & EDHF (Figures 2.4 and 3.2), endothelial denudation (Figure 4.1, 4.2, 4.3 and 4.4) and exogenous NO donor (Figure 2.4 and 3.2) between male and female groups on a high salt diet suggest a possible differential pathological effect of salt between males and females and the mechanisms at play in the development of wall stiffness. The results from this thesis emphasize the impact of high salt consumption on endothelial function. Results from this study suggest that high salt consumption negatively influences NO bioavailability and increases sensitivity to vessel constrictor effects in male Dahl salt-sensitive rats. This observation is consistent with previous studies suggesting that EDHF plays an important role in females compared to males, with EDHF compensating for loss or reduced NO bioavailability in females (McCulloch & Randall, 1998; Scotland et al., 2005).

Arterial wall stiffness is a maladaptive response of the vessel to the changes in mechanical and hemodynamic stress characterized by alterations in the structure and function of the arterial wall. The pathophysiological changes that result in arterial wall stiffness can also be separated into structural and cellular remodeling (Feihl et al., 2008; Renna et al., 2013). The structural changes

in arterial wall stiffness encompass the changes in the composition of the ECM components, primarily collagen and elastin (Méndez-Barbero et al., 2021; Renna et al., 2013), while cellular changes involve a dysfunction of the endothelium and the proliferation and switch from a contractile to a synthetic phenotype of the underlying VSMCs (Félétou, 2011; Lemarié et al., 2010; Méndez-Barbero et al., 2021; Vanhoutte et al., 2017; Yannoutsos et al., 2014). Although several mechanisms are thought to be involved in both the structural and cellular changes that result in the development of wall stiffness, the contributions of MMP-9 (Busti et al., 2010; Cabral et al., 2008; Díez, 2007), NADPH (Canugovi et al., 2019; Drummond et al., 2011; Fortuno et al., 2005) and beta-integrin (Pierre Boutouyrie et al., 2011; Louis et al., 2007; Safar, 2010) are suggested to be central to the remodeling of the arterial wall. Immunohistochemical analysis from this study indicates sex-specific differences in the various biomarkers of arterial remodeling (Figures 3.5, 3.6, 3.7 and 4.9).

The results from the second study emphasize the contributions of MMP-9 in arterial remodeling with an increased expression of MMP-9 and ECM turnover in the male groups on a high salt diet compared to the corresponding females (Figure 3.5). The mechanisms involved in the induction and related expression of MMP-9 remain unclear but seem to suggest both humoral and local responses to the vessel wall stress due to a high salt diet and elevated blood pressure.

Furthermore, our results suggest a possible negative influence of salt intake on endothelial function via increases in oxidative stress, resulting in a reduction in NO bioavailability and endothelial damage in the male groups, which could account for these differences. Oxidative stress resulting from an imbalance between producing and removing reactive oxygen species (ROS) is a crucial factor contributing to arterial wall remodeling. As an essential mediator of vascular cell physiology modulating the activity of several signaling molecules, ROS are also

involved in endothelial dysfunction, vascular inflammation, and arterial remodeling in pathophysiological conditions (Montezano et al., 2015; Paravicini & Touyz, 2008; Touyz & Schiffrin, 2004; Wind et al., 2010). NADPH serves as the primary source of ROS in the vascular system. NADPH is involved in several cellular functions, including growth, proliferation, differentiation, fibrosis, cytoskeletal regulation, apoptosis and contraction of the vascular wall. Furthermore, NADPH is involved in hypertension, inflammation, restenosis and other vascular pathologies (Chen et al., 2018). Increased oxidative stress due to NAPDH oxidase-derived ROS released from vascular cells under stress and pathophysiological conditions is associated with arterial remodeling (Fortuno et al., 2005; Montezano et al., 2015; Touyz & Schiffrin, 2004).

A reduced NO bioavailability characterizes endothelial dysfunction. Results from the first study using SNP, an endogenous NO donor, resulted in a significant reduction in CYM, indicating the vital role of NO in modulating vascular tone, especially in males compared to females (Figure 2.4). Endothelium-dependent relaxation is attenuated by increased levels of endogenous superoxide anions that convert NO into peroxynitrite, thereby impairing the eNOS-dependent relaxation. Elevated blood pressure has been reported to induce the production of superoxide anions via the membrane NADPH. Increased superoxide production resulting in endothelial dysfunction has been observed in hypertensive animal models of hypertension (Jiménez et al., 2007; Murdoch et al., 2011; Sanchez et al., 2006; Wind et al., 2010). This observation is consistent with our current findings that suggest elevated NADPH expression with hypertension, especially in males compared to females (Figure 3.6).

The results from Chapter 3 also implicate the role of VSMC as a source of the mechanistic differences in arterial stiffness via alterations in the cytoskeleton and integrin interactions with the ECM. The ECM-integrin-cytoskeleton interactions play an essential role in mechanosensing,

allowing VSMCs to sense and respond to changes in intraluminal pressure and maintain vascular wall tone. In response to increased wall stress in pathological conditions, integrin expression triggers downstream signals in the myogenic response of resistance arteries that protect vital organs or promote synthetic VSMC phenotypes involved in VSMC proliferation and migration (Goldschmidt et al., 2001; Ojha et al., 2022; Yip et al., 2010). Increased expression of β1-Integrin in Chapter 3 emphasizes the role of VSMC in salt-induced wall stiffness via alterations in ECM-integrin-cytoskeleton interaction observed in males and females on high salt consumption (Figure 3.7). Furthermore, this observation aligns with the greater increase in CYM in the presence of phenylephrine in male versus female hypertensive animals, and normotensive males observed in Chapter 2.

The study in Chapters 3 and 4 highlights the role of ion channels in regulating vascular tone and arterial stiffness via the activation of both the established conventional vascular ion channels (L-type Ca channels) and the novel mechanosensitive ion channels (Piezo 1). For the first time, we have shown the sex-specific roles of these channels in both endothelial and VSMCs of Dahl salt-sensitive rats fed on a high salt diet. Verapamil caused significant changes in CYM within the males but not the female groups (Figure 3.1). These findings indicate a sex-specific sensitivity in the L-type calcium channels that can significantly influence arterial biomechanics in males but not females, as discussed in Chapter 3.

5.6 Piezo 1 mechanosensitive ion channels

Piezo 1 mechanosensitive ion channels are primarily found in peripheral tissues, including endothelial cells and VSMCs and play a crucial role in vascular development and homeostasis (Beech & Kalli, 2019; Douguet et al., 2019). Activation of Piezo 1 mechanosensitive ion channels is thought to be involved in the modulation of the myogenic and trophic effects of the

vessel wall (Endesh, 2018; Garcia Robledo MD, 2019; Robledo, 2019). The study in Chapter 4 reports a differential expression of Piezo 1 mechanosensitive ion channels in small mesenteric arteries in males and females on high salt, suggesting an elevated Piezo-1 channel expression in pathological conditions (Figure 4.9). More importantly, results from the functional studies in endothelium intact and denuded vessels using Yoda and GsMTx-4 suggest a different vasoregulatory role of Piezo 1 channels that is either endothelium-specific (originating from Piezo 1 channels expressed by the endothelium) or VSMC-specific (originating from Piezo 1 channels expressed by the VSMC) (Figure 4.2, 4.3 and 4.4), with a more significant impact in males than females as discussed in Chapter 4. Further studies would be required to assess the contributions of the endothelium-specific and VSMC-specific Piezo 1 channels as a potential pharmacological target in the modulation of vascular stiffness.

5.7 Control of vascular tone on arterial wall remodeling

A vicious cycle of events between structural alterations and loss of endothelial cell function has been suggested to occur in small mesenteric arteries in a hypertensive state (Versari et al., 2009a; Yannoutsos et al., 2014). Modifications in mesenteric artery walls due to elevated blood pressure alter the vascular reserve and blood flow vital to organs (Christensen & Mulvany, 2001; Takala, 1996). Factors that influence the structure and function of the arterial wall contribute to the stiffness and progression of wall remodeling (De Meyer & Herman, 1997; Drexler, 1998; Gibbons, 1997; Nagao & Vanhoutte, 1993; Rubanyi, 1991; Su, 2015). Arterial wall elasticity is modulated by VSMC tone. The loss of vasodilatory effects from the endothelium and increased levels of vasoconstriction due to factors released from endothelial cells, sympathetic nerves, and humoral sources results in the initiation and progression of arterial wall remodeling.

5.8 Limitations

There are some limitations associated with the investigation that require discussion. While pressure myography allows the biomechanics of an arterial wall segment to be assessed *in vitro*, the function is evaluated without perivascular tethering, circulating factors, sympathetic nerve input and, importantly, blood flow, which induces shear stress, when compared with *in vivo*. In addition, while the effects of a number of pharmacological agents were examined in the current thesis, other interventions could have been used with other vasoactive drugs.

As previously discussed, due to the complex nature of the vessel wall, the various indices used to estimate arterial stiffness present some limitations. A shortcoming in the use of compliance as a measure of arterial stiffness is that the compliance of the vessel wall depends on the changes in volume with distending pressure, which is influenced by the size of the lumen and the vessel wall. Furthermore, despite the compensation of the non-linear curve observed from the stress/strain relationship of the arterial wall defined as the slope (CYM), a limitation to using CYM is that the slope does not accurately define the viscoelastic properties of the vessel wall. Regardless of this limitation, CYM provides a static measure of the elastic contributions from all the components of the blood vessel wall, providing a single number for defining arterial wall stiffness.

Likewise, other analytical techniques, such as Western blots, could have been used to explore further the various biochemical markers of arterial stiffness and Piezo 1 channels to quantify any differences between normal and diseased states in males versus females.

Regardless of these limitations, these studies provide insights into understanding the functional (i.e., pharmacomechanical coupling) and morphological changes in blood vessels of male and

female animals on high salt diet and the function of the various pharmacological agents in arterial wall biomechanics.

5.9 Conclusion

Arterial stiffness and remodeling is a leading marker of cardiovascular risk and mortality. This thesis examined the contributions of a high salt diet to arterial stiffness and some of the possible mechanisms involved. The data presented in Chapters 2 - 4 emphasizes significant sex-specific differences in the manifestation of arterial wall stiffness due to high salt consumption and the complex pathophysiological mechanisms that are closely interrelated and could influence the arterial wall's structure (Figure 5.1). Furthermore, this thesis established the role of the various sex-specific mechanisms responsible for the differences in vascular stiffening in males and females. Additionally, this work highlighted the differential expression and role of vascular mechanosensitive channels in regulating resistance artery biomechanics in physiological and pathophysiological conditions, thus providing insights that could be used to develop novel sex-specific cardiovascular-related therapies and treatments.

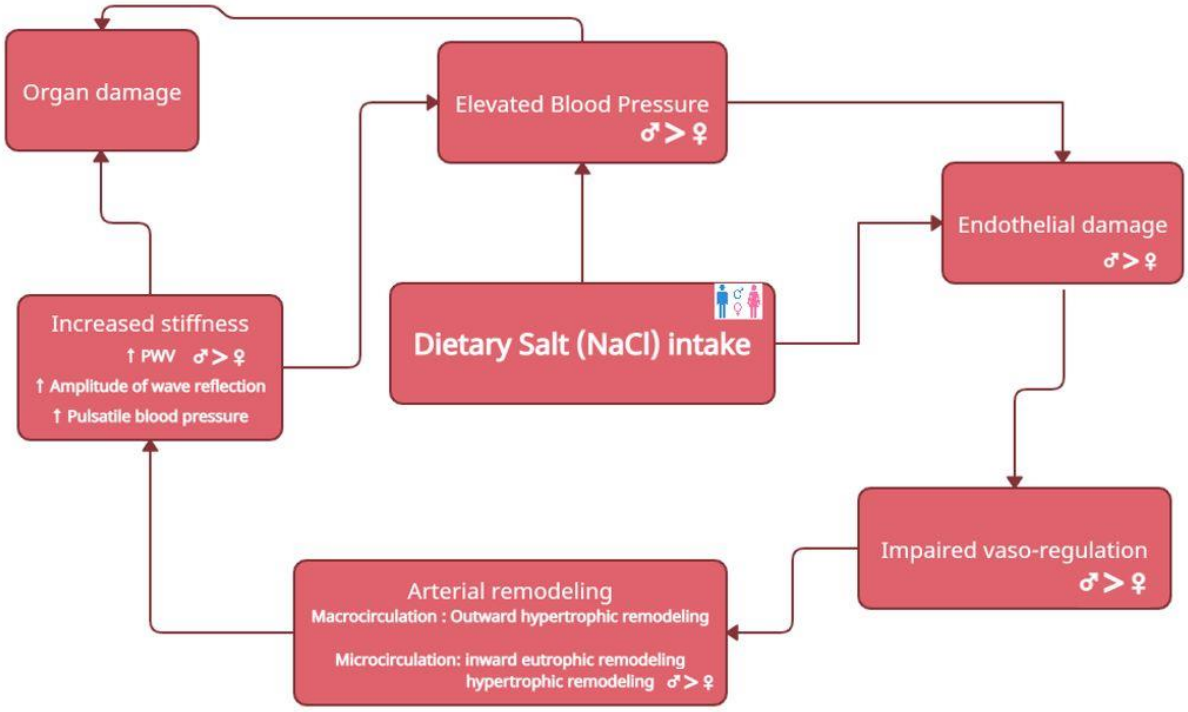

Figure 5.1: Overview of the structural modification and loss of EC function due to high salt intake as a proposed factor in the crosstalk between micro-and-macro-circulation.

References

Abais-Battad, J. M., Alsheikh, A. J., Pan, X., Fehrenbach, D. J., Dasinger, J. H., Lund, H., . . . Mattson, D. L. (2019). Dietary Effects on Dahl Salt-Sensitive Hypertension, Renal Damage, and the T Lymphocyte Transcriptome. *Hypertension*, *74*(4), 854-863. doi: 10.1161/HYPERTENSIONAHA.119.12927.

Achike, F. I., & Dai, S. (1990). Cardiovascular responses to verapamil and nifedipine in hypoventilated and hyperventilated rats. *Br J Pharmacol*, *100*(1), 102-106. doi: 10.1111/j.1476-5381.1990.tb12059.x.

Adams, D. J., Barakeh, J., Laskey, R., & Van Breemen, C. (1989). Ion channels and regulation of intracellular calcium in vascular endothelial cells. *FASEB J*, *3*(12), 2389-2400. doi: 10.1096/fasebj.3.12.2477294.

Adams, R. H., & Alitalo, K. (2007). Molecular regulation of angiogenesis and lymphangiogenesis. *Nat Rev Mol Cell Biol*, *8*(6), 464-478. doi: 10.1038/nrm2183.

Adamson, S. L. (1999). Arterial pressure, vascular input impedance, and resistance as determinants of pulsatile blood flow in the umbilical artery. *European Journal of Obstetrics & Gynecology and Reproductive Biology*, *84*(2), 119-125.

Agbaje, A. O. (2022). Arterial stiffness precedes hypertension and metabolic risks in youth: a review. *J Hypertens*, *40*(10), 1887-1896. doi: 10.1097/HJH.0000000000003239.

Aguiar, S. L. F., Miranda, M. C. G., Guimaraes, M. A. F., Santiago, H. C., Queiroz, C. P., Cunha, P. D. S., . . . Faria, A. M. C. (2017). High-Salt Diet Induces IL-17-Dependent Gut Inflammation and Exacerbates Colitis in Mice. *Front Immunol*, *8*, 1969. doi: 10.3389/fimmu.2017.01969.

Ahimastos, A. A., Formosa, M., Dart, A. M., & Kingwell, B. A. (2003). Gender differences in large artery stiffness pre- and post puberty. *J Clin Endocrinol Metab*, *88*(11), 5375-5380. doi: 10.1210/jc.2003-030722.

Ahmed, S., & Warren, D. T. (2018). Vascular smooth muscle cell contractile function and mechanotransduction. *Vessel Plus*, *2*(11).

Aird, W. C. (2007). Phenotypic heterogeneity of the endothelium: II. Representative vascular beds. *Circ Res*, *100*(2), 174-190. doi: 10.1161/01.RES.0000255690.03436.ae.

Alberts, B., Johnson, A., Lewis, J., Raff, M., Roberts, K., & Walter, P. (2002). Ion channels and the electrical properties of membranes. In *Molecular Biology of the Cell. 4th edition*. Garland Science.

Almohanna, A. M. (2019). *An Investigation into the Effects of Extracellular Acidification on Mouse Uterine Contraction and Possible Mechanisms of Action*.The University of Liverpool (United Kingdom).

Althoff, T. F., & Offermanns, S. (2015). G-protein-mediated signaling in vascular smooth muscle cells—implications for vascular disease. *Journal of Molecular Medicine*, *93*, 973-981.

Anderson, E. A., Sinkey, C. A., Lawton, W. J., & Mark, A. L. (1989). Elevated sympathetic nerve activity in borderline hypertensive humans. Evidence from direct intraneural recordings. *Hypertension*, *14*(2), 177-183. doi: 10.1161/01.hyp.14.2.177.

Anderson, T. J. (2006). Arterial stiffness or endothelial dysfunction as a surrogate marker of vascular risk. *Canadian Journal of Cardiology*, *22*, 72B-80B.

Appel, L. J., Frohlich, E. D., Hall, J. E., Pearson, T. A., Sacco, R. L., Seals, D. R., . . . Van Horn, L. V. (2011). The Importance of Population-Wide Sodium Reduction as a Means to

Prevent Cardiovascular Disease and Stroke A Call to Action From the American Heart Association. *Circulation*, *123*(10), 1138-1143. doi: 10.1161/CIR.0b013e31820d0793.

Arnal, J.-F., El Amrani, A.-I., Chatellier, G., Menard, J., & Michel, J.-B. (1993). Cardiac weight in hypertension induced by nitric oxide synthase blockade. *Hypertension*, *22*(3), 380-387.

Arribas, S. M., Hinek, A., & Gonzalez, M. C. (2006). Elastic fibres and vascular structure in hypertension. *Pharmacol Ther*, *111*(3), 771-791. doi: 10.1016/j.pharmthera.2005.12.003.

Ashida, T., Kawano, Y., Yoshimi, H., Akabane, S., Kuramochi, M., & Omae, T. (1991). Effects of ouabain and verapamil on endothelin-1-induced contraction of mesenteric artery in young spontaneously hypertensive rats. *J Cardiovasc Pharmacol*, *17 Suppl 7*, S174-176. doi: 10.1097/00005344-199100177-00049.

Avolio, A. (2013). Arterial stiffness. *Pulse*, *1*(1), 14-28.

Bacakova, L., Travnickova, M., Filova, E., Matějka, R., Stepanovska, J., Musilkova, J., . . . Molitor, M. (2018). The role of vascular smooth muscle cells in the physiology and pathophysiology of blood vessels. *Muscle Cell and Tissue-Current Status of Research Field*, *1*, 13.

Baldo, M. P., Brant, L. C., Cunha, R. S., Molina, M. d. C. B., Griep, R. H., Barreto, S. M., . . . Mill, J. G. (2019). The association between salt intake and arterial stiffness is influenced by a sex-specific mediating effect through blood pressure in normotensive adults: the ELSA-Brasil study. *The Journal of Clinical Hypertension*, *21*(12), 1771-1779.

Ball, S. G. (1989). The sympathetic nervous system and converting enzyme inhibition. *J Cardiovasc Pharmacol*, *13 Suppl 3*, S17-21. doi: 10.1097/00005344-198900133-00005.

Baltgaile, G. (2012). Arterial wall dynamics. *Perspectives in Medicine*, *1*(1-12), 146-151.

Bank, A. J., & Kaiser, D. R. (2002). Arterial wall mechanics. *Pan Vascular Medicine: Integrated Clinical Management*, 151-161.

Bank, A. J., Wang, H., Holte, J. E., Mullen, K., Shammas, R., & Kubo, S. H. (1996). Contribution of collagen, elastin, and smooth muscle to in vivo human brachial artery wall stress and elastic modulus. *Circulation*, *94*(12), 3263-3270. doi: 10.1161/01.cir.94.12.3263.

Barbaro, N. R., Fontana, V., Modolo, R., De Faria, A. P., Sabbatini, A. R., Fonseca, F. H., . . . Moreno, H. (2015). Increased arterial stiffness in resistant hypertension is associated with inflammatory biomarkers. *Blood Pressure*, *24*(1), 7-13. doi: 10.3109/08037051.2014.940710.

Bauer, V., & Sotníková, R. (2010). Nitric oxide—the endothelium-derived relaxing factor and its role in endothelial functions. *General physiology and biophysics*, *29*(4), 319.

Bax, M., Romanov, V., Junday, K., Giannoulatou, E., Martinac, B., Kovacic, J. C., . . . Graham, R. M. (2022). Arterial dissections: Common features and new perspectives. *Frontiers in cardiovascular medicine*, *9*, 1055862.

Beech, D. J. (2007). Ion channel switching and activation in smooth-muscle cells of occlusive vascular diseases. *Biochem Soc Trans*, *35*(Pt 5), 890-894. doi: 10.1042/BST0350890.

Beech, D. J. (2018). Endothelial Piezo1 channels as sensors of exercise. *J Physiol*, *596*(6), 979-984. doi: 10.1113/JP274396.

Beech, D. J., & Kalli, A. C. (2019). Force Sensing by Piezo Channels in Cardiovascular Health and Disease. *Arterioscler Thromb Vasc Biol*, *39*(11), 2228-2239. doi: 10.1161/ATVBAHA.119.313348.

Belanger, K. M., Crislip, G. R., Gillis, E. E., Abdelbary, M., Musall, J. B., Mohamed, R., . . . Sullivan, J. C. (2020). Greater t regulatory cells in females attenuate doca-salt–induced increases in blood pressure versus males. *Hypertension*, *75*(6), 1615-1623.

Belik, J., & Stephens, N. L. (1993). Developmental differences in vascular smooth muscle mechanics in pulmonary and systemic circulations. *J Appl Physiol (1985)*, *74*(2), 682-687. doi: 10.1152/jappl.1993.74.2.682.

Benetos, A., Waeber, B., Izzo, J., Mitchell, G., Resnick, L., Asmar, R., & Safar, M. (2002). Influence of age, risk factors, and cardiovascular and renal disease on arterial stiffness: clinical applications. *Am J Hypertens*, *15*(12), 1101-1108. doi: 10.1016/s0895-7061(02)03029-7.

Bergel, D. H. (1960). *The visco-elastic properties of the arterial wall* Queen Mary University of London].

Bevan, J. A., & Laher, I. (1991). Pressure and flow-dependent vascular tone. *FASEB J*, *5*(9), 2267-2273. doi: 10.1096/fasebj.5.9.1860618.

Bevan, R. D., & Bevan, J. A. (1984). Structural Change in the Blood Vessel Wall. In *Fundamental Fault in Hypertension* (pp. 296-306). Springer.

Bibbins-Domingo, K., Chertow, G. M., Coxson, P. G., Moran, A., Lightwood, J. M., Pletcher, M. J., & Goldman, L. (2010). Projected effect of dietary salt reductions on future cardiovascular disease. *N Engl J Med*, *362*(7), 590-599. doi: 10.1056/NEJMoa0907355.

Böhm, F., & Pernow, J. (2007). The importance of endothelin-1 for vascular dysfunction in cardiovascular disease. *Cardiovascular Research*, *76*(1), 8-18.

Boutouyrie, P., Lacolley, P., Briet, M., Regnault, V., Stanton, A., Laurent, S., & Mahmud, A. (2011). Pharmacological modulation of arterial stiffness. *Drugs*, *71*(13), 1689-1701. doi: 10.2165/11593790-000000000-00000.

Boutouyrie, P., Lacolley, P., Briet, M., Regnault, V., Stanton, A., Laurent, S., & Mahmud, A. (2011). Pharmacological modulation of arterial stiffness. *Drugs*, *71*, 1689-1701.

Boyle, G. L. J. (2001). Arterial remodelling: mechanisms of altered artery structure and their diagnostic implications for pathologists. *Progress in Pathology: Volume 5*, *5*, 135.

Briones, A. M., Xavier, F. E., Arribas, S. M., González, M. C., Rossoni, L. V., Alonso, M. J., & Salaices, M. (2006). Alterations in structure and mechanics of resistance arteries from ouabain-induced hypertensive rats. *American Journal of Physiology-Heart and Circulatory Physiology*, *291*(1), H193-H201.

Brooke, B. S., Bayes-Genis, A., & Li, D. Y. (2003). New insights into elastin and vascular disease. *Trends in Cardiovascular Medicine*, *13*(5), 176-181. doi: Pii S1050-1738(03)00065-3

Doi 10.1016/S1050-1738(03)00065-3.

Brown, I. A. M., Diederich, L., Good, M. E., DeLalio, L. J., Murphy, S. A., Cortese-Krott, M. M., . . . Isakson, B. E. (2018). Vascular Smooth Muscle Remodeling in Conductive and Resistance Arteries in Hypertension. *Arterioscler Thromb Vasc Biol*, *38*(9), 1969-1985. doi: 10.1161/ATVBAHA.118.311229.

Brozovich, F. V., Nicholson, C. J., Degen, C. V., Gao, Y. Z., Aggarwal, M., & Morgan, K. G. (2016). Mechanisms of Vascular Smooth Muscle Contraction and the Basis for Pharmacologic Treatment of Smooth Muscle Disorders. *Pharmacol Rev*, *68*(2), 476-532. doi: 10.1124/pr.115.010652.

Bruno, R. M., Ghiadoni, L., Seravalle, G., Dell'oro, R., Taddei, S., & Grassi, G. (2012). Sympathetic regulation of vascular function in health and disease. *Front Physiol*, *3*, 284. doi: 10.3389/fphys.2012.00284.

Busse, R., Edwards, G., Feletou, M., Fleming, I., Vanhoutte, P. M., & Weston, A. H. (2002). EDHF: bringing the concepts together. *Trends Pharmacol Sci*, *23*(8), 374-380. doi: 10.1016/s0165-6147(02)02050-3.

Busse, R., Trogisch, G., & Bassenge, E. (1985). The role of endothelium in the control of vascular tone. *Basic Res Cardiol*, *80*(5), 475-490. doi: 10.1007/BF01907912.

Busti, C., Falcinelli, E., Momi, S., & Gresele, P. (2010). Matrix metalloproteinases and peripheral arterial disease. *Intern Emerg Med*, *5*(1), 13-25. doi: 10.1007/s11739-009-0283-y.

Byrne, C. J., Khurana, S., Kumar, A., & Tai, T. C. (2018). Inflammatory Signaling in Hypertension: Regulation of Adrenal Catecholamine Biosynthesis. *Front Endocrinol (Lausanne)*, *9*, 343. doi: 10.3389/fendo.2018.00343.

Cabral-Pacheco, G. A., Garza-Veloz, I., Castruita-De la Rosa, C., Ramirez-Acuna, J. M., Perez-Romero, B. A., Guerrero-Rodriguez, J. F., . . . Martinez-Fierro, M. L. (2020). The Roles of Matrix Metalloproteinases and Their Inhibitors in Human Diseases. *Int J Mol Sci*, *21*(24), 9739. doi: 10.3390/ijms21249739.

Cabral, G. A., Raborn, E. S., Griffin, L., Dennis, J., & Marciano-Cabral, F. (2008). CB2 receptors in the brain: role in central immune function. *Br J Pharmacol*, *153*(2), 240-251. doi: 10.1038/sj.bjp.0707584.

Cai, Z., Gong, Z., Li, Z., Li, L., & Kong, W. (2021). Vascular Extracellular Matrix Remodeling and Hypertension. *Antioxid Redox Signal*, *34*(10), 765-783. doi: 10.1089/ars.2020.8110.

Camasão, D., & Mantovani, D. (2021). The mechanical characterization of blood vessels and their substitutes in the continuous quest for physiological-relevant performances. A critical review. *Materials Today Bio*, *10*, 100106.

Campinho, P., Vilfan, A., & Vermot, J. (2020). Blood Flow Forces in Shaping the Vascular System: A Focus on Endothelial Cell Behavior. *Front Physiol*, *11*, 552. doi: 10.3389/fphys.2020.00552.

Canugovi, C., Stevenson, M. D., Vendrov, A. E., Hayami, T., Robidoux, J., Xiao, H., . . . Madamanchi, N. R. (2019). Increased mitochondrial NADPH oxidase 4 (NOX4) expression in aging is a causative factor in aortic stiffening. *Redox Biology*, *26*, 101288. doi: ARTN 101288

10.1016/j.redox.2019.101288.

Cappuccio, F. P. (2013). Cardiovascular and other effects of salt consumption. *Kidney Int Suppl (2011)*, *3*(4), 312-315. doi: 10.1038/kisup.2013.65.

Carlson, S. H., Shelton, J., White, C. R., & Wyss, J. M. (2000). Elevated sympathetic activity contributes to hypertension and salt sensitivity in diabetic obese Zucker rats. *Hypertension*, *35*(1 Pt 2), 403-408. doi: 10.1161/01.hyp.35.1.403.

Caro, C. G., Pedley, T. J., Schroter, R., & Seed, W. (2012). *The mechanics of the circulation*.Cambridge University Press.

Cecelja, M., & Chowienczyk, P. (2012). Role of arterial stiffness in cardiovascular disease. *JRSM Cardiovasc Dis*, *1*(4), 1-10. doi: 10.1258/cvd.2012.012016.

Cecelja, M., Jiang, B. Y., McNeill, K., Kato, B., Ritter, J., Spector, T., & Chowienczyk, P. (2009). Increased Wave Reflection Rather Than Central Arterial Stiffness Is the Main Determinant of Raised Pulse Pressure in Women and Relates to Mismatch in Arterial

Dimensions A Twin Study. *Journal of the American College of Cardiology*, *54*(8), 695-703. doi: 10.1016/j.jacc.2009.04.068.

Chachisvilis, M., Zhang, Y. L., & Frangos, J. A. (2006). G protein-coupled receptors sense fluid shear stress in endothelial cells. *Proc Natl Acad Sci U S A*, *103*(42), 15463-15468. doi: 10.1073/pnas.0607224103.

Chatzizisis, Y. S., Coskun, A. U., Jonas, M., Edelman, E. R., Feldman, C. L., & Stone, P. H. (2007). Role of endothelial shear stress in the natural history of coronary atherosclerosis and vascular remodeling: molecular, cellular, and vascular behavior. *Journal of the American College of Cardiology*, *49*(25), 2379-2393. doi: 10.1016/j.jacc.2007.02.059.

Chen, G., & Cheung, D. W. (1996). Modulation of endothelium-dependent hyperpolarization and relaxation to acetylcholine in rat mesenteric artery by cytochrome P450 enzyme activity. *Circ Res*, *79*(4), 827-833. doi: 10.1161/01.res.79.4.827.

Chen, Q., Jin, M., Yang, F., Zhu, J., Xiao, Q., & Zhang, L. (2013). Matrix metalloproteinases: inflammatory regulators of cell behaviors in vascular formation and remodeling. *Mediators Inflamm*, *2013*, 928315. doi: 10.1155/2013/928315.

Chen, Q., Wang, Q., Zhu, J., Xiao, Q., & Zhang, L. (2018). Reactive oxygen species: key regulators in vascular health and diseases. *Br J Pharmacol*, *175*(8), 1279-1292. doi: 10.1111/bph.13828.

Cheng, J., Wen, J., Wang, N., Wang, C., Xu, Q., & Yang, Y. (2019). Ion Channels and Vascular Diseases. *Arterioscler Thromb Vasc Biol*, *39*(5), e146-e156. doi: 10.1161/ATVBAHA.119.312004.

Chirinos, J. A. (2012). Arterial stiffness: basic concepts and measurement techniques. *J Cardiovasc Transl Res*, *5*(3), 243-255. doi: 10.1007/s12265-012-9359-6.

Chobanian, A. V., Bakris, G. L., Black, H. R., Cushman, W. C., Green, L. A., Izzo Jr, J. L., . . . Wright Jr, J. T. (2003). Seventh report of the joint national committee on prevention, detection, evaluation, and treatment of high blood pressure. *Hypertension*, *42*(6), 1206-1252.

Christensen, K. L., & Mulvany, M. J. (2001). Location of resistance arteries. *J Vasc Res*, *38*(1), 1-12. doi: 10.1159/000051024.

Chrysant, S. G. (2016). Effects of High Salt Intake on Blood Pressure and Cardiovascular Disease: The Role of COX Inhibitors. *Clin Cardiol*, *39*(4), 240-242. doi: 10.1002/clc.22536.

Cipollone, F., Cicolini, G., & Bucci, M. (2008). Cyclooxygenase and prostaglandin synthases in atherosclerosis: recent insights and future perspectives. *Pharmacol Ther*, *118*(2), 161-180. doi: 10.1016/j.pharmthera.2008.01.002.

Cocciolone, A. J., Hawes, J. Z., Staiculescu, M. C., Johnson, E. O., Murshed, M., & Wagenseil, J. E. (2018). Elastin, arterial mechanics, and cardiovascular disease. *Am J Physiol Heart Circ Physiol*, *315*(2), H189-H205. doi: 10.1152/ajpheart.00087.2018.

Cohen, R. A., & Vanhoutte, P. M. (1995). Endothelium-dependent hyperpolarization. Beyond nitric oxide and cyclic GMP. *Circulation*, *92*(11), 3337-3349. doi: 10.1161/01.cir.92.11.3337.

Colafella, K. M. M., & Denton, K. M. (2018). Sex-specific differences in hypertension and associated cardiovascular disease. *Nat Rev Nephrol*, *14*(3), 185-201. doi: 10.1038/nrneph.2017.189.

Collier, S. R., Frechette, V., Sandberg, K., Schafer, P., Ji, H., Smulyan, H., & Fernhall, B. (2011). Sex differences in resting hemodynamics and arterial stiffness following 4 weeks

of resistance versus aerobic exercise training in individuals with pre-hypertension to stage 1 hypertension. *Biol Sex Differ*, *2*(1), 9. doi: 10.1186/2042-6410-2-9.

Conger, J. D. (1994). Endothelial regulation of vascular tone. *Hosp Pract (Off Ed)*, *29*(10), 117-122, 125-116. doi: 10.1080/21548331.1994.11443095.

Cook, N. R., Cutler, J. A., Obarzanek, E., Buring, J. E., Rexrode, K. M., Kumanyika, S. K., . . . Whelton, P. K. (2007). Long term effects of dietary sodium reduction on cardiovascular disease outcomes: observational follow-up of the trials of hypertension prevention (TOHP). *BMJ*, *334*(7599), 885-888. doi: 10.1136/bmj.39147.604896.55.

Cooke, J. P. (2000). The endothelium: a new target for therapy. *Vasc Med*, *5*(1), 49-53. doi: 10.1177/1358836X0000500108.

Cooper, D., & Dimri, M. (2021). Biochemistry, Calcium Channels. In *StatPearls [Internet]*. StatPearls Publishing.

Cosson, E., Herisse, M., Laude, D., Thomas, F., Valensi, P., Attali, J. R., . . . Dabire, H. (2007). Aortic stiffness and pulse pressure amplification in Wistar-Kyoto and spontaneously hypertensive rats. *Am J Physiol Heart Circ Physiol*, *292*(5), H2506-2512. doi: 10.1152/ajpheart.00732.2006.

Coutinho, T., Borlaug, B. A., Pellikka, P. A., Turner, S. T., & Kullo, I. J. (2013). Sex differences in arterial stiffness and ventricular-arterial interactions. *Journal of the American College of Cardiology*, *61*(1), 96-103. doi: 10.1016/j.jacc.2012.08.997.

Covic, A., & Siriopol, D. (2015). Pulse wave velocity ratio: the new “gold standard” for measuring arterial stiffness. In (Vol. 65, pp. 289-290): Am Heart Assoc.

Cox, R. H. (1975). Arterial wall mechanics and composition and the effects of smooth muscle activation. *Am J Physiol*, *229*(3), 807-812. doi: 10.1152/ajplegacy.1975.229.3.807.

Cox, R. H. (1983). Comparison of arterial wall mechanics using ring and cylindrical segments. *Am J Physiol*, *244*(2), H298-303. doi: 10.1152/ajpheart.1983.244.2.H298.

Cribbs, L. L. (2001). Vascular smooth muscle calcium channels: could "T" be a target? In (Vol. 89, pp. 560-562): Am Heart Assoc.

Crowe, A. R., & Yue, W. (2019). Semi-quantitative Determination of Protein Expression using Immunohistochemistry Staining and Analysis: An Integrated Protocol. *Bio Protoc*, *9*(24), e3465-e3465. doi: 10.21769/BioProtoc.3465.

Cui, N., Hu, M., & Khalil, R. A. (2017). Biochemical and Biological Attributes of Matrix Metalloproteinases. *Prog Mol Biol Transl Sci*, *147*, 1-73. doi: 10.1016/bs.pmbts.2017.02.005.

Daemen, J. (2013). Diastolic dysfunction and arterial stiffness: the chicken or the egg. *Neth Heart J*, *21*(5), 219-221. doi: 10.1007/s12471-013-0405-z.

Daiber, A., Steven, S., Weber, A., Shuvaev, V. V., Muzykantov, V. R., Laher, I., . . . Munzel, T. (2017). Targeting vascular (endothelial) dysfunction. *Br J Pharmacol*, *174*(12), 1591-1619. doi: 10.1111/bph.13517.

Davenport, A. P., Hyndman, K. A., Dhaun, N., Southan, C., Kohan, D. E., Pollock, J. S., . . . Maguire, J. J. (2016). Endothelin. *Pharmacol Rev*, *68*(2), 357-418. doi: 10.1124/pr.115.011833.

Davies, P. F., & Tripathi, S. C. (1993). Mechanical stress mechanisms and the cell. An endothelial paradigm. *Circ Res*, *72*(2), 239-245. doi: 10.1161/01.res.72.2.239.

Davis, M. J., Earley, S., Li, Y. S., & Chien, S. (2023). Vascular mechanotransduction. *Physiol Rev*, *103*(2), 1247-1421. doi: 10.1152/physrev.00053.2021.

Davis, M. J., & Hill, M. A. (1999). Signaling mechanisms underlying the vascular myogenic response. *Physiol Rev*, *79*(2), 387-423. doi: 10.1152/physrev.1999.79.2.387.

De Meyer, G. R., & Herman, A. G. (1997). Vascular endothelial dysfunction. *Prog Cardiovasc Dis*, *39*(4), 325-342. doi: 10.1016/s0033-0620(97)80031-x.

Decano, J. L., Pasion, K. A., Black, N., Giordano, N. J., Herrera, V. L., & Ruiz-Opazo, N. (2016). Sex-specific genetic determinants for arterial stiffness in Dahl salt-sensitive hypertensive rats. *BMC Genet*, *17*(1), 19. doi: 10.1186/s12863-015-0324-7.

Díez, J. (2007). Arterial stiffness and extracellular matrix. *Atherosclerosis, Large Arteries and Cardiovascular Risk*, *44*, 76-95.

Díez, J. (2014). Structural alterations in arterial stiffness: role of arterial fibrosis. *Blood Pressure and Arterial Wall Mechanics in Cardiovascular Diseases*, 205-213.

Dogan, M. F., Yildiz, O., Arslan, S. O., & Ulusoy, K. G. (2019). Potassium channels in vascular smooth muscle: a pathophysiological and pharmacological perspective. *Fundam Clin Pharmacol*, *33*(5), 504-523. doi: 10.1111/fcp.12461.

Doughty, J. M., Plane, F., & Langton, P. D. (1999). Charybdotoxin and apamin block EDHF in rat mesenteric artery if selectively applied to the endothelium. *Am J Physiol*, *276*(3), H1107-1112. doi: 10.1152/ajpheart.1999.276.3.H1107.

Douguet, D., Patel, A., Xu, A., Vanhoutte, P. M., & Honore, E. (2019). Piezo Ion Channels in Cardiovascular Mechanobiology. *Trends Pharmacol Sci*, *40*(12), 956-970. doi: 10.1016/j.tips.2019.10.002.

Drexler, H. (1998). Factors involved in the maintenance of endothelial function. *Am J Cardiol*, *82*(10A), 3S-4S. doi: 10.1016/s0002-9149(98)00667-5.

Drummond, G. R., Selemidis, S., Griendling, K. K., & Sobey, C. G. (2011). Combating oxidative stress in vascular disease: NADPH oxidases as therapeutic targets. *Nature Reviews Drug Discovery*, *10*(6), 453-471. doi: 10.1038/nrd3403.

DuPont, J. J., Kenney, R. M., Patel, A. R., & Jaffe, I. Z. (2019). Sex differences in mechanisms of arterial stiffness. *Br J Pharmacol*, *176*(21), 4208-4225. doi: 10.1111/bph.14624.

Eble, J. A., & Niland, S. (2009). The extracellular matrix of blood vessels. *Curr Pharm Des*, *15*(12), 1385-1400. doi: 10.2174/138161209787846757.

Edis, A. J., & Shepherd, J. T. (1970). Autonomic control of the peripheral vascular system. *Arch Intern Med*, *125*(4), 716-724.

Edwards, D. H. (2013). Local, integrated control of blood flow: Professor Tudor Griffith Memorial. *Auton Neurosci*, *178*(1-2), 4-8. doi: 10.1016/j.autneu.2013.02.023.

Eguchi, S., Hirata, Y., Imai, T., & Marumo, F. (1993). Endothelin receptor subtypes are coupled to adenylate cyclase via different guanyl nucleotide-binding proteins in vasculature. *Endocrinology*, *132*(2), 524-529. doi: 10.1210/endo.132.2.7678793.

Eid, A. H., El-Yazbi, A. F., Zouein, F., Arredouani, A., Ouhtit, A., Rahman, M. M., . . . Abou-Saleh, H. (2018). Inositol 1,4,5-Trisphosphate Receptors in Hypertension. *Front Physiol*, *9*, 1018. doi: 10.3389/fphys.2018.01018.

Eisenach, J. H., Gullixson, L. R., Kost, S. L., Joyner, M. J., Turner, S. T., & Nicholson, W. T. (2012). Sex differences in salt sensitivity to nitric oxide dependent vasodilation in healthy young adults. *J Appl Physiol (1985)*, *112*(6), 1049-1053. doi: 10.1152/japplphysiol.01197.2011.

Endesh, N. E. M. (2018). *Contractile functions of Piezo1 channels in murine arteries* University of Leeds].

Engberink, R. H. G. O., Rorije, N. M. G., van der Heide, J. J. H., van den Born, B. J. H., & Voget, L. (2015). Role of the Vascular Wall in Sodium Homeostasis and Salt Sensitivity. *Journal of the American Society of Nephrology*, *26*(4), 777-783. doi: 10.1681/Asn.2014050430.

Eoh, J. H., Shen, N., Burke, J. A., Hinderer, S., Xia, Z., Schenke-Layland, K., & Gerecht, S. (2017). Enhanced elastin synthesis and maturation in human vascular smooth muscle tissue derived from induced-pluripotent stem cells. *Acta Biomater*, *52*, 49-59. doi: 10.1016/j.actbio.2017.01.083.

Feihl, F., Liaudet, L., Levy, B. I., & Waeber, B. (2008). Hypertension and microvascular remodelling. *Cardiovascular Research*, *78*(2), 274-285. doi: 10.1093/cvr/cvn022.

Feihl, F., Liaudet, L., & Waeber, B. (2009). The macrocirculation and microcirculation of hypertension. *Curr Hypertens Rep*, *11*(3), 182-189. doi: 10.1007/s11906-009-0033-6.

Félétou, M. (2011). The endothelium, Part I: Multiple functions of the endothelial cells--focus on endothelium-derived vasoactive mediators. Colloquium series on integrated systems physiology: From molecule to function.

Félétou, M., & Vanhoutte, P. M. (2004). EDHF: new therapeutic targets? *Pharmacological research*, *49*(6), 565-580.

Fels, B., & Kusche-Vihrog, K. (2020). It takes more than two to tango: mechanosignaling of the endothelial surface. *Pflugers Arch*, *472*(4), 419-433. doi: 10.1007/s00424-020-02369-2.

Fitch, R. M., Vergona, R., Sullivan, M. E., & Wang, Y. X. (2001). Nitric oxide synthase inhibition increases aortic stiffness measured by pulse wave velocity in rats. *Cardiovascular Research*, *51*(2), 351-358. doi: 10.1016/s0008-6363(01)00299-1.

Folkow, B. (1987). Structure and function of the arteries in hypertension. *Am Heart J*, *114*(4 Pt 2), 938-948. doi: 10.1016/0002-8703(87)90591-6.

Fortuno, A., San Jose, G., Moreno, M. U., Diez, J., & Zalba, G. (2005). Oxidative stress and vascular remodelling. *Exp Physiol*, *90*(4), 457-462. doi: 10.1113/expphysiol.2005.030098.

Frismantiene, A., Philippova, M., Erne, P., & Resink, T. J. (2018). Smooth muscle cell-driven vascular diseases and molecular mechanisms of VSMC plasticity. *Cell Signal*, *52*, 48-64. doi: 10.1016/j.cellsig.2018.08.019.

Frisoli, T. M., Schmieder, R. E., Grodzicki, T., & Messerli, F. H. (2012). Salt and hypertension: is salt dietary reduction worth the effort? *The American journal of medicine*, *125*(5), 433-439.

Fronek, K., & Zweifach, B. W. (1975). Microvascular pressure distribution in skeletal muscle and the effect of vasodilation. *American Journal of Physiology-Legacy Content*, *228*(3), 791-796.

Gallo, G., Volpe, M., & Savoia, C. (2021). Endothelial Dysfunction in Hypertension: Current Concepts and Clinical Implications. *Front Med (Lausanne)*, *8*, 798958. doi: 10.3389/fmed.2021.798958.

Gamoh, S., Shiba, T., DiPette, D. J., & Yamamoto, R. (2019). Differences in the response to periarterial nerve stimulation or exogenous noradrenaline infusion in the mesenteric vascular bed with the intestinal tract harvested from commonly used rat models of hypertension. *Clinical and Experimental Pharmacology and Physiology*, *46*(5), 427-434.

Gao, Y. (2022). Neurotransmitters. In *Biology of Vascular Smooth Muscle: Vasoconstriction and Dilatation* (pp. 111-130). Springer.

Gao, Y. Z., Saphirstein, R. J., Yamin, R., Suki, B., & Morgan, K. G. (2014). Aging impairs smooth muscle-mediated regulation of aortic stiffness: a defect in shock absorption function? *Am J Physiol Heart Circ Physiol*, *307*(8), H1252-1261. doi: 10.1152/ajpheart.00392.2014.

Garcia Robledo MD, J. (2019). Piezo1: Proteins for mechanotransduction and integration of endothelial shear stress & intravascular pressure.

Garland, C. J., Hiley, C. R., & Dora, K. A. (2011). EDHF: spreading the influence of the endothelium. *Br J Pharmacol*, *164*(3), 839-852. doi: 10.1111/j.1476-5381.2010.01148.x.

Ghosh, D., Syed, A. U., Prada, M. P., Nystoriak, M. A., Santana, L. F., Nieves-Cintron, M., & Navedo, M. F. (2017). Calcium Channels in Vascular Smooth Muscle. *Adv Pharmacol*, *78*, 49-87. doi: 10.1016/bs.apha.2016.08.002.

Gibbons, G. H. (1997). Endothelial function as a determinant of vascular function and structure: a new therapeutic target. *Am J Cardiol*, *79*(5A), 3-8. doi: 10.1016/s0002-9149(97)00122-7.

Gibbons, G. H., & Dzau, V. J. (1994). The emerging concept of vascular remodeling. *N Engl J Med*, *330*(20), 1431-1438. doi: 10.1056/NEJM199405193302008.

Gilbert, J. S., & Nijland, M. J. (2008). Sex differences in the developmental origins of hypertension and cardiorenal disease. *Am J Physiol Regul Integr Comp Physiol*, *295*(6), R1941-1952. doi: 10.1152/ajpregu.90724.2008.

Gkaliagkousi, E., & Douma, S. (2009). The pathogenesis of arterial stiffness and its prognostic value in essential hypertension and cardiovascular diseases. *Hippokratia*, *13*(2), 70-75.

Glasser, S. P., Arnett, D. K., McVeigh, G. E., Finkelstein, S. M., Bank, A. J., Morgan, D. J., & Cohn, J. N. (1997). Vascular compliance and cardiovascular disease: a risk factor or a marker? *Am J Hypertens*, *10*(10 Pt 1), 1175-1189. doi: 10.1016/s0895-7061(97)00311-7.

Goldschmidt, M. E., McLeod, K. J., & Taylor, W. R. (2001). Integrin-mediated mechanotransduction in vascular smooth muscle cells: frequency and force response characteristics. *Circ Res*, *88*(7), 674-680. doi: 10.1161/hh0701.089749.

Gomez Sandoval, Y.-H., Emehdi Atef, M., Levesque, L.-O., Li, Y., & B Anand-Srivastava, M. (2014). Endothelin-1 signaling in vascular physiology and pathophysiology. *Current vascular pharmacology*, *12*(2), 202-214.

Goto, K., & Kitazono, T. (2022). Chloride Ions, Vascular Function and Hypertension. *Biomedicines*, *10*(9), 2316. doi: 10.3390/biomedicines10092316.

Gough, N. R. (2008). NADPH Sensor Regulates NO Production. *Science Signaling*, *1*(16), ec142-ec142.

Grey, E., Bratteli, C., Glasser, S. P., Alinder, C., Finkelstein, S. M., Lindgren, B. R., & Cohn, J. N. (2003). Reduced small artery but not large artery elasticity is an independent risk marker for cardiovascular events. *American journal of hypertension*, *16*(4), 265-269.

Griffith, O. W., & Stuehr, D. J. (1995). Nitric oxide synthases: properties and catalytic mechanism. *Annu Rev Physiol*, *57*(1), 707-736. doi: 10.1146/annurev.ph.57.030195.003423.

Grillo, A., Salvi, L., Coruzzi, P., Salvi, P., & Parati, G. (2019). Sodium Intake and Hypertension. *Nutrients*, *11*(9), 1970. doi: 10.3390/nu11091970.

Guajardo, I., Ayer, A., Johnson, A. D., Ganz, P., Mills, C., Donovan, C., . . . Dubin, R. F. (2018). Sex differences in vascular dysfunction and cardiovascular outcomes: The cardiac,

endothelial function, and arterial stiffness in ESRD (CERES) study. *Hemodial Int*, *22*(1), 93-102. doi: 10.1111/hdi.12544.

Gundiah, N., Ratcliffe, M. B., & Pruitt, L. A. (2009). The biomechanics of arterial elastin. *J Mech Behav Biomed Mater*, *2*(3), 288-296. doi: 10.1016/j.jmbbm.2008.10.007.

Guo, X., Lu, X., Yang, J., & Kassab, G. S. (2014). Increased aortic stiffness elevates pulse and mean pressure and compromises endothelial function in Wistar rats. *Am J Physiol Heart Circ Physiol*, *307*(6), H880-887. doi: 10.1152/ajpheart.00265.2014.

Ha, S. K. (2014). Dietary salt intake and hypertension. *Electrolyte Blood Press*, *12*(1), 7-18. doi: 10.5049/EBP.2014.12.1.7.

Hall, J. E., & Hall, M. E. (2020). *Guyton and Hall textbook of medical physiology e-Book*.Elsevier Health Sciences.

Halper, J. (2018). Basic Components of Vascular Connective Tissue and Extracellular Matrix. *Adv Pharmacol*, *81*, 95-127. doi: 10.1016/bs.apha.2017.08.012.

Hansen, M. B., Dresner, L. S., & Wait, R. B. (1998). Profile of neurohumoral agents on mesenteric and intestinal blood flow in health and disease. *Physiol Res*, *47*(5), 307-327.

Hassanisaber, H., Rouleau, L., & Faucheux, N. (2019). Effect of BMP-9 on endothelial cells and its role in atherosclerosis. *Front Biosci (Landmark Ed)*, *24*(6), 994-1023. doi: 10.2741/4764.

Hays, T. T., Ma, B., Zhou, N., Stoll, S., Pearce, W. J., & Qiu, H. (2018). Vascular smooth muscle cells direct extracellular dysregulation in aortic stiffening of hypertensive rats. *Aging Cell*, *17*(3), e12748. doi: 10.1111/acel.12748.

He, F. J., Li, J., & MacGregor, G. A. (2013). Effect of longer-term modest salt reduction on blood pressure. *Cochrane database of systematic reviews*, (4).

He, F. J., & MacGregor, G. A. (2007). Salt, blood pressure and cardiovascular disease. *Curr Opin Cardiol*, *22*(4), 298-305. doi: 10.1097/HCO.0b013e32814f1d8c.

He, J., Gu, D., Chen, J., Jaquish, C. E., Rao, D. C., Hixson, J. E., . . . GenSalt Collaborative Research, G. (2009). Gender difference in blood pressure responses to dietary sodium intervention in the GenSalt study. *J Hypertens*, *27*(1), 48-54. doi: 10.1097/hjh.0b013e328316bb87.

Heistad, D. D., & Marcus, M. L. (1979). Role of vasa vasorum in nourishment of the aorta. *Blood Vessels*, *16*(5), 225-238. doi: 10.1159/000158209.

Hill, M., & Davis, M. (2012). Local control of microvascular perfusion. Colloquium Series on Integrated Systems Physiology: From Molecule to Function.

Hill, M. A., Sun, Z., Martinez-Lemus, L., & Meininger, G. A. (2007). New technologies for dissecting the arteriolar myogenic response. *Trends Pharmacol Sci*, *28*(7), 308-315. doi: 10.1016/j.tips.2007.05.006.

Holme, M. R., & Sharman, T. (2020). Sodium nitroprusside.

Holzapfel, G. A., Gasser, T. C., & Ogden, R. W. (2000). A new constitutive framework for arterial wall mechanics and a comparative study of material models. *Journal of Elasticity*, *61*(1-3), 1-48. doi: Doi 10.1023/A:1010835316564.

Honoré, E., Martins, J. R., Penton, D., Patel, A., & Demolombe, S. (2015). The piezo mechanosensitive ion channels: may the force be with you! *Reviews of Physiology, Biochemistry and Pharmacology Vol. 169*, 25-41.

Huang, A., Sun, D., Koller, A., & Kaley, G. (1998). Gender difference in flow-induced dilation and regulation of shear stress: role of estrogen and nitric oxide. *Am J Physiol*, *275*(5), R1571-1577. doi: 10.1152/ajpregu.1998.275.5.R1571.

Hübner, C. A., Schroeder, B. C., & Ehmke, H. (2015). Regulation of vascular tone and arterial blood pressure: role of chloride transport in vascular smooth muscle. *Pflügers Archiv-European Journal of Physiology*, *467*, 605-614.

Hughes, A. D. (1995). Calcium channels in vascular smooth muscle cells. *J Vasc Res*, *32*(6), 353-370. doi: 10.1159/000159111.

Humphrey, J. D. (1995). Mechanics of the arterial wall: review and directions. *Crit Rev Biomed Eng*, *23*(1-2), 1-162.

Humphrey, J. D., & Schwartz, M. A. (2021). Vascular Mechanobiology: Homeostasis, Adaptation, and Disease. *Annu Rev Biomed Eng*, *23*, 1-27. doi: 10.1146/annurev-bioeng-092419-060810.

Iftinca, M. (2011). Neuronal T–type calcium channels: What's new? Iftinca: T–type channel regulation. *Journal of medicine and life*, *4*(2), 126.

Inagami, T., Naruse, M., & Hoover, R. (1995). Endothelium - as an Endocrine Organ. *Annual Review of Physiology*, *57*(1), 171-189.

Intengan, H. D., Deng, L. Y., Li, J. S., & Schiffrin, E. L. (1999). Mechanics and composition of human subcutaneous resistance arteries in essential hypertension. *Hypertension*, *33*(1 Pt 2), 569-574. doi: 10.1161/01.hyp.33.1.569.

Intengan, H. D., & Schiffrin, E. L. (1998). Mechanical properties of mesenteric resistance arteries from Dahl salt-resistant and salt-sensitive rats: role of endothelin-1. *J Hypertens*, *16*(12 Pt 2), 1907-1912. doi: 10.1097/00004872-199816121-00009.

Intengan, H. D., & Schiffrin, E. L. (2000). Structure and mechanical properties of resistance arteries in hypertension: role of adhesion molecules and extracellular matrix determinants. *Hypertension*, *36*(3), 312-318. doi: 10.1161/01.hyp.36.3.312.

Intengan, H. D., & Schiffrin, E. L. (2001). Vascular remodeling in hypertension: roles of apoptosis, inflammation, and fibrosis. *Hypertension*, *38*(3 Pt 2), 581-587. doi: 10.1161/hy09t1.096249.

Jackson. (2021). Myogenic Tone in Peripheral Resistance Arteries and Arterioles: The Pressure Is On! *Front Physiol*, *12*, 699517. doi: 10.3389/fphys.2021.699517.

Jackson, W. F. (2000). Ion channels and vascular tone. *Hypertension*, *35*(1 Pt 2), 173-178. doi: 10.1161/01.hyp.35.1.173.

Jackson, W. F. (2017). Potassium Channels in Regulation of Vascular Smooth Muscle Contraction and Growth. *Adv Pharmacol*, *78*, 89-144. doi: 10.1016/bs.apha.2016.07.001.

Jackson, W. F. (2021). Myogenic Tone in Peripheral Resistance Arteries and Arterioles: The Pressure Is On! *Frontiers in Physiology*, *12*. doi: ARTN 699517

10.3389/fphys.2021.699517.

Jacob, M., Chappell, D., & Becker, B. F. (2016). Regulation of blood flow and volume exchange across the microcirculation. *Crit Care*, *20*(1), 319. doi: 10.1186/s13054-016-1485-0.

Jacob, M. P. (2003). Extracellular matrix remodeling and matrix metalloproteinases in the vascular wall during aging and in pathological conditions. *Biomed Pharmacother*, *57*(5-6), 195-202. doi: 10.1016/s0753-3322(03)00065-9.

Jadeja, R. N., Rachakonda, V., Bagi, Z., & Khurana, S. (2015). Assessing Myogenic Response and Vasoactivity In Resistance Mesenteric Arteries Using Pressure Myography. *J Vis Exp*, 10.3791/50997(101), e50997. doi: 10.3791/50997.

Jaminon, A., Reesink, K., Kroon, A., & Schurgers, L. (2019). The Role of Vascular Smooth Muscle Cells in Arterial Remodeling: Focus on Calcification-Related Processes. *Int J Mol Sci*, *20*(22), 5694. doi: 10.3390/ijms20225694.

Janić, M., Lunder, M., & Šabovič, M. (2014). Arterial stiffness and cardiovascular therapy. *BioMed research international*, *2014*.

Jiang, J., Zheng, J. P., Li, Y., Gan, Z., Jiang, Y., Huang, D., . . . Ke, Y. (2016). Differential contribution of endothelium-derived relaxing factors to vascular reactivity in conduit and resistance arteries from normotensive and hypertensive rats. *Clin Exp Hypertens*, *38*(4), 393-398. doi: 10.3109/10641963.2016.1148155.

Jiménez, R., López-Sepúlveda, R., Kadmiri, M., Romero, M., Vera, R., Sánchez, M., . . . Dueñas, M. (2007). Polyphenols restore endothelial function in DOCA-salt hypertension: role of endothelin-1 and NADPH oxidase. *Free Radical Biology and Medicine*, *43*(3), 462-473.

Johansson, B. (1989). Myogenic tone and reactivity: definitions based on muscle physiology. *J Hypertens Suppl*, *7*(4), S5-8; discussion S9.

Kajuluri, L. P., Singh, K., & Morgan, K. G. (2021). Vascular aging, the vascular cytoskeleton and aortic stiffness. *Explor Med*, *2*, 186-197. doi: 10.37349/emed.2021.00041.

Kalani, A., Pushpakumar, S. B., Vacek, J. C., Tyagi, S. C., & Tyagi, N. (2016). Inhibition of MMP-9 attenuates hypertensive cerebrovascular dysfunction in Dahl salt-sensitive rats. *Mol Cell Biochem*, *413*(1-2), 25-35. doi: 10.1007/s11010-015-2623-8.

Kanbay, M., Chen, Y., Solak, Y., & Sanders, P. W. (2011). Mechanisms and consequences of salt sensitivity and dietary salt intake. *Curr Opin Nephrol Hypertens*, *20*(1), 37-43. doi: 10.1097/MNH.0b013e32834122f1.

Karnovsky, M. J. (1964). The Localization of Cholinesterase Activity in Rat Cardiac Muscle by Electron Microscopy. *J Cell Biol*, *23*(2), 217-232. doi: 10.1083/jcb.23.2.217.

Katusic, Z. S. (1996). Superoxide anion and endothelial regulation of arterial tone. *Free Radic Biol Med*, *20*(3), 443-448. doi: 10.1016/0891-5849(96)02116-8.

Katz, A. M., Hager, W. D., Messineo, F. C., & Pappano, A. J. (1985). Cellular actions and pharmacology of calcium-channel blockers. *Am J Emerg Med*, *3*(6 Suppl), 1-9. doi: 10.1016/0735-6757(85)90226-8.

Kaur, G., Verma, S. K., Singh, D., & Singh, N. K. (2023). Role of G-Proteins and GPCRs in Cardiovascular Pathologies. *Bioengineering (Basel)*, *10*(1), 76. doi: 10.3390/bioengineering10010076.

Kawasaki, T., Delea, C. S., Bartter, F. C., & Smith, H. (1978). The effect of high-sodium and low-sodium intakes on blood pressure and other related variables in human subjects with idiopathic hypertension. *Am J Med*, *64*(2), 193-198. doi: 10.1016/0002-9343(78)90045-1.

Kefauver, J. M., Ward, A. B., & Patapoutian, A. (2020). Discoveries in structure and physiology of mechanically activated ion channels. *Nature*, *587*(7835), 567-576. doi: 10.1038/s41586-020-2933-1.

Khamdaeng, T., Luo, J., Vappou, J., Terdtoon, P., & Konofagou, E. (2012). Arterial stiffness identification of the human carotid artery using the stress–strain relationship in vivo. *Ultrasonics*, *52*(3), 402-411.

Kihara, M., Utagawa, N., Mano, M., Nara, Y., Horie, R., & Yamori, Y. (1985). Biochemical aspects of salt-induced, pressure-independent left ventricular hypertrophy in rats. *Heart and Vessels*, *1*, 212-215.

Kim, E. D., Ballew, S. H., Tanaka, H., Heiss, G., Coresh, J., & Matsushita, K. (2019). Short-Term Prognostic Impact of Arterial Stiffness in Older Adults Without Prevalent

Cardiovascular Disease. *Hypertension*, *74*(6), 1373-1382. doi: 10.1161/Hypertensionaha.119.13496.

Kim, J.-Y., Park, J. B., Kim, D. S., Kim, K. S., Jeong, J. W., Park, J. C., . . . Chung, N. (2015). Gender difference in arterial stiffness in a multicenter cross-sectional study: the Korean Arterial Aging Study (KAAS). *Pulse*, *2*(1-4), 11-17.

Kim, J. Y., Park, J. B., Kim, D. S., Kim, K. S., Jeong, J. W., Park, J. C., . . . investigators, K. (2014). Gender Difference in Arterial Stiffness in a Multicenter Cross-Sectional Study: The Korean Arterial Aging Study (KAAS). *Pulse (Basel)*, *2*(1-4), 11-17. doi: 10.1159/000365267.

Kingwell, B. A., Medley, T. L., Waddell, T. K., Cole, T. J., Dart, A. M., & Jennings, G. L. (2001). Large artery stiffness: structural and genetic aspects. *Clin Exp Pharmacol Physiol*, *28*(12), 1040-1043. doi: 10.1046/j.1440-1681.2001.03580.x.

Kobayashi, N., Hata, N., Kume, N., Yokoyama, S., Shinada, T., Tomita, K., . . . Yamamoto, M. (2011). Matrix Metalloproteinase-9 for the Earliest Stage Acute Coronary Syndrome– Comparison With High-Sensitivity Troponin T–. *Circulation Journal*, *75*(12), 2853-2861.

Kolh, P., D'Orio, V., Lambermont, B., Gerard, P., Gommes, C., & Limet, R. (2000). Increased aortic compliance maintains left ventricular performance at lower energetic cost. *Eur J Cardiothorac Surg*, *17*(3), 272-278. doi: 10.1016/s1010-7940(00)00341-9.

Krüger-Genge, A., Blocki, A., Franke, R.-P., & Jung, F. (2019). Vascular endothelial cell biology: an update. *International journal of molecular sciences*, *20*(18), 4411.

Kshatri, A. S., Gonzalez-Hernandez, A., & Giraldez, T. (2018). Physiological Roles and Therapeutic Potential of Ca(2+) Activated Potassium Channels in the Nervous System. *Front Mol Neurosci*, *11*, 258. doi: 10.3389/fnmol.2018.00258.

Kuchan, M. J., & Frangos, J. A. (1993). Shear stress regulates endothelin-1 release via protein kinase C and cGMP in cultured endothelial cells. *Am J Physiol*, *264*(1 Pt 2), H150-156. doi: 10.1152/ajpheart.1993.264.1.H150.

Kusche-Vihrog, K., Schmitz, B., & Brand, E. (2015). Salt controls endothelial and vascular phenotype. *Pflugers Arch*, *467*(3), 499-512. doi: 10.1007/s00424-014-1657-1.

Lacolley, P., Regnault, V., Nicoletti, A., Li, Z. L., & Michel, J. B. (2012). The vascular smooth muscle cell in arterial pathology: a cell that can take on multiple roles. *Cardiovascular Research*, *95*(2), 194-204. doi: 10.1093/cvr/cvs135.

Lacolley, P., Regnault, V., Segers, P., & Laurent, S. (2017). Vascular smooth muscle cells and arterial stiffening: relevance in development, aging, and disease. *Physiological reviews*, *97*(4), 1555-1617.

Lacolley, P., Regnault, V., Segers, P., & Laurent, S. (2017). Vascular Smooth Muscle Cells and Arterial Stiffening: Relevance in Development, Aging, and Disease. *Physiol Rev*, *97*(4), 1555-1617. doi: 10.1152/physrev.00003.2017.

Lacy, P. S., Pilkington, G., Hanvesakul, R., Fish, H. J., Boyle, J. P., & Thurston, H. (2000). Evidence against potassium as an endothelium-derived hyperpolarizing factor in rat mesenteric small arteries. *Br J Pharmacol*, *129*(3), 605-611. doi: 10.1038/sj.bjp.0703076.

Laher, I., & Van Breemen, C. (2012). Regulation of Calcium Sensitivity. *The Resistance Vasculature: A Publication of the University of Vermont Center for Vascular Research*, 305.

Laurent, S. (1995). Arterial wall hypertrophy and stiffness in essential hypertensive patients. *Hypertension*, *26*(2), 355-362. doi: 10.1161/01.hyp.26.2.355.

Laurent, S., Agabiti-Rosei, C., Bruno, R. M., & Rizzoni, D. (2022). Microcirculation and Macrocirculation in Hypertension: A Dangerous Cross-Link? *Hypertension*, *79*(3), 479-490. doi: 10.1161/HYPERTENSIONAHA.121.17962.

Laurent, S., & Boutouyrie, P. (2013). Arterial Stiffness and Cardiovascular Events in Hypertensives. *Current Cardiovascular Risk Reports*, *7*, 238-243.

Laurent, S., & Boutouyrie, P. (2015). The structural factor of hypertension: large and small artery alterations. *Circ Res*, *116*(6), 1007-1021. doi: 10.1161/CIRCRESAHA.116.303596.

Laurent, S., & Boutouyrie, P. (2020). Interrelationships Between Micro-and Macrocirculation. In *Microcirculation in Cardiovascular Diseases* (pp. 103-119). Springer.

Laurent, S., Hulot, J.-S., & Boutouyrie, P. (2019). Role of Central Blood Pressure and Arterial Stiffening. *Hypertension and Heart Failure: Epidemiology, Mechanisms and Treatment*, 135-154.

Leblanc, C., & Tabrizchi, R. (2018). Role of β2-and β3-adrenoceptors in arterial stiffness in a state of hypertension. *European journal of pharmacology*, *819*, 136-143.

Lee, H. Y., & Oh, B. H. (2010). Aging and arterial stiffness. *Circ J*, *74*(11), 2257-2262. doi: 10.1253/circj.cj-10-0910.

Lee, R. M., Garfield, R. E., Forrest, J. B., & Daniel, E. E. (1983). Morphometric study of structural changes in the mesenteric blood vessels of spontaneously hypertensive rats. *Blood Vessels*, *20*(2), 57-71. doi: 10.1159/000158460.

Lee, R. M., & Smeda, J. S. (1985). Primary versus secondary structural changes of the blood vessels in hypertension. *Can J Physiol Pharmacol*, *63*(4), 392-401. doi: 10.1139/y85-070.

Lemarié, C. A., Tharaux, P.-L., & Lehoux, S. (2010). Extracellular matrix alterations in hypertensive vascular remodeling. *Journal of molecular and cellular cardiology*, *48*(3), 433-439.

Levick, J. R. (2013). *An introduction to cardiovascular physiology*.Butterworth-Heinemann.

Li, X., Shen, B., Yao, X. Q., & Yang, D. (2009). Synthetic chloride channel regulates cell membrane potentials and voltage-gated calcium channels. *J Am Chem Soc*, *131*(38), 13676-13680. doi: 10.1021/ja902352g.

Liao, D., Arnett, D. K., Tyroler, H. A., Riley, W. A., Chambless, L. E., Szklo, M., & Heiss, G. (1999). Arterial stiffness and the development of hypertension. The ARIC study. *Hypertension*, *34*(2), 201-206. doi: 10.1161/01.hyp.34.2.201.

Lim, H. S., & Lip, G. Y. (2008). Arterial stiffness: beyond pulse wave velocity and its measurement. *J Hum Hypertens*, *22*(10), 656-658. doi: 10.1038/jhh.2008.47.

Lincoln, T. M., Dey, N., & Sellak, H. (2001). Signal transduction in smooth muscle - Invited review: cGMP-dependent protein kinase signaling mechanisms in smooth muscle: from the regulation of tone to gene expression. *Journal of Applied Physiology*, *91*(3), 1421-1430. doi: DOI 10.1152/jappl.2001.91.3.1421.

Linde, C. I., Karashima, E., Raina, H., Zulian, A., Wier, W. G., Hamlyn, J. M., . . . Golovina, V. A. (2012). Increased arterial smooth muscle Ca2+ signaling, vasoconstriction, and myogenic reactivity in Milan hypertensive rats. *Am J Physiol Heart Circ Physiol*, *302*(3), H611-620. doi: 10.1152/ajpheart.00950.2011.

London, G. M., & Pannier, B. (2010). Arterial functions: how to interpret the complex physiology. *Nephrol Dial Transplant*, *25*(12), 3815-3823. doi: 10.1093/ndt/gfq614.

López-López, J. R., Cidad, P., & Pérez-García, M. T. (2018). Kv channels and vascular smooth muscle cell proliferation. *Microcirculation*, *25*(1), e12427.

Louis, H., Kakou, A., Regnault, V., Labat, C., Bressenot, A., Gao-Li, J., . . . Li, Z. (2007). Role of α1β1-integrin in arterial stiffness and angiotensin-induced arterial wall hypertrophy in mice. *American Journal of Physiology-Heart and Circulatory Physiology*, *293*(4), H2597-H2604.

Louis, W. J., Tabei, R., & Spector, S. (1971). Effects of sodium intake on inherited hypertension in the rat. *Lancet*, *2*(7737), 1283-1286. doi: 10.1016/s0140-6736(71)90603-9.

Luft, F. C. (2012). Molecular mechanisms of arterial stiffness: new insights. *J Am Soc Hypertens*, *6*(6), 436-438. doi: 10.1016/j.jash.2012.10.004.

Luo, W., Liu, B., & Zhou, Y. (2016). The endothelial cyclooxygenase pathway: Insights from mouse arteries. *Eur J Pharmacol*, *780*, 148-158. doi: 10.1016/j.ejphar.2016.03.043.

Luscher, T. F., & Barton, M. (2000). Endothelins and endothelin receptor antagonists: therapeutic considerations for a novel class of cardiovascular drugs. *Circulation*, *102*(19), 2434-2440. doi: 10.1161/01.cir.102.19.2434.

Lüscher, T. F., & Tanner, F. C. (1993). Endothelial regulation of vascular tone and growth. *American journal of hypertension*, *6*(7_Pt_2), 283S-293S.

Ma, Y., Choi, J., Hourlier-Fargette, A., Xue, Y., Chung, H. U., Lee, J. Y., . . . Huang, Y. (2018). Relation between blood pressure and pulse wave velocity for human arteries. *Proc Natl Acad Sci U S A*, *115*(44), 11144-11149. doi: 10.1073/pnas.1814392115.

Magder, S. (2018). The meaning of blood pressure. *Crit Care*, *22*(1), 257. doi: 10.1186/s13054-018-2171-1.

Malfait, F. (2018). Vascular aspects of the Ehlers-Danlos Syndromes. *Matrix Biol*, *71-72*, 380-395. doi: 10.1016/j.matbio.2018.04.013.

Malmsten, C. L. (1986). Prostaglandins, thromboxanes, and leukotrienes in inflammation. *Am J Med*, *80*(4B), 11-17. doi: 10.1016/0002-9343(86)90073-2.

Man, W., & Wang, Y. (2017). Age-associated arterial remodelling. *EC Cardiology*.

Mandegar, M., Remillard, C. V., & Yuan, J. X. (2002). Ion channels in pulmonary arterial hypertension. *Prog Cardiovasc Dis*, *45*(2), 81-114. doi: 10.1053/pcad.2002.127491.

Manrique, C., Lastra, G., Ramirez-Perez, F. I., Haertling, D., DeMarco, V. G., Aroor, A. R., . . . Garro, M. (2016). Endothelial estrogen receptor-α does not protect against vascular stiffness induced by Western diet in female mice. *Endocrinology*, *157*(4), 1590-1600.

Marasciulo, F. L., Montagnani, M., & Potenza, M. A. (2006). Endothelin-1: the yin and yang on vascular function. *Curr Med Chem*, *13*(14), 1655-1665. doi: 10.2174/092986706777441968.

Marque, V., Van Essen, H., Struijker-Boudier, H. A., Atkinson, J., & Lartaud-Idjouadiene, I. (2001). Determination of aortic elastic modulus by pulse wave velocity and wall tracking in a rat model of aortic stiffness. *J Vasc Res*, *38*(6), 546-550. doi: 10.1159/000051090.

Martinez-Quinones, P., McCarthy, C. G., Watts, S. W., Klee, N. S., Komic, A., Calmasini, F. B., . . . Wenceslau, C. F. (2018). Hypertension Induced Morphological and Physiological Changes in Cells of the Arterial Wall. *Am J Hypertens*, *31*(10), 1067-1078. doi: 10.1093/ajh/hpy083.

Martins, S. M., Trabuco, J. R., Monteiro, G. A., & Prazeres, D. M. CHALLENGES AND LATEST TRENDS.

Masi, S., Uliana, M., & Virdis, A. (2019). Angiotensin II and vascular damage in hypertension: Role of oxidative stress and sympathetic activation. *Vascul Pharmacol*, *115*, 13-17. doi: 10.1016/j.vph.2019.01.004.

Matsumoto, T., Sugita, S., & Nagayama, K. (2016). Tensile properties of smooth muscle cells, elastin, and collagen fibers. *Vascular Engineering: New Prospects of Vascular Medicine and Biology with a Multidiscipline Approach*, 127-140.

Mayet, J., & Hughes, A. (2003). Cardiac and vascular pathophysiology in hypertension. *Heart*, *89*(9), 1104-1109. doi: 10.1136/heart.89.9.1104.

McCulloch, A. I., & Randall, M. D. (1998). Sex differences in the relative contributions of nitric oxide and EDHF to agonist-stimulated endothelium-dependent relaxations in the rat isolated mesenteric arterial bed. *Br J Pharmacol*, *123*(8), 1700-1706. doi: 10.1038/sj.bjp.0701781.

McLoone, V. I., Ringwood, J. V., & Van Vliet, B. N. (2009). A multi-component model of the dynamics of salt-induced hypertension in Dahl-S rats. *BMC physiology*, *9*, 1-11.

Méndez-Barbero, N., Gutiérrez-Muñoz, C., & Blanco-Colio, L. M. (2021). Cellular crosstalk between endothelial and smooth muscle cells in vascular wall remodeling. *International journal of molecular sciences*, *22*(14), 7284.

Meneely, G. R., Lemley-Stone, J., & Darby, W. J. (1961). Changes in blood pressure and body sodium of rats fed sodium and potassium chloride. *Am J Cardiol*, *8*(4), 527-532. doi: 10.1016/0002-9149(61)90130-8.

Mensah, E. A., Daneshtalab, N., & Tabrizchi, R. (2022). Differential biomechanics in resistance arteries of male compared with female Dahl hypertensive rats. *Journal of hypertension*, *40*(3), 596-605.

Mensah, E. A., Daneshtalab, N., & Tabrizchi, R. (2024). Effects of vasoactive substances on biomechanics of small resistance arteries of male and female Dahl salt-sensitive rats. *Pharmacology Research & Perspectives*, *12*(2), e1180.

Messas, E., Pernot, M., & Couade, M. (2013). Arterial wall elasticity: state of the art and future prospects. *Diagn Interv Imaging*, *94*(5), 561-569. doi: 10.1016/j.diii.2013.01.025.

Mitchell, G. F. (2009). Arterial Stiffness and Wave Reflection: Biomarkers of Cardiovascular Risk. *Artery Res*, *3*(2), 56-64. doi: 10.1016/j.artres.2009.02.002.

Mitchell, G. F., Hwang, S. J., Vasan, R. S., Larson, M. G., Pencina, M. J., Hamburg, N. M., . . . Benjamin, E. J. (2010). Arterial stiffness and cardiovascular events: the Framingham Heart Study. *Circulation*, *121*(4), 505-511. doi: 10.1161/CIRCULATIONAHA.109.886655.

Mitchell, J. A., Kirkby, N. S., Ahmetaj-Shala, B., Armstrong, P. C., Crescente, M., Ferreira, P., . . . Warner, T. D. (2021). Cyclooxygenases and the cardiovascular system. *Pharmacol Ther*, *217*, 107624. doi: 10.1016/j.pharmthera.2020.107624.

Montezano, A. C., Dulak-Lis, M., Tsiropoulou, S., Harvey, A., Briones, A. M., & Touyz, R. M. (2015). Oxidative stress and human hypertension: vascular mechanisms, biomarkers, and novel therapies. *Can J Cardiol*, *31*(5), 631-641. doi: 10.1016/j.cjca.2015.02.008.

Mooney, M. (1940). A theory of large elastic deformation. *Journal of Applied Physics*, *11*(9), 582-592. doi: Doi 10.1063/1.1712836.

Moreira, M. C., da Silva, E. F., Silveira, L. L., de Paiva, Y. B., de Castro, C. H., Freiria-Oliveira, A. H., . . . Pedrino, G. R. (2014). High sodium intake during postnatal phases induces an increase in arterial blood pressure in adult rats. *Br J Nutr*, *112*(12), 1923-1932. doi: 10.1017/S0007114514002918.

Morgado, M., Cairrao, E., Santos-Silva, A. J., & Verde, I. (2012). Cyclic nucleotide-dependent relaxation pathways in vascular smooth muscle. *Cell Mol Life Sci*, *69*(2), 247-266. doi: 10.1007/s00018-011-0815-2.

Mozaffarian, D., Fahimi, S., Singh, G. M., Micha, R., Khatibzadeh, S., Engell, R. E., . . . Chronic Diseases Expert, G. (2014). Global sodium consumption and death from cardiovascular causes. *N Engl J Med*, *371*(7), 624-634. doi: 10.1056/NEJMoa1304127.

Mozos, I., Malainer, C., Horbanczuk, J., Gug, C., Stoian, D., Luca, C. T., & Atanasov, A. G. (2017). Inflammatory Markers for Arterial Stiffness in Cardiovascular Diseases. *Front Immunol*, *8*, 1058. doi: 10.3389/fimmu.2017.01058.

Mulvany, M. J., Baumbach, G. L., Aalkjaer, C., Heagerty, A. M., Korsgaard, N., Schiffrin, E. L., & Heistad, D. D. (1996). Vascular remodeling. *Hypertension*, *28*(3), 505-506.

Münzel, T., Heitzer, T., & Harrison, D. (1997). The physiology and pathophysiology of the nitric oxide/superoxide system. *Herz*, *22*(3), 158.

Murdoch, C. E., Alom-Ruiz, S. P., Wang, M., Zhang, M., Walker, S., Yu, B., . . . Shah, A. M. (2011). Role of endothelial Nox2 NADPH oxidase in angiotensin II-induced hypertension and vasomotor dysfunction. *Basic Res Cardiol*, *106*(4), 527-538. doi: 10.1007/s00395-011-0179-7.

Myers, J., & Morgan, T. (1983). The effect of sodium intake on the blood pressure related to age and sex. *Clin Exp Hypertens A*, *5*(1), 99-118. doi: 10.3109/10641968309048813.

Myers, P. R., Minor, R. L., Guerra, R., Bates, J. N., & Harrison, D. G. (1990). Vasorelaxant Properties of the Endothelium-Derived Relaxing Factor More Closely Resemble S-Nitrosocysteine Than Nitric-Oxide. *Nature*, *345*(6271), 161-163. doi: DOI 10.1038/345161a0.

Myllyharju, J., & Kivirikko, K. I. (2001). Collagens and collagen-related diseases. *Ann Med*, *33*(1), 7-21. doi: 10.3109/07853890109002055.

Nagao, T., & Vanhoutte, P. M. (1993). Endothelium-derived hyperpolarizing factor and endothelium-dependent relaxations. *Am J Respir Cell Mol Biol*, *8*(1), 1-6. doi: 10.1165/ajrcmb/8.1.1.

Nagasawa, S., Handa, H., Naruo, Y., Moritake, K., & Hayashi, K. (1982). Experimental cerebral vasospasm arterial wall mechanics and connective tissue composition. *Stroke*, *13*(5), 595-600. doi: 10.1161/01.str.13.5.595.

Nakano, D., & Pollock, D. M. (2009). Contribution of endothelin a receptors in endothelin 1–dependent natriuresis in female rats. *Hypertension*, *53*(2), 324-330.

Nausch, L. W., Bonev, A. D., Heppner, T. J., Tallini, Y., Kotlikoff, M. I., & Nelson, M. T. (2012). Sympathetic nerve stimulation induces local endothelial Ca2+ signals to oppose vasoconstriction of mouse mesenteric arteries. *Am J Physiol Heart Circ Physiol*, *302*(3), H594-602. doi: 10.1152/ajpheart.00773.2011.

Nelson, M. T., Conway, M. A., Knot, H. J., & Brayden, J. E. (1997). Chloride channel blockers inhibit myogenic tone in rat cerebral arteries. *J Physiol*, *502 (Pt 2)*(Pt 2), 259-264. doi: 10.1111/j.1469-7793.1997.259bk.x.

Nichols, W. W., Heffernan, K. S., & Chirinos, J. A. (2015). Overview of the normal structure and function of the macrocirculation and microcirculation. *Arterial Disorders: Definition, Clinical Manifestations, Mechanisms and Therapeutic Approaches*, 13-46.

Nichols, W. W., Pierce, G. L., & Braith, R. W. (2007). Does hormone treatment alter arterial properties in postmenopausal women? *Expert review of endocrinology & metabolism*, *2*(5), 653-665.

Nilius, B., & Droogmans, G. (2001). Ion channels and their functional role in vascular endothelium. *Physiol Rev*, *81*(4), 1415-1459. doi: 10.1152/physrev.2001.81.4.1415.

Nishiwaki, M., Kurobe, K., Kiuchi, A., Nakamura, T., & Matsumoto, N. (2014). Sex differences in flexibility-arterial stiffness relationship and its application for diagnosis of arterial stiffening: a cross-sectional observational study. *PLoS One*, *9*(11), e113646. doi: 10.1371/journal.pone.0113646.

Nissen, R., Cardinale, G. J., & Udenfriend, S. (1978). Increased turnover of arterial collagen in hypertensive rats. *Proc Natl Acad Sci U S A*, *75*(1), 451-453. doi: 10.1073/pnas.75.1.451.

Nobles, M., Benians, A., & Tinker, A. (2005). Heterotrimeric G proteins precouple with G protein-coupled receptors in living cells. *Proc Natl Acad Sci U S A*, *102*(51), 18706-18711. doi: 10.1073/pnas.0504778102.

Noori, M., Savvidou, M., & Williams, D. (2007). *Endothelial factors*.Cambridge University Press Cambridge, UK.

Nourse, J. L., & Pathak, M. M. (2017). How cells channel their stress: Interplay between Piezo1 and the cytoskeleton. Seminars in cell & developmental biology.

O'Rourke, M. F., & Mancia, G. (1999). Arterial stiffness. *Journal of hypertension*, *17*(1), 1-4.

O'Rourke, S. T. (1996). Effects of potassium channel blockers on resting tone in isolated coronary arteries. *J Cardiovasc Pharmacol*, *27*(5), 636-642. doi: 10.1097/00005344-199605000-00004.

Ogola, B. O., Zimmerman, M. A., Clark, G. L., Abshire, C. M., Gentry, K. M., Miller, K. S., & Lindsey, S. H. (2018). New insights into arterial stiffening: does sex matter? *American Journal of Physiology-Heart and Circulatory Physiology*, *315*(5), H1073-H1087.

Ojha, K. R., Shin, S. Y., Padgham, S., Leon Olmedo, F., Guo, B., Han, G., . . . Trache, A. (2022). Age-Associated Dysregulation of Integrin Function in Vascular Smooth Muscle. *Front Physiol*, *13*, 913673. doi: 10.3389/fphys.2022.913673.

Orie, N. N., & Clapp, L. H. (2011). Role of prostanoid IP and EP receptors in mediating vasorelaxant responses to PGI2 analogues in rat tail artery: Evidence for Gi/o modulation via EP3 receptors. *Eur J Pharmacol*, *654*(3), 258-265. doi: 10.1016/j.ejphar.2010.12.005.

Orshal, J. M., & Khalil, R. A. (2004). Gender, sex hormones, and vascular tone. *Am J Physiol Regul Integr Comp Physiol*, *286*(2), R233-249. doi: 10.1152/ajpregu.00338.2003.

Ottolini, M., Hong, K., & Sonkusare, S. K. (2019). Calcium signals that determine vascular resistance. *Wiley Interdisciplinary Reviews-Systems Biology and Medicine*, *11*(5), e1448. doi: ARTN e1448

10.1002/wsbm.1448.

Owen, C. A., & Roberts, M. (2007). Arterial vascular hemodynamics. *Journal of Diagnostic Medical Sonography*, *23*(3), 129-140.

Ozkor, M. A., & Quyyumi, A. A. (2011). Endothelium-derived hyperpolarizing factor and vascular function. *Cardiol Res Pract*, *2011*, 156146. doi: 10.4061/2011/156146.

Palombo, C., & Kozakova, M. (2016). Arterial stiffness, atherosclerosis and cardiovascular risk: Pathophysiologic mechanisms and emerging clinical indications. *Vascul Pharmacol*, *77*, 1-7. doi: 10.1016/j.vph.2015.11.083.

Pan, Q., Wang, R., Reglin, B., Fang, L., Yan, J., Cai, G., . . . Ning, G. (2018). Pulse wave velocity in the microcirculation reflects both vascular compliance and resistance: insights from computational approaches. *Microcirculation*, *25*(5), e12458.

Parai, K., & Tabrizchi, R. (2005). Effects of chloride substitution in isolated mesenteric blood vessels from Dahl normotensive and hypertensive rats. *Journal of cardiovascular pharmacology*, *46*(1), 105-114.

Paravicini, T. M., & Touyz, R. M. (2008). NADPH oxidases, reactive oxygen species, and hypertension: clinical implications and therapeutic possibilities. *Diabetes Care*, *31 Suppl 2*(Supplement_2), S170-180. doi: 10.2337/dc08-s247.

Park, J. B., & Schiffrin, E. L. (2001). Small artery remodeling is the most prevalent (earliest?) form of target organ damage in mild essential hypertension. *Journal of hypertension*, *19*(5), 921-930.

Patel, D. J., Vaishnav, R. N., Gow, B. S., & Kot, P. A. (1974). Hemodynamics. *Annu Rev Physiol*, *36*(1), 125-154. doi: 10.1146/annurev.ph.36.030174.001013.

Pechère-Bertschi, A., & Burnier, M. (2004). Female sex hormones, salt, and blood pressure regulation. *American journal of hypertension*, *17*(10), 994-1001.

Penela, P., Murga, C., Ribas, C., Tutor, A. S., Peregrin, S., & Mayor, F., Jr. (2006). Mechanisms of regulation of G protein-coupled receptor kinases (GRKs) and cardiovascular disease. *Cardiovascular Research*, *69*(1), 46-56. doi: 10.1016/j.cardiores.2005.09.011.

Perez-Zoghbi, J. F., Karner, C., Ito, S., Shepherd, M., Alrashdan, Y., & Sanderson, M. J. (2009). Ion channel regulation of intracellular calcium and airway smooth muscle function. *Pulm Pharmacol Ther*, *22*(5), 388-397. doi: 10.1016/j.pupt.2008.09.006.

Peters, J., Mack, G. W., & Lister, G. (2001). The importance of the peripheral circulation in critical illnesses. *Intensive Care Med*, *27*(9), 1446-1458. doi: 10.1007/s001340101034.

Pfister, S. L. (2011). Role of lipoxygenase metabolites of arachidonic acid in enhanced pulmonary artery contractions of female rabbits. *Hypertension*, *57*(4), 825-832. doi: 10.1161/HYPERTENSIONAHA.110.168716.

Pirahanchi, Y., Marsidi, J. L., & Brown, K. N. (2019). Physiology, Endothelial Derived Relaxation Factor.

Plant, A. L., Bhadriraju, K., Spurlin, T. A., & Elliott, J. T. (2009). Cell response to matrix mechanics: focus on collagen. *Biochim Biophys Acta*, *1793*(5), 893-902. doi: 10.1016/j.bbamcr.2008.10.012.

Pollock, D. M., Keith, T. L., & Highsmith, R. F. (1995). Endothelin receptors and calcium signaling. *FASEB J*, *9*(12), 1196-1204. doi: 10.1096/fasebj.9.12.7672512.

Powles, J., Fahimi, S., Micha, R., Khatibzadeh, S., Shi, P., Ezzati, M., . . . Mozaffarian, D. (2013). Global, regional and national sodium intakes in 1990 and 2010: a systematic analysis of 24 h urinary sodium excretion and dietary surveys worldwide. *BMJ open*, *3*(12), e003733.

Prewitt, R. L., Rice, D. C., & Dobrian, A. D. (2002). Adaptation of resistance arteries to increases in pressure. *Microcirculation*, *9*(4), 295-304. doi: 10.1038/sj.mn.7800143.

Pries, A. R., Secomb, T. W., & Gaehtgens, P. (1996). Biophysical aspects of blood flow in the microvasculature. *Cardiovascular Research*, *32*(4), 654-667.

Puetz, S., Lubomirov, L. T., & Pfitzer, G. (2009). Regulation of smooth muscle contraction by small GTPases. *Physiology (Bethesda)*, *24*(6), 342-356. doi: 10.1152/physiol.00023.2009.

Pulous, F. E., & Petrich, B. G. (2019). Integrin-dependent regulation of the endothelial barrier. *Tissue Barriers*, *7*(4), 1685844.

Qiu, H. Y., Zhu, Y., Sun, Z., Trzeciakowski, J. P., Gansner, M., Depre, C., . . . Vatner, S. F. (2010). Vascular Smooth Muscle Cell Stiffness As a Mechanism for Increased Aortic Stiffness With Aging. *Circulation research*, *107*(5), 615-U117. doi: 10.1161/Circresaha.110.221846.

Quinn, U., Tomlinson, L. A., & Cockcroft, J. R. (2012). Arterial stiffness. *JRSM Cardiovasc Dis*, *1*(6), 1-8. doi: 10.1258/cvd.2012.012024.

Rapp, J. P. (1982). Dahl salt-susceptible and salt-resistant rats. A review. *Hypertension*, *4*(6), 753-763. doi: 10.1161/01.hyp.4.6.753.

Rembold, C. M. (1992). Regulation of contraction and relaxation in arterial smooth muscle. *Hypertension*, *20*(2), 129-137. doi: 10.1161/01.hyp.20.2.129.

Renna, N. F., de Las Heras, N., & Miatello, R. M. (2013). Pathophysiology of vascular remodeling in hypertension. *Int J Hypertens*, *2013*, 808353. doi: 10.1155/2013/808353.

Retailleau, K., Duprat, F., Arhatte, M., Ranade, S. S., Peyronnet, R., Martins, J. R., . . . Honore, E. (2015). Piezo1 in Smooth Muscle Cells Is Involved in Hypertension-Dependent Arterial Remodeling. *Cell Rep*, *13*(6), 1161-1171. doi: 10.1016/j.celrep.2015.09.072.

Rhee, M.-Y., Lee, H.-Y., & Park, J. B. (2008). Measurements of arterial stiffness: methodological aspects. *Korean Circulation Journal*, *38*(7), 343-350.

Ribeiro-Silva, J. C., Nolasco, P., Krieger, J. E., & Miyakawa, A. A. (2021). Dynamic Crosstalk between Vascular Smooth Muscle Cells and the Aged Extracellular Matrix. *International journal of molecular sciences*, *22*(18), 10175. doi: ARTN 10175

10.3390/ijms221810175.

Robert, V., Van Thiem, N., Cheav, S. L., Mouas, C., Swynghedauw, B., & Delcayre, C. (1994). Increased cardiac types I and III collagen mRNAs in aldosterone-salt hypertension. *Hypertension*, *24*(1), 30-36. doi: 10.1161/01.hyp.24.1.30.

Robertson, A. M., & Watton, P. N. (2013). Mechanobiology of the arterial wall. *Transport in biological Media*, *2013*, 275-347.

Robledo, J. G. (2019). *Piezo1: Proteins for mechanotransduction and integration of endothelial shear stress & intravascular pressure* The University of Western Ontario (Canada)].

Rode, B., Shi, J., Endesh, N., Drinkhill, M. J., Webster, P. J., Lotteau, S. J., . . . Beech, D. J. (2017). Piezo1 channels sense whole body physical activity to reset cardiovascular homeostasis and enhance performance. *Nat Commun*, *8*(1), 350. doi: 10.1038/s41467-017-00429-3.

Rodríguez-Iturbe, B., Franco, M., Tapia, E., Quiroz, Y., & Johnson, R. J. (2012). Renal inflammation, autoimmunity and salt-sensitive hypertension. *Clinical and Experimental Pharmacology and Physiology*, *39*(1), 96-103.

Rossi, P., Frances, Y., Kingwell, B. A., & Ahimastos, A. A. (2011). Gender differences in artery wall biomechanical properties throughout life. *J Hypertens*, *29*(6), 1023-1033. doi: 10.1097/HJH.0b013e328344da5e.

Rubanyi, G. M. (1991). Endothelium-derived relaxing and contracting factors. *J Cell Biochem*, *46*(1), 27-36. doi: 10.1002/jcb.240460106.

Sader, M. A., & Celermajer, D. S. (2002). Endothelial function, vascular reactivity and gender differences in the cardiovascular system. *Cardiovascular Research*, *53*(3), 597-604. doi: 10.1016/s0008-6363(01)00473-4.

Safar, M., & O'Rourke, M. F. (2006). *Arterial Stiffness in Hypertension: Handbook of Hypertension Series* (Vol. 23). Elsevier Health Sciences.

Safar, M. E. (2007). Arterial stiffness: a simplified overview in vascular medicine. *Adv Cardiol*, *44*, 1-18. doi: 10.1159/000096699.

Safar, M. E. (2010). Arterial aging—hemodynamic changes and therapeutic options. *Nature Reviews Cardiology*, *7*(8), 442-449.

Safar, M. E., & Struijker-Boudier, H. (2010). Cross-talk between macro-and microcirculation. *Acta physiologica*, *198*(4), 417-430.

Safar, M. E., Temmar, M., Kakou, A., Lacolley, P., & Thornton, S. N. (2009). Sodium intake and vascular stiffness in hypertension. *Hypertension*, *54*(2), 203-209. doi: 10.1161/HYPERTENSIONAHA.109.129585.

Safar, M. E., Thuilliez, C., Richard, V., & Benetos, A. (2000). Pressure-independent contribution of sodium to large artery structure and function in hypertension. *Cardiovascular Research*, *46*(2), 269-276. doi: 10.1016/s0008-6363(99)00426-5.

Said, M. A., Eppinga, R. N., Lipsic, E., Verweij, N., & van der Harst, P. (2018). Relationship of Arterial Stiffness Index and Pulse Pressure With Cardiovascular Disease and Mortality. *J Am Heart Assoc*, *7*(2), e007621. doi: 10.1161/JAHA.117.007621.

Sanchez, A., Contreras, C., Villalba, N., Martinez, P., Martinez, A. C., Briones, A., . . . Prieto, D. (2010). Altered arachidonic acid metabolism via COX-1 and COX-2 contributes to the

endothelial dysfunction of penile arteries from obese Zucker rats. *Br J Pharmacol*, *159*(3), 604-616. doi: 10.1111/j.1476-5381.2009.00553.x.

Sanchez, M., Galisteo, M., Vera, R., Villar, I. C., Zarzuelo, A., Tamargo, J., . . . Duarte, J. (2006). Quercetin downregulates NADPH oxidase, increases eNOS activity and prevents endothelial dysfunction in spontaneously hypertensive rats. *J Hypertens*, *24*(1), 75-84. doi: 10.1097/01.hjh.0000198029.22472.d9.

Sanders, M. W., Fazzi, G. E., Janssen, G. M., Blanco, C. E., & De Mey, J. G. (2005). High sodium intake increases blood pressure and alters renal function in intrauterine growth–retarded rats. *Hypertension*, *46*(1), 71-75.

Sandoo, A., van Zanten, J. J., Metsios, G. S., Carroll, D., & Kitas, G. D. (2010). The endothelium and its role in regulating vascular tone. *Open Cardiovasc Med J*, *4*, 302-312. doi: 10.2174/1874192401004010302.

Sandow, S. L., Gzik, D. J., & Lee, R. M. (2009). Arterial internal elastic lamina holes: relationship to function? *Journal of anatomy*, *214*(2), 258-266.

Saphirstein, R. J., & Morgan, K. G. (2014). The contribution of vascular smooth muscle to aortic stiffness across length scales. *Microcirculation*, *21*(3), 201-207. doi: 10.1111/micc.12101.

Sasaki, M., Hori, M. T., Hino, T., Golub, M. S., & Tuck, M. L. (1997). Elevated 12-lipoxygenase activity in the spontaneously hypertensive rat. *Am J Hypertens*, *10*(4 Pt 1), 371-378.

Sauzeau, V., Sevilla, M. A., Rivas-Elena, J. V., de Alava, E., Montero, M. J., Lopez-Novoa, J. M., & Bustelo, X. R. (2006). Vav3 proto-oncogene deficiency leads to sympathetic hyperactivity and cardiovascular dysfunction. *Nat Med*, *12*(7), 841-845. doi: 10.1038/nm1426.

Savoia, C. (2019). Vascular Remodeling. *Textbook of Vascular Medicine*, 193-201.

Schiffrin, E. L. (1992). Reactivity of small blood vessels in hypertension: relation with structural changes. State of the art lecture. *Hypertension*, *19*(2 Suppl), II1-9. doi: 10.1161/01.hyp.19.2_suppl.ii1-a.

Schiffrin, E. L. (2020). How Structure, Mechanics, and Function of the Vasculature Contribute to Blood Pressure Elevation in Hypertension. *Can J Cardiol*, *36*(5), 648-658. doi: 10.1016/j.cjca.2020.02.003.

Schiffrin, E. L., & Hayoz, D. (1997). How to assess vascular remodelling in small and medium-sized muscular arteries in humans. *J Hypertens*, *15*(6), 571-584. doi: 10.1097/00004872-199715060-00002.

Scotland, R. S., Madhani, M., Chauhan, S., Moncada, S., Andresen, J., Nilsson, H., . . . Ahluwalia, A. (2005). Investigation of vascular responses in endothelial nitric oxide synthase/cyclooxygenase-1 double-knockout mice: key role for endothelium-derived hyperpolarizing factor in the regulation of blood pressure in vivo. *Circulation*, *111*(6), 796-803. doi: 10.1161/01.CIR.0000155238.70797.4E.

Secomb, T. W. (2016). Hemodynamics. *Compr Physiol*, *6*(2), 975-1003. doi: 10.1002/cphy.c150038.

Segal, S. (2000). Integration of blood flow control to skeletal muscle: key role of feed arteries. *Acta Physiologica Scandinavica*, *168*(4), 511-518.

Segal, S. S., & Duling, B. R. (1986). Communication between feed arteries and microvessels in hamster striated muscle: segmental vascular responses are functionally coordinated. *Circulation research*, *59*(3), 283-290.

Senior, K. R. (2010). *Blood: physiology and circulation*.The Rosen Publishing Group, Inc.

Shadwick, R. E. (1999). Mechanical design in arteries. *J Exp Biol*, *202*(Pt 23), 3305-3313. doi: 10.1242/jeb.202.23.3305.

Sharman, J. E., Davies, J. E., Jenkins, C., & Marwick, T. H. (2009). Augmentation index, left ventricular contractility, and wave reflection. *Hypertension*, *54*(5), 1099-1105. doi: 10.1161/HYPERTENSIONAHA.109.133066.

Sheng, Y., & Zhu, L. (2018). The crosstalk between autonomic nervous system and blood vessels. *International journal of physiology, pathophysiology and pharmacology*, *10*(1), 17.

Shirwany, N. A., & Zou, M. H. (2010). Arterial stiffness: a brief review. *Acta Pharmacol Sin*, *31*(10), 1267-1276. doi: 10.1038/aps.2010.123.

Silva, A. G., Goroso, D. G., & Silva, R. R. (2019). SCHSim: A Simulator of Elastic Arterial Vessels Using Windkessel Models. Latin American Conference on Biomedical Engineering.

Simmonds, S. S., Lay, J., & Stocker, S. D. (2014). Dietary salt intake exaggerates sympathetic reflexes and increases blood pressure variability in normotensive rats. *Hypertension*, *64*(3), 583-589. doi: 10.1161/HYPERTENSIONAHA.114.03250.

Simon, G., Jaeckel, M., & Illyes, G. (2003). Development of structural vascular changes in salt-fed rats. *Am J Hypertens*, *16*(6), 488-493. doi: 10.1016/s0895-7061(03)00568-5.

Snyder, S. H., & Bredt, D. S. (1992). Biological roles of nitric oxide. *Sci Am*, *266*(5), 68-71, 74-67. doi: 10.1038/scientificamerican0592-68.

Sobey, C. G. (2001). Potassium channel function in vascular disease. *Arterioscler Thromb Vasc Biol*, *21*(1), 28-38. doi: 10.1161/01.atv.21.1.28.

Sofola, O. A., Knill, A., Hainsworth, R., & Drinkhill, M. (2002). Change in endothelial function in mesenteric arteries of Sprague-Dawley rats fed a high salt diet. *J Physiol*, *543*(Pt 1), 255-260. doi: 10.1113/jphysiol.2002.022277.

Sokolis, D. P., & Iliopoulos, D. C. (2014). Impaired mechanics and matrix metalloproteinases/inhibitors expression in female ascending thoracic aortic aneurysms. *J Mech Behav Biomed Mater*, *34*, 154-164. doi: 10.1016/j.jmbbm.2014.02.015.

Sokolis, D. P., Kefaloyannis, E. M., Kouloukoussa, M., Marinos, E., Boudoulas, H., & Karayannacos, P. E. (2006). A structural basis for the aortic stress–strain relation in uniaxial tension. *Journal of biomechanics*, *39*(9), 1651-1662.

Sorokin, V., Vickneson, K., Kofidis, T., Woo, C. C., Lin, X. Y., Foo, R., & Shanahan, C. M. (2020). Role of Vascular Smooth Muscle Cell Plasticity and Interactions in Vessel Wall Inflammation. *Front Immunol*, *11*, 599415. doi: 10.3389/fimmu.2020.599415.

Stables, M. J., & Gilroy, D. W. (2011). Old and new generation lipid mediators in acute inflammation and resolution. *Prog Lipid Res*, *50*(1), 35-51. doi: 10.1016/j.plipres.2010.07.005.

Stankevičius, E., Kėvelaitis, E., Vainorius, E., & Simonsen, U. (2003). Role of nitric oxide and other endothelium-derived factors. *Medicina (Kaunas)*, *39*(4), 333-341.

Stefanovska, A., & Bracic, M. (1999). Physics of the human cardiovascular system. *Contemporary Physics*, *40*(1), 31-55. doi: Doi 10.1080/001075199181693.

Stegemann, J. P., Hong, H., & Nerem, R. M. (2005). Mechanical, biochemical, and extracellular matrix effects on vascular smooth muscle cell phenotype. *J Appl Physiol (1985)*, *98*(6), 2321-2327. doi: 10.1152/japplphysiol.01114.2004.

Struijker-Boudier, H. A. (2014). Large Arteries, Microcirculation, and Mechanisms of Hypertension. In *Blood Pressure and Arterial Wall Mechanics in Cardiovascular Diseases* (pp. 15-21). Springer.

Su, J. B. (2015). Vascular endothelial dysfunction and pharmacological treatment. *World J Cardiol*, *7*(11), 719-741. doi: 10.4330/wjc.v7.i11.719.

Sullivan, S., Hammadah, M., Wilmot, K., Ramadan, R., Pearce, B. D., Shah, A., . . . Kim, J. H. (2018). Young women with coronary artery disease exhibit higher concentrations of interleukin-6 at baseline and in response to mental stress. *Journal of the American Heart Association*, *7*(23), e010329.

Sumpio, B. E., Riley, J. T., & Dardik, A. (2002). Cells in focus: endothelial cell. *Int J Biochem Cell Biol*, *34*(12), 1508-1512. doi: 10.1016/s1357-2725(02)00075-4.

Susic, D., & Frohlich, E. D. (2012). Salt consumption and cardiovascular, renal, and hypertensive diseases: clinical and mechanistic aspects. *Curr Opin Lipidol*, *23*(1), 11-16. doi: 10.1097/MOL.0b013e32834d9c52.

Syeda, R., Xu, J., Dubin, A. E., Coste, B., Mathur, J., Huynh, T., . . . Patapoutian, A. (2015). Chemical activation of the mechanotransduction channel Piezo1. *Elife*, *4*, e07369. doi: 10.7554/eLife.07369.

Takahashi, T., Tomiyama, H., Aboyans, V., Kumai, K., Nakano, H., Fujii, M., . . . Chikamori, T. (2021). Association of pulse wave velocity and pressure wave reflection with the ankle-brachial pressure index in Japanese men not suffering from peripheral artery disease. *Atherosclerosis*, *317*, 29-35.

Takala, J. (1996). Determinants of splanchnic blood flow. *Br J Anaesth*, *77*(1), 50-58. doi: 10.1093/bja/77.1.50.

Tanaka, Y., Yamaki, F., Koike, K., & Toro, L. (2004). New insights into the intracellular mechanisms by which PGI2 analogues elicit vascular relaxation: cyclic AMP-independent, Gs-protein mediated-activation of MaxiK channel. *Current Medicinal Chemistry-Cardiovascular & Hematological Agents*, *2*(3), 257-265.

Taylor, B. N., & Cassagnol, M. (2022). Alpha adrenergic receptors. In *StatPearls [Internet]*. StatPearls Publishing.

Tesauro, M., Mauriello, A., Rovella, V., Annicchiarico-Petruzzelli, M., Cardillo, C., Melino, G., & Di Daniele, N. (2017). Arterial ageing: from endothelial dysfunction to vascular calcification. *J Intern Med*, *281*(5), 471-482. doi: 10.1111/joim.12605.

Thompson, J., & Khalil, R. A. (2003). Gender differences in the regulation of vascular tone. *Clin Exp Pharmacol Physiol*, *30*(1-2), 1-15. doi: 10.1046/j.1440-1681.2003.03790.x.

Tomiyama, H., Komatsu, S., Shiina, K., Matsumoto, C., Kimura, K., Fujii, M., . . . Yamashina, A. (2018). Effect of wave reflection and arterial stiffness on the risk of development of hypertension in Japanese men. *Journal of the American Heart Association*, *7*(10), e008175.

Tomiyama, H., Shiina, K., Nakano, H., Iwasaki, Y., Matsumoto, C., Fujii, M., . . . Yamashina, A. (2020). Arterial stiffness and pressure wave reflection in the development of isolated diastolic hypertension. *Journal of hypertension*, *38*(10), 2000-2007.

Tomiyama, H., & Yamashina, A. (2010). Non-invasive vascular function tests: their pathophysiological background and clinical application. *Circ J*, *74*(1), 24-33. doi: 10.1253/circj.cj-09-0534.

Touyz, R. M. (2005). Intracellular mechanisms involved in vascular remodelling of resistance arteries in hypertension: role of angiotensin II. *Exp Physiol*, *90*(4), 449-455. doi: 10.1113/expphysiol.2005.030080.

Touyz, R. M., Alves-Lopes, R., Rios, F. J., Camargo, L. L., Anagnostopoulou, A., Arner, A., & Montezano, A. C. (2018). Vascular smooth muscle contraction in hypertension. *Cardiovascular Research*, *114*(4), 529-539. doi: 10.1093/cvr/cvy023.

Touyz, R. M., Montezano, A. C., & Rosendorff, C. (2013). Vascular Function. *Essential Cardiology: Principles and Practice*, 45-65.

Touyz, R. M., & Schiffrin, E. L. (2000). Signal transduction mechanisms mediating the physiological and pathophysiological actions of angiotensin II in vascular smooth muscle cells. *Pharmacol Rev*, *52*(4), 639-672.

Touyz, R. M., & Schiffrin, E. L. (2004). Reactive oxygen species in vascular biology: implications in hypertension. *Histochem Cell Biol*, *122*(4), 339-352. doi: 10.1007/s00418-004-0696-7.

Townsend, R. R., Wilkinson, I. B., Schiffrin, E. L., Avolio, A. P., Chirinos, J. A., Cockcroft, J. R., . . . American Heart Association Council on, H. (2015). Recommendations for Improving and Standardizing Vascular Research on Arterial Stiffness: A Scientific Statement From the American Heart Association. *Hypertension*, *66*(3), 698-722. doi: 10.1161/HYP.0000000000000033.

Tschanz, S. A., Burri, P. H., & Weibel, E. R. (2011). A simple tool for stereological assessment of digital images: the STEPanizer. *J Microsc*, *243*(1), 47-59. doi: 10.1111/j.1365-2818.2010.03481.x.

Tucker, W. D., Arora, Y., & Mahajan, K. (2017). Anatomy, blood vessels.

Turlo, K. A., Scapa, J., Bagher, P., Jones, A. W., Feil, R., Korthuis, R. J., . . . Iruela-Arispe, M. L. (2013). β1-integrin is essential for vasoregulation and smooth muscle survival in vivo. *Arteriosclerosis, thrombosis, and vascular biology*, *33*(10), 2325-2335.

Tykocki, N. R., Boerman, E. M., & Jackson, W. F. (2017). Smooth Muscle Ion Channels and Regulation of Vascular Tone in Resistance Arteries and Arterioles. *Compr Physiol*, *7*(2), 485-581. doi: 10.1002/cphy.c160011.

Uetake, Y., Ikeda, H., Irie, R., Tejima, K., Matsui, H., Ogura, S., . . . Shimosawa, T. (2015). High-salt in addition to high-fat diet may enhance inflammation and fibrosis in liver steatosis induced by oxidative stress and dyslipidemia in mice. *Lipids Health Dis*, *14*(1), 6. doi: 10.1186/s12944-015-0002-9.

Ugural, A. C., & Fenster, S. K. (2011). *Advanced mechanics of materials and applied elasticity*.Pearson Education.

Unwin, N. (1989). The structure of ion channels in membranes of excitable cells. *Neuron*, *3*(6), 665-676. doi: 10.1016/0896-6273(89)90235-3.

Van de Voorde, J., & Vanheel, B. (2000). EDHF-mediated relaxation in rat gastric small arteries: influence of ouabain/Ba2+ and relation to potassium ions. *J Cardiovasc Pharmacol*, *35*(4), 543-548. doi: 10.1097/00005344-200004000-00005.

van Varik, B. J., Rennenberg, R. J., Reutelingsperger, C. P., Kroon, A. A., de Leeuw, P. W., & Schurgers, L. J. (2012). Mechanisms of arterial remodeling: lessons from genetic diseases. *Front Genet*, *3*, 290. doi: 10.3389/fgene.2012.00290.

Van Vliet, B. N., Chafe, L. L., Halfyard, S. J., & Leonard, A. M. (2006). Distinct rapid and slow phases of salt-induced hypertension in Dahl salt-sensitive rats. *J Hypertens*, *24*(8), 1599-1606. doi: 10.1097/01.hjh.0000239296.25260.e0.

Vanhoutte, P., Shimokawa, H., Feletou, M., & Tang, E. (2017). Endothelial dysfunction and vascular disease–a 30th anniversary update. *Acta physiologica*, *219*(1), 22-96.

Vasan, R. S., Short, M. I., Niiranen, T. J., Xanthakis, V., DeCarli, C., Cheng, S., . . . Mitchell, G. F. (2019). Interrelations Between Arterial Stiffness, Target Organ Damage, and Cardiovascular Disease Outcomes. *Journal of the American Heart Association*, *8*(14), e012141. doi: ARTN e012141

10.1161/JAHA.119.012141.

Veerasamy, M., Ford, G. A., Neely, D., Bagnall, A., MacGowan, G., Das, R., & Kunadian, V. (2014). Association of aging, arterial stiffness, and cardiovascular disease: a review. *Cardiol Rev*, *22*(5), 223-232. doi: 10.1097/CRD.0000000000000009.

Velez-Roa, S., Ciarka, A., Najem, B., Vachiery, J. L., Naeije, R., & van de Borne, P. (2004). Increased sympathetic nerve activity in pulmonary artery hypertension. *Circulation*, *110*(10), 1308-1312. doi: 10.1161/01.CIR.0000140724.90898.D3.

Vermeersch, S. J., Rietzschel, E. R., De Buyzere, M. L., Van Bortel, L. M., Gillebert, T. C., Verdonck, P. R., . . . Boutouyrie, P. (2009). Distance measurements for the assessment of carotid to femoral pulse wave velocity. *J Hypertens*, *27*(12), 2377-2385. doi: 10.1097/HJH.0b013e3283313a8a.

Versari, D., Daghini, E., Virdis, A., Ghiadoni, L., & Taddei, S. (2009a). Endothelial dysfunction as a target for prevention of cardiovascular disease. *Diabetes Care*, *32 Suppl 2*(Suppl 2), S314-321. doi: 10.2337/dc09-S330.

Versari, D., Daghini, E., Virdis, A., Ghiadoni, L., & Taddei, S. (2009b). Endothelium-dependent contractions and endothelial dysfunction in human hypertension. *Br J Pharmacol*, *157*(4), 527-536. doi: 10.1111/j.1476-5381.2009.00240.x.

Vögler, O., Barceló, J. M., Ribas, C., & Escribá, P. V. (2008). Membrane interactions of G proteins and other related proteins. *Biochimica et Biophysica Acta (BBA)-Biomembranes*, *1778*(7-8), 1640-1652.

Volkers, L., Mechioukhi, Y., & Coste, B. (2015). Piezo channels: from structure to function. *Pflugers Arch*, *467*(1), 95-99. doi: 10.1007/s00424-014-1578-z.

Vollmer, W. M., Sacks, F. M., Ard, J., Appel, L. J., Bray, G. A., Simons-Morton, D. G., . . . Group, D. A.-S. T. C. R. (2001). Effects of diet and sodium intake on blood pressure: subgroup analysis of the DASH-sodium trial. *Ann Intern Med*, *135*(12), 1019-1028. doi: 10.7326/0003-4819-135-12-200112180-00005.

Wagenseil, J. E., & Mecham, R. P. (2007). New insights into elastic fiber assembly. *Birth Defects Research Part C: Embryo Today: Reviews*, *81*(4), 229-240.

Wagenseil, J. E., & Mecham, R. P. (2009). Vascular extracellular matrix and arterial mechanics. *Physiol Rev*, *89*(3), 957-989. doi: 10.1152/physrev.00041.2008.

Wagenseil, J. E., & Mecham, R. P. (2012). Elastin in large artery stiffness and hypertension. *J Cardiovasc Transl Res*, *5*(3), 264-273. doi: 10.1007/s12265-012-9349-8.

Walsh, M. P., Kargacin, G. J., Kendrick-Jones, J., & Lincoln, T. M. (1995). Intracellular mechanisms involved in the regulation of vascular smooth muscle tone. *Can J Physiol Pharmacol*, *73*(5), 565-573. doi: 10.1139/y95-072.

Wang, Y., Shi, J., & Tong, X. (2021). Cross-Talk between Mechanosensitive Ion Channels and Calcium Regulatory Proteins in Cardiovascular Health and Disease. *Int J Mol Sci*, *22*(16), 8782. doi: 10.3390/ijms22168782.

Webb, R. C. (2003). Smooth muscle contraction and relaxation. *Adv Physiol Educ*, *27*(1-4), 201-206. doi: 10.1152/advan.00025.2003.

Weinberger, M. H., & Fineberg, N. S. (1991). Sodium and volume sensitivity of blood pressure. Age and pressure change over time. *Hypertension*, *18*(1), 67-71. doi: 10.1161/01.hyp.18.1.67.

Westerhof, N., Lankhaar, J. W., & Westerhof, B. E. (2009). The arterial Windkessel. *Med Biol Eng Comput*, *47*(2), 131-141. doi: 10.1007/s11517-008-0359-2.

White, R. M., Rivera, C. O., & Davison, C. A. (2000). Nitric oxide-dependent and -independent mechanisms account for gender differences in vasodilation to acetylcholine. *J Pharmacol Exp Ther*, *292*(1), 375-380.

Williams, B. (1998). Mechanical influences on vascular smooth muscle cell function. *J Hypertens*, *16*(12 Pt 2), 1921-1929. doi: 10.1097/00004872-199816121-00011.

Wind, S., Beuerlein, K., Armitage, M. E., Taye, A., Kumar, A. H., Janowitz, D., . . . Schmidt, H. H. (2010). Oxidative stress and endothelial dysfunction in aortas of aged spontaneously hypertensive rats by NOX1/2 is reversed by NADPH oxidase inhibition. *Hypertension*, *56*(3), 490-497. doi: 10.1161/HYPERTENSIONAHA.109.149187.

Wu, Y., Han, X., Gao, J., Wang, Y., Zhu, C., Huang, Z., . . . Wu, S. (2021). Individual and combined contributions of age-specific and sex-specific pulse pressure and brachial-ankle pulse wave velocity to the risk of new-onset diabetes mellitus. *BMJ Open Diabetes Res Care*, *9*(1), e001942. doi: 10.1136/bmjdrc-2020-001942.

Wynne, B. M., Chiao, C. W., & Webb, R. C. (2009). Vascular Smooth Muscle Cell Signaling Mechanisms for Contraction to Angiotensin II and Endothelin-1. *J Am Soc Hypertens*, *3*(2), 84-95. doi: 10.1016/j.jash.2008.09.002.

Xu, J., & Shi, G. P. (2014). Vascular wall extracellular matrix proteins and vascular diseases. *Biochim Biophys Acta*, *1842*(11), 2106-2119. doi: 10.1016/j.bbadis.2014.07.008.

Yamaguchi, A., Botta, E., & Holinstat, M. (2022). Eicosanoids in inflammation in the blood and the vessel. *Front Pharmacol*, *13*, 997403. doi: 10.3389/fphar.2022.997403.

Yang, C., Kwan, Y. W., Au, A. L. S., Poon, C. C. W., Zhang, Q. A., Chan, S. W., . . . Leung, G. P. H. (2010). 14,15-Epoxyeicosatrienoic acid induces vasorelaxation through the prostaglandin EP

receptors in rat mesenteric artery. *Prostaglandins & Other Lipid Mediators*, *93*(1-2), 44-51. doi: 10.1016/j.prostaglandins.2010.06.004.

Yang, J., Clark, J. W., Jr., Bryan, R. M., & Robertson, C. (2003). The myogenic response in isolated rat cerebrovascular arteries: smooth muscle cell model. *Med Eng Phys*, *25*(8), 691-709. doi: 10.1016/s1350-4533(03)00100-0.

Yannoutsos, A., Levy, B. I., Safar, M. E., Slama, G., & Blacher, J. (2014). Pathophysiology of hypertension: interactions between macro and microvascular alterations through endothelial dysfunction. *J Hypertens*, *32*(2), 216-224. doi: 10.1097/HJH.0000000000000021.

Yasmin, McEniery, C. M., Wallace, S., Dakham, Z., Pulsalkar, P., Maki-Petaja, K., . . . Wilkinson, I. B. (2005). Matrix metalloproteinase-9 (MMP-9), MMP-2, and serum elastase activity are associated with systolic hypertension and arterial stiffness. *Arterioscler Thromb Vasc Biol*, *25*(2), 372. doi: 10.1161/01.ATV.0000151373.33830.41.

Yip, K.-P., Balasubramanian, L., & Sham, J. S. (2010). Integrin-mediated mechanotransduction in vascular smooth muscle cells. In *Mechanosensitivity and Mechanotransduction* (pp. 3-24). Springer.

Ylitalo, P., Hepp, R., Mohring, J., & Gross, F. (1976). Effects of varying sodium intake on blood pressure and renin-angiotensin system in subtotally nephrectomized rats. *J Lab Clin Med*, *88*(5), 807-816.

Yuan, B., & Leenen, F. (1991). Dietary sodium intake and left ventricular hypertrophy in normotensive rats. *American Journal of Physiology-Heart and Circulatory Physiology*, *261*(5), H1397-H1401.

Yue, B. (2014). Biology of the extracellular matrix: an overview. *J Glaucoma*, *23*(8 Suppl 1), S20-23. doi: 10.1097/IJG.0000000000000108.

Yun, S., Budatha, M., Dahlman, J. E., Coon, B. G., Cameron, R. T., Langer, R., . . . Schwartz, M. A. (2016). Interaction between integrin α5 and PDE4D regulates endothelial inflammatory signalling. *Nature cell biology*, *18*(10), 1043-1053.

Zamponi, G. W., Striessnig, J., Koschak, A., & Dolphin, A. C. (2015). The Physiology, Pathology, and Pharmacology of Voltage-Gated Calcium Channels and Their Future Therapeutic Potential. *Pharmacological Reviews*, *67*(4), 821-870. doi: 10.1124/pr.114.009654.

Zewde, T., & Mattson, D. L. (2004). Inhibition of cyclooxygenase-2 in the rat renal medulla leads to sodium-sensitive hypertension. *Hypertension*, *44*(4), 424-428. doi: 10.1161/01.HYP.0000140924.91479.03.

Zicha, J., Dobešová, Z., Vokurková, M., Rauchová, H., Hojná, S., Kadlecová, M., . . . Kuneš, J. (2012). Age-dependent salt hypertension in Dahl rats: fifty years of research. *Physiological research*, *61*.

Zieman, S. J., Melenovsky, V., & Kass, D. A. (2005). Mechanisms, pathophysiology, and therapy of arterial stiffness. *Arterioscler Thromb Vasc Biol*, *25*(5), 932-943. doi: 10.1161/01.ATV.0000160548.78317.29.

Zoungas, S., & Asmar, R. P. (2007). Arterial stiffness and cardiovascular outcome. *Clin Exp Pharmacol Physiol*, *34*(7), 647-651. doi: 10.1111/j.1440-1681.2007.04654.x.

Zygmunt, P. M., Edwards, G., Weston, A. H., Davis, S. C., & Hogestatt, E. D. (1996). Effects of cytochrome P450 inhibitors on EDHF-mediated relaxation in the rat hepatic artery. *Br J Pharmacol*, *118*(5), 1147-1152. doi: 10.1111/j.1476-5381.1996.tb15517.x.

Appendix A

Ethics approval

All procedures on animals were carried out in accordance with the guidelines of the Canadian Council on Animal Care, with the approval of the Institutional Animal Care Committee of Memorial University of Newfoundland (Protocol No. 20-22-RT) and the Canadian Council of Animal Care (Guide to Care and Use of Experimental Animals, Vol 1, 2nd Edition).

Appendix B

Baseline lumen diameters (μm) of the third-order mesenteric arteries measured at the initial pressure of 3.99967 KPa.

Table 1.1. Baseline blood vessel diameters (μm) at the pressure of 3.99967 KPa in isolated third-order mesenteric arteries of Dahl salt-sensitive male (M) and female (F) rats on regular (R) or high salt (HS; 4% NaCl) diets for 6-7 weeks. Each value is expressed as a mean ± SEM (n = 14). Complied data of the values from experiments of Chapter 2 and Chapter 3.

M (R diet)	M (HS diet)	F (R diet)	F (HS diet)
234.4±5.3[a]	272.0±9.5[b]	191.6±1.7	190.6±1.5

[a]Significantly different from F (R diet); $P < 0.05$

[b]Significantly different from F (HS diet); $P < 0.05$

Baseline lumen diameters (μm) of the third-order mesenteric arteries measured at the initial pressure of 1.99984 KPa.

Table 1.2. Baseline blood vessel diameters (μm) at the pressure of 1.99984 KPa in the isolated third-order mesenteric arteries of Dahl salt-sensitive male (M) and female (F) rats on regular(R) or high salt (HS; (4% NaCl) diets for 6-7 weeks for each experimental group in intact and denuded vessels. Each value is expressed as a mean ± SEM (n = 8).

Groups (Intact Vessels)	M (R diet)	M (HS diet)	F (R diet)	F (HS diet)
Vehicle	221.6±10.0[b]	242.9±13.0[c]	190.3±4.0	195.5±20.0
Yoda	214.5±9.1[b]	249.8±12.9[c]	184.8±2.3	186.3±3.0
GsMTx-4	211.0±4.3[b]	234.9±10.8[c]	190.1±2.4	198.0±5.0
PE+Yoda	221.1±3.2[b]	243.6±10.9[c]	184.8±2.6	190.3±8.3

Groups (Denuded Vessels)	M (R diet)	M (HS diet)	F (R diet)	F (HS diet)
Vehicle	213.5±8.0[b]	237.9±7.8[ac]	193.4±5.6	194.4±2.4
Yoda	202.0±4.8	244.3±13.0[ac]	191.8±6.1	192.1±4.1
GsMTx-4	215.4±2.7[b]	242.6±12.2[ac]	187.1±2.4	186.8±3.9
PE+Yoda	206.7±3.3[b]	237.0±6.2[ac]	187.3±2.3	194.3±2.3

[a]Significantly different from M (R diet); $P < 0.05$

[b]Significantly different from F (R diet); $P < 0.05$

[c]Significantly different from F (HS diet); $P < 0.05$

PE; Phenylephrine

GsMTx-4; Grammostola mechanotoxin.

Appendix C

Table 2.1: Drugs/Compounds used in this study.

Drug/Compounds	Supplier	Solvent	Bath concentration
Phenylephrine hydrochloride	Sigma Aldrich (Montreal, Canada)	Distilled water	0.3 μM
L-N^{ω}-Nitro arginine methyl ester	Sigma Aldrich (Montreal, Canada)	Distilled water	0.3 μM
Verapamil	Sigma Aldrich (Montreal, Canada)	Distilled water	0.3 μM
$BaCl_2$	Sigma Aldrich (Montreal, Canada)	Distilled water	100 μM
Ouabain	Sigma Aldrich (Montreal, Canada)	Distilled water	100 μM
Sodium nitroprusside	Sigma Aldrich (Montreal, Canada)	Distilled water	0.3 μM
Yoda	Bio-Techne Canada (Tocris Bioscience), ON, Canada	DMSO	10 μM
Grammostola Mechanotoxin 4 (GsMTx-4)	Alomone labs, JBP, Israel	DMSO	2 μM

Equivalent volumes of the vehicles:

I. ddH_2O (double distilled water)
II. DMSO

Table 2.2: Antibodies used in this study.

Product name	Supplier	Description	Concentration
Anti-MMP9 antibody [EP1254] ab76003	Abcam, MA, USA	Rabbit monoclonal [EP1254]	1: 200
Anti-Integrin beta 1 antibody [EPR16895] ab179471	Abcam, MA, USA	Rabbit monoclonal [EPR16895]	1: 250
Anti-NADPH oxidase 4 antibody [UOTR1B493] ab133303	Abcam, MA, USA	Rabbit monoclonal [UOTR1B493]	1: 100
Anti-Piezo1 Antibody (#APC-087) (1: 200)	Alomone labs, JBP, Israel	Polyclonal	1: 200

Table 2.3: Composition of solutions used in this study.

Solution	Chemicals	Concentration (mM)
Modified Krebs Buffer	NaCl	120
	KCl	4
	$MgCl_2.6H_2O$	1.2
	$CaCl_2H_2O$	1.5
	$NaHCO_3$	25
	KH_2PO_4	1.2
	Glucose	11
	EDTA	0.1

Appendix D

Table 3.1: 2018 Teklad Global 18% Protein Rodent Diet (Teklad Diets, Madison, WI, USA)

Ingredients: inclusion)- Ground wheat, ground corn, wheat middlings, dehulled soybean meal, corn gluten meal, soybean oil, calcium carbonate, dicalcium phosphate, brewers dried yeast, iodized salt, L-lysine, DL-methionine, choline chloride, magnesium oxide, vitamin E acetate, menadione sodium bisulfite complex (source of vitamin K activity), manganous oxide, ferrous sulfate, zinc oxide, niacin, calcium pantothenate, copper sulfate, pyridoxine hydrochloride, riboflavin, thiamin mononitrate, vitamin A acetate, calcium iodate, vitamin B12 supplement, folic acid, biotin, vitamin D3 supplement, cobalt carbonate.

Macronutrients	**Minerals**
Crude Protein % 18.4 Fat (ether extract) [a] % 6.0 Carbohydrate (available) [b] % 44.2 Crude Fiber % 3.8 Neutral Detergent Fiber [c] % 14.7 Ash % 5.5 Energy Density d kcal/g (kJ/g) 3.1 (13.0) Calories from Protein % 24 Calories from Fat % 18 Calories from Carbohydrate % 58	Calcium % 1.0 Phosphorus % 0.7 Non-Phytate Phosphorus % 0.4 Sodium % 0.2 Potassium % 0.6 Chloride % 0.4 Magnesium % 0.2 Zinc mg/kg 70 Manganese mg/kg 100 Copper mg/kg 15 Iodine mg/kg 6 Iron mg/kg 200 Selenium mg/kg 0.23
Amino Acids	**Vitamins**
Aspartic Acid % 1.4 Glutamic Acid % 3.4 Alanine % 1.1 Glycine % 0.8 Threonine % 0.7 Proline % 1.6 Serine % 1.1 Leucine % 1.8 Isoleucine % 0.8 Valine % 0.9 Phenylalanine % 1.0	Vitamin A e, f IU/g 15.0 Vitamin D3 e, g IU/g 1.5 Vitamin E IU/kg 110 Vitamin K3 (menadione) mg/kg 50 Vitamin B1 (thiamin) mg/kg 17 Vitamin B2 (riboflavin) mg/kg 15 Niacin (nicotinic acid) mg/kg 70 Vitamin B6 (pyridoxine) mg/kg 18 Pantothenic Acid mg/kg 33 Vitamin B12 (cyanocobalamin) mg/kg 0.08

Tyrosine % 0.6 Methionine % 0.4 Cystine % 0.3 Lysine % 0.9 Histidine % 0.4 Arginine % 1.0 Tryptophan % 0.2	Biotin mg/kg 0.40 Folate mg/kg 4 Choline mg/kg 1200
Fatty Acids	**Other**
C16:0 Palmitic % 0.7 C18:0 Stearic % 0.2 C18:1ω9 Oleic % 1.2 C18:2ω6 Linoleic % 3.1 C18:3ω3 Linolenic % 0.3 Total Saturated % 0.9 Total Monounsaturated % 1.3 Total Polyunsaturated % 3.4	Cholesterol mg/kg --

Table 3.2: Calculated nutrient composition of stroke prone rodent diet (Zeigler Bros., Inc. Gardners, PA, USA)

Ingredients: Wheat Middlings, Corn, Rice Bran, Dehulled Soybean Meal, Wheat Bran, Fishmeal, Dried Sflim Milfl, Soy Oil, Salt, Limestone, Ferrous Sulfate, Magnesium Oxide, Manganese Oxide, Copper Sulfate, Cobalt Carbonate, Potassium Iodide, Choline Chloride, Vitamin D3 Supplement, dl-Alpha Tocopheryl Acetate (Vitamin E Supplement), Inositol, Niacin, Menadione Sodium Bisulfite Complex (Source of Vitamin K Activity), Riboflavin, Calcium Pantothenate, Vitamin A Acetate, Pyridoxine Hydrochloride, Thiamine Mononitrate, Biotin, Vitamin B12 Supplement, Folic Acid.

Amino Acid Concentration (% of total diet)	**Mineral Concentration**			**Vitamin Concentration**
Arginine 0.75	Calcium	%	0.86	Vitamin A IU/g 10.41
Lysine 0.70	Phosphorous	%	0.50	Vitamin D
Methionine 0.23	Potassium	%	0.55	3 IU/g 2.02
Cystine 0.18	Sodium	%	0.39	Alpha-Tocopherol IU/kg 62.17
Tryptophan 0.15	Magnesium	%	0.15	Thiamine ppm 12.07
Glycine 0.58	Iron	ppm	178.00	Riboflavin ppm 12.47
Histidine 0.28	Zinc	ppm	24.00	Niacin ppm 84.93
Leucine 0.97	Manganese	ppm	75.95	Pantothenic Acid ppm 22.47
Isoleucine 0.55	Copper	ppm	8.36	Choline ppm 1711.89
Phenylalanine 0.52	Cobalt	ppm	2.54	Pyrodoxine ppm 12.71
Tyrosine 0.39	Iodine	ppm	2.72	Folic Acid ppm 1.29
Threonine 0.46				Biotin ppm 0.24
Valine 0.61				Vitamin B12 Mcg/kg 11.63
				Vitamin K ppm 5.04